

Design of New Classes of 1,3-Dipoles and Dynamic Amide Bond Formation

Huseyin Erguven

*A thesis submitted to McGill University in partial fulfillment of the requirements
of the degree of Doctor of Philosophy*

Department of Chemistry
McGill University
Montreal, Quebec, Canada
H3A 0B8

December, 2019

© Huseyin Erguven, 2019

Abstract

This thesis describes discoveries in two general areas of research: the design of new classes of mesoionic heterocycles and their application in 1,3-dipolar cycloaddition reactions; and the development of an alternative approach for the dynamic formation of amide bonds. Each of the studies are directed toward creating more efficient and/or broadly applicable platforms to address these two challenges, and do so with easily generated reagents.

In Chapter 2, we describe the development of a new class of mesoionic 1,3-dipole derived from 2-pyridyl acyl chlorides and imines. This work was inspired by one of the earliest examples of mesoionic heterocycles, Besthorn's red. Besthorn's red is a well-known dye, and does not demonstrate cycloaddition reactivity due to its extended conjugation. We aimed to reduce this extended conjugation in this dipolar core by modifying its components. As was hoped, this new pyridine-based mesoionic heterocycle demonstrates cycloaddition reactivity with alkynes to generate indolizines. This method was exploited to synthesize a range of substituted indolizines from alkynes, imines and pyridyl acyl chlorides.

In Chapter 3, we report the generation of another class of 1,3-dipole; the carbonyl-ylide version of phosphamünchnones. The latter is a phosphorus-containing 1,3-dipole previously discovered by our research group, and can be generated from the one pot reaction of imines, acyl chlorides and phosphonites. In order to generate their carbonyl-ylide analogs, we replaced the imine component with aldehydes. The weak nucleophilicity of aldehydes was overcome via *in situ* generation of potent acyl triflate electrophiles from acyl chlorides and silver triflate. The acyl triflate electrophiles can undergo rapid coupling with aldehydes and phosphonite, and upon deprotonation create a new oxygen-containing 1,3-dipole. Coupling the formation of these

substrates with 1,3-dipolar cycloaddition offers a modular approach to synthesize substituted furans via the one pot coupling of aldehydes, acyl chlorides and alkynes.

Chapter 4 describes our discovery of a new method for dynamic formation of amides. This was achieved via the reversible reaction between imines and acyl chlorides to form α -chloroamides. Although the reaction of imines and acyl chlorides is a well-known route to generate N-acyl iminium salts in synthetic chemistry, its dynamic features have not been investigated in the context of dynamic covalent chemistry (DCvC). A variety of experiments were performed to demonstrate that this transformation is indeed dynamic, and offers a route to access amides in a reversible fashion at ambient conditions, without a catalyst, and from readily available and tunable imines and acyl chlorides. In addition, the reaction can be coupled with hydrolysis to generate robust amide products.

Chapter 4 also discloses a preliminary study on the use of this dynamic reaction to generate amide-containing macromolecules such as polyamides and macrocycles. The latter is especially important, since formation of macrocyclic amides using irreversible amide bond formation reactions typically requires ultra-high dilutions or specially designed substrates. As an alternative, we demonstrate here that these products can be accessed in high yields from diimines and diacyl chlorides without high dilution, and where thermodynamic control can be exploited to favor the formation of macrocycles or polymers.

Résumé

Cette thèse décrit des découvertes dans deux domaines de recherche généraux : la conception de nouvelles classes d'hétérocycles mésoioniques et leur application dans la réaction de cyclisation 1,3-dipolaire et le développement d'une approche alternative pour la formation dynamique de liens amides. Chacune de ces études est dirigée vers la création de nouvelles plateformes plus efficaces et/ou applicables de manière générale pour aborder ces deux défis, et de faire cela avec des réactifs générés facilement.

Dans le chapitre 2, nous décrivons le développement d'une nouvelle classe de 1,3-dipôle mésoionique obtenue à partir de chlorure de 2-pyridylacyle et d'imines. Ce projet fut inspiré par l'un des premiers exemples d'hétérocycles mésoioniques, le rouge de Besthorn. Le rouge de Besthorn un colorant bien connu, et ne montre aucune réactivité de cycloaddition en raison de sa conjugaison étendue. Nous visons à réduire cette conjugaison étendue dans ce corps dipolaire en modifiant ses composantes. Comme nous l'espérons, ce nouvel hétérocycle mésoionique à base de pyridine montre de la réactivité de cycloaddition avec des alcynes pour générer des indolizines. Cette méthode fut exploitée pour synthétiser une gamme d'indolizines substituées à partir d'alcynes, d'imines, et de chlorure de pyridylacyle.

Dans le chapitre 3, nous reportons la génération d'une autre classe de 1,3-dipôles, la version ylure de carbonyle du phospho-münchnones. Ce dernier, un 1,3-dipôle contenant un phosphore, a été découvert précédemment par notre groupe de recherche et peut être généré à partir d'une réaction «one pot» d'imines, de chlorures d'acyle et de phosphonites. Afin de générer leurs analogues ylure de carbonyle, nous avons remplacé la composante imine par des aldéhydes. La faible nucléophilie des aldéhydes fut surmontée par la génération *in situ* de triflates d'acyle

fortement électrophiles à partir de chlorure d'acyle et de triflate d'argent. Les électrophiles de type triflate d'acyle peuvent rapidement subir un couplage avec des aldéhydes et phosphonites, suivie d'une déprotonation, créant un nouveau 1,3-dipôle contenant un oxygène. Jumeler la formation de ces substrats avec l'addition 1,3-dipolaire offre une approche modulaire pour synthétiser des furanes substitués via le couplage «one pot» d'aldéhydes, de chlorure d'acyles et d'alcyne.

Le chapitre 4 décrit notre découverte d'une nouvelle méthode pour la formation dynamique d'amides. Ceci fut atteint via la réaction réversible entre des imines et des chlorures d'acyle pour former des α -chloroamides. Bien que la réaction des imines et des chlorures d'acyle soit une voie bien connue pour générer des sels d'imines *N*-acylées en chimie de synthèse, ses caractéristiques dynamiques n'ont pas fait l'objet d'études dans le contexte de la chimie covalente dynamique.

Le chapitre 4 divulgue aussi une étude préliminaire sur l'utilisation de cette réaction dynamique pour générer des macromolécules contenant des amides tels que des polyamides et des macrocycles. Ces derniers sont particulièrement importants, puisque la formation d'amides macrocycliques utilisant la formation irréversible de liens amides requière typiquement de très grandes dilutions ou des substrats spécialement choisis. Comme alternative, nous montrons ici que ces produits peuvent être accessibles avec de hauts rendements à partir de diimines et des chlorures de diacyle sans grande dilution, où le contrôle thermodynamique peut être exploité pour favoriser la formation de macrocycles ou de polymères.

Acknowledgements

I would like to thank my supervisor Professor Bruce A. Arndtsen for his support and guidance during my studies. I am inspired to be a better scientist after being a member of his group.

I am thankful to former members of our group, Dr. Jeffrey Quesnel, Dr. Fabio Lorenzini and Dr. Boran Xu for their help during my first years. I also want to mention the other former members for providing a warm and fun working environment; Dr. Laure Kayser, Dr. Jevgenijs Tjutrins. Dr. Gerardo Martin Torres, Victoria Jackiewicz, Maximiliano De La Higuera Macias, Anthony Lau, Nigel Braun, Neda Firoozi, Alexander Fabrikant, Omkar Kulkarni, Dr. Mohammad Ghanbari and Oliver Williams. I'd also like to mention the two brilliant undergraduate students I worked with, Kaitlyn Nelson and Tongyue Liang.

I am also grateful to the current members of Arndtsen group for their help and company: Garrison Kinney, Yi Liu, Pierre-Louis Lagueux-Tremblay, Taleah Levesque, Sébastien Roy, Anthony Labelle, Angela Kaiser, Jose Zgheib. I especially thank Cuihan Zhou for our collaboration on my last project. I'll miss every member of this great collection of people.

I'd like to mention Dr. Hatem Titi, Dr. Violeta Toader and Jean-Louis Do for their effort and time for several characterizations during my studies. I also thank the NMR facility manager Dr. Robin Stein and the mass spectrometry facility managers Dr. Nadim Saadeh and Dr. Alexander Wahba for almost all the characterization data presented in this thesis. I would also like to acknowledge the rest of the department staff: Chantal Marotte, Rick Rossi, Weihua Wang, Jean-Philippe Guay, Sandra Aerssen and Linda Del Paggio.

My family have been the primary motivation for being able to pursue my degree. I thank my brothers Emre and Emirhan, and my parents for their endless support and company. Sizleri çok seviyorum.

Contributions of Co-Authors

This thesis consists of five chapters. Chapter 1 is an introduction to the work described in this thesis. Chapter 2 is a published manuscript. Chapter 3 will be submitted, and Chapter 4 has been submitted for publication. The work presented in this thesis was carried out as part of my doctoral dissertation in chemistry under the supervision of Dr. Bruce Arndtsen. Thus, he is the corresponding author on all the manuscripts and assisted in editing this thesis. I performed all the experiments reported in these manuscripts, except where noted below:

Chapter 2: “Development and Cycloaddition Reactivity of a New Class of Pyridine-Based Mesoionic 1,3-Dipole” *Angew. Chem. Int. Ed.* **2017**, 56, 6078. Evan N. Keyzer and David C. Leitch synthesized the 1,3-dipole **2.2n** and crystallized it for X-ray analysis. X-ray structural analysis was performed by Laure V. Kayser.

Chapter 3: Cuihan Zhou performed some of the screening reactions in Table 3.1, as well as screening of various solvents and triflate salts mentioned in this chapter.

Chapter 4: “A Versatile Approach to Dynamic Amide Bond Formation with Imine Nucleophiles” *Chem. Eur. J.* doi:10.1002/chem.202001140. Evan N. Keyzer performed preliminary investigations of dynamic imine/acyl chloride reaction. X-ray structural analysis of **4.9b** was performed by Hatem Titi.

Table of Contents

Abstract	iii
Résumé.....	v
Acknowledgements.....	vii
Contributions of Co-Authors	ix
Table of Contents	x
List of Schemes.....	xiii
List of Figures.....	xvi
List of Tables	xvi
Abbreviations	xviii
CHAPTER 1: Introduction: Mesoionic Heterocycles and Dynamic Covalent Chemistry	
1.1 Perspective	1
1.2 Mesoionic Heterocycles and Their Cycloaddition Reactivity	3
1.2.1 Early Examples of Mesoionic Heterocycles	4
1.2.2 Stability of Mesoionic Heterocycles.....	7
1.2.3 Synthesis and Cycloaddition Reactivity of Mesoionic Heterocycles	9
1.2.3.1 Münchnones.....	10
1.2.3.2 Phospha-Münchnones.....	19
1.2.3.3 Mesoionic Imidazoles (1,3-Diazolium-4-olates)	23
1.2.3.4 Isomünchnones	25
1.2.3.5 Oxamünchnones.....	28
1.3 Dynamic Covalent Chemistry and Amides.....	31
1.3.1 Emergence of Dynamic Covalent Chemistry.....	32
1.3.2 Common Reactions in Dynamic Covalent Chemistry	33
1.3.2.1 Imine Formation and Exchange	34
1.3.2.2 Disulfide Exchange.....	37
1.3.2.3 Boronic Acid Derivatives	39
1.3.2.4 Alkene and Alkyne Metathesis	41

1.3.2.5 Examples of Other Dynamic Covalent Reactions	43
1.3.3 Dynamic Covalent Chemistry of Amides	45
1.3.3.1 Thermal Exchange	46
1.3.3.2 Catalytic Transamidation Reactions	46
1.3.3.3 Peptide-Based Dynamic Covalent Chemistry	50
1.3.3.4 Formation of Amides by Post-Synthetic Modifications	52
1.4 Overview of Thesis	54
1.5 References	56
CHAPTER 2: Development and Cycloaddition Reactivity of a New Class of Pyridine-Based Mesoionic 1,3-Dipole	
2.0 Preface	64
2.1 Introduction	64
2.2 Results and Discussion	66
2.3 Conclusions	74
2.4 Experimental Section	76
2.4.1 General Procedures	76
2.4.2 Experimental Procedures	76
2.4.3 Characterization Data	78
2.5 References	89
CHAPTER 3: Multicomponent Synthesis of Furans via a New Class of Phosphorus-Based 1,3-Dipole	
3.0 Preface	94
3.1 Introduction	94
3.2 Results and Discussion	99
3.3 Conclusions	107
3.4 Experimental Section	107
3.4.1 General Procedures	107
3.4.2 Experimental Procedures	108
3.4.3 Characterization Data	110
3.5 References	115

CHAPTER 4: A Versatile Approach to Dynamic Amide Bond Formation with Imine Nucleophiles

4.0 Preface	119
4.1 Introduction.....	120
4.2 Results and Discussion	123
4.2.1 Reversibility of Imine/Acyl Chloride Reaction	123
4.2.2 Control of Equilibrium.....	123
4.2.3 Dynamic Exchange	127
4.2.4 Controlled Generation of Secondary and Tertiary Amide Products	130
4.2.5 Coupling Exchange and Hydrolysis.....	132
4.2.6 Utility in Macrocyclization	133
4.3 Conclusions.....	136
4.4 Experimental Section	136
4.4.1 General Procedures	136
4.4.2 Experimental Procedures	137
4.4.3 Characterization Data.....	147
4.5 References.....	155

CHAPTER 5: Summary, Conclusions and Future Work

5.1 Conclusions and Contributions to Original Knowledge	160
5.2 Suggestions for Future Work	162
5.3 References.....	165

Appendix I	A-1
-------------------------	-----

Appendix II	A-2
--------------------------	-----

Appendix III	A-22
---------------------------	------

List of Schemes

Scheme 1.1	Resonance structures of a 1,3-dipole (azide) and its 1,3 dipolar cycloaddition reaction with an alkyne	1
Scheme 1.2	Common exchange reactions used in DCvC.....	2
Scheme 1.3	Synthesis of dehydrodithizone	4
Scheme 1.4	Synthesis of endo-thiodihydrothiodiaxoles and endo- thiotriazolines	5
Scheme 1.5	Synthesis of Besthorn's red.....	5
Scheme 1.6	Synthesis of sydnones	6
Scheme 1.7	Synthesis of münchnones	6
Scheme 1.8	Cycloaddition reactions of sydnones and münchnones with alkynes.	9
Scheme 1.9	Synthesis of münchnones via dehydration with acetic anhydride.....	10
Scheme 1.10	Synthesis of münchnones via 4-component Ugi reaction	11
Scheme 1.11	Palladium-catalyzed carbonylative münchnone synthesis and its mechanism	12
Scheme 1.12	Palladium-catalyzed double carbonylative münchnone synthesis	13
Scheme 1.13	General cycloaddition reactivity of münchnones with alkynes	14
Scheme 1.14	Synthesis of pyrrole containing biologically active molecules via münchnones	15
Scheme 1.15	Synthesis of atorvastatin via cycloaddition of münchnones	16
Scheme 1.16	Cycloaddition reactions between münchnones and a) alkenes with a leaving group and b) alkenes without a leaving group c) alkenes followed by proton migration	17
Scheme 1.17	Cycloaddition reactions between münchnones and a) imines with a leaving group and b) phosphalkynes c) diazo compounds	18
Scheme 1.18	Formation of phosphamünchnone from imine, acyl chloride and phosphonite.....	19
Scheme 1.19	Enantioselective cycloaddition via chiral phosphites.....	22
Scheme 1.20	Synthesis of mesoionic imidazoles from imidoyl chloride	23

Scheme 1.21	Synthesis of mesoionic imidazole from amidines and α -bromo acyl chlorides (a) and cycloaddition of münchnones with isocyanates (b)	24
Scheme 1.22	Cycloaddition reactivity of mesoionic imidazoles with alkynes and alkenes.....	25
Scheme 1.23	Synthesis of isomünchnones from α -diazoidimides.....	26
Scheme 1.24	Synthesis of isomünchnones from α -ketoimides.....	26
Scheme 1.25	General cycloaddition reactivity of isomünchnones	27
Scheme 1.26	Synthesis of furans from polymer-supported isomünchnones	27
Scheme 1.27	Synthesis of 2-pyridones from isomünchnones and alkenes.....	28
Scheme 1.28	Synthesis and trapping of possible oxamünchnone intermediate by cyclodehydration of O-acetyl mandelic acid (a) and cyclization of α -diazo anhydride (b).....	29
Scheme 1.29	In situ trapping of oxamünchnones with alkenes	29
Scheme 1.30	Synthesis and in situ trapping of 1,3-oxathiolium-4-olate	30
Scheme 1.31	Formation of Zn^{2+} templated cyclic tetramers of 2-aminobenzaldehyde (a) and Ni^{2+} complexes of imine containing tetradentate ligands (b)	33
Scheme 1.32	Formation of dynamic imine libraries through a) partial hydrolysis and b) amination.....	35
Scheme 1.33	Formation of tetramers or trimers of 2-aminobenzaldehyde.....	35
Scheme 1.34	Synthesis of dynamic imine rotaxanes through hydrogen bonding	36
Scheme 1.35	Synthesis and reduction of imine macrocycles	37
Scheme 1.36	General representation of disulfide exchange	38
Scheme 1.37	Selective formation and capture of peptide containing cyclic disulfide hexamers	39
Scheme 1.38	General representation of boronic acid ester exchange.....	39
Scheme 1.39	Synthesis of a porous COF by dehydration of 1,4-benzenediboronic acid...40	40
Scheme 1.40	Mechanism of alkene metathesis.....	41
Scheme 1.41	Synthesis arylenevinylene macrocycles (AVMs) through olefin metathesis	42
Scheme 1.42	Formation of polymers or macrocycles through alkyne metathesis.....	43

Scheme 1.43	Examples of other DCvC reactions	44
Scheme 1.44	Conventional synthesis of amides from amines and carboxylic acid derivatives	45
Scheme 1.45	Amide interchange reactions at high temperatures	46
Scheme 1.46	a) AlCl ₃ promoted b) Copper catalyzed transamidation reactions	47
Scheme 1.47	a) Amide metathesis at room temperature using Zr(NMe ₂) ₄ as catalyst b) Proposed mechanism for transamidation c) Formation of stable metallated amide 1.21 with secondary amides	49
Scheme 1.48	Enzyme-assisted transamidation driven by self-assembly	50
Scheme 1.49	General mechanism of native chemical ligation (NCL).....	51
Scheme 1.50	Amide metathesis through native chemical ligation	52
Scheme 1.51	Preparation of amide-based COF via post-synthetic modification	53
Scheme 2.1	Mesoionic 1,3-dipoles and cycloaddition.....	66
Scheme 2.2	Synthesis of pyridine-based 1,3-dipole 2.2a	67
Scheme 2.3	Cycloaddition reactivity of pyridine-based 1,3-dipole 2.2	71
Scheme 2.4	Targeted synthesis of fluorescent indolizine 2.5	74
Scheme 3.1	Common approaches to furan synthesis.....	96
Scheme 3.2	Furan synthesis via mesoionic 1,3-dipoles.....	97
Scheme 3.3	1,3-Dipolar cycloaddition routes to furans.....	99
Scheme 3.4	Mechanistic postulate for furan synthesis	100
Scheme 3.5	Synthesis of fused-ring oxazole 3.5n via intramolecular cycloaddition	105
Scheme 3.6.	³¹ P NMR analysis of 3.2o	106
Scheme 4.1	Efficient Trapping of the Dynamically Formed 4.3 to Access Secondary and Tertiary Amides.....	131
Scheme 5.1	Synthesis of pyridine-based münchnones	163
Scheme 5.2	Palladium-catalyzed carbonylative synthesis of oxamünchnones	164
Scheme 5.3	Isocyanide-mediated synthesis of furans.....	164
Scheme 5.4	Synthesis of macrocyclic phosphamünchnones and pyrroles.....	165

List of Figures

Figure 1.1	General structure and resonance in mesoionic heterocycles	3
Figure 1.2	Representative examples of mesoionic heterocycles	7
Figure 1.3	Examples of stable mesoionic compounds.....	8
Figure 1.4	Three Sustmann Types for 1,3-dipolar cycloaddition reactions.....	14
Figure 1.5	X-ray crystal structure of a phospho-münchnone.....	21
Figure 1.6	Kinetic vs. Thermodynamic Control	32
Figure 2.1	Crystal structure of 2.2n	70
Figure 4.1	Dynamic covalent approaches to amides	122
Figure 4.2	Reaction of 4.1a and 4.2a	124
Figure 4.3	Dynamic exchange of 4.3 with imines	128
Figure 4.4	Dynamic exchange between amides 4.3	129
Figure 4.5	Kinetic and Thermodynamic Controlled Generation and Trapping of Secondary Amides via 4.3	132
Figure 4.6	Controlled generation of amide macrocycles or polymers.....	135
Figure 4.7	[4.1a]*[4.2a] vs [4.3aa] plot used to determine the K_{eq} value of 4.3aa in CD_3CN	138
Figure 4.8	van't Hoff plot for formation of 4.3aa in CD_3CN	140

List of Tables

Table 1.1	Calculated heats of hydrogenation of mesoionic heterocycles	8
Table 1.2	Phospho-münchnone mediated pyrrole synthesis from imines, acyl chlorides and alkenes	20
Table 1.3	Cycloaddition regioselectivity of different mesoionic heterocycles.....	22
Table 1.4	Metal catalyzed transamidation of secondary amides	47
Table 2.1	Substrate scope for 1,3-dipole 2.2a formation.....	69
Table 2.2	Modular synthesis of indolizines via mesoionic 1,3-dipole 2.2	73

Table 3.1	Synthesis of furan 3.5a via cycloaddition.....	101
Table 3.2	Substrate diversity of tetrasubstituted furan synthesis.....	104
Table 4.1	Influence of imine, acyl chloride and halide on dynamic formation of amides 4.3	126
Table 4.2	Equilibrium data for 4.3aa in CD ₃ CN	138
Table 4.3	Data for van't Hoff plot for formation of 4.3aa in CD ₃ CN.....	139

Abbreviations

Å	Ångstrom
Ac	acetate
Ac ₂ O	acetic anhydride
AgOTf	silver trifloromethanesulfonate
Ar	aryl
n-BuLi	n-butyl lithium
Bn	benzyl
br	broad
catechyl	o-O ₂ C ₆ H ₄
°C	degrees Celsius
cat.	catalyst
COF	Covalent organic framework
Cy	cyclohexyl
δ	chemical shift
d	doublet
dba	dibenzylideneacetone
DBU	1,8-diazabicyclo[5,4,0]undec-7-ene
DCC	1,3-dicyclohexylcarbodiimide
DCvC	Dynamic Covalent Chemistry
DCM	dichloromethane
DCE	1,2 dichloroethane
DIPEA	diisopropylethylamine (Hünigs base)
DMAD	dimethylacetylene dicarboxylate
DMF	<i>N,N</i> -dimethylformamide
DMSO	dimethylsulphoxide
eq	equivalents
ESI-MS	electrospray ionization mass spectrometry

Et	ethyl
EtOAc	ethyl acetate
EWG	Electron withdrawing group
h	hour(s)
Hex	hexyl
HRMS	high resolution mass spectrometry
Hz	hertz
i-Pr	Isopropyl
LiHMDS	Lithium hexamethyldisilazane (Lithium bis(trimethylsilyl)amide)
J	coupling constant
L	ligand
m	multiplet
mg	milligram
min	minute(s)
ml	milliliter
mmol	millimol
MS	mass spectrum
m/z	mass-to-charge ratio
NMR	nuclear magnetic resonance
Nu	nucleophile
OTf	trifloromethanesulfonate
Ph	Phenyl
pH	negative logarithm of hydrogen ion concentration
pKa	negative logarithm of equilibrium constant for association
PMP	p-MeOC ₆ H ₄
ppm	parts per million
p-Tolyl	p-MeC ₆ H ₄
q	Quartet
r.t.	room temperature

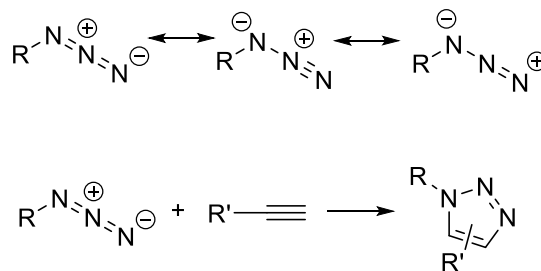
s	singlet
sec	second(s)
t	triplet
t-Bu	tert-butyl
THF	tetrahydrofuran
TMSBr	trimethylsilyl bromide
TMSI	trimethylsilyl iodide
TMSOTf	trimethylsilyl trifluoromethanesulfonate
Ts	toluenesulfonyl
Δ	reflux

CHAPTER 1

Introduction: Mesoionic Heterocycles and Dynamic Covalent Chemistry

1.1. Perspective

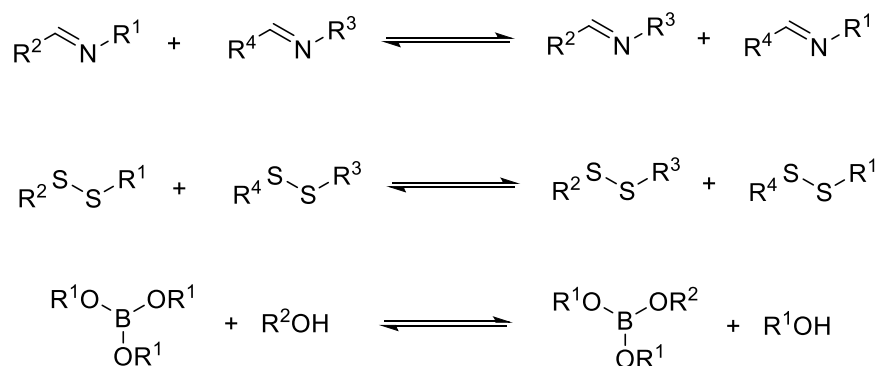
1,3-dipoles are classically defined as compounds with four delocalized electrons shared over three atoms. These molecules bear a positive and negative charge in all possible covalent resonance structures. The most prominent feature of such compounds is their cycloaddition reactions, where an unsaturated substrate (a dipolarophile) reacts with the 1,3-dipole to generate a five-membered ring. This type of reactivity offers a convergent method to form heterocyclic products from relatively simple reagents, and as such has become a prominent field in synthetic organic chemistry, with applications ranging from total synthesis to the assembly of pharmaceutically relevant structures. A representative 1,3-dipole is shown in Scheme 1.1 with azides, which can undergo cycloaddition with alkynes (i.e. Huisgen cycloaddition, a prototypical “click”¹ reaction).²



Scheme 1.1 Resonance structures of a 1,3-dipole (azide) and its 1,3 dipolar cycloaddition reaction with an alkyne.

Mesoionic heterocycles are a special class of 1,3-dipoles, where the charges are delocalized in a 5 membered-ring. These compounds can act as more stable versions of their corresponding acyclic 1,3-dipoles, and thus undergo cycloaddition reactions. The first part of this introduction chapter will discuss the synthesis and cycloaddition reactions of mesoionic heterocycles.

The second part of this introduction chapter will focus on dynamic covalent chemistry (DCvC). DCvC offers a strategy to use reversible covalent bond formation reactions to generate complex molecular architectures. This rapidly developing field can be considered as a branch of supramolecular chemistry, where rapid equilibration and error-correcting features are essential, but it does not rely on weak non-covalent interactions. Therefore, DCvC has potential to access robust, highly-organized materials, which can prove useful for many of their potential applications. While a range of reactions have been found to be relevant for DCvC, the most commonly used functional groups in this field are imines, disulfides and boronic acid derivatives (Scheme 1.2). This chapter will give a summary of these reactions and their applications in DCvC. The incorporation of amides in DCvC will also be discussed, which is one of the research subjects of this thesis.

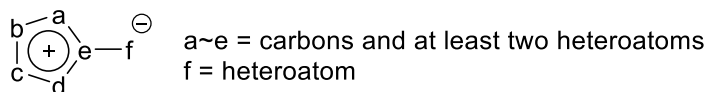


Scheme 1.2 Common exchange reactions used in DCvC.

1.2. Mesoionic Heterocycles and Their Cycloaddition Reactivity

The first use of the term “mesoionic” (mesomeric + ionic) can be traced back to 1949 in a publication by Ollis and Baker.³ The commonly accepted definition of a mesoionic heterocycle is:⁴ “...a five-membered heterocycle which cannot be represented satisfactorily by any one covalent or polar structure and possesses a sextet of electrons in association with the five atoms comprising the ring.”

a) General structure of mesoionic heterocycles



b) Example of resonance structures in Münchnones

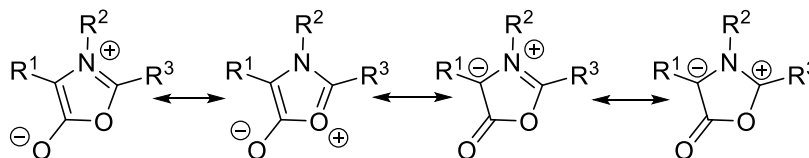


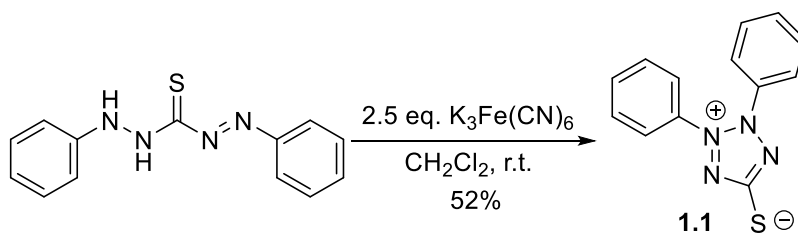
Figure 1.1 General structure and resonance in mesoionic heterocycles.

The typical representation of a mesoionic heterocycle is shown in Figure 1.1. This contains at least 2 heteroatoms in the ring, whereas the exocyclic atom (f) is also a heteroatom and is often associated with the negative charge. The heteroatoms in these systems are usually nitrogen and oxygen, however, variants with sulfur, selenium and phosphorus are also known. As illustrated with 1,3-oxazolium 5-oxalates (münchnones, Figure 1.1b), the charges in the heterocycle are stabilized by delocalization. In addition, these inner salts can act as masked 1,3-dipoles and can undergo cycloaddition reactions with a variety of dipolarophiles. This reactivity offers access to a

broad range of heterocycles depending on the dipolarophile and 1,3-dipole employed, and constitutes the main utility of mesoionic heterocycles.

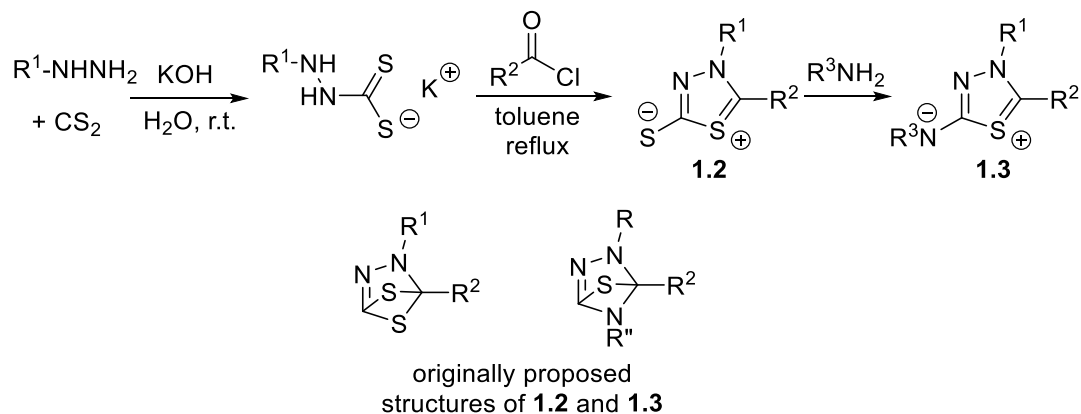
1.2.1. Early Examples of Mesoionic Heterocycles

Although the term ‘mesoionic’ has been a part of the literature for 70 years, examples to this class of molecule can be found in reports from over a century ago. In 1882, Fischer and Besthorn described the formation of the dehydrodithizone **1.1** (Scheme 1.3) by oxidation of dithizone.⁵ It is important to note that the correct dipolar structures for these early examples were assigned several decades after their initial synthesis.



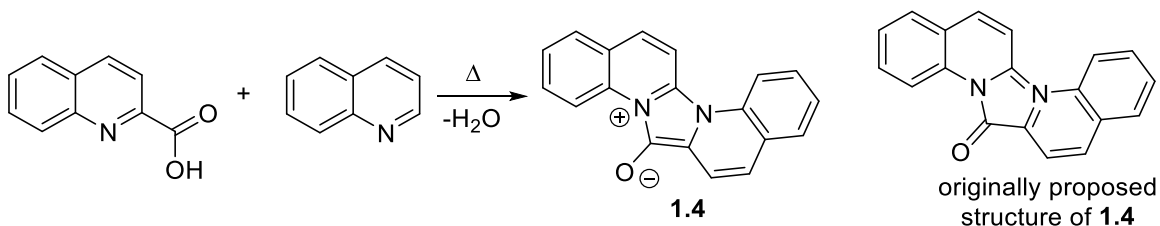
Scheme 1.3 Synthesis of dehydrodithizone

Subsequent contributions to the field came from Busch and coworkers in 1895, where they described the preparation of new compounds similar to dehydrodithizone (**1.1**), the mesoionics **1.2** and **1.3** (Scheme 1.4) from hydrazines, carbon disulfide and acyl chlorides.⁶ These products were initially proposed to have neutral bicyclic structure. Schönberg much later pointed out that such small bicyclic scaffolds bearing double bonds would not conform to Bredt’s rule, and proposed their currently accepted zwitterionic form.⁷



Scheme 1.4 Synthesis of endo-thiodihydrothiodiazoles (**1.2**) and endo-thiotriazolines (**1.3**) (no yields were reported)

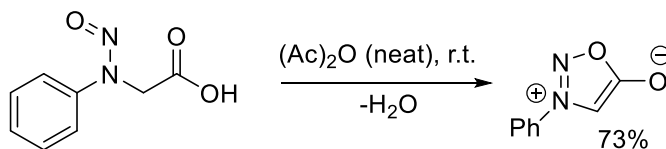
Besthorn et al. added a new member to this class of molecules in 1894, the pigment Besthorn's red (**1.4**), which was generated upon the condensation of 2-quinoline carboxylic acid and quinoline.⁸ Their initial structure assignment included a pentavalent nitrogen, which was corrected to be a dipolar core by Krollpfeiffer in 1937.⁹



Scheme 1.5 Synthesis of Besthorn's red

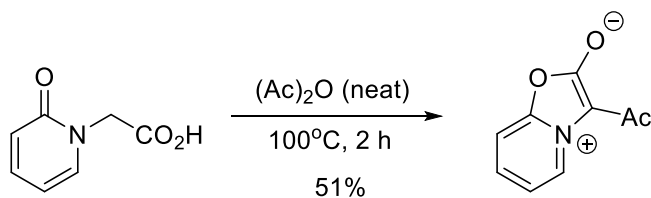
Sydnones, one of the most well-known examples to mesoionic heterocycles, were first prepared in 1935 by Earl and Mackney¹⁰ by dehydration of N-nitroso N-phenylglycine using acetic anhydride (Scheme 1.6). Similar to the previous cases, accurate assignment of the dipolar structure

was revealed later by Ollis and Baker,¹ when they introduced the term “mesoionic compounds”. This soon led to a re-investigation for other members of these type of molecules from previous reports.^{3,6,11-13}



Scheme 1.6 Synthesis of sydnone

One of the most prominent classes of mesoionic heterocycles are münchnones, which were first reported in 1958 by Lawson and Miles.¹⁴ Their original synthesis involved cyclodehydration of 2-pyridone *N*-acetic acid using acetic anhydride (Scheme 1.7). Münchnones are named after the city Munich (München), where their 1,3-dipolar cycloaddition reactivity was first noted by Huisgen in 1964.¹⁵



Scheme 1.7 Synthesis of münchnone

Subsequent studies in the field demonstrated that a diverse array of variants of münchnones or sydnone can be generated. Examples of these include those where the nitrogen and oxygen in the ring are exchanged (isomünchnones),¹⁶ or the heteroatoms are replaced with

other units (e.g. sydnone imines,¹⁷ münchnone imines,¹⁸ thiomünchnones¹⁹ or thioisomünchnones;²⁰ Figure 1.2).

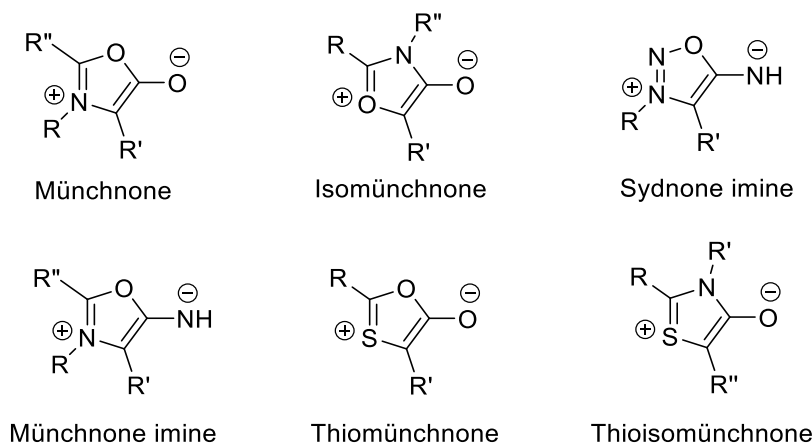


Figure 1.2 Representative examples of mesoionic heterocycles

1.2.2. Stability of Mesoionic Heterocycles

The lifetime of mesoionic compounds under ambient conditions can vary between seconds to months or longer, depending on their structure and substitution pattern. Mesoionic compounds are typically much more stable than their corresponding acyclic 1,3-dipoles due to their aromaticity and extra resonance stability. However, their charged structure still makes them reactive, and many are sensitive towards air and moisture. Substituting mesoionic compounds with aromatic groups can help increase their stability through extended conjugation. Further stabilization can be obtained by incorporating an electron withdrawing or donor group on positions where there is significant build-up of negative or positive charge, respectively. As examples, the extended conjugation in Besthorn's red **1.4** (Scheme 1.5) and thioisomünchnone²⁰ **1.5** can make the dipoles indefinitely stable in air. Similarly, stable versions of münchnones,²¹ and isomünchnones¹⁶ incorporating extended conjugation and/or electron withdrawing units on the ring have been

isolated as air-stable solids (**1.6**, **1.7**), and have been characterized by X-ray crystallography (e.g. **1.6**). The extended conjugation in sydnone **1.8** has made it stable enough to be used in vivo, where it displays antibacterial²² or antitumor activity.²³

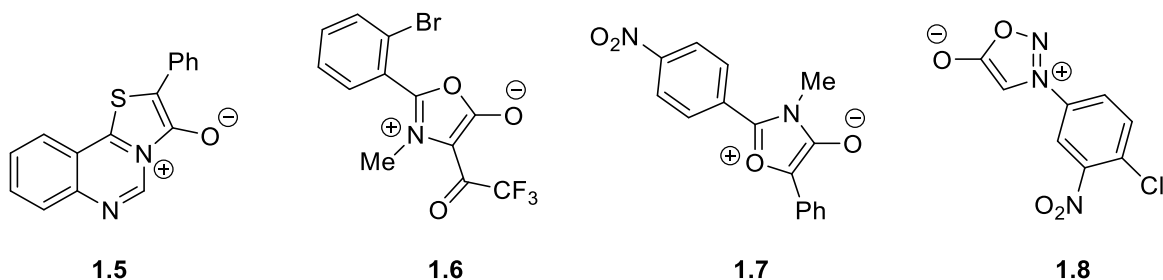


Figure 1.3 Examples of stable mesoionic compounds

In addition to their substitution pattern, the stability of a mesoionic compound also depends on the structure itself, and in particular the nature of the heteroatoms in the ring. For example, a computational study by Hamaguchi probing the relative heat of hydrogenation concluded that resonance stability of mesoionic systems with oxygen instead of nitrogen is lower due to low energy level of oxygen p-orbitals.²⁴ The latter can be seen in the more negative heat of hydrogenation of dipoles such as oxamünchnones relative to their nitrogen-containing analogues (Table 1.1).

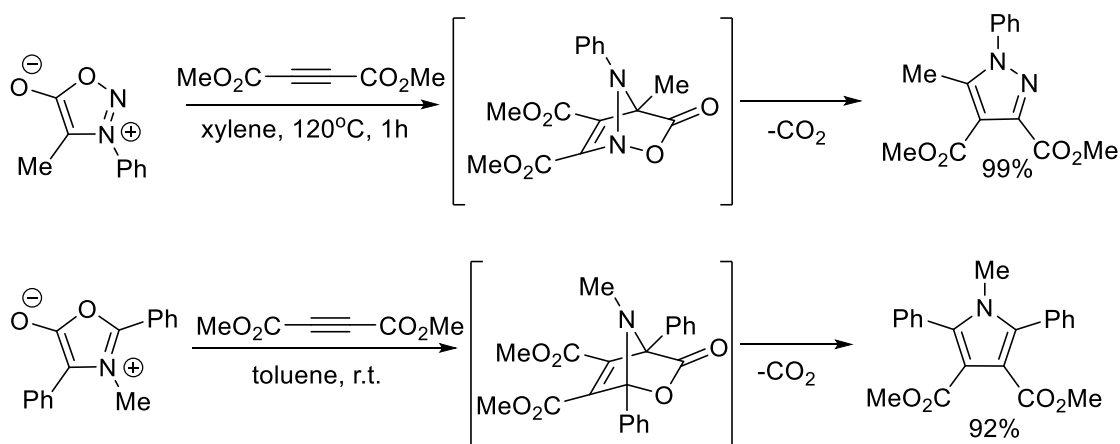
	Mesoionic imidazole	Münchnone	Isomünchnone	Oxamünchnone
calculated heat of hydrogenation (kcal/mol)	-18.8	-26.9	-36.5	-44.5

Table 1.1 Calculated heats of hydrogenation of mesoionic heterocycles

These findings are correlated with experimental observations: mesoionic imidazoles,²⁵ münchnones²¹ and isomünchnones¹⁶ have been isolated as stable solids, whereas 1,3-dioxolylium-4-olates (oxamünchnones) have only been generated and used *in situ*, even with an electron withdrawing p-nitrophenyl group on C4 position.²⁶

1.2.3. Synthesis and Cycloaddition Reactivity of Mesoionic Heterocycles

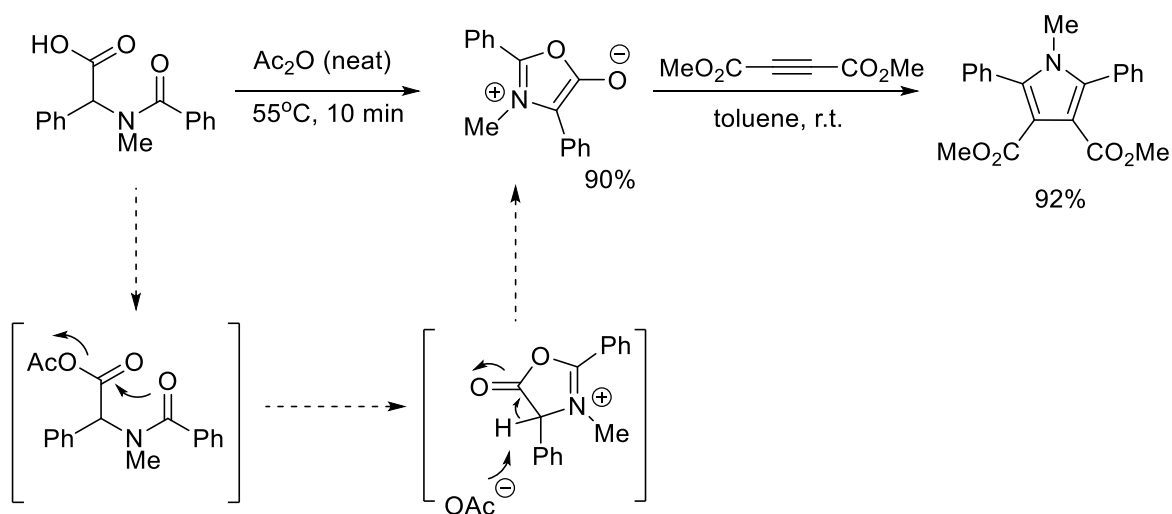
Although mesoionic heterocycles have existed for a long time, their reactivity did not attract significant attention until the research of Huisgen in 1962.²⁷ In this pioneering studies, Huisgen demonstrated that the cycloaddition of alkynes with sydnones and münchnones led to formation of pyrazoles and pyrroles, respectively (Scheme 1.8).¹⁵ These studies have stimulated significant research efforts directed towards the discovery of efficient platforms to assemble mesoionic heterocycles and exploit these (often *in situ*) in cycloaddition reactivity. Provided below are highlights of these efforts with various key derivatives of münchnones, which are the focus of subsequent research in this thesis.



Scheme 1.8 Cycloaddition reactions of sydnones and münchnones with alkynes.

1.2.3.1. Münchnones

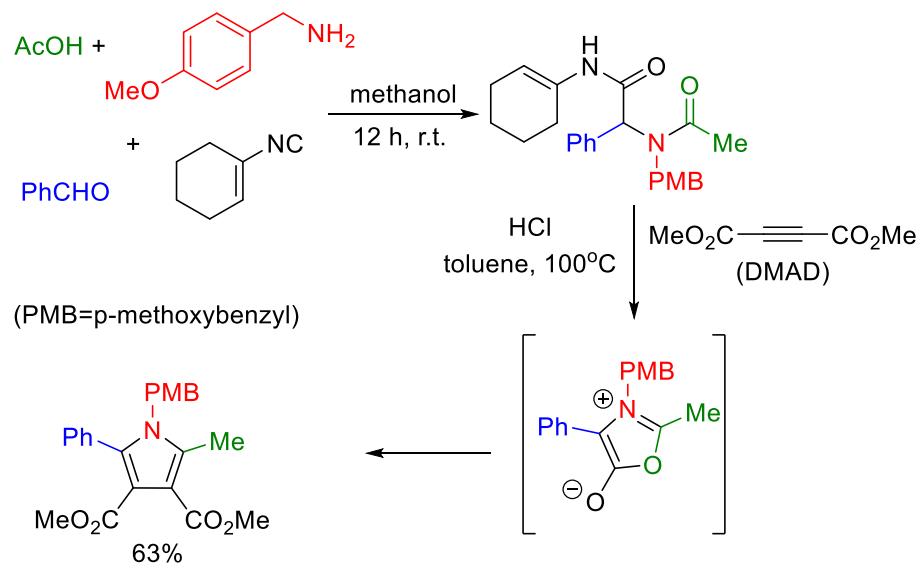
As noted above (Scheme 1.7), münchnones were first prepared via the cyclodehydration of *N*-acyl amino acids. This still represents the most common route to prepare these dipoles. The cyclization is typically performed with the aid of acetic anhydride¹⁵ or carbodiimides²⁸ such as dicyclohexylcarbodiimide (DCC), and commonly requires high temperatures (Scheme 1.9). These reagents presumably activate the carboxylic acid towards nucleophilic attack of the amide oxygen, which is followed by deprotonation. Although air-stable münchnones have been isolated,²¹ these compounds are often prepared and trapped with dipolarophiles in situ to yield the cycloaddition product.



Scheme 1.9 Synthesis of münchnones via dehydration with acetic anhydride

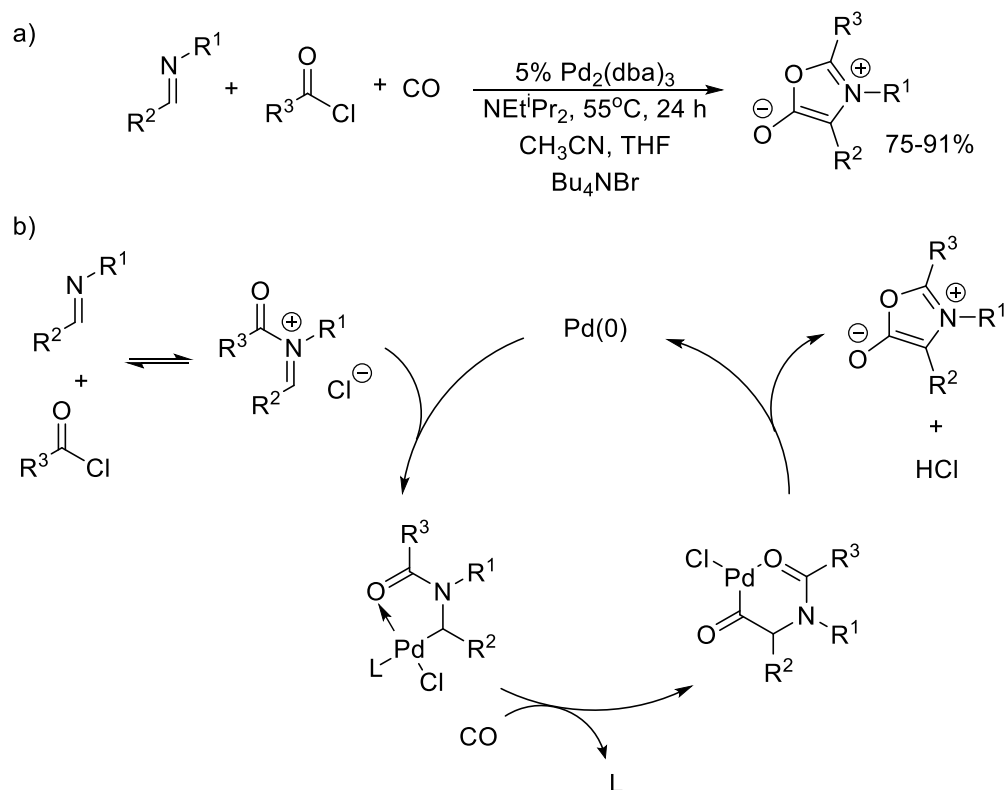
The *N*-acyl amino acid building blocks for münchnones are often synthesized via multistep protocols.²⁹ However, alternate approaches have been described. For example, the 4-component Ugi reaction has been used in münchnone chemistry. This multicomponent pathway initially converts carboxylic acid, amine, aldehyde and isocyanide to a *N*-acyl amino acid (Scheme 1.10).³⁰

The subsequent heating of this product in acid promotes cyclodehydration, and leads to the in situ formation of a münchnone for cycloaddition with an alkyne.



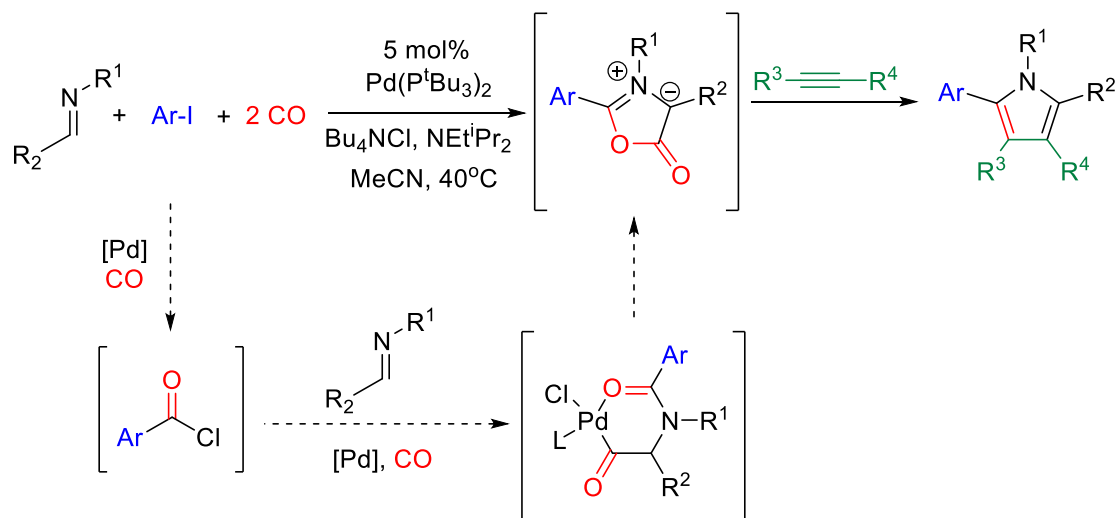
Scheme 1.10 Synthesis of münchnones via 4-component Ugi reaction

Our research group has developed the first metal-catalyzed synthesis of münchnones (Scheme 1.11).³¹ This reaction has been shown to proceed via the initial formation of an *N*-acyl iminium from imine and acyl chloride. The latter can undergo oxidative addition to palladium center followed by CO insertion. Reductive elimination and deprotonation generates the substituted münchnones in moderate to good yields. Overall, this allows a modular synthesis of münchnones from readily available imines, acyl chlorides and carbon monoxide.



Scheme 1.11 Palladium-catalyzed carbonylative münchnone synthesis and its mechanism

In a more recent study, this chemistry has been further improved by combining it with the in situ formation of acyl chlorides by Pd-catalyzed carbonylation of aryl iodides.³² This enables the formation of münchnones from more stable starting materials, and can also be broadly diversified (Scheme 1.12).



Scheme 1.12 Palladium-catalyzed double carbonylative münchnone synthesis

1,3-dipolar cycloaddition reactivity is likely the most heavily exploited feature of mesoionic heterocycles such as münchnones. Most mesoionic heterocycles are nucleophilic (HOMO-controlled) dipoles due to their carbon-based cores (and thus relatively high energy π -orbitals). As a result, they often undergo Type 1 cycloaddition, where the HOMO of the dipole pairs with the LUMO of the dipolarophile (Figure 1.4).³³ Electron withdrawing substituents on the dipolarophile lower the LUMO energy, and therefore improves the overlap. As such, a common alkyne employed in these cycloadditions is dimethylacetylene dicarboxylate (DMAD), which is often used in trapping mesoionic heterocycles as a preliminary test of their existence. Indeed, Gribble has noted in his review of mesoionic heterocycles that: “If DMAD is unable to ambush a suspected mesoionic heterocycle, then the latter most probably has not been generated!”.³⁴ In addition to alkynes, other dipolarophiles have been utilized in this chemistry, such as alkenes, imines, nitriles and carbonyl compounds.

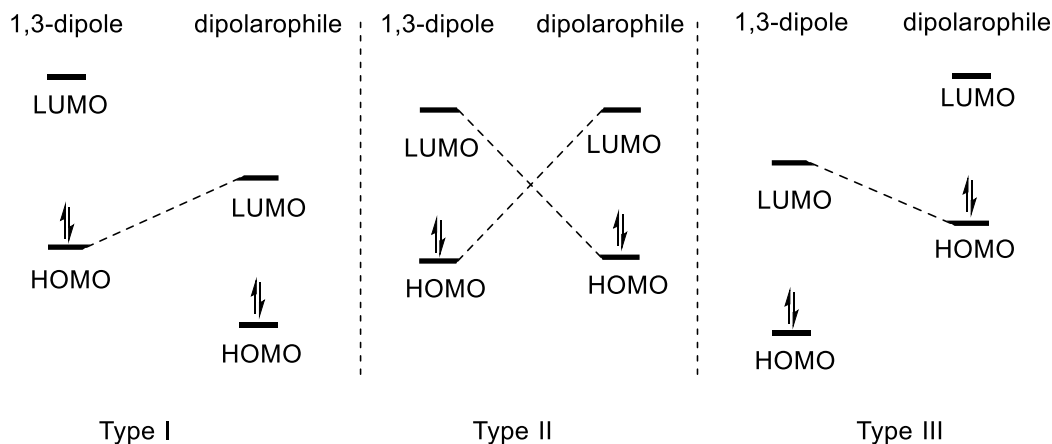
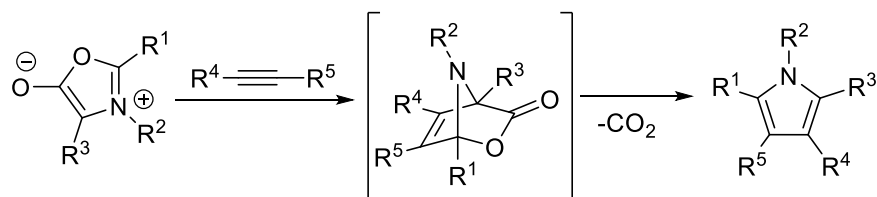


Figure 1.4 Three Sustmann Types for 1,3-dipolar cycloaddition reactions

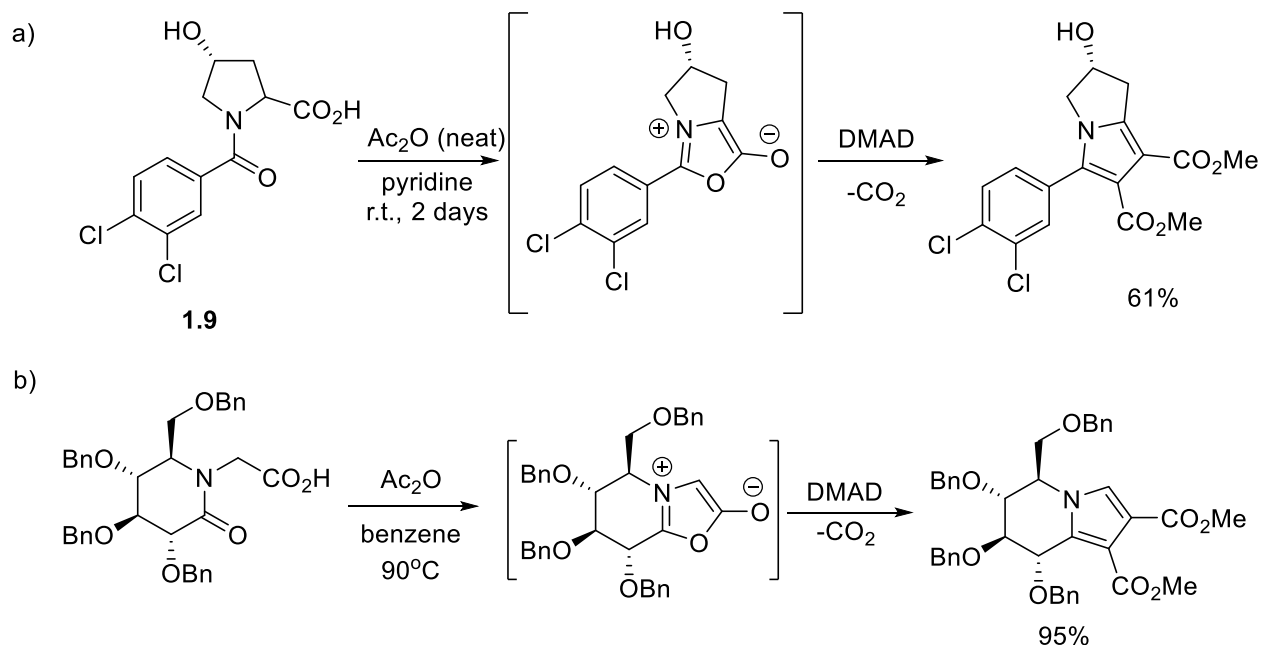
In the case of münchnones, alkynes are often employed in cycloaddition. Their reaction initially forms a bicyclic intermediate, which undergoes retro-cycloaddition to eliminate CO_2 and aromatize to generate pyrroles (Scheme 1.13). This provides a strong overall driving force for the reaction and forms a robust product.



Scheme 1.13 General cycloaddition reactivity of münchnones with alkynes

The versatility and convergent nature of münchnone/alkyne cycloaddition has been applied in many areas. These include a number of studies in drug discovery. As representative examples, Anderson and coworkers³⁵ explored this reactivity to access potential antileukemic agents (Scheme 1.14a). In this case, **1.9**, which can be derived from 4-hydroxyproline, is used in the in situ formation of münchnone, which undergoes rapid cycloaddition with DMAD to afford

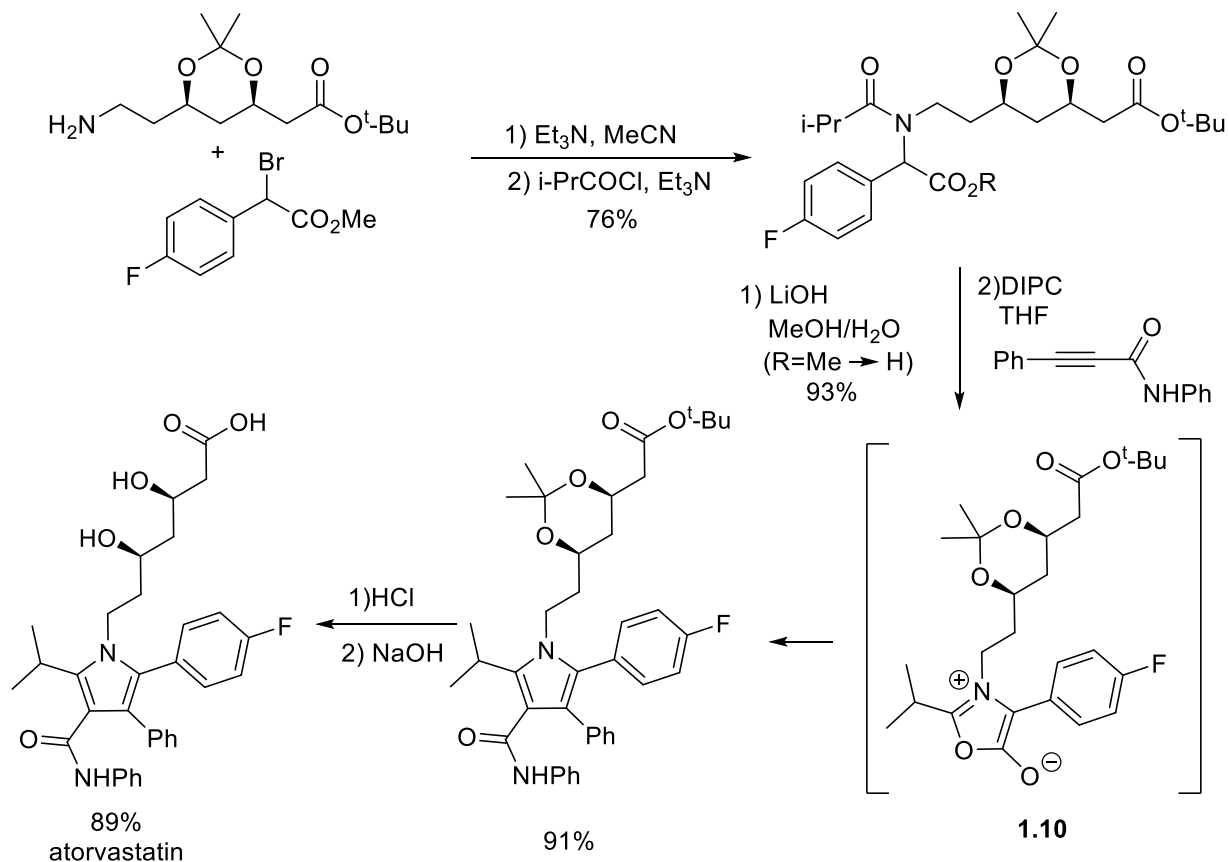
bicyclic products. In situ trapping of münchnones has also been used to generate pyrrole containing novel inhibitors of β -D-glucosidases from carbohydrate derived substrates. (Scheme 1.14b).³⁶



Scheme 1.14 Synthesis of pyrrole containing biologically active molecules via münchnones

Perhaps the most famous application of münchnones is in the early synthesis of Lipitor, a drug for the prevention of cardiovascular disease.³⁷ Roth et al. at Parke-Davis first prepared their precursor to atorvastatin (Lipitor) via the regioselective cycloaddition of an electron deficient alkyne with a münchnone.³⁸ Gribble later demonstrated that this reaction could be performed on the münchnone incorporating the protected chiral side chain (Scheme 1.15).³⁹ Of note, the cycloaddition of **1.10** is highly regioselective in this case, where the electron deficient substituent is directed away from C(4). The latter is consistent with the expected build-up of negative charge on this carbon. However, subsequent studies have shown that münchnone cycloadditions with

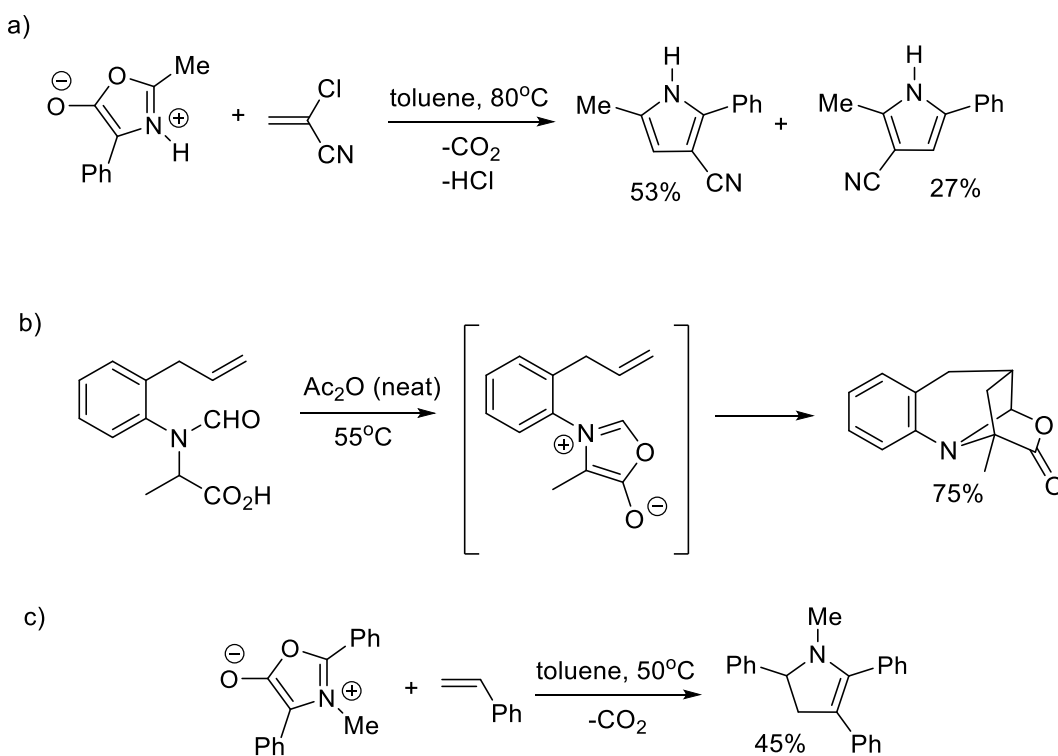
unsymmetrical alkynes, even those with a strong electronic bias, are not highly regioselective (*vide infra*).⁴⁰⁻⁴²



Scheme 1.15 Synthesis of atorvastatin via cycloaddition of münchnones

1,3-Dipolar cycloaddition reactions of münchnones with alkenes can be summarized under two different categories. Alkenes with a good leaving group, such as chloride, nitro or nitrile substituents, can be used as alkyne equivalents. In these, cycloaddition leads again to the formation of a bicyclic product. From here, CO_2 and HX ($\text{X}=\text{leaving group}$) elimination leads again to aromatization and the formation of pyrroles (Scheme 1.16a).⁴³ Alternatively, cycloaddition reactions of alkenes without a leaving group lead to the generation of more stable bicyclic products,

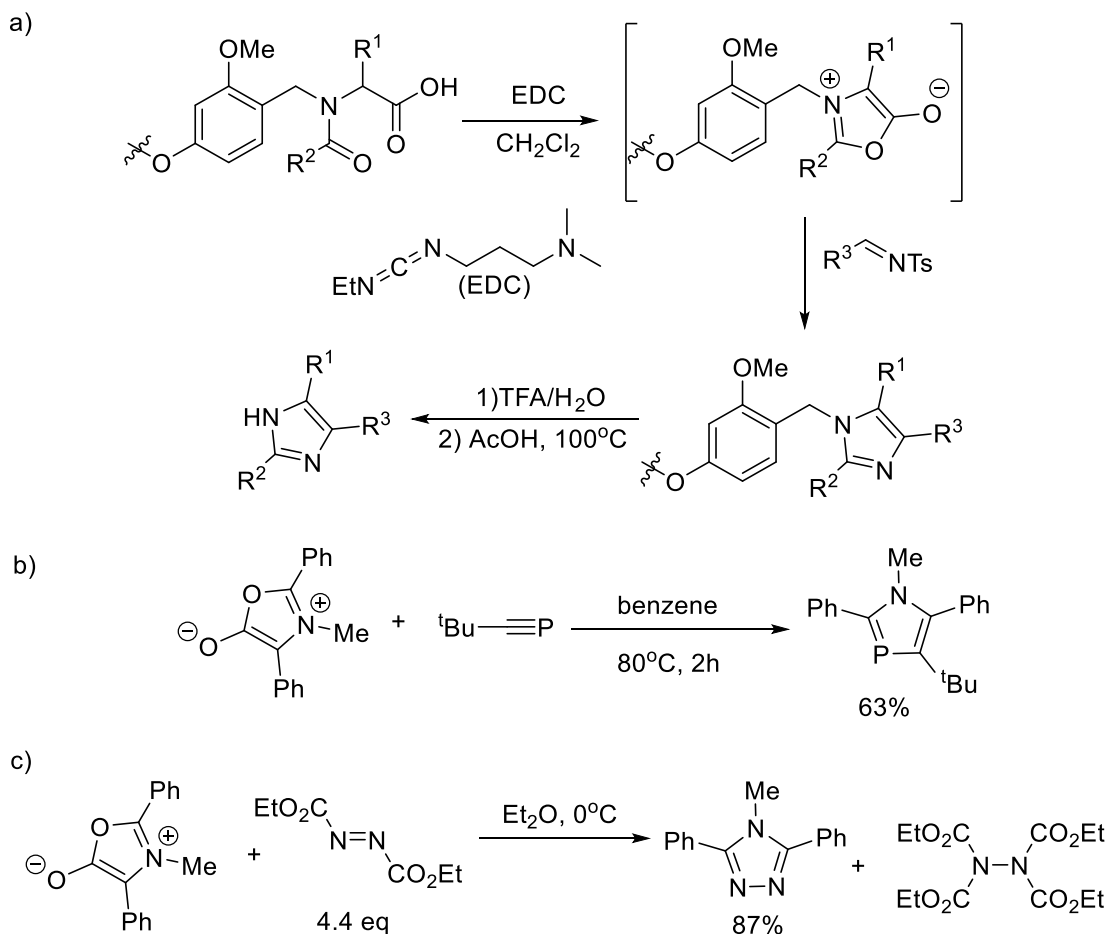
as elimination of CO₂ would form a new 1,3-dipole that cannot readily aromatize. This method is often applied to intramolecular cycloadditions, where cage-like complex structures can be obtained in one step (Scheme 1.16b).⁴⁴⁻⁴⁵ As shown in Scheme 1.16c, these alkenes can also lead to the build-up of other products, such as the partially reduced pyrrolines, upon proton migration.⁴⁶



Scheme 1.16 Cycloaddition reactions between münchnones and a) alkenes with a leaving group and b) alkenes without a leaving group c) alkenes followed by proton migration

In addition to alkynes or alkenes, heteroatom-containing dipolarophiles have also been used in Münchnone cycloaddition. Examples of these are given in Scheme 1.17.⁴⁷⁻⁵¹ These reactions are performed more rarely, as they often are not as easily generalized as alkyne cycloaddition. Nevertheless, there have been several reports of the use of electron deficient *N*-

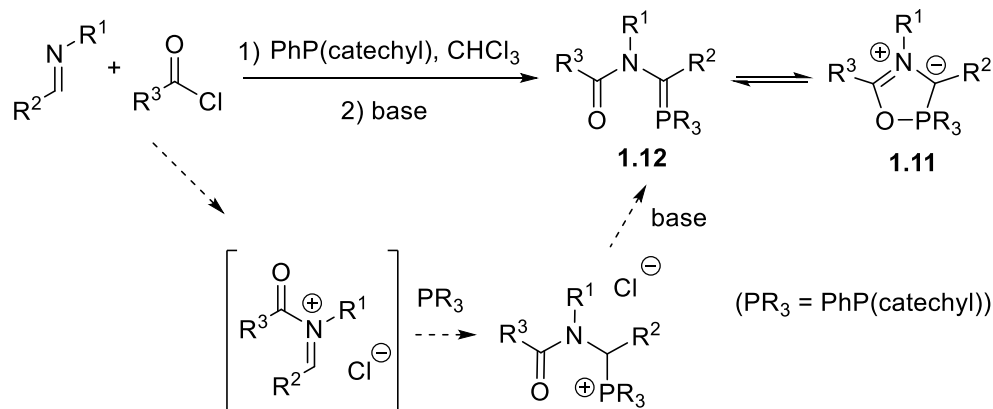
sulfonyl imine cycloaddition to münchnones (Scheme 1.17a). These substrates can also aromatize upon sulfinic acid loss to in this case offer a streamlined synthesis of imidazoles.



Scheme 1.17 Cycloaddition reactions between münchnones and a) imines with a leaving group and b) phosphalkynes c) diazo compounds

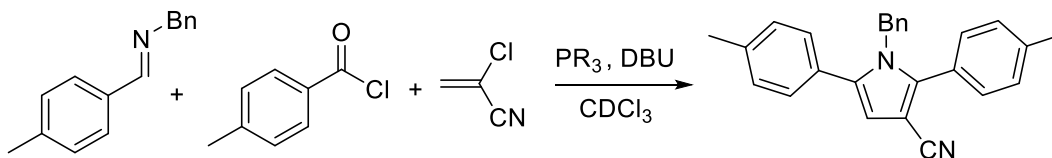
1.2.3.2. Phospha-Münchnones

Our research group has developed a new variant of münchnones in the form of the phosphorus-containing heterocycle **1.11**, dubbed phospho-münchnones. First reported in 2007,⁵² these unusual dipolar compounds can be easily generated in the one pot reaction of imines, acyl chlorides and phosphonites (Scheme 1.18).



Scheme 1.18 Formation of phospho-münchnone from imine, acyl chloride and phosphonite

1.11 exists in equilibrium with its acyclic Wittig tautomer **1.12**, and this equilibrium is strongly influenced by the phosphorus reagent used in the reaction. In principle, chelation of the amide oxygen to phosphorus is more favored when PR₃ unit is electron poor. However, this must be balanced with the ability of PR₃ to undergo nucleophilic attack in the first step to form the phosphonium salt. Experimental results support this duality: when electron rich triphenylphosphine is used, the phosphonium salt is readily generated, but the deprotonation does not lead to cycloaddition and instead generates a Wittig-type product (Table 1.2). In contrast, triphenylphosphite reacts sluggishly with the iminium salt, but does participate in cycloaddition to form pyrrole in moderate yield. The phosphonite PhP(catechyl) provides a balance between these two extremes, and forms pyrrole product in near quantitative yield and in minutes at ambient temperature.



PR ₃	temp(°C)	time(h)	yield (%)	³¹ P of 1.11 or 1.12 (ppm)
PPh ₃	80	-	0	10.2
Ph ₂ P(OPh)	80	-	0	-
PhP(OPh) ₂	65	48	80	-
PhP(O-p-CNPh) ₂	50	11	81	-
P(OPh) ₃	23	15	53	30.2, -44.0 (1.2;1)
PhP(catechyl)	23	0.5	95	-16.9

Table 1.2 Phospha-münchnone mediated pyrrole synthesis from imines, acyl chlorides and alkenes

The ³¹P NMR chemical shifts of the intermediates involved in this reaction (**1.11** or **1.12**) correlate with the observed cycloaddition reactivities. Thus, PPh₃ generates an intermediate with ³¹P NMR shifts in the typical region for Wittig reagents **1.12** (typically between δ 40 to -9 ppm), whereas the reactive intermediate form with PhP(catechyl) has an upfield ³¹P NMR shift (-16.9 ppm), suggestive of the formation of a 5-coordinate phosphorus (i.e. **1.11**).⁵³ Triphenylphosphite shows two signals, implying it exists as both **1.11** and **1.12** in solution. This analysis is confirmed with X-ray crystallography, which shows the intermediate generated with PhP(catechyl) is indeed a 1,3-dipole (Figure 1.5).⁵⁴ This has a strong P-O interaction in this structure (1.79 Å), and all other bond lengths and angles in the ring are similar to münchnones. The structure points to an additional, important role of the catechyl unit in the formation of this 1,3-dipole, where its bond angle on phosphorus favors a five-coordinated, pseudotrigonal bipyramidal geometry in which catechyl can adopt an equatorial/axial geometry with a bond angle of 91°. This angle strain presumably destabilizes the tetrahedral phosphorus in **1.11**, and favors cyclization.

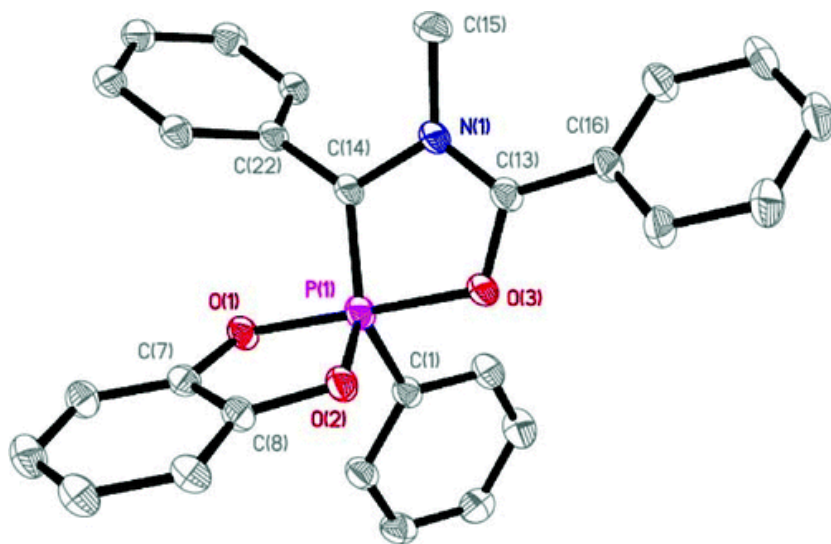
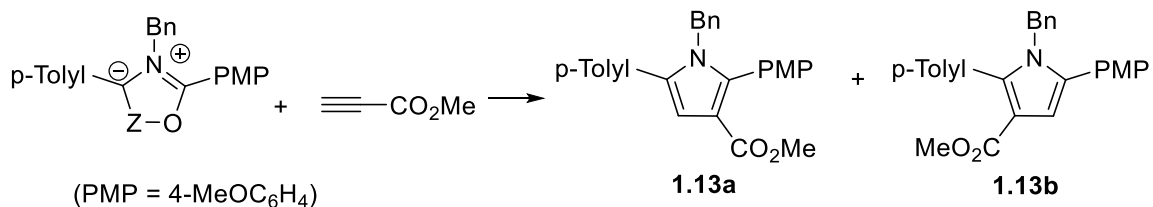


Figure 1.5 X-ray crystal structure of a phosphamünchnone

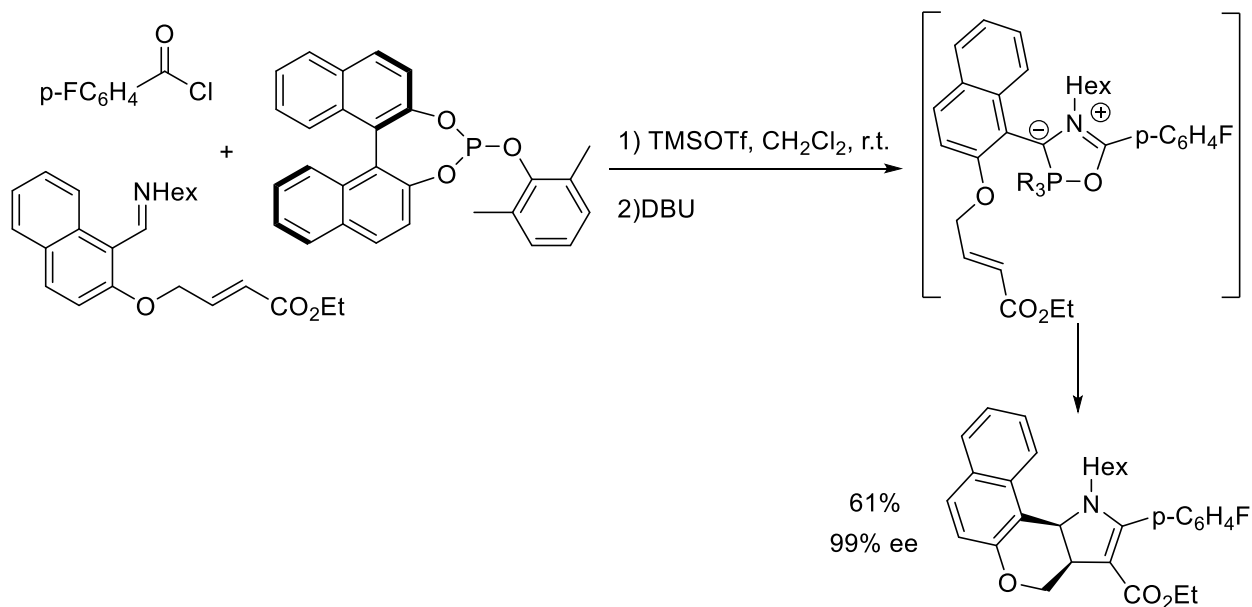
In addition to representing a new version of münchnones, the incorporation of the phosphorus into the backbone of **1.11** provides an avenue to modulate cycloaddition selectivity. A comparative study of cycloaddition regioselectivity for different mesoionic heterocycles was performed by our research group (Table 1.3).⁴² Münchnones display poor regiocontrol in cycloaddition with terminal alkynes such as methyl propiolate. Similar results were noted with the münchnone-imines. In contrast, phosphamünchnones display high regioselectivity in this cycloaddition, where it is believed the strongly polarized P-C bond, together with the large PR_3 unit, which act in concert to direct the ester unit away from phosphorus and form **1.13a** in high yield and regioselectivity.



Z	yield (%)	(1.13a):(1.13b)
C=O	65	73:27
C=N(cyclohexyl)	85	88:12
PPh(Catechyl)	91	95:5

Table 1.3 Cycloaddition regioselectivity of different mesoionic heterocycles

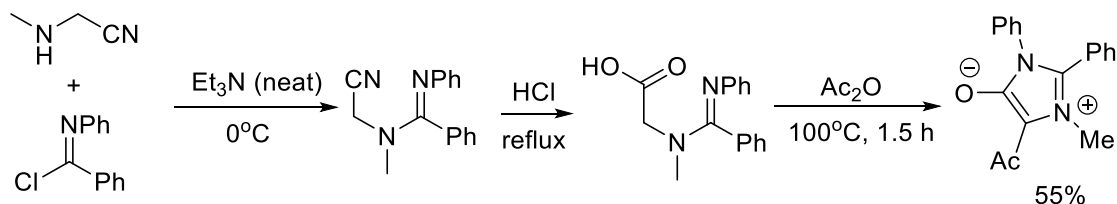
The phosphorus unit can also be exploited to control enantioselectivity. This was demonstrated with the use of a chiral binol-derived phosphite,⁵⁵ which allows the formation of polycyclic pyrrolines in up to 99% ee (Scheme 1.19).



Scheme 1.19 Enantioselective cycloaddition via chiral phosphites

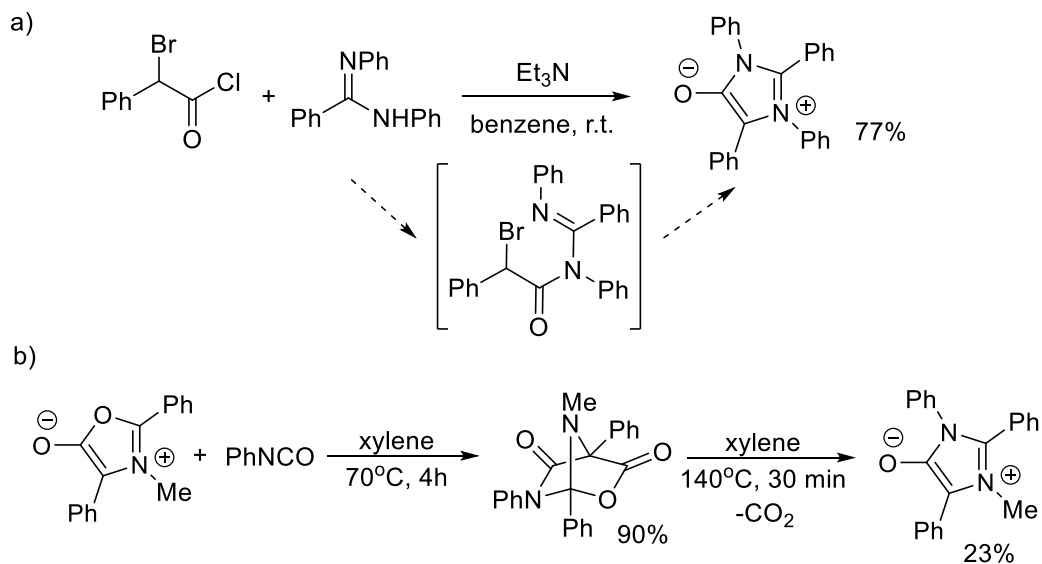
1.2.3.3. Mesoionic Imidazoles (1,3-Diazolium-4-olates)

Another mesoionic core that is relevant to the research in this thesis is mesoionic imidazoles. They have attracted less attention compared to münchnones. One possible reason is their more complicated synthesis. An early synthesis of mesoionic imidazoles was reported by Lawson,¹⁴ and involves the reaction of imidoyl chlorides with methylaminoacetonitrile to generate *N*-imidoyl amino acids. The latter can be converted to the mesoionic core upon first acid catalyzed hydrolysis followed by cyclodehydration (Scheme 1.20). The mesoionic imidazole product is acylated by the anhydride in this process.



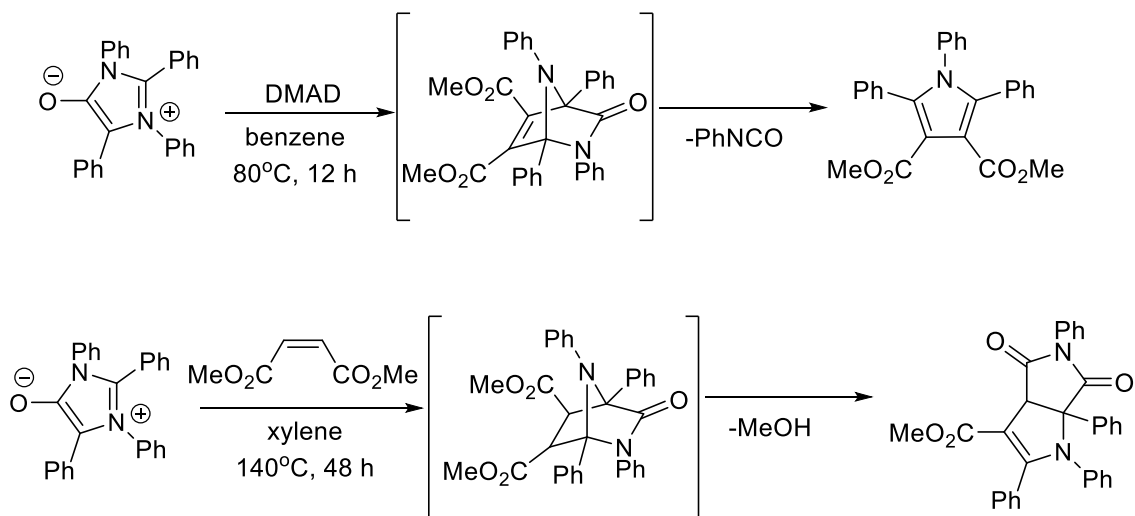
Scheme 1.20 Synthesis of mesoionic imidazoles from imidoyl chloride

A more recent report by Potts showed that mesoionic imidazoles can be synthesized in one step by the reaction of *N,N'*-disubstituted amidines and α -bromo acyl chlorides in the presence of a base (Scheme 1.21a).²⁵ In this case, initial *N*-acylation of the amidine is believed to be followed by cyclization and loss of HBr . While this approach is effective, the synthesis requires the initial assembly of the substituted amidine reagent. Alternatively, this mesoionic core can be obtained from the cycloaddition reaction between isocyanates and münchnones.⁵⁶ In this reaction, heating an isocyanate with a münchnone results in [3+2] cycloaddition to initially form a stable bicyclic intermediate. This cycloadduct was then heated at higher temperatures to release carbon dioxide and generate the mesoionic imidazolium core, albeit with low yields (Scheme 1.21b).



Scheme 1.21 Synthesis of mesoionic imidazole from amidines and α -bromo acyl chlorides (a) and cycloaddition of münchnones with isocyanates (b)

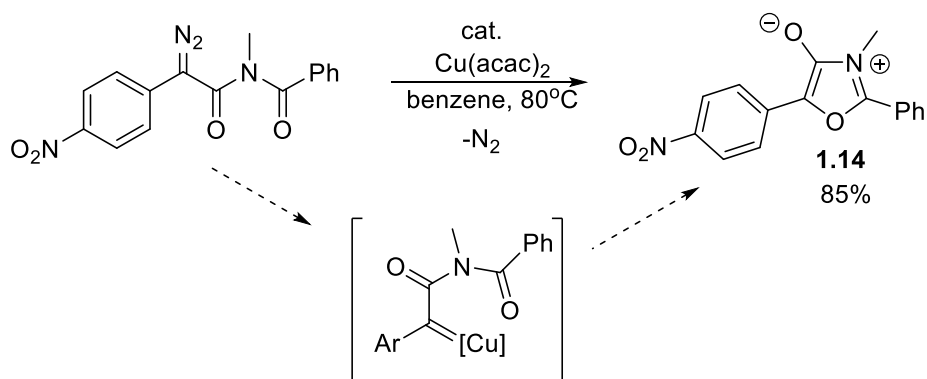
Cycloaddition reactions of 1,3-diazolium 4-olates has not seen the same attention as the münchnones, although there are few reports.⁵⁷⁻⁵⁸ These demonstrate these dipoles react with electron poor alkynes in a similar fashion to münchnones to form pyrroles after, in this case, isocyanate loss (Scheme 1.22). In contrast, electron deficient alkenes such as dimethyl maleate react to form a bicyclic intermediate which undergoes a rearrangement to form a fused-ring pyrroline.⁵⁷



Scheme 1.22 Cycloaddition reactivity of mesoionic imidazoles with alkynes and alkenes (no yields were reported)

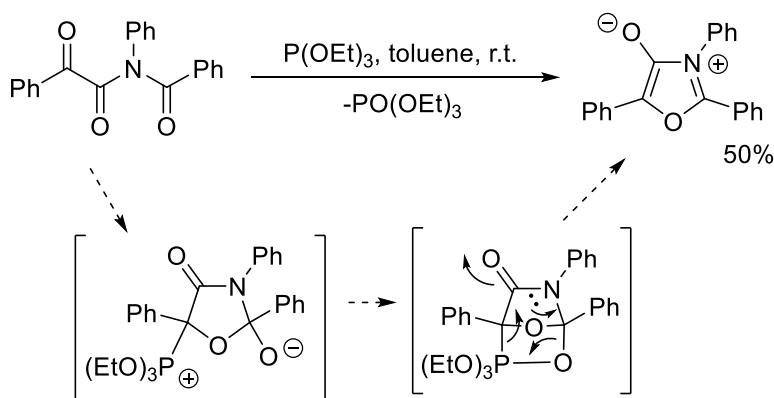
1.2.3.4. Isomünchnones

Another variant of münchnones are isomünchnones. These 1,3-dipoles are often prepared and trapped *in situ* with a dipolarophile, although stable versions with electron withdrawing groups on C5 have been isolated. Isomünchnones were first generated by the copper catalyzed cyclization of α -diazoimides (Scheme 1.23). This reaction is believed to involve the formation of a Cu-carbenoid, which undergoes cyclization with the amide oxygen to form **1.14**.⁵⁹



Scheme 1.23 Synthesis of isomünchnones from α -diazoimides

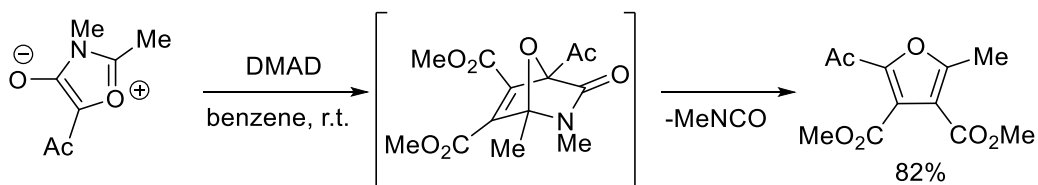
Isomünchnones can also be generated via deoxygenation of α -ketoimides (Scheme 1.24). Haddadin and coworkers used triethyl phosphite to abstract an oxygen from these starting materials, which yields isomünchnones upon cyclization.⁶⁰



Scheme 1.24 Synthesis of isomünchnones from α -ketoimides

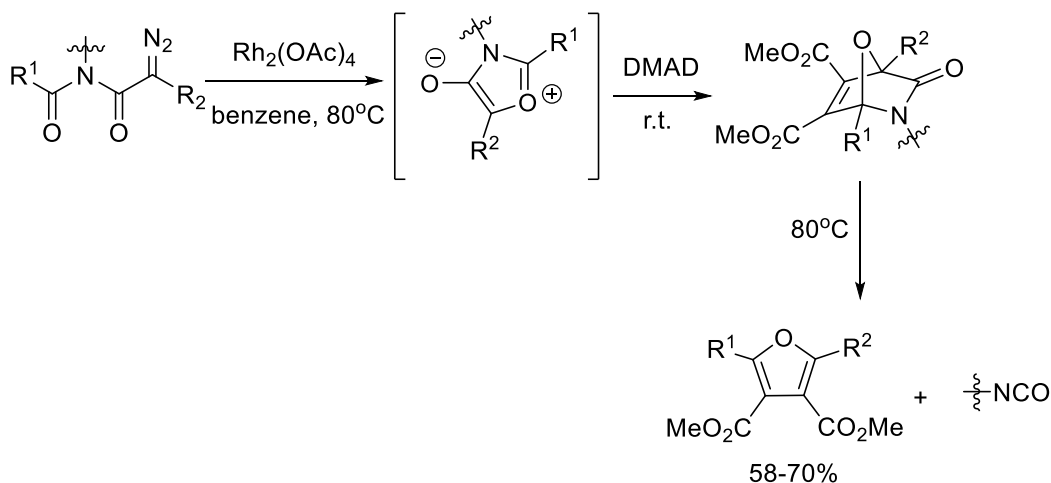
Isomünchnones are utilized as masked carbonyl ylides in cycloaddition reactions.³⁴ This reactivity has been explored with a variety of dipolarophiles, including alkenes and alkynes. Cycloaddition proceeds via a mechanism similar to that of münchnones, however, the bicyclic intermediates formed with isomünchnones are more stable and can be isolated in most cases

(Scheme 1.25).⁶¹ The synthesis of the corresponding furan from these intermediates often requires elevated temperatures. This feature of isomünchnones was exploited by Padwa⁶²⁻⁶³ and Harwood⁶⁴ for preparation of numerous polycyclic structures.



Scheme 1.25 General cycloaddition reactivity of isomünchnones

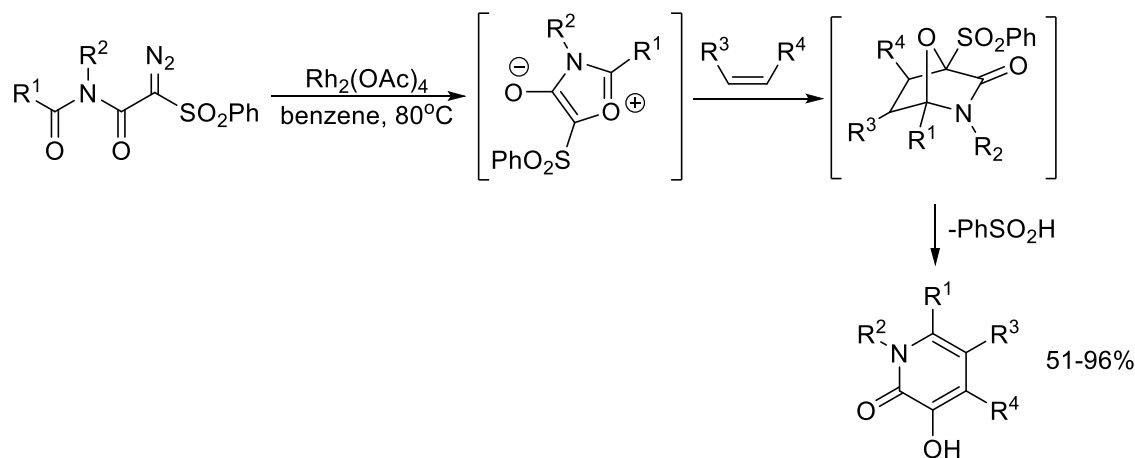
An interesting synthesis of furans via isomünchnones was demonstrated by Gallop et al.⁶⁵ In this study, polymer-supported isomünchnones were synthesized using an amine resin. Cycloaddition with alkynes at room temperature resulted in formation of the corresponding bicyclic product, which releases the furan upon heating. Since the isocyanate fragment is not incorporated into the furan product, it stays on the resin (Scheme 1.26).



Scheme 1.26 Synthesis of furans from polymer-supported isomünchnones

Isomünchnones can also be applied to the synthesis of 6-membered ring products, as demonstrated by Padwa.⁶³ In this chemistry, the bicyclic cycloadduct of sulfonyl-containing

isomünchnones and alkenes undergoes a rearrangement via release of sulfinic acid (Scheme 1.27). This approach offers a useful method to access polycyclic 2-pyridones; and it has been applied to total synthesis of biologically active molecules.⁶⁶⁻⁶⁷

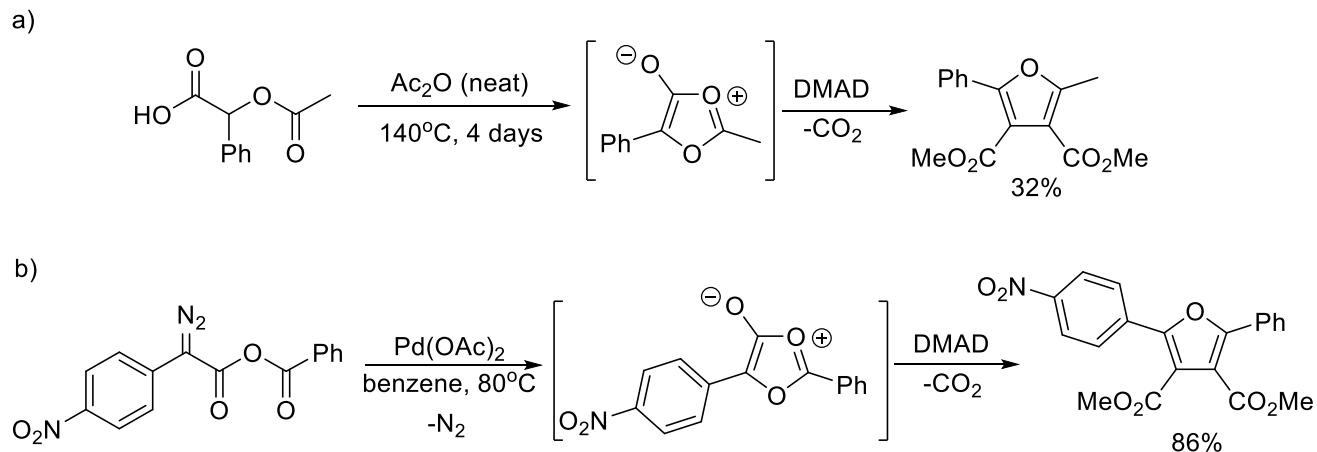


Scheme 1.27 Synthesis of 2-pyridones from isomünchnones and alkenes

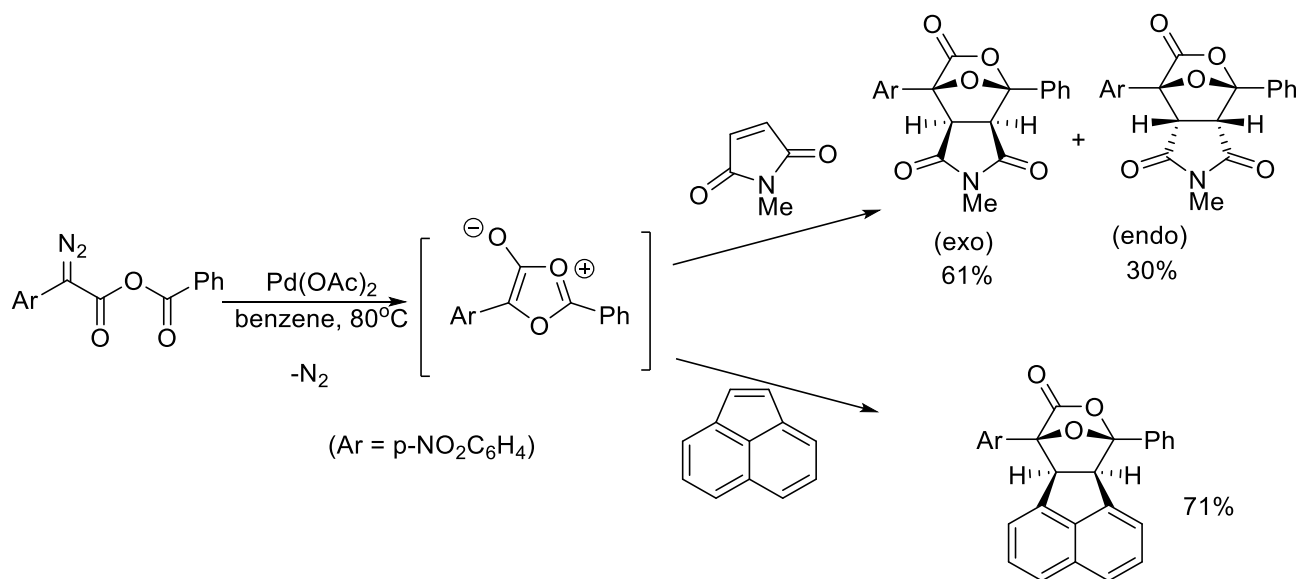
1.2.3.5. Oxamünchnones

In contrast to the mesoionic heterocycles mentioned above, the fully oxygen version of münchnones, oxamünchnones, have not been isolated. Their low stability is presumably related to their lower aromatic stabilization (Section 1.2.2), together with the weaker nucleophilicity of the ester unit, which may favor the formation of their reactive ketene tautomer. The in situ formation of these elusive dipoles was first reported by Berk,⁶⁸ where cyclodehydration of *O*-acetyl mandelic acid in the presence of dimethylacetylene dicarboxylate (DMAD) resulted in formation of the corresponding furan (Scheme 1.28a). Hamaguchi later reported that oxamünchnones can be generated in a similar fashion to isomünchnones from diazo compounds.⁶⁹ In this case, the palladium catalyzed cyclization of α -diazo anhydrides in the presence of DMAD resulted in good yields of the corresponding substituted furan (Scheme 1.28b). In both methods, no stable product

was isolated in the absence of a dipolarophile. The latter method can also be applied to alkene cycloaddition to generate bicyclic products (Scheme 1.29).⁶⁹



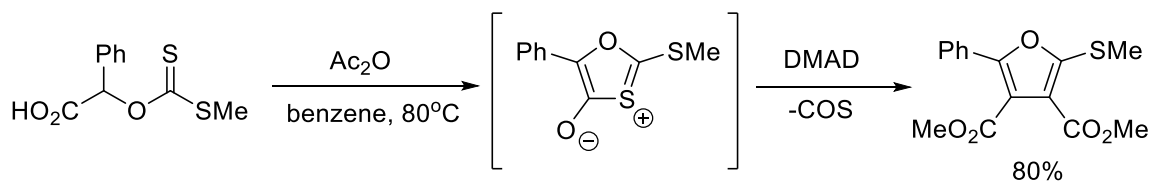
Scheme 1.28 Synthesis and trapping of possible oxamünchnone intermediate by cyclodehydration of O-acetyl mandelic acid (a) and cyclization of α -diazo anhydride (b)



Scheme 1.29 In situ trapping of oxamünchnones with alkenes

The sulfur-containing variants of oxamünchnones are also known (e.g. 1,3-oxathiolium-4-olates). However, studies on synthesis and cycloaddition reactivity of such 1,3-

dipoles are very limited. In a report by Gotthardt and coworkers, this mesoionic heterocycle was trapped *in situ* with an alkyne to generate the corresponding furan product (Scheme 1.30).⁷⁰



Scheme 1.30 Synthesis and in situ trapping of 1,3-oxathiolium-4-olate

1.3. Dynamic Covalent Chemistry and Amides

Synthetic organic chemistry often employs irreversible, kinetically controlled transformations to generate a single, stable product. This ensures that the desired product does not revert back to the starting materials, and instead forms bonds that are by themselves robust. The latter is important when the structural integrity of products is needed for its application (e.g. pharmaceuticals, polymers, etc.). While this approach has proven extremely powerful, it also has intrinsic limitations. Perhaps most notably, these reactions can often only be used to generate one, or sometimes two, bonds at a time, and even in these scenarios controlling product selectivity by kinetic influences can be challenging. This can make the synthesis of large, complex products a challenging and time-consuming process, as these require multiple steps to assemble.

In contrast, supramolecular chemistry often relies on non-covalent interactions such as hydrogen bonding, metal coordination, van der Waals forces or π -stacking to achieve the self-assembly of complex structures. Since the forces involved in these interactions are weak, products are often generated in a reversible fashion at ambient conditions. In this scenario, selectivity is ultimately controlled by the thermodynamic features of the product(s). Unlike traditional kinetic-controlled reactions, multiple bonding interactions can be formed simultaneously to access complex architectures with often high product selectivity. Unfortunately, the required use of weak interactions also leads to products that are often not kinetically robust, and can disassemble when conditions are changed. In order to address this issue, the concept of dynamic covalent chemistry (DCvC) has been developed. As the name suggests, DCvC exploits reactions that generate more robust covalent bonds, but does so under conditions where they are reversibly generated. These can therefore allow the application of supramolecular chemistry principles to the generation of covalent products.

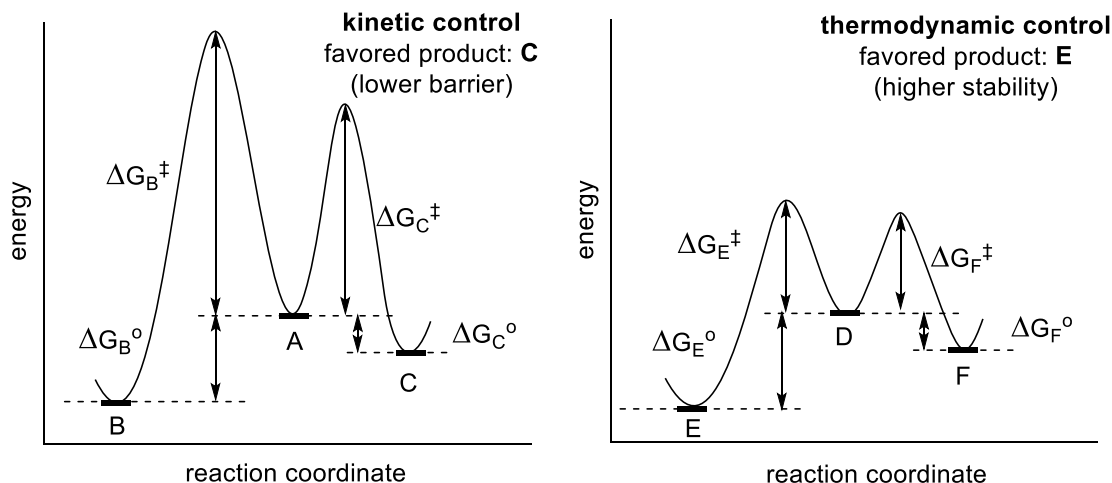
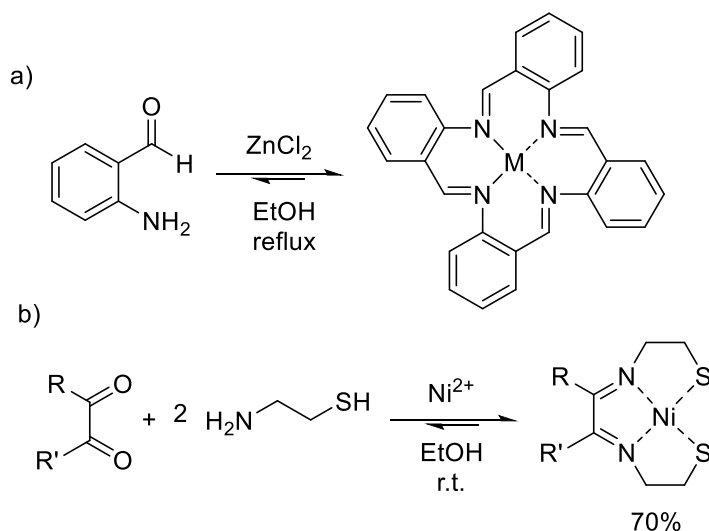


Figure 1.6 Kinetic vs. Thermodynamic Control

1.3.1. Emergence of Dynamic Covalent Chemistry

The concept of dynamic covalent chemistry is a relatively recent addition to the literature. This name was first proposed by Rowan et al. in 2002.⁷¹ However, actual use of the principles of DCvC predates this nomenclature by many decades. One of the earliest recognized examples of dynamic covalent chemistry was reported by Seidel in 1926.⁷² In this study, a cyclic tetramer of 2-aminobenzaldehyde was selectively generated in the presence of Zn^{2+} cations (Scheme 1.31a). However, the full characterization of this product was not reported until 1965 in a study by Busch.⁷³ The concept of templated imine macrocycle synthesis was pioneered by Busch⁷⁴ during 1960s (e.g. Scheme 1.31b). Nevertheless, it has only been in the past ca. 15 years that the true power of this technique is recognized in supramolecular chemistry. These studies have demonstrated how complex covalent architectures can be generated by exploiting certain classes of covalent bond forming reactions that are reversible at near ambient conditions. Examples of its applications include the assembly of covalent molecular cages,⁷⁵ reversible polymerizations,⁷⁶⁻⁷⁷ covalent organic frameworks (COF),⁷⁸⁻⁷⁹ dynamic drug design,⁸⁰⁻⁸¹ and many others.^{71, 82} Most of

these systems rely on the error-checking, adaptive nature and proof-reading properties of dynamic covalent chemistry to generate highly ordered architectures.



Scheme 1.31 Formation of Zn²⁺ templated cyclic tetramers of 2-aminobenzaldehyde (a) and Ni²⁺ complexes of imine containing tetradentate ligands (b)

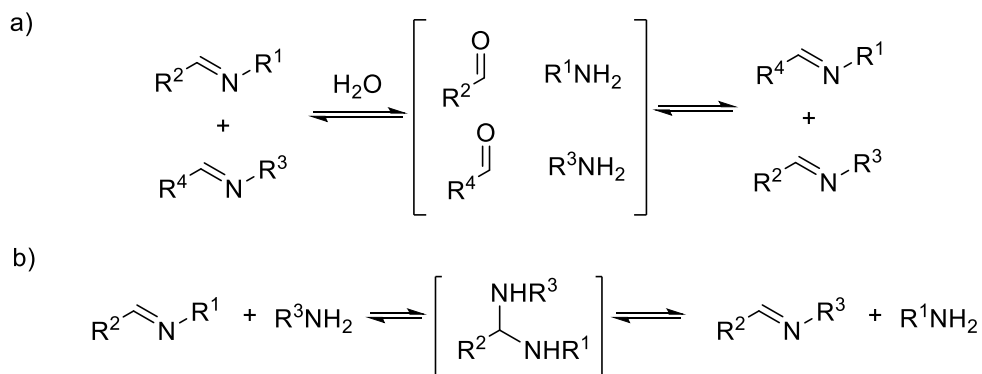
1.3.2. Common Reactions in Dynamic Covalent Chemistry

While all reactions are in principle reversible, the kinetic stability of most covalent organic bonds precludes their use in dynamic reactions under accessible conditions. For a reaction to be useful in DCvC, the timeframe of reversibility should be short. In supramolecular chemistry, bonds with a lifetime in the range of $1 \text{ ms} < \tau < 1 \text{ min}$ can be ideal, since they can undergo rapid exchange, yet are stable enough to be detected by common techniques.⁸³ In practice, most dynamic covalent systems have much longer lifetimes. These reactions typically reach equilibrium within 24 hours at accessible conditions (< ca. 100°C, but ideally ambient temperature). In addition, many systems use catalysts to lower this barrier to allow exchange.

A dynamic covalent reaction should reach equilibrium from both forward and reverse directions. In addition, the exchange of components between different members of the dynamic library should be possible. In order to obtain robust products, these reactions often also require a way to “turn off” the reversibility, such as changing the conditions, removing catalysts, or transforming the labile products to more kinetically stable versions by further chemical modifications. Described below are some of the most common reactions that are utilized in dynamic covalent chemistry.

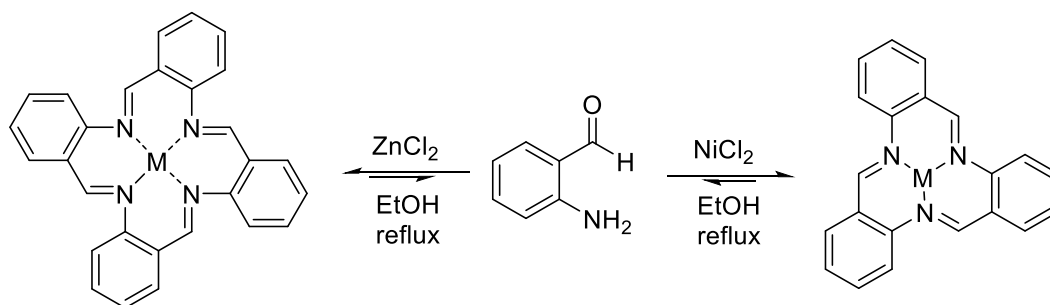
1.3.2.1. Imine Formation and Exchange

The most heavily exploited reaction in dynamic covalent chemistry is the formation of imines from primary amines and aldehydes/ketones. This broad use is driven in part by the availability of the components (amines, aldehydes) as well as the properties of the imine products.⁸⁴ There are several mechanisms by which imines can undergo exchange. In most cases, the presence of water results in the partial hydrolysis of imine to form amines and aldehydes, which can be followed by imine formation with different aldehydes or amines, thus generating a dynamic library of products (Scheme 1.32). Alternatively, imines can undergo exchange or metathesis under anhydrous conditions via the intermediacy of aminals. Either pathway can be accelerated by addition of Lewis or Brønsted acids.⁸⁵



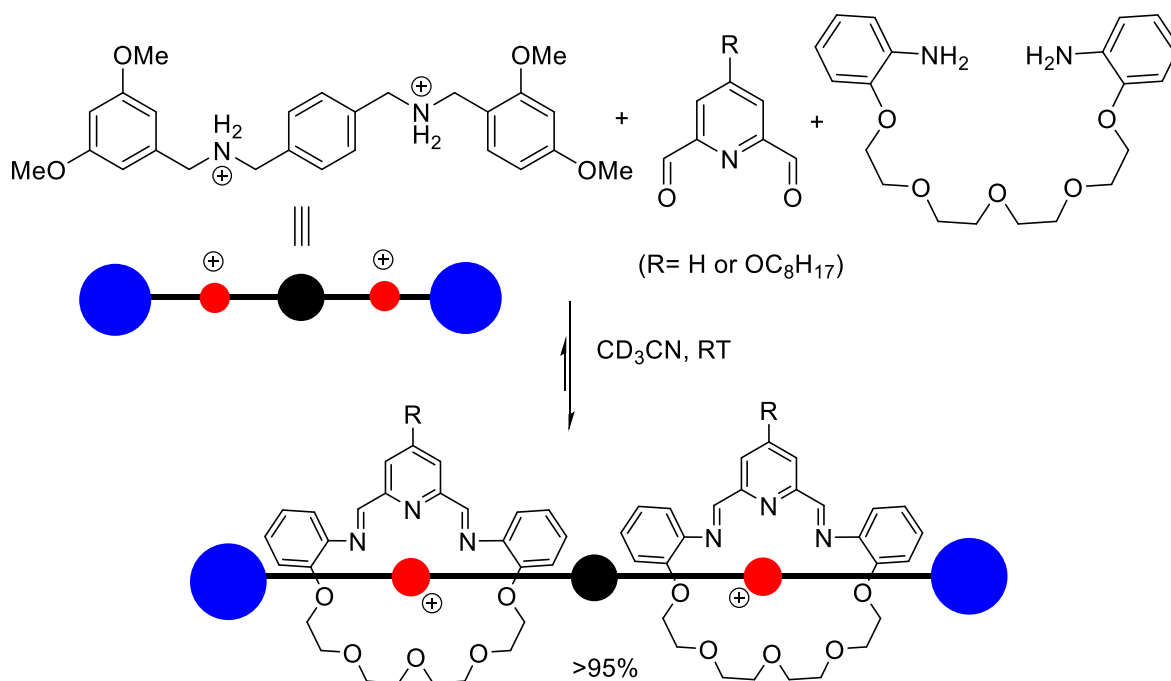
Scheme 1.32 Formation of dynamic imine libraries through a) partial hydrolysis and b) amination

An important feature of imines is their ability to coordinate to Brønsted or Lewis acids via the lone pair on nitrogen. This has been exploited to influence the relative stability of products in a broad range of systems. As a representative example, one of the first applications of dynamic covalent chemistry was in the metal templated synthesis of macrocyclic imines (noted above in Scheme 1.31a). Subsequent investigations on this system revealed that different structures can be obtained by changing the metal cation.⁸⁶ Thus, if ZnCl₂ is replaced with the smaller NiCl₂ in reaction with 2-aminobenzaldehyde, the cyclic trimer is instead generated as the major product (Scheme 1.33).



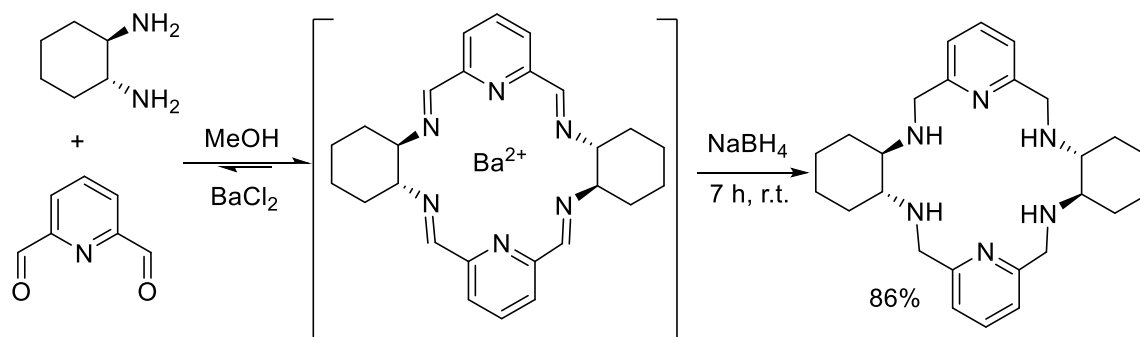
Scheme 1.33 Formation of tetramers or trimers of 2-aminobenzaldehyde

Hydrogen bonding can also be exploited to control imine product formation. As an example, Stoddart has utilized the dynamic formation of imines to construct rotaxanes (Scheme 1.34).⁸⁷ In this system, the reaction of 2,6-pyridinedicarboxaldehyde and tetraethylene glycol bis(2-aminophenyl)ether in the presence of a protonated amine template was found to lead to the selective formation of oligorotaxanes bearing [1+1] imine rings. The selectivity in this system was attributed to hydrogen bonding between the ammonium unit and [1+1] imine macrocycle. The rotaxane is held together with the stopper aromatic units at both ends. Upon reaching the equilibrium, these dynamic macrocyclic imines were reduced to kinetically stable amines using $\text{BH}_3 \cdot \text{THF}$.



Scheme 1.34 Synthesis of dynamic imine rotaxanes through hydrogen bonding

Imine reduction is a common way to “fix” imine containing structures as isolable products. This was also illustrated in an example by Gotor to access amine containing macrocycles (Scheme 1.35).⁸⁸



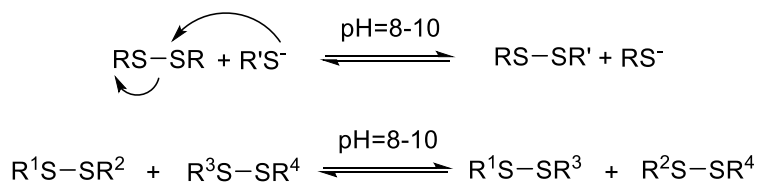
Scheme 1.35 Synthesis and reduction of imine macrocycles

Imines have been exploited in a wide range of other areas of DCvC, with examples ranging from drug discovery to polymers, covalent organic frameworks and molecular cages. This topic has been reviewed.^{84, 89-91}

1.3.2.2. Disulfide Exchange

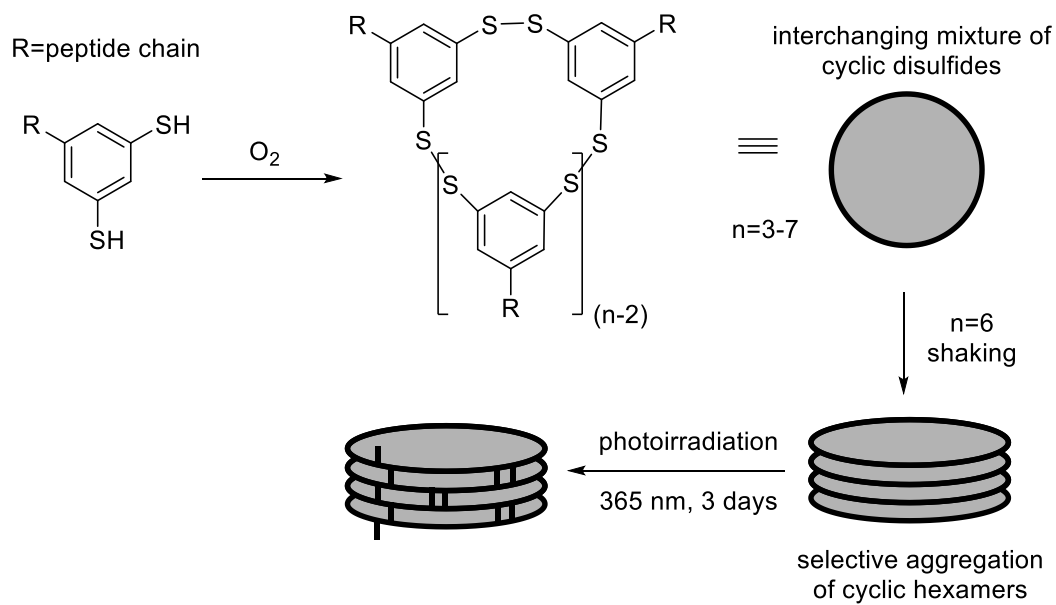
Disulfides are likely the second most prominent functionality encountered in dynamic covalent chemistry.⁹² Disulfide bond formation is highly relevant to biochemical systems, where they are the most common crosslinks in proteins. However, disulfides can also undergo exchange reaction in organic solvents under basic conditions. This exchange of thiol units is usually driven by nucleophilic attack of a thiolate anion to a disulfide bond, which leads to the formation of a new disulfide and thiolate (Scheme 1.36). One of the main advantages of this chemistry is the simple control of reversibility with pH, which influences the concentration of the thiolate anion. Thus, mildly basic conditions (pH=8-10) are ideal for exchange, while the reversibility can be

turned off by acidifying the mixture (pH<8). Other exchange methods are also reported using nucleophiles or metal catalysis.⁹³ Of note, the exchange of disulfides can also be stopped by oxidation of sulfur to a sulfoxide or sulfone.



Scheme 1.36 General representation of disulfide exchange

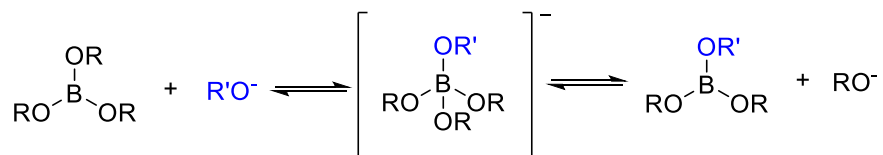
As with the imines, DCvC with disulfides has been applied to a range of areas, including the synthesis of macrocyclic or polymeric materials.⁹³ As one example, the compatibility of disulfide bonds with biological systems allows the design of interesting hybrid peptide products. Thus, Otto has exploited the dynamic formation of disulfide bonds to form peptide-containing macrocycles (Scheme 1.37).⁹⁴ In this system, slow oxidation of a peptide-tethered aromatic dithiol results in formation of a dynamic library of cyclic disulfides (n=3-7). However, only the cyclic hexamer (n=6) is able to aggregate and precipitate due to strong peptide-peptide hydrogen bonding. Since disulfide formation is reversible, precipitation drives the equilibrium towards the hexameric product. Subsequent photoirradiation was used to promote homolytic S-S cleavage and rearrangement to covalently link the stacks together.



Scheme 1.37 Selective formation and capture of peptide containing cyclic disulfide hexamers

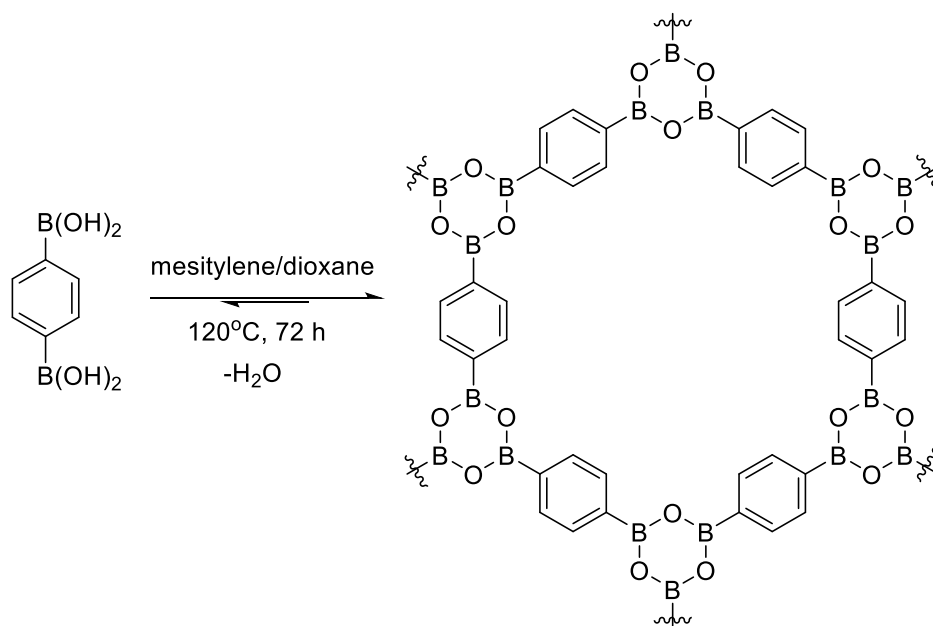
1.3.2.3. Boronic Acid Derivatives

The reversible formation and cleavage of B-O-B bonds has also been an extremely useful tool in dynamic covalent chemistry.⁹⁵ The starting materials for these reactions are often boronic ($\text{RB}(\text{OR})_2$) or boric ($\text{B}(\text{OR})_3$) acid derivatives, which are also broadly available or easily generated. The dynamic nature of the B-O bond in these systems arises from the electrophilic, formally unsaturated boron center, which can interact reversibly with nucleophiles to form a borate. Therefore, this chemistry requires the presence of nucleophiles (e.g. H_2O or ROH) to be dynamic (Scheme 1.38).



Scheme 1.38 General representation of boronic acid ester exchange

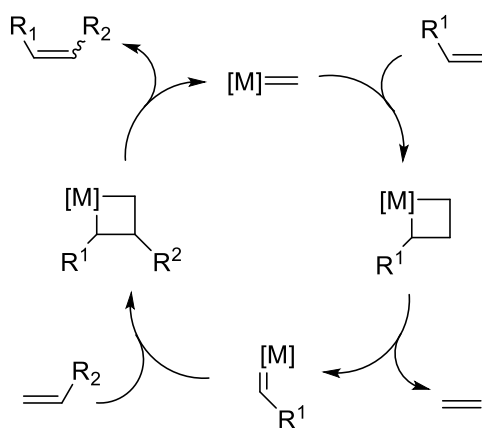
While this reaction has also been exploited in many areas,⁹⁵ the trigonal planar geometry of boron center has proven particularly useful for the preparation of highly ordered 2D or 3D stacked structures. The error-checking features of dynamic chemistry allow convenient formation of such complex materials. As an example, Yaghi has shown that well-ordered boronic ester containing covalent organic frameworks (COF) can be generated by the condensation of a simple diboronic acid (Scheme 1.39).⁹⁶ Selectivity in this case is driven by the near 120° bond angles at boron and oxygen, which favors the formation of a planar 6-membered B-O ring. X-ray diffraction analysis of this COF reveals that the layers are stacked in a staggered fashion, similar to graphite, where B-O interactions between layers drives the close packing. The use of larger aromatic units leads to eclipsed stacking, due to overriding π - π interactions.



Scheme 1.39 Synthesis of a porous COF by dehydration of 1,4-benzenediboronic acid

1.3.2.4. Alkene and Alkyne Metathesis

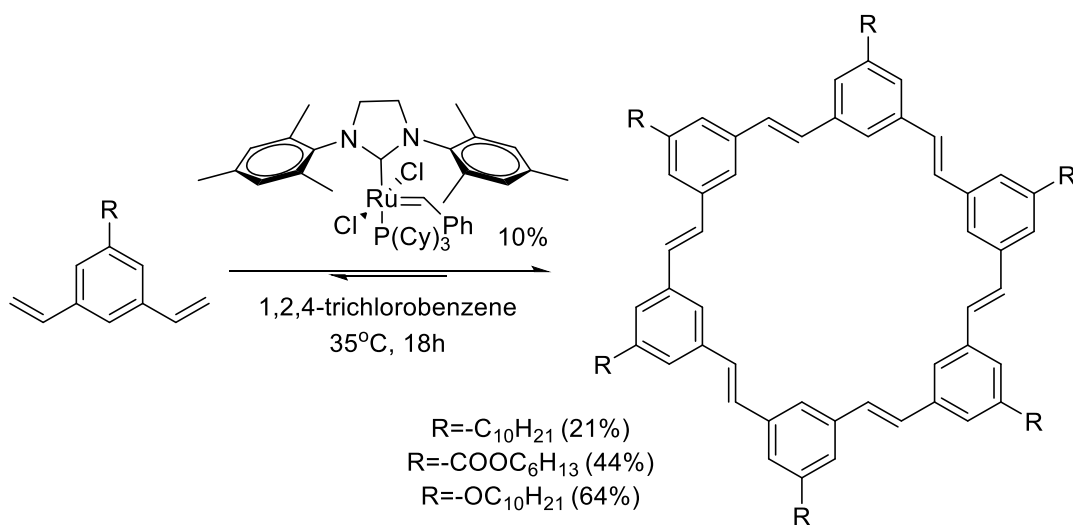
Transition metal catalysis has also been found to be an important tool in creating dynamic reactions. The most common of these is olefin metathesis, and the related alkyne metathesis. Alkene and alkyne bonds are not dynamic under normal conditions. However, in the presence of metal-carbene (or -carbyne) catalysts, alkenes (or alkynes) can undergo a scrambling of substituents (Scheme 1.40). As illustrated with alkenes, this is driven by the ability of certain metal-carbene complexes to undergo a rapid 2+2 cycloaddition and retro-cycloaddition to exchange the carbene unit with the alkene. The catalyst system used in these reactions varies between alkenes and alkynes. Ruthenium-based Grubbs or Grubbs-Hoveyda catalysts are common for alkene metathesis,⁹⁷ while Schrock-type molybdenum or tungsten based catalysts often enable alkyne metathesis.⁹⁸ Of note, alkene and alkyne metathesis reactions often have good functional group tolerance, which allows applications where other orthogonal dynamic covalent reactions can be used in the same system.⁹⁹



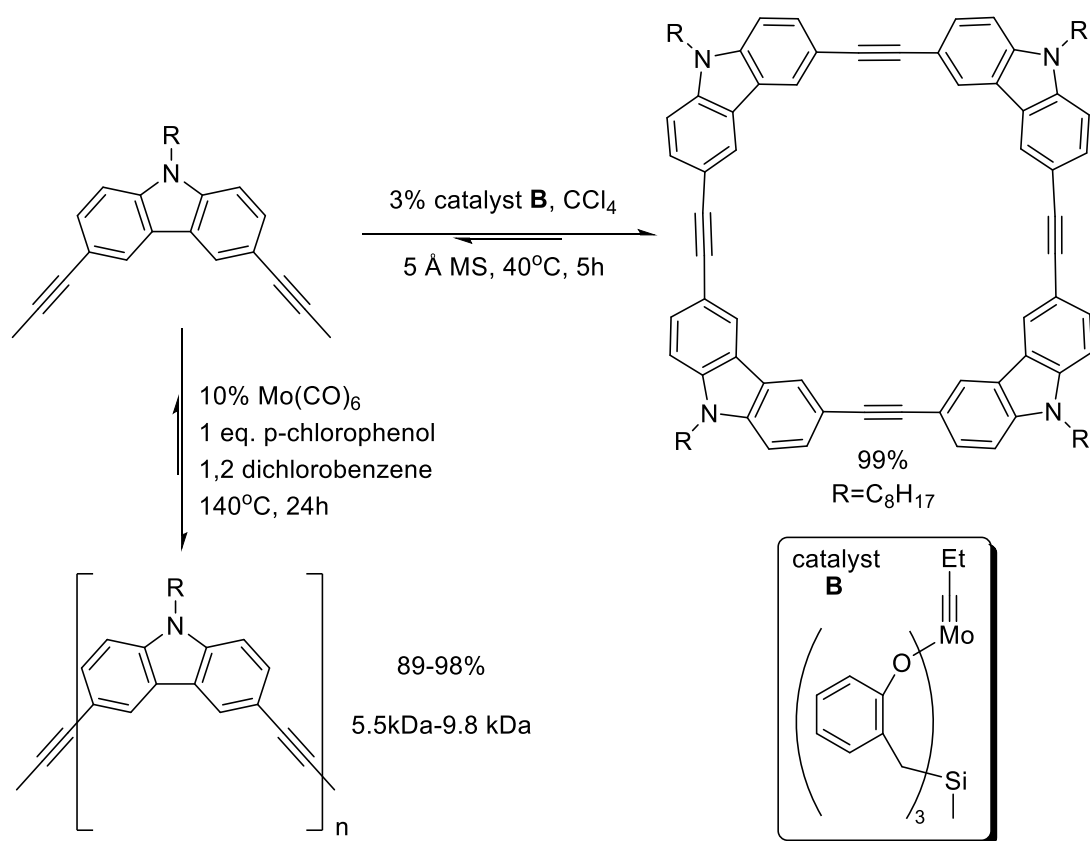
Scheme 1.40 Mechanism of alkene metathesis

Alkene and alkyne metathesis has been used to assemble a range of robust products. As one example, Zhang has demonstrated that alkene metathesis with Grubb's second generation

catalyst can allow the selective build-up of the macrocyclic hexamer of 1,3-divinylarenes (Scheme 1.41).¹⁰⁰ Nevertheless, a common challenge for this chemistry is to find active catalysts that can allow establishment of the equilibrium in short times, and in some cases, thermodynamically less stable products may be obtained due to low activity of the catalyst. The latter was illustrated by Zhang, where polymers or macrocycles can be obtained from the same alkyne-containing carbazole monomer using different catalysts (Scheme 1.42).¹⁰¹



Scheme 1.41 Synthesis arylenevinylene macrocycles (AVMs) through olefin metathesis

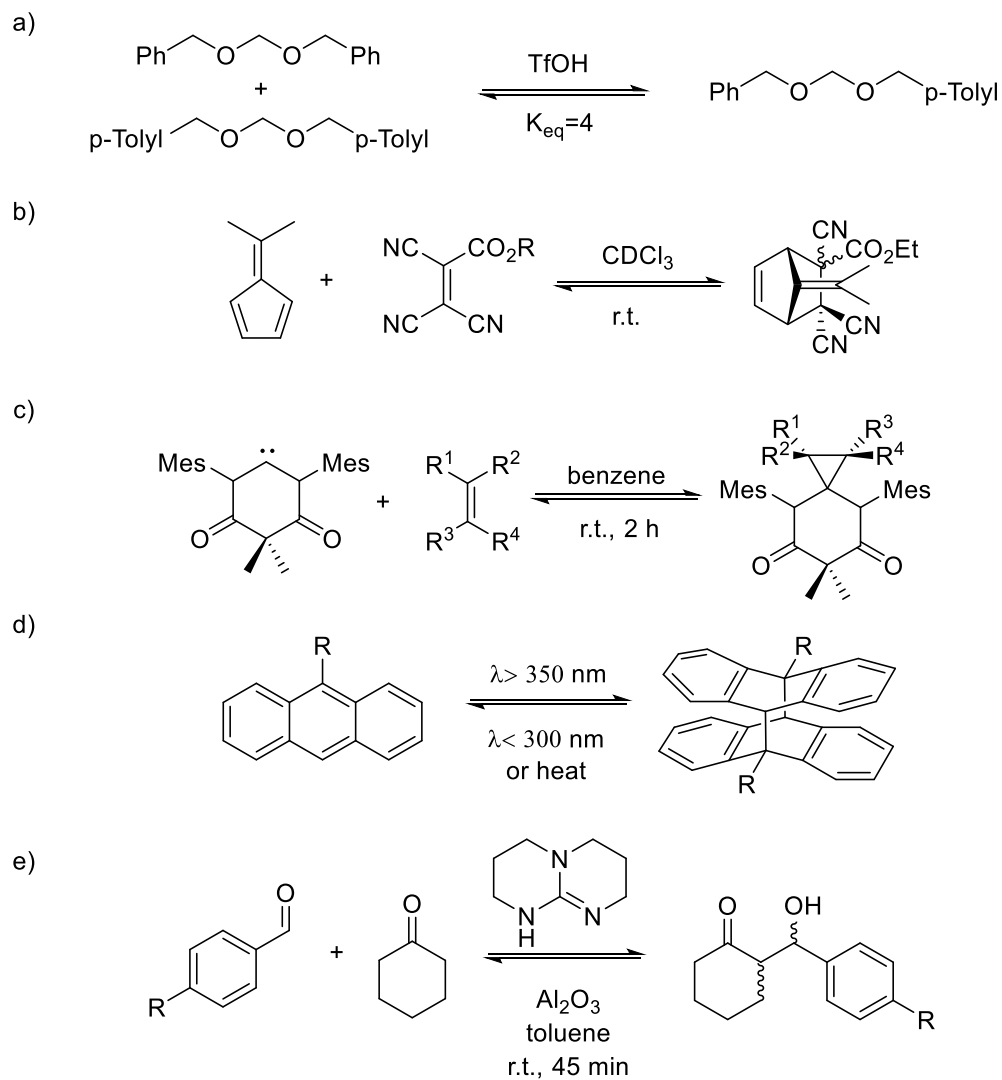


Scheme 1.42 Formation of polymers or macrocycles through alkyne metathesis

1.3.2.5. Examples of Other Dynamic Covalent Reactions

A wide range of other organic reactions have been found to be dynamic. As representative examples, while the C-O covalent bond is typically stable, acetals can undergo dynamic exchange under acidic conditions (Scheme 1.43a).¹⁰² Alternatively, a range of pericyclic reactions has also been found to be dynamic. Indeed, one of the early examples of modern DCvC by Lehn in 2005 involved the use of fulvenes as dienes and electron poor cyanoolefins as dipolarophiles in the reversible Diels-Alder cycloaddition (Scheme 1.43b).¹⁰³ Other examples include [2+1] carbene additions (Scheme 1.43c),¹⁰⁴ or [4+4]-anthracene photodimerizations (Scheme 1.43d).¹⁰⁵ Similarly, the aldol reaction is well known to be reversible, and has been exploited in DCvC

(Scheme 1.43e).^{106,107} In addition to these, various other covalent bond forming reactions have been shown to be reversible and found use in dynamic chemistry.¹⁰⁸⁻¹¹³

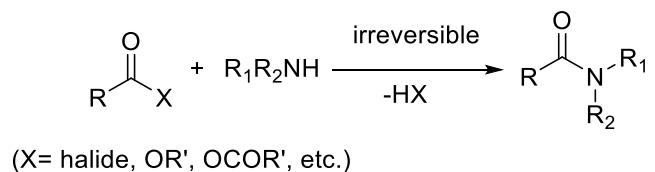


Scheme 1.43 Examples of other DCvC reactions, including a) Acetal scrambling b) Diels-Alder cycloaddition c) [2+1] carbene addition d) [4+4]-anthracene photodimerizations e) aldol reaction

1.3.3. Dynamic Covalent Chemistry of Amides

Although dynamic covalent chemistry has been used in a wide range of applications, the functional groups generated in these reactions (imines, disulfides, boronic acid esters etc.) are often not those that have found extensive use in common synthetic materials. This is a natural result of the moderate bond strengths that are typically required for reversibility. Catalytic approaches have provided solutions for a few functional groups (e.g. alkene or alkyne metathesis), but the generation of many relevant and robust functional groups via DCvC is still a challenge.

The application of amide bond formation in dynamic covalent chemistry represents a particularly interesting target. The amide functionality is ubiquitous in both natural and synthetic materials. For example, amides are present in most of marketed pharmaceuticals and biomolecules.¹¹⁴ Building blocks of life, amino acids, are connected through amide bonds to form proteins. Amides are also extremely important in the manufacture of materials. For example, commonly used polymers such as nylon or Kevlar contain amide connections. Much of the utility of amides is derived from their high thermodynamic stability. The carbonyl-nitrogen bond strength in amides can be up to 90-100 kcal/mol, due in part to resonance stabilization. In addition, amides are easily accessible from available building blocks, amines and carboxylic acid derivatives (Scheme 1.44).

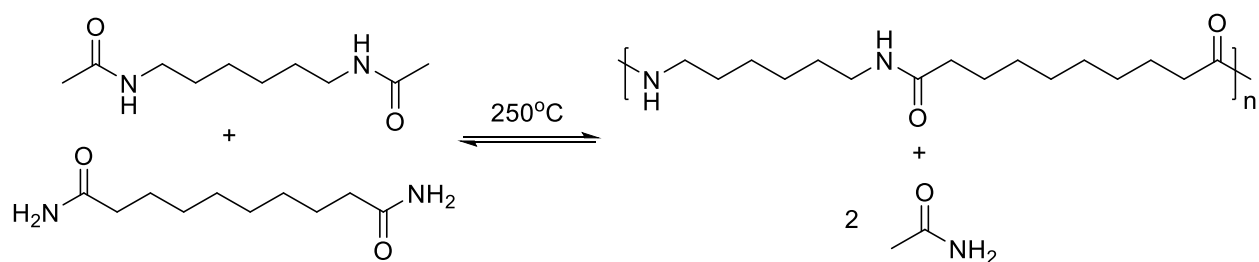


Scheme 1.44 Conventional synthesis of amides from amines and carboxylic acid derivatives

As a result of their high C-N bond strengths, amides are often generated under kinetic control, and are not amenable to DCvC. Nevertheless, there have been efforts to render amide bond formation dynamic. A highlight of these is given below.

1.3.3.1. Thermal Exchange

While the amide bonds are strong, the carbonyl carbon is electrophilic, and it is known that amides can undergo exchange at very high temperatures. In one of the earliest studies on this subject by Houtz (Scheme 1.45), exchange between diamides were shown to take place at 250°C.¹¹⁵ Unfortunately, these are extremely harsh conditions, and would prove incompatible with many relevant functionalities.

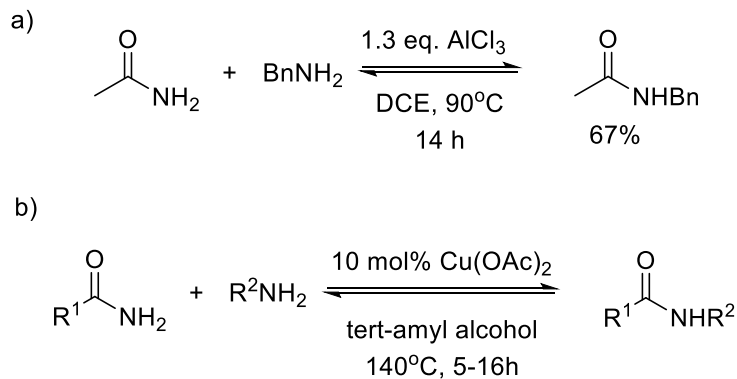


Scheme 1.45 Amide interchange reactions at high temperatures

1.3.3.2. Catalytic Transamidation Reactions

There have been studies directed towards using either stoichiometric reagents or catalysts to lower the barrier to amide exchange with free amines (transamidation). For example, early work by Bertrand utilized super-stoichiometric quantities of aluminum chloride to promote transamidation at 90°C in a period of several hours to a day (Scheme 1.46a).¹¹⁶ Alternatively,

Beller has shown that copper acetate can be an efficient catalyst for transamidation between primary amides and amines, albeit still at high temperatures (Scheme 1.46b).¹¹⁷



Scheme 1.46 a) AlCl_3 promoted b) Copper catalyzed transamidation reactions

A significant contribution to this field came from Gellman and Stahl in 2003 with the use of metal-amide salts as catalysts. Exchange reactions in this study still required temperatures up to 90°C , but resulted in efficient equilibration with only 5% of catalyst.¹¹⁸ Most promising results came from the use of $\text{Al}(\text{NMe}_2)_3$, which can establish similar ratios of products from both forward and reverse directions, indicating presence of a true equilibrium (Table 1.4).

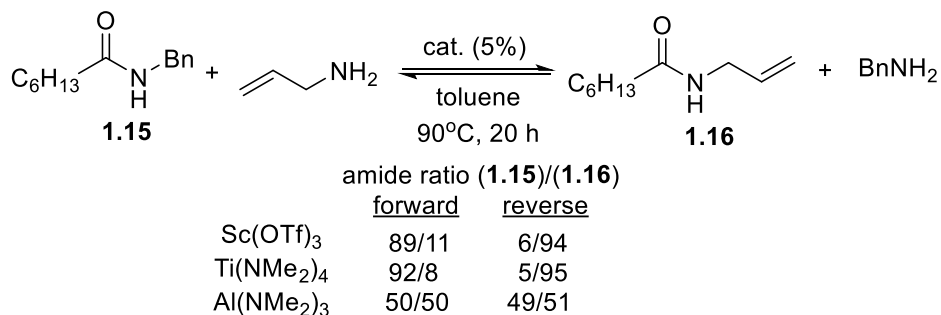
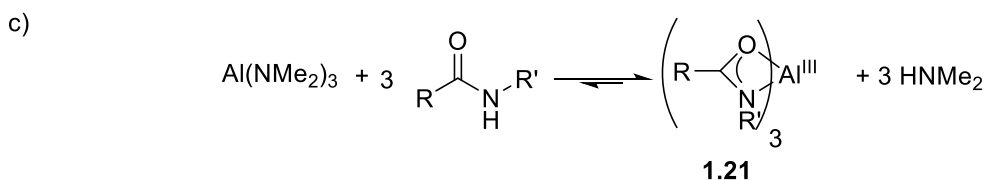
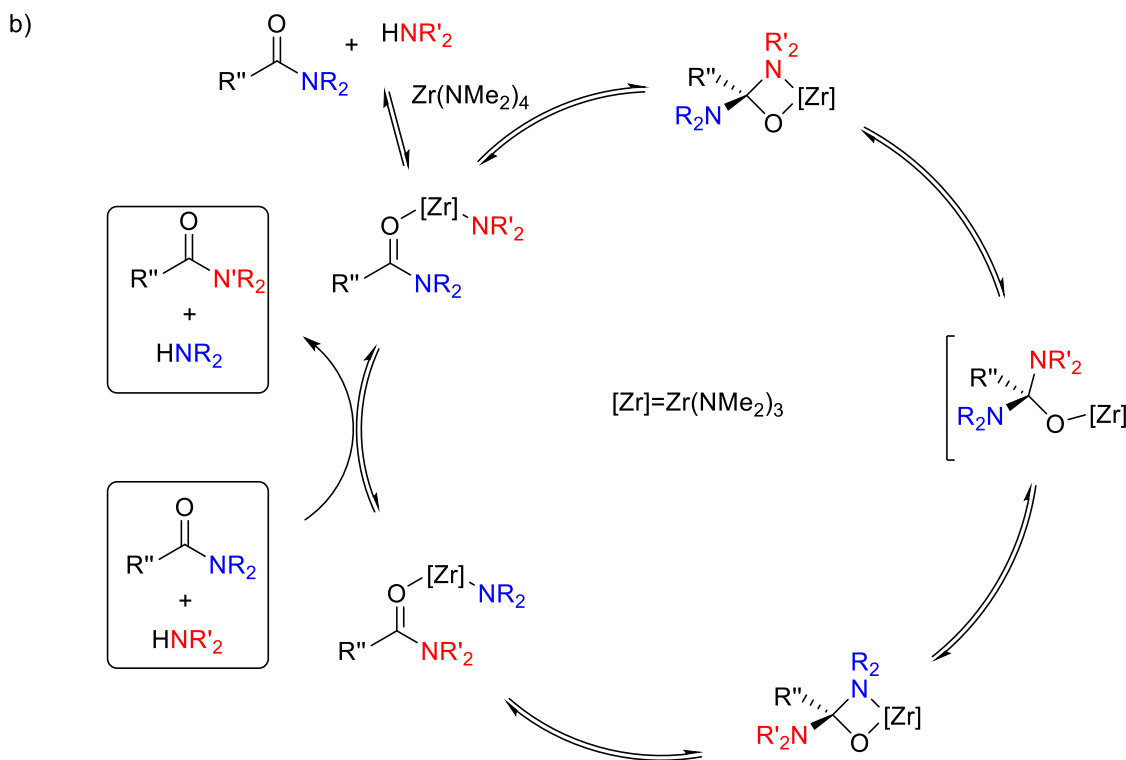
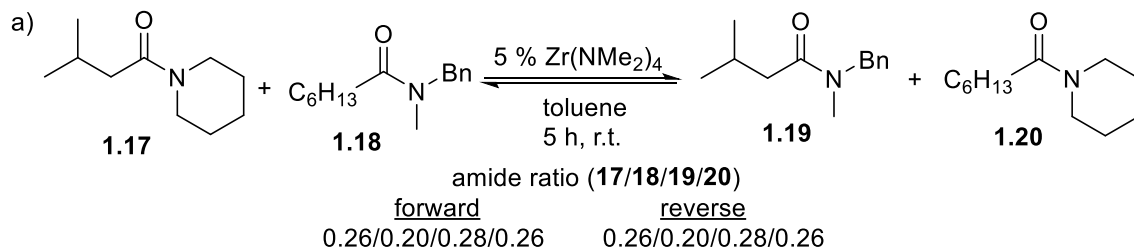


Table 1.4 Metal catalyzed transamidation of secondary amides

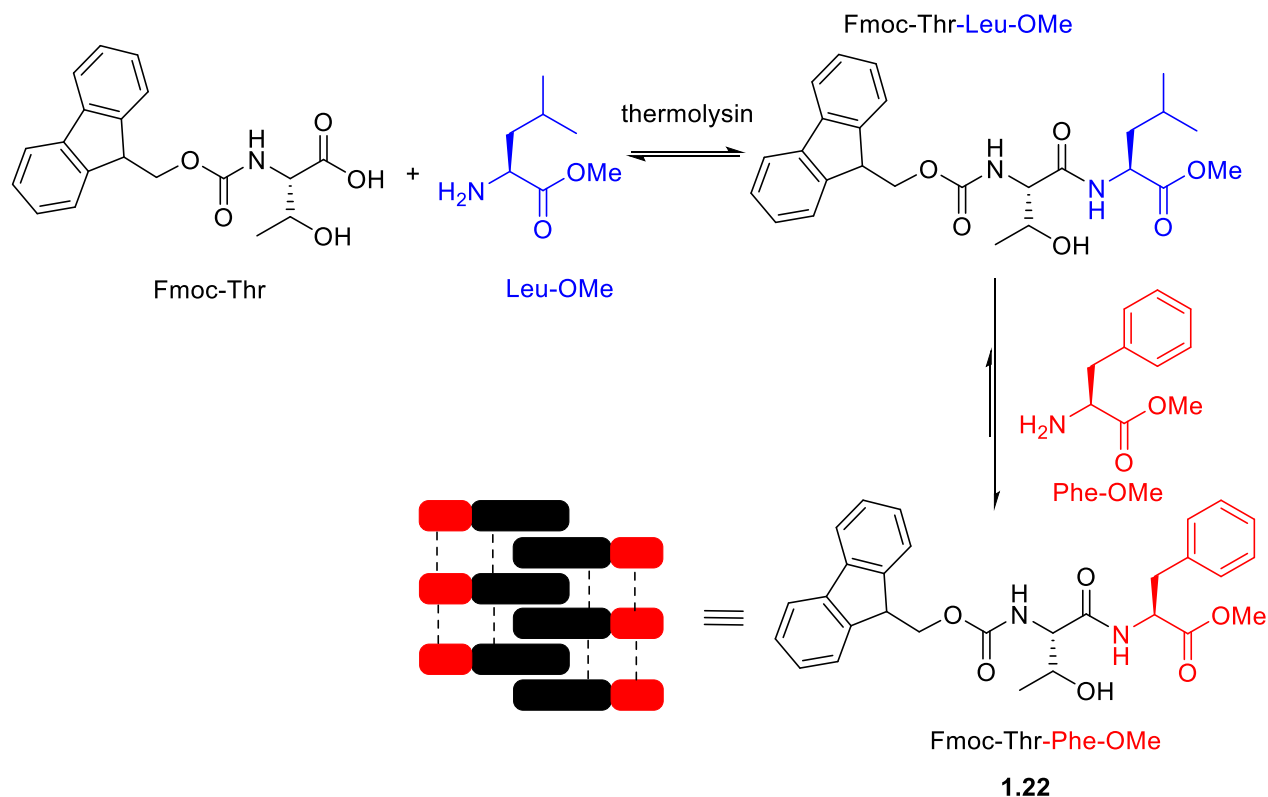
In contrast to the transamidation reactions above, the dynamic exchange between two different amides with metal catalysts has proven much more challenging. The most significant work in this area was also developed by Gellman and Stahl.¹¹⁹ In this study, they demonstrate that $\text{Zr}(\text{NMe}_2)_4$ is a highly active catalyst for amide metathesis, and these reactions can reach equilibrium from both directions within 5 hours at room temperature (Scheme 1.47a). The activity of this catalyst is postulated to arise from a dual activation from Zr center, where both the amide carbonyl group and amido nucleophile are activated in proximity of each other (Scheme 1.47b). Unfortunately, this system was only active for unfunctionalized tertiary amides, as secondary amides react to form stable, metallated amides **1.21** (Scheme 1.47c).



Scheme 1.47 a) Amide metathesis at room temperature using $Zr(NMe_2)_4$ as catalyst b) Proposed mechanism for transamidation c) Formation of stable metallated amide **1.21** with secondary amides

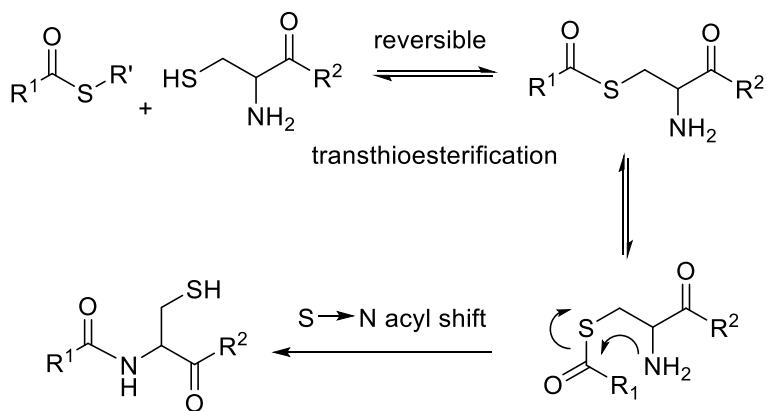
1.3.3.3. Peptide-Based Dynamic Covalent Chemistry

As an alternate to synthetic metal catalysts, it is well-known that peptide sequences can be reversibly cleaved with a variety of enzymes. Thus, the chemistry of proteins and peptides in cells can be dynamic, and half-life for exchange in the presence of enzymes can be as low as hours to days (compared to 7 years in water).¹²⁰ These enzymatic systems have been utilized in peptide-based synthetic DCvC. For example, Ulijn and coworkers demonstrated that the enzyme thermolysin can catalyze exchange in dipeptides derivatized with aromatic Fmoc (fluorenylmethyloxycarbonyl) groups. The favored self-assembly of the phenylalanine incorporated dipeptides into nanofibres in water (due in part to π -stacking) drives this reaction to the selective formation of **1.22** (Scheme 1.48).

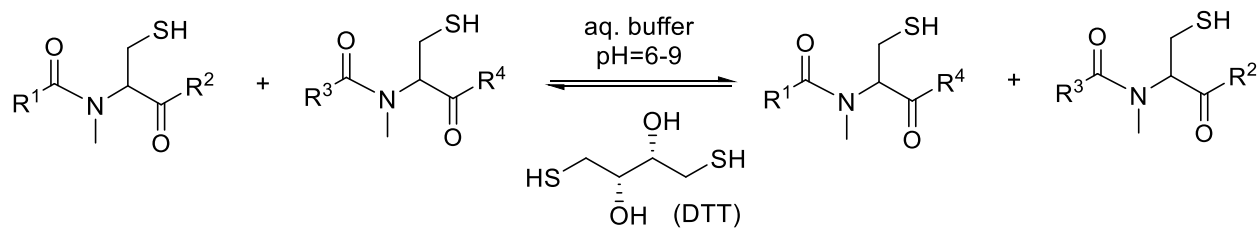


Scheme 1.48 Enzyme-assisted transamidation driven by self-assembly

Another approach to transamidation in peptides is to use native chemical ligation (NCL).¹²¹ In this, the thiol of an *N*-terminal cysteine residue undergoes transthioesterification with the thioester of a *C*-terminal peptide (Scheme 1.49). This step is reversible and can be catalyzed by thiol additives. The generation of the new thioester is followed by a *S*-to-*N*-acyl shift and thus formation of a new peptide bond. While the generation of a peptide in this final step is typically irreversible, research has shown that this can be rendered reversible by modifications to the substrate. For example, Giuseppone and coworkers have employed *N*-methylated cysteine residues to facilitate *N*- to *S*-acyl shift in a native chemical ligation platform.¹²² Incorporation of a tertiary amide significantly enhances the rate of *cis*-*trans* isomerization of the amide bond, which is a requirement for this step. With the help of a thiol additive (DTT) and mildly basic conditions to increase thiolate concentrations, amide metathesis between peptides with *N*-methyl cysteine residue was achieved (Scheme 1.50).



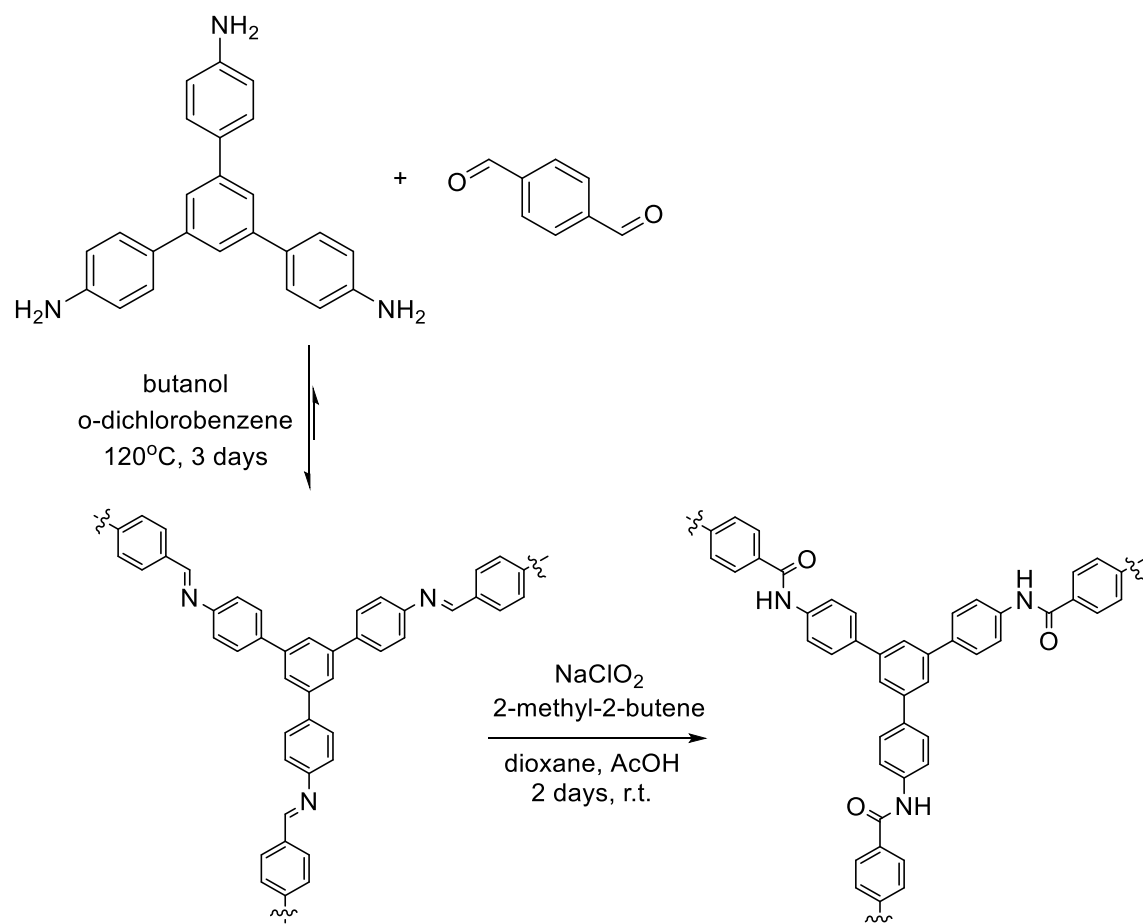
Scheme 1.49 General mechanism of native chemical ligation (NCL)



Scheme 1.50 Amide metathesis through native chemical ligation

1.3.3.4. Formation of Amides by Post-Synthetic Modifications

Finally, post synthetic modification on dynamic systems has also been employed to apply DCvC to amides. This has recently been reported by Yaghi in the assembly of amide containing COFs.¹²³ To generate amides, the authors first used dynamic imine formation to selectively assemble a crystalline COF from amines and aldehydes. Imines have been shown by Tomioka to be susceptible to oxidation to amides by NaClO_2 .¹²⁴ By coupling imine formation with this oxidation, Yaghi was able to generate a robust amide-based COF network (Scheme 1.51).



Scheme 1.51 Preparation of amide-based COF via post-synthetic modification

1.4. Overview of Thesis

1,3-dipolar cycloaddition reactions of mesoionic heterocycles offers a convergent approach to assemble five-membered ring products. However, the application of these reactions is often limited due to challenging synthesis of mesoionic compounds themselves. Recently, new methods have been developed to access these molecules in a more efficient fashion, including our lab's synthesis of münchnones and phosphamünchnones from readily available imines, acyl chlorides and either carbon monoxide (with palladium catalysis) or phosphonites. When combined with their cycloaddition reactivity with various dipolarophiles, this opened modular routes to the synthesis of nitrogen-containing heterocycles. Despite these results, and efforts by other labs, many of the other mesoionic heterocycles noted in section 1.2 are less available for use in cycloaddition.

To address these challenges, we have undertaken a study to discover alternative classes of 1,3-dipoles that might be generated in a modular fashion and exploited in cycloaddition. We describe in Chapter 2 the development a new class of mesoionic heterocycle derived from 2-pyridyl acyl chlorides and imines. The synthesis of this 1,3-dipole was inspired by Besthorn's red, one of the earliest examples of mesoionic heterocycles (Section 1.2.1). In order to induce cycloaddition reactivity in this inert dipole, we reduce the extended conjugation in this structure by using pyridines and imines as components, rather than quinolines. As was hoped, these pyridine-based 1,3-dipoles can undergo cycloaddition with a range of alkynes, and thereby offer a straightforward method to prepare substituted indolizines from imines, alkynes and pyridyl acyl chlorides.

Chapter 3 describes our efforts to generate another class of 1,3-dipole: carbonyl-ylide analogs of phosphamünchnones (Section 1.2.3.2). This can be accomplished by replacing imines in the synthesis of phosphamünchnones with aldehydes. In order to overcome the weak

nucleophilicity of aldehydes, we generated potent acyl triflate electrophiles in situ from acyl chlorides and silver triflate, which undergo spontaneous coupling with aldehydes and then the phosphonite PhP(catechyl). Although the stability of this new 1,3-dipole is lower than phosphamünchnones, they can conveniently be trapped with alkyne cycloaddition to provide a new route to assemble furans in one pot from in this case aldehydes, acyl chlorides and alkynes.

In Chapter 4, we describe the discovery of a new approach to the dynamic formation of amides via the reversible reaction of imines and acyl chlorides to form α -chloroamides. Although this reaction is a well-known in synthetic chemistry as a route to generate *N*-acyl iminium salts, its dynamic properties have not been probed in the context of dynamic covalent chemistry (DCvC, Section 1.3). We have performed a variety of experiments to prove the dynamic nature of the reaction between imines and acyl chlorides, including exchange and scrambling reactions. This approach allows dynamic formation of amides under ambient conditions, without a catalyst, and, importantly, from readily available and easily tuned components (imines and acyl chlorides). Moreover, the reaction can be coupled with simple hydrolysis to freeze this dynamic reaction and obtain robust secondary amide products.

Within Chapter 4, we also describe a preliminary study on the use of this dynamic reaction to synthesize amide-containing macromolecules such as polyamides and macrocycles. The latter is especially important, since formation of macrocyclic amides via irreversible reactions typically requires ultrahigh dilution, or the use of specifically designed substrates. We show here that these structures can instead be generated in high yield from diimines and diacyl chlorides, at normal concentrations, and where thermodynamic features can be used to shuttle the systems between macrocyclic and polymeric products. Overall, this offers a new method to generate amide macrocycles under thermodynamic control.

1.5. References

- (1) Kolb, H. C.; Finn, M. G.; Sharpless, K. B., *Angew. Chem. Int. Ed.* **2001**, *40*, 2004-2021.
- (2) Huisgen, R., *Proc. Chem. Soc.* **1961**, 357-396.
- (3) Baker, W.; Ollis, W. D.; Poole, V. D., *J. Chem. Soc.* **1949**, 307-314.
- (4) Newton, C. G.; Ramsden, C. A., *Tetrahedron* **1982**, *38*, 2965-3011.
- (5) Fischer, E., *Liebigs Ann.* **1882**, *212*, 316-339.
- (6) Baker, W.; Ollis, W. D., *Quarterly Reviews, Chemical Society* **1957**, *11*, 15-29.
- (7) Schönberg, A., *J. Chem. Soc.* **1938**, 824-825.
- (8) Besthorn, E.; Jaeglé, G., *Ber. Dtsch. Chem. Ges.* **1894**, *27*, 907-914.
- (9) Krollpfeiffer, F.; Schneider, K., *Liebigs Ann.* **1937**, *530*, 34-50.
- (10) Earl, J. C.; Mackney, A. W., *J. Chem. Soc.* **1935**, 899-900.
- (11) Hill, R. A. W.; Sutton, L. E., *J. Chem. Soc.* **1949**, 746-753.
- (12) Baker, W.; Ollis, W.; Poole, V., *J. Chem. Soc.* **1950**, 1542-1551.
- (13) a) Lawson, A.; Miles, D., *J. Chem. Soc.* **1959**, 2865-2871. b) Arulsamy, N.; Bohle, D. S., *Angew. Chem. Int. Ed.* **2002**, *41*, 2089-2091.
- (14) Lawson, A.; Miles, D. H., *J. Chem. Soc.* **1959**, 2865-2871.
- (15) Huisgen, R.; Gotthardt, H.; Bayer, H. O.; Schaefer, F. C., *Angew. Chem. Int. Ed.* **1964**, *3*, 136-137.
- (16) Hamaguchi, M.; Ibata, T., *Tetrahedron Lett.* **1974**, *15*, 4475-4476.
- (17) a) Greco, C. V.; Nyberg, W. H.; Cheng, C., *J. Med. Chem.* **1962**, *5*, 861-865. b) Bohle, D. S.; Perepichka, I., *J. Org. Chem.* **2009**, *74*, 1621-1626.
- (18) Götz, M.; Zeile, K., *Tetrahedron* **1970**, *26*, 3185-3193.
- (19) Potts, K. T.; Chen, S. J.; Kane, J.; Marshall, J. L., *J. Org. Chem.* **1977**, *42*, 1633-1638.

- (20) Potts, K. T.; Murphy, P., *J. Chem. Soc., Chem. Commun.* **1984**, 20, 1348-1349.
- (21) Boyd, G. V.; Davies, C. G.; Donaldson, J. D.; Silver, J.; Wright, P. H., *J. Chem. Soc.* **1975**, 12, 1280-1282.
- (22) Moustafa, M. A.; Gineinah, M. M.; Nasr, M. N.; Bayoumi, W. A. H., *Arch. Pharm.* **2004**, 337, 427-433.
- (23) Galuppo, L. F.; dos Reis Lívero, F. A.; Martins, G. G.; Cardoso, C. C.; Beltrame, O. C.; Klassen, L. M. B.; Canuto, A. V. d. S.; Echevarria, A.; Telles, J. E. Q.; Klassen, G.; Acco, A., *Basic Clin. Pharmacol. Toxicol.* **2016**, 119, 41-50.
- (24) Hamaguchi, M.; Tomida, N.; Mochizuki, E.; Oshima, T., *Tetrahedron Lett.* **2003**, 44, 7945-7948.
- (25) Potts, K. T.; Chen, S. J., *J. Org. Chem.* **1977**, 42, 1639-1644.
- (26) Hamaguchi, M.; Nagai, T., *J. Chem. Soc., Chem. Commun.* **1985**, 19, 1319-1321.
- (27) Huisgen, R.; Grashey, R.; Gotthardt, H.; Schmidt, R., *Angew. Chem. Int. Ed.* **1962**, 1, 48-49.
- (28) Potts, K. T.; Yao, S., *J. Org. Chem.* **1979**, 44, 977-979.
- (29) Bailey, P. D., *An introduction to peptide chemistry*. John Wiley and Sons: **1990**.
- (30) Keating, T. A.; Armstrong, R. W., *J. Am. Chem. Soc.* **1996**, 118, 2574-2583.
- (31) Dhawan, R.; Dghaym, R. D.; Arndtsen, B. A., *J. Am. Chem. Soc.* **2003**, 125, 1474-1475.
- (32) Torres, G. M.; Quesnel, J. S.; Bijou, D.; Arndtsen, B. A., *J. Am. Chem. Soc.* **2016**, 138, 7315-7324.
- (33) Sustmann, R., *Pure Appl. Chem.* **1974**, 40, 569.
- (34) Gribble, G. W., Mesoionic Ring Systems. In *Synthetic Applications of 1,3-Dipolar Cycloaddition Chemistry Toward Heterocycles and Natural Products*, **2002**, pp 681-753.
- (35) Anderson, W. K.; Chang, C. P.; McPherson Jr, H. L., *J. Med. Chem.* **1983**, 26, 1333-1338.

- (36) Granier, T.; Gaiser, F.; Hintermann, L.; Vasella, A., *Helv. Chim. Acta* **1997**, *80*, 1443-1456.
- (37) Baumann, M.; Baxendale, I. R.; Ley, S. V.; Nikbin, N., *Beilstein J. Org. Chem.* **2011**, *7*, 442-495.
- (38) Roth, B. D., *Prog. Med. Chem.* **2002**, *40*, 1-22.
- (39) Lopchuk, J. M.; Gribble, G. W., *Tetrahedron Lett.* **2015**, *56*, 3208-3211.
- (40) Gribble, G. W., *Oxazoles: synthesis, reactions, and spectroscopy*. John Wiley & Sons: **2003**; Vol. 60.
- (41) Lopchuk, J. M.; Hughes, R. P.; Gribble, G. W., *Org. Lett.* **2013**, *15*, 5218-5221.
- (42) Morin, M. S. T.; St-Cyr, D. J.; Arndtsen, B. A.; Krenske, E. H.; Houk, K. N., *J. Am. Chem. Soc.* **2013**, *135*, 17349-17358.
- (43) Benages, I. A.; Albonico, S. M., *J. Org. Chem.* **1978**, *43*, 4273-4276.
- (44) Padwa, A.; Lim, R.; MacDonald, J. G.; Gingrich, H. L.; Kellar, S. M., *J. Org. Chem.* **1985**, *50*, 3816-3823.
- (45) Bélanger, G.; April, M.; Dauphin, É.; Roy, S., *J. Org. Chem.* **2007**, *72*, 1104-1111.
- (46) Gotthardt, H.; Huisgen, R., *Chem. Ber.* **1970**, *103*, 2625-2638.
- (47) a) Bilodeau, M. T.; Cunningham, A. M., *J. Org. Chem.* **1998**, *63*, 2800-2801. b) Dalla Croce, P.; Ferraccioli, R.; La Rosa, C., *Tetrahedron* **1999**, *55*, 201-210.
- (48) Rösch, W.; Richter, H.; Regitz, M., *Chem. Ber.* **1987**, *120*, 1809-1813.
- (49) Huisgen, R.; Funke, E.; Schaefer, F. C.; Gotthardt, H.; Brunn, E., *Tetrahedron Lett.* **1967**, *8*, 1809-1814.
- (50) Siamaki, A. R.; Arndtsen, B. A., *J. Am. Chem. Soc.* **2006**, *128*, 6050-6051.
- (51) Zaman, S.; Mitsuru, K.; Abell, A. D., *Org. Lett.* **2005**, *7*, 609-611.
- (52) St. Cyr, D. J.; Arndtsen, B. A., *J. Am. Chem. Soc.* **2007**, *129*, 12366-12367.

- (53) Tebby, J. C., *Handbook of Phosphorus-31 Nuclear Magnetic Resonance Data*. CRC, **2017**.
- (54) St-Cyr, D. J.; Morin, M. S. T.; Bélanger-Gariépy, F.; Arndtsen, B. A.; Krenske, E. H.; Houk, K. N., *J. Org. Chem.* **2010**, *75*, 4261-4273.
- (55) Morin, M. S. T.; Arndtsen, B. A., *Org. Lett.* **2014**, *16*, 1056-1059.
- (56) Toshie, S.; Hiroshi, K., *Bull. Chem. Soc. Jpn.* **1970**, *43*, 3941-3942.
- (57) Singh, G.; Pande, P. S., *Tetrahedron Lett.* **1974**, *15*, 2169-2170.
- (58) Barba, F.; Batanero, B., *Tetrahedron Lett.* **1994**, *35*, 6355-6356.
- (59) Hamaguchi, M.; Ibata, T., *Tetrahedron Lett.* **1974**, *15*, 4475-4476.
- (60) Haddadin, M. J.; Kattan, A. M.; Freeman, J. P., *J. Org. Chem.* **1982**, *47*, 723-725.
- (61) Padwa, A.; Hertzog, D. L.; Chinn, R. L., *Tetrahedron Lett.* **1989**, *30*, 4077-4080.
- (62) Padwa, A.; Brodney, M. A.; Marino, J. P.; Sheehan, S. M., *J. Org. Chem.* **1997**, *62*, 78-87.
- (63) Padwa, A.; Sheehan, S. M.; Straub, C. S., *J. Org. Chem.* **1999**, *64*, 8648-8659.
- (64) Drew, M. G. B.; Fengler-Veith, M.; Harwood, L. M.; Jahans, A. W., *Tetrahedron Lett.* **1997**, *38*, 4521-4524.
- (65) Gowravaram, M. R.; Gallop, M. A., *Tetrahedron Lett.* **1997**, *38*, 6973-6976.
- (66) Goldberg, S. I.; Lipkin, A. H., *J. Org. Chem.* **1972**, *37*, 1823-1825.
- (67) Kuethe, J. T.; Padwa, A., *J. Org. Chem.* **1997**, *62*, 774-775.
- (68) Berk, H. C.; Zwickelmaier, K. E.; Franz, J. E., *Synth. Commun.* **1980**, *10*, 707-710.
- (69) Hamaguchi, M.; Nagai, T., *J. Chem. Soc., Chem. Commun.* **1985**, *4*, 190-191.
- (70) Gotthardt, H.; Weissshuhn, M. C.; Dörhöfer, K., *Angew. Chem. Int. Ed.* **1975**, *14*, 422-422.

- (71) Rowan, S. J.; Cantrill, S. J.; Cousins, G. R. L.; Sanders, J. K. M.; Stoddart, J. F., *Angew. Chem. Int. Ed.* **2002**, *41*, 898-952.
- (72) Seidel, F., *Ber. Dtsch. Chem. Ges.* **1926**, *59*, 1894-1908.
- (73) Melson, G. A.; Busch, D. H., *J. Am. Chem. Soc.* **1965**, *87*, 1706-1710.
- (74) Thompson, M. C.; Busch, D. H., *J. Am. Chem. Soc.* **1962**, *84*, 1762-1763.
- (75) Jin, Y.; Wang, Q.; Taynton, P.; Zhang, W., *Acc. Chem. Res.* **2014**, *47*, 1575-1586.
- (76) Zhang, Y.; Barboiu, M., *Chem. Rev.* **2016**, *116*, 809-834.
- (77) Moulin, E.; Cormos, G.; Giuseppone, N., *Chem. Soc. Rev.* **2012**, *41*, 1031-1049.
- (78) Feng, X.; Ding, X.; Jiang, D., *Chem. Soc. Rev.* **2012**, *41*, 6010-6022.
- (79) Ding, S.-Y.; Wang, W., *Chem. Soc. Rev.* **2013**, *42*, 548-568.
- (80) Corbett, P. T.; Leclaire, J.; Vial, L.; West, K. R.; Wietor, J.-L.; Sanders, J. K. M.; Otto, S., *Chem. Rev.* **2006**, *106*, 3652-3711.
- (81) Ramström, O.; Lehn, J.-M., *Nat. Rev. Drug Discov.* **2002**, *1*, 26-36.
- (82) Jin, Y.; Yu, C.; Denman, R. J.; Zhang, W., *Chem. Soc. Rev.* **2013**, *42*, 6634-6654.
- (83) Aida, T.; Meijer, E. W.; Stupp, S. I., *Science* **2012**, *335*, 813-817.
- (84) Belowich, M. E.; Stoddart, J. F., *Chem. Soc. Rev.* **2012**, *41*, 2003-2024.
- (85) Leussing, D. L.; Leach, B. E., *J. Am. Chem. Soc.* **1971**, *93*, 3377-3384.
- (86) Tait, A. M.; Busch, D. H.; Wilshire, J.; Lever, A. B. P., *Inorg. Synth.*, **1978**, *18*, 30.
- (87) Wu, J.; Leung, K. C.-F.; Stoddart, J. F., *Proc. Natl. Acad. Sci. U.S.A.* **2007**, *104*, 17266-17271.
- (88) González-Álvarez, A.; Alfonso, I.; López-Ortiz, F.; Aguirre, Á.; García-Granda, S.; Gotor, V., *Eur. J. Org. Chem.* **2004**, *2004*, 1117-1127.
- (89) Acharyya, K.; Mukherjee, P. S., *Angew. Chem. Int. Ed.* **2019**, *58*, 8640-8653.
- (90) Meyer, C. D.; Joiner, C. S.; Stoddart, J. F., *Chem. Soc. Rev.* **2007**, *36*, 1705-1723.

- (91) Segura, J. L.; Mancheño, M. J.; Zamora, F., *Chem. Soc. Rev.* **2016**, *45*, 5635-5671.
- (92) Schaufelberger, F., Timmer, B.J. and Ramström, O. Principles of Dynamic Covalent Chemistry. In *Dynamic Covalent Chemistry*, **2017**, pp 1-30.
- (93) Black, S. P.; Sanders, J. K. M.; Stefankiewicz, A. R., *Chem. Soc. Rev.* **2014**, *43*, 1861-1872.
- (94) Li, J.; Carnall, J. M. A.; Stuart, M. C. A.; Otto, S., *Angew. Chem. Int. Ed.* **2011**, *50*, 8384-8386.
- (95) Nishiyabu, R.; Kubo, Y.; James, T. D.; Fossey, J. S., *Chem. Commun.* **2011**, *47*, 1124-1150.
- (96) Côté, A. P.; Benin, A. I.; Ockwig, N. W.; O'Keeffe, M.; Matzger, A. J.; Yaghi, O. M., *Science* **2005**, *310*, 1166-1170.
- (97) Vougioukalakis, G. C.; Grubbs, R. H., *Chem. Rev.* **2010**, *110*, 1746-1787.
- (98) Jyothish, K.; Zhang, W., *Angew. Chem. Int. Ed.* **2011**, *50*, 8478-8480.
- (99) Okochi, K. D.; Jin, Y.; Zhang, W., *Chem. Commun.* **2013**, *49* (39), 4418-4420.
- (100) Jin, Y.; Zhang, A.; Huang, Y.; Zhang, W., *Chem. Comm.* **2010**, *46*, 8258-8260.
- (101) Yang, H.; Liu, Z.; Zhang, W., *Adv. Synth. Catal.* **2013**, *355*, 885-890.
- (102) Cacciapaglia, R.; Di Stefano, S.; Mandolini, L., *J. Am. Chem. Soc.* **2005**, *127*, 13666-13671.
- (103) Boul, P. J.; Reutenauer, P.; Lehn, J.-M., *Org. Lett.* **2005**, *7*, 15-18.
- (104) Moerdyk, J. P.; Bielawski, C. W., *Nat. Chem.* **2012**, *4*, 275-280.
- (105) Xu, J.-F.; Chen, Y.-Z.; Wu, L.-Z.; Tung, C.-H.; Yang, Q.-Z., *Org. Lett.* **2013**, *15*, 6148-6151.
- (106) Martinez-Castaneda, A.; Rodriguez-Solla, H.; Concellon, C.; del Amo, V., *Org. Biomol. Chem.* **2012**, *10*, 1976-81.

- (107) Vongvilai, P.; Angelin, M.; Larsson, R.; Ramström, O., *Angew. Chem. Int. Ed.* **2007**, *46*, 948-950.
- (108) Ying, H.; Zhang, Y.; Cheng, J., *Nat. Comm.* **2014**, *5*, 3218.
- (109) Holler, M.; Allenbach, N.; Sonet, J.; Nierengarten, J.-F., *Chem. Comm.* **2012**, *48*, 2576-2578.
- (110) Brachvogel, R.-C.; von Delius, M., *Chem. Sci.* **2015**, *6*, 1399-1403.
- (111) Rowan, S. J.; Brady, P. A.; Sanders, J. K. M., *Angew. Chem. Int. Ed.* **1996**, *35*, 2143-2145.
- (112) Shi, B.; Greaney, M. F., *Chem. Comm.* **2005**, *7*, 886-888.
- (113) Ji, S.; Cao, W.; Yu, Y.; Xu, H., *Angew. Chem. Int. Ed.* **2014**, *53*, 6781-6785.
- (114) Roughley, S. D.; Jordan, A. M., *J. Med. Chem.* **2011**, *54*, 3451-3479.
- (115) Beste, L. F.; Houtz, R. C., *J. Polym. Sci.* **1952**, *8*, 395-407.
- (116) Bon, E.; Bigg, D. C. H.; Bertrand, G., *J. Org. Chem.* **1994**, *59*, 4035-4036.
- (117) Zhang, M.; Imm, S.; Bähn, S.; Neubert, L.; Neumann, H.; Beller, M., *Angew. Chem. Int. Ed.* **2012**, *51*, 3905-3909.
- (118) Eldred, S. E.; Stone, D. A.; Gellman, S. H.; Stahl, S. S., *J. Am. Chem. Soc.* **2003**, *125*, 3422-3423.
- (119) Stephenson, N. A.; Zhu, J.; Gellman, S. H.; Stahl, S. S., *J. Am. Chem. Soc.* **2009**, *131*, 10003-10008.
- (120) Eden, E.; Geva-Zatorsky, N.; Issaeva, I.; Cohen, A.; Dekel, E.; Danon, T.; Cohen, L.; Mayo, A.; Alon, U., *Science* **2011**, *331*, 764-8.
- (121) Dawson, P.; Muir, T.; Clark-Lewis, I.; Kent, S., *Science* **1994**, *266*, 776-779.
- (122) Ruff, Y.; Garavini, V.; Giuseppone, N., *J. Am. Chem. Soc.* **2014**, *136*, 6333-6339.
- (123) Waller, P. J.; Lyle, S. J.; Osborn Popp, T. M.; Diercks, C. S.; Reimer, J. A.; Yaghi, O. M., *J. Am. Chem. Soc.* **2016**, *138*, 15519-15522.

(124) Mohamed, M. A.; Yamada, K.-I.; Tomioka, K., *Tetrahedron Lett.* **2009**, *50*, 3436-3438.

CHAPTER 2

Development and Cycloaddition Reactivity of a New Class of Pyridine-Based Mesoionic 1,3-Dipole¹

2.0 Preface

1,3-Diazolium-4-olates (mesoionic imidazoles), discussed in section 1.2.3.3., are one of the lesser-known members of mesoionic heterocycles. Their synthesis often involves multiple steps and complex starting materials. An early example to this class of 1,3-dipole, Besthorn's Red, can be easily prepared from a carboxylic acid and quinoline, however, it does not demonstrate cycloaddition reactivity. Described below is a modified version of this 1,3-dipole, synthesized from readily available starting materials such as pyridine-based acyl chlorides and imines. Combined with its improved cycloaddition reactivity with alkynes, this provides a new route to synthesize substituted indolizines under mild conditions using simple building blocks. This work was published in *Angew. Chem. Int. Ed.* **2017**, *56*, 6078.

2.1 Introduction

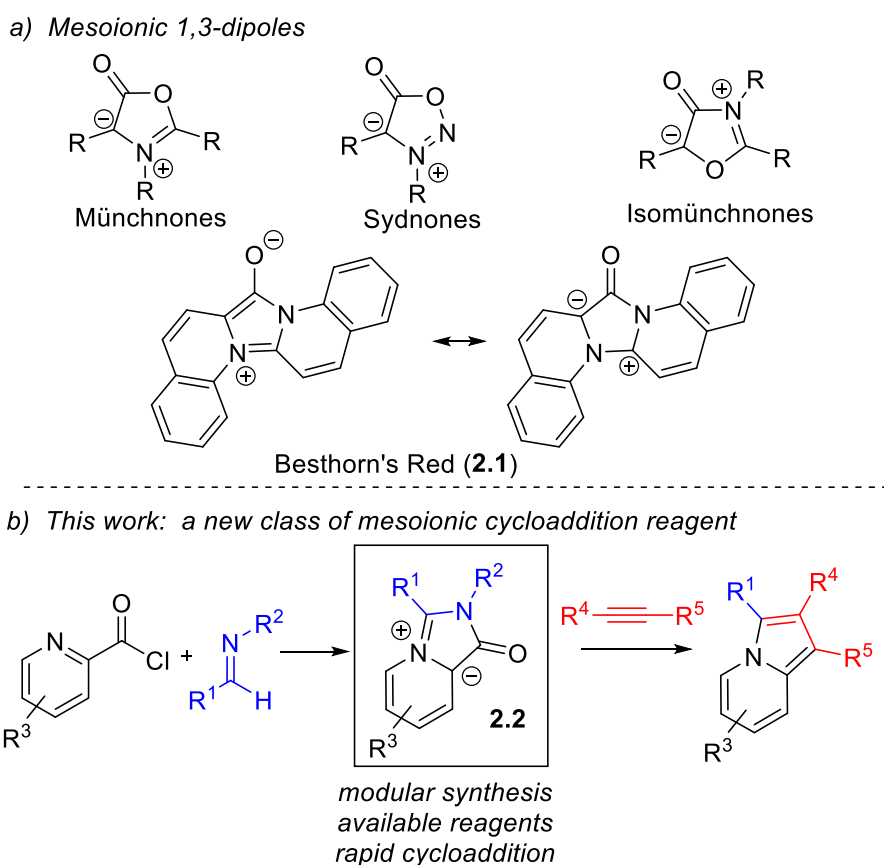
1,3-Dipolar cycloaddition has become one of the central synthetic approaches to construct five-membered ring heterocycles.² Relative to the more classical assembly of heterocycles by cyclization of pre-synthesized substrates, dipolar cycloadditions can provide access to these products in a convergent fashion, where one reactant is often a readily available unsaturated dipolarophile (alkyne, alkene, imine, etc). These cycloadditions can also be rapid reactions, which,

when coupled with the orthogonality of this chemistry to more traditional organic reactions, has opened its application in a diverse array of areas (i.e. a variant of “click” reactions).³ Examples include not just organic heterocycle synthesis, but also biochemical studies,⁴ polymer chemistry,⁵ materials science,⁶ and many other topics.

Key to the utility of 1,3-dipolar cycloaddition is access to these reactive dipoles, many of which were pioneered through the early work of Huisgen and others.⁷ One notable class are mesoionic heterocycles (e.g. Scheme 2.1a).⁸ In contrast to many 1,3-dipoles, mesoionic dipoles can be considered of “intermediate” ionicity, and multiple aromatic resonance structures can be drawn for each of these compounds. An important feature of mesoionic heterocycles is their stability, where resonance can make many of these reagents sufficiently robust for isolation. Nevertheless, the use of many variants of mesoionics can be limited by the required steps needed to build-up their structure, which can detract from their utility in heterocycle synthesis.

We have recently become interested in the design of new classes of mesoionic dipoles, and in particular those that might be more easily generated from available substrates.⁹ In considering potential structures, we noted that one of the earliest isolated mesoionic heterocycles was quinoline-based compound **2.1** (Scheme 2.1a), commonly known as Besthorn’s Red. This red pigment was generated by Besthorn in 1894,¹⁰ with subsequent studies by Krollpfeiffer¹¹ demonstrating it to contain the now accepted mesoionic structure. Besthorn’s Red has not been shown to participate in 1,3-dipolar cycloaddition reactivity, presumably due to its extended conjugation and resonance stabilization. Nevertheless, in light of its facile synthesis from quinolines, we questioned if this platform might be modified to access to an alternative class of mesoionic 1,3-dipolar cycloaddition reagents. We describe here our studies towards this goal. These demonstrate that the reaction of imines with pyridine-based acyl chlorides can allow the

generation of a new type of 1,3-dipolar cycloaddition reagent **2.2** (Scheme 2.1b). Compounds **2.2** undergo rapid 1,3-dipolar cycloaddition reactions with alkynes. The latter opens a route to construct families of pharmaceutically relevant indolizines,¹² where this structure is generated in one pot from simply imines, heterocyclic acyl chlorides, and alkynes.

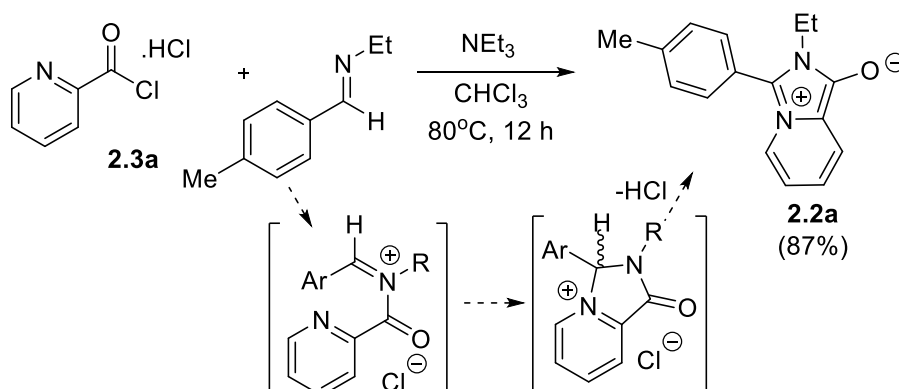


Scheme 2.1 Mesoionic 1,3-dipoles and cycloaddition

2.2 Results and Discussion

Our initial studies probed the reaction of the acyl chloride of picolinic acid (**2.3a**) with the imine *p*-tolyl(H)C=Nbn (Scheme 2.2). Combining these reagents at 80 °C leads to formation of a green solution over the course of 12 h, suggestive of the potential formation of the chromophoric 1,3-dipole. However, ¹H NMR analysis shows this reaction is not clean, and includes the

formation of significant amounts of protonated imine and other products. After testing several reaction conditions, it was found that simple Et₃N can serve as an effective base for this transformation, and leads to the near quantitative formation of **2.2a**. Dipole **2.2a** can be isolated as a green solid in 87% yield by extraction with toluene. ¹H and ¹³C NMR analysis are consistent with the structure shown, including upfield shifts in the pyridinyl hydrogens (to δ 6.0-7.5 ppm) and carbonyl carbon (δ 150.6 ppm), indicative of delocalization of charge onto the carbonyl oxygen and pyridine.

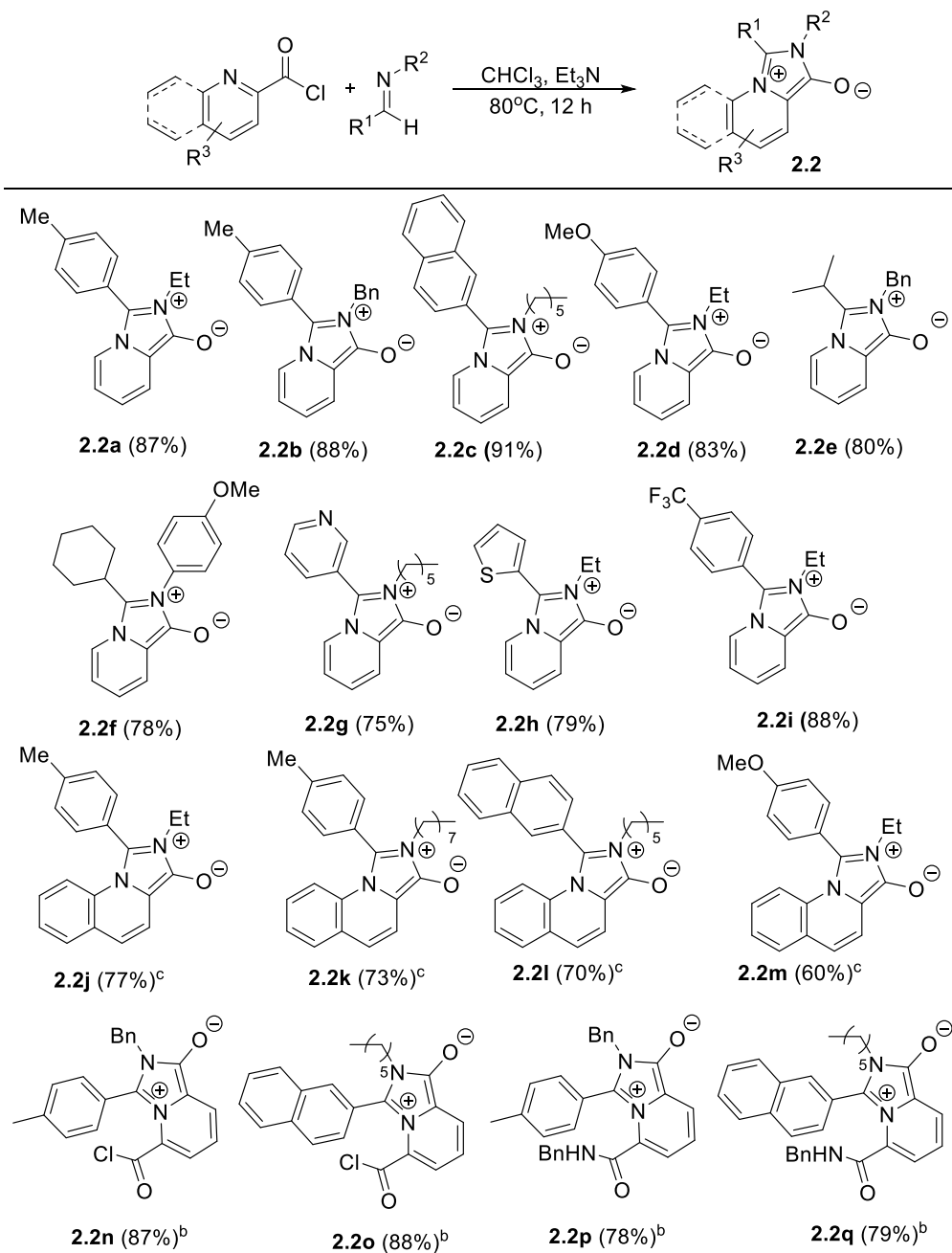


Scheme 2.2 Synthesis of pyridine-based 1,3-dipole **2.2a**

A feature of **2.2a** is its generation from available acyl chlorides and imines. As such, it is straightforward to prepare a range of new variants of this dipole. Table 2.1 demonstrates the substrate scope for this transformation. For example, the imine can be systematically varied to incorporate a number of different nitrogen substituents, such as *N*-benzyl (**2.2b**) or -aromatic (**2.2f**) units. Similarly, the imine carbon can be modulated to include various substituted aromatics with electron withdrawing (**2.2i**) or donor (**2.2d,m**) groups. Heteroaromatic substituents are also well tolerated (**2.2g,h**), as are more sensitive enolizable alkyl-substituted imines (**2.2e,f**). The pyridine can be replaced with a diacyl chloride (**2.2n,o**), and a quinoline (**2.2j-m**). The former react rapidly with imines (3 h at ambient temperature) and can be further derivatized to access other dipoles

(2.2p,q). Notably, many of these modifications leads to a significant color change, and can allow the formation of dipoles with colors ranging from red (**2.2j-m**) to blue (**2.2n,o**) to green (**2.2a-i**).

Table 2.1 Substrate scope for 1,3-dipole **2.2** formation^a



[a] Acyl chloride (0.3 mmol), imine (0.3 mmol) and Et₃N (90 mg, 0.9 mmol) in 3 mL CHCl₃ for 12 h at 80 °C. [b] 3 h at rt. [c] Et₃N (60 mg, 0.6 mmol).

In the case of dipole **2.2n**, crystals suitable for X-ray structural analysis can be obtained by crystallization from dichloromethane/pentane. The crystal structure of **2.2n** is shown in Figure 2.1, and demonstrates it is indeed a new mesoionic heterocycle. Of note, the N1-C1 (1.343(2) Å) and N2-C1 (1.376(2) Å) bonds in **2.2n** are close to symmetrical, and intermediate between single and double bonds. In addition, the C8-O2 bond (1.228(2) Å) is similar to that in typical amides (PhCONMe₂, C=O 1.231 Å).¹³ This, together with a C2-C3 length between a single and double bond (1.428(2) Å) and upfield pyridinyl ¹H NMR resonances, suggests the formal negative charge is likely delocalized throughout the carbonyl and heterocyclic system.

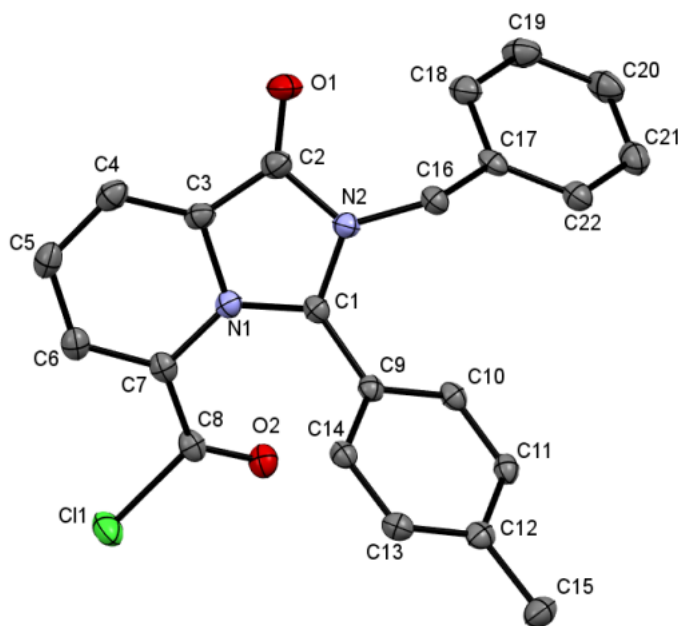
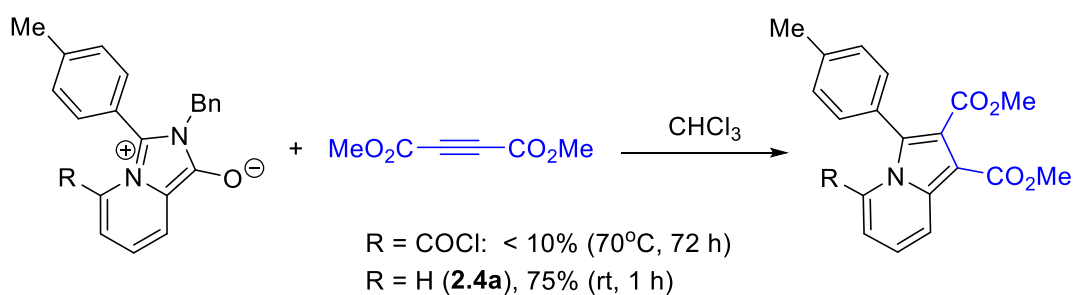


Figure 2.1 Crystal structure of **2.2n**. Select bond lengths [Å]: N1–C1 1.343(2), N2–C1 1.376(2), O1–C2 1.228(2), C3–C2 1.428(2), C3–C4 1.370(2), C2–N2 1.402(2), C11–C8 1.8035(17), O2–C8 1.197(2)

With the ability to form these mesoionic heterocycles in hand, we next questioned if the 1,3-dipole core of **2.2** can allow their participation in cycloaddition chemistry. For this, it was

envisioned that the reduced aromaticity of **2.2** relative to Besthorn's Red could allow alkyne cycloaddition across the carbon skeleton to be followed by irreversible isocyanate liberation (which cannot occur with **2.1**) as a route to build-up indolizines. Initial studies with the crystallographically characterized **2.2n** show that while it does react sluggishly with the electron poor alkyne dimethylacetylene dicarboxylate (DMAD), it forms indolizine in very low yield (Scheme 2.3). However, removing the electron withdrawing acyl chloride functionality on the pyridine (e.g. dipole **2.2b**), which presumably creates a more nucleophilic dipole, leads to a rapid cycloaddition with the electron poor DMAD within less than 1 h at ambient temperature, and the formation of indolizine **2.4a** in good yield (75%).



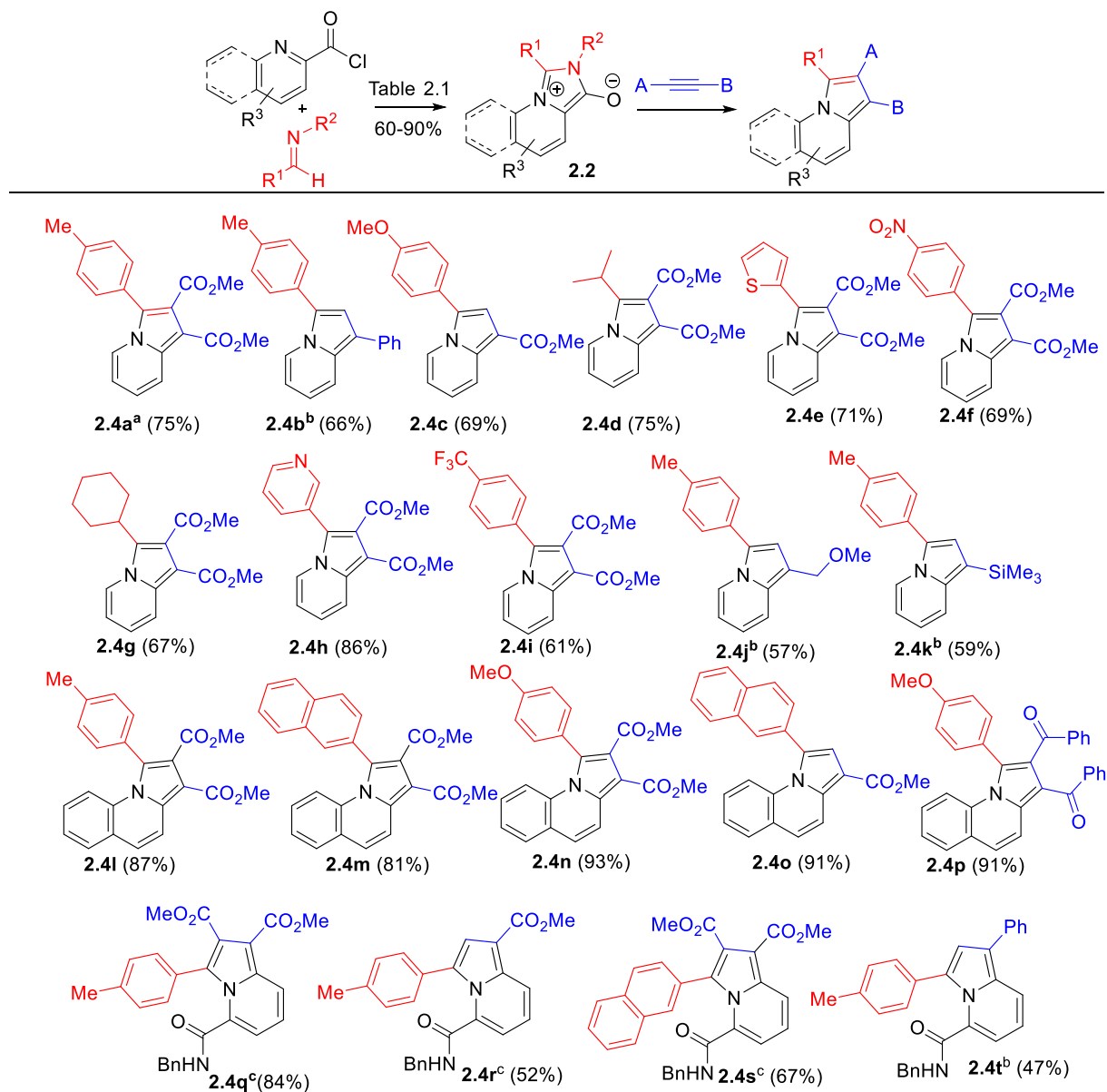
Scheme 2.3 Cycloaddition reactivity of pyridine-based 1,3-dipole **2.2**

As illustrated in Table 2.2, the generation of **2.2** can be coupled with alkyne cycloaddition to create a modular synthesis of indolizines. A range of alkynes can participate in cycloaddition with in situ generated **2.2**. While electron poor alkynes undergo most rapid reaction (e.g. methyl propiolate, DMAD, and diketoalkynes), mild heating can also allow reactions to proceed with more electron rich alkynes, such as phenylacetylene (**2.4b,t**), those with functional groups (**2.4j**), and even TMS acetylene (**2.4k**).¹⁴ In the case of terminal alkynes, only one regioisomeric product is isolated, wherein the alkyne substituent is directed away from the 2-carbon of the imidazolium

core. As this selectivity is consistent with both electron poor and electron rich alkynes, it presumably arises from steric interactions with the R¹ substituent in the imidazolium dipole **2.2**.

The dipole **2.2** can also be tuned. In the case of the pyridinyl unit, this can allow the synthesis of various quinoline-based heterocycles (**2.4l–p**), and functionalized pyridine derivatives (**2.4q–t**). The cycloaddition reactivity shows a strong dependence upon the electronics of these substituents. While the simple pyridine- and quinoline-derived dipoles react within 30 min at ambient temperature with DMAD, the more electron deficient dipoles **2.2p** and **2.2q** require 10 h, and the most electron poor **2.2o** does not react at all. As with the trends in alkyne substituents, this is consistent with the dipole **2.2** behaving as the electron-rich component in the cycloaddition reaction, similar to that noted with related N-alkylated pyridinium 1,3-dipoles.¹⁵ Finally, the imine unit in **2.2** can also be modified to tune the 2-substituent in the indolizine. This includes the incorporation of functionalized aromatics with electron donor or withdrawing substituents (**2.4c,i**), alkyl units (**2.4d,g**), and even other heterocycles (**2.4e,h**). Overall combining the formation of **2.2** with alkyne cycloaddition can provide a novel method to build-up families of indolizines, wherein any of the pyridinyl, imine and alkyne substituents can be systematically modified.

Table 2.2 Modular synthesis of indolizines via mesoionic 1,3-dipole **2.2**

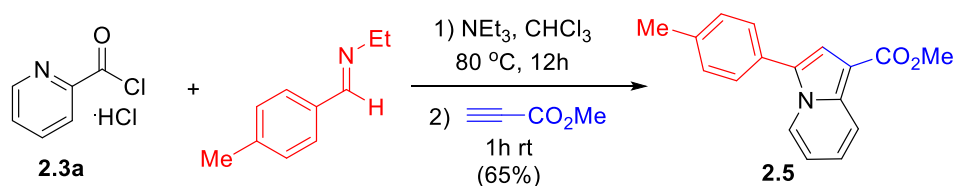


[a] **2.2** formed as in Table 2.1, alkyne (0.3 mmol) in 2 mL CHCl₃, 1 h at ambient temperature.

[b] 65°C, 24 h. [c] 10 h.

Indolizines are present in a range of pharmaceutically relevant products as well as electronic materials.^{11,16} Typical synthetic approaches to these products include cyclizations with synthetic pyridine or pyrrole derivatives,¹⁷⁻¹⁹ substitution on preformed indolizines,²⁰ or 1,3-

dipolar cycloaddition with pyridinium ylides.²¹ **2.2** can be considered a stabilized, mesoionic analogue to these latter 1,3-dipoles, and offers the ability to incorporate a range of aryl, heteroaryl and alkyl units into the 3-indolizine position from simple imines. As an illustration of the utility of this approach, ester-substituted indolizines such as **2.5** (Scheme 2.4) has been shown by Lan and You to be strong blue emitting materials of use in fluorescence imaging.^{20a} In contrast to its synthesis by substitution on pre-synthesized indolizines, **2.5** can be directly generated from **2.3a**, an imine and an alkyne. In addition to forming **2.5**, the systematic tuning of each the substrates can in principle allow access to a range of new variants of these products, and from reagents that are either commercially available (e.g. **2.3a**, alkynes) or easily generated (imines).



Scheme 2.4 Targeted synthesis of fluorescent indolizine **2.5**

2.3 Conclusions

In conclusion, a new class of mesoionic, pyridine-based 1,3-dipolar cycloaddition reagent has been developed. These dipoles are stable, easily generated from available substrates, yet can undergo rapid cycloaddition with alkynes to provide a route to synthesize indolizines. Considering the broad variety of dipolar cycloaddition substrates available, as well as the accessibility of **2.2**, this should provide straightforward access to a range of pyridine-based heterocyclic products. Studies directed towards the latter are in progress.

2.4 Experimental Section²²

2.4.1 General Procedures

All manipulations were conducted in a glovebox under a nitrogen atmosphere. Unless otherwise noted, all reagents were purchased from commercial sources and used without purification. Solvents were dried by using a solvent purifier system. Solvents were stored over activated 3Å molecular sieves inside the glovebox. Deuterated acetonitrile and benzene were stirred over calcium hydride, vacuum transferred, degassed, and stored over 4Å molecular sieves. Imines were prepared using standard literature procedures.²³ Nuclear magnetic resonance (NMR) characterization was performed on 400 MHz spectrometers for proton and 101 MHz for carbon. ¹H and ¹³C NMR chemical shifts were referenced to residual solvent. ¹H and ¹³C NMR spectra to show the purity are available in the supporting information of the publication.¹ Mass spectra were recorded on a high-resolution electrospray ionization quadrupole mass spectrometer.

2.4.2 Experimental Procedures

Typical Preparation of 1,3-Dipoles 2.2 In a glovebox, 2-pyridinecarbonyl chloride hydrochloride (53 mg, 0.30 mmol), (p-tolyl)HC=NEt (44 mg, 0.30 mmol) and Et₃N (91 mg, 0.90 mmol) were dissolved in 3 ml of chloroform, and then transferred into a 25 ml Schlenk tube along with a stir bar. Tube was sealed and taken out of the glovebox, and placed in a 80°C oil bath for 12 hours (in the case of **2.2n,o**, the reaction was simply stirred at ambient temperature for 3 h; for **2.2i-o**, 2 equiv. of Et₃N was used). After the completion of reaction, mixture is taken into glovebox, and the solvent and excess Et₃N were removed in vacuo. The crude product was dissolved in 3 ml toluene, the protonated Et₃N was removed by filtration through a frit, and any remaining imine was washed away with pentane, affording dipole **2.2a** as a green solid (66 mg, 87 % yield). In the case of the

dipoles generated with quinolinyl acyl chloride (**2.2j-m**), and dipoles **2.2b,h**, some impurities were generated in the dipole that could not be removed by washing. These were instead removed after conversion to indolizines via column chromatography.

Preparation of Amide-Substituted 1,3-Dipoles The above procedure for the generation of dipole **2.2n** was followed. To the crude reaction mixture was added benzylamine (32 mg, 0.30 mmol) and Et₃N (61 mg, 0.60 mmol), and the solution was stirred for 30 min. Following this, the excess base and solvent was removed in vacuo, followed by precipitation of the amide-substituted dipole from acetonitrile at -35°C to afford **2.2p** as an orange solid (80%, 107 mg, 0.24 mmol).

Typical Formation of Indolizines 2.4 The dipole **2.2b** (83 mg, 0.264 mmol) generated as above was immediately dissolved in 2 mL CHCl₃, and to this solution was added the dimethylacetylene dicarboxylate (43 mg, 0.30 mmol). The mixture was stirred for 1h at ambient temperature. In the case of less electron efficient alkynes, the mixture was warmed to 65 °C for 18 h. Excess benzylamine can be added after this time to react with the liberated isocyanate. The solvent was removed in vacuo, and the indolizine product **2.4a** was isolated by column chromatography (40% ethyl acetate, 60 % hexanes) as a pale yellow solid (75%, 64 mg, 0.198 mmol).

Crystallization of 2.2n Compound **2.2n** was prepared as noted above, and base removed by stirring over K₃PO₄. Single crystals are grown by vapour diffusion of pentane into a dichloromethane solution of **2.2n** at room temperature. The X-ray crystal structure is available at the Cambridge Crystallographic Data Centre (CCDC) under the deposition number 1507654.

2.4.3 Characterization Data

2-ethyl-3-(p-tolyl)imidazo[1,5-a]pyridin-2-ium-1-olate (2.2a) Green solid, 66 mg, 87%. ¹H NMR (400 MHz, CDCl₃) δ 7.49 (dt, *J* = 8.9, 1.2 Hz, 1H), 7.37 – 7.32 (m, 3H), 7.30 (d, *J* = 8.3 Hz, 2H), 6.38 (t, *J* = 7.5 Hz, 1H), 6.02 (ddd, *J* = 8.9, 6.4, 0.7 Hz, 1H), 4.03 (q, *J* = 7.2 Hz, 2H), 2.42 (s, 3H), 1.23 (t, *J* = 7.2 Hz, 4H). ¹³C NMR (101 MHz, CDCl₃) δ 150.6, 140.4, 130.5, 129.2, 122.5, 121.6, 119.3, 116.6, 115.9, 110.3, 109.0, 36.7, 21.5, 14.9. HRMS (ESI⁺) for C₁₆H₁₆N₂O; calculated 252.1257, found 252.1258 (error m/z = -0.3 ppm)

2-benzyl-3-(p-tolyl)imidazo[1,5-a]pyridin-2-ium-1-olate (2.2b) Green solid, 83 mg, 88%. ¹H NMR (400 MHz, CDCl₃) δ 7.59 (d, *J* = 9.0 Hz, 1H), 7.38 (d, *J* = 7.3 Hz, 1H), 7.29 – 7.20 (m, 5H), 7.15 – 7.09 (m, 4H), 6.43 (ddd, *J* = 7.4, 6.5, 1.3 Hz, 1H), 6.08 (ddd, *J* = 9.0, 6.4, 0.7 Hz, 1H), 5.19 (s, 2H), 2.42 (s, 3H). ¹³C NMR (101 MHz, CDCl₃) δ 151.1, 140.4, 137.1, 130.3, 129.5, 129.3, 128.5, 127.54, 127.47, 122.9, 121.4, 119.6, 116.7, 110.3, 109.2, 44.9, 21.5. HRMS (ESI⁺) for C₂₁H₁₈N₂O; calculated 314.1414, found 314.1414 (error m/z = 0.0 ppm)

2-hexyl-3-(naphthalen-2-yl)imidazo[1,5-a]pyridin-2-ium-1-olate (2.2c) Green solid, 94 mg, 91%. ¹H NMR (400 MHz, CDCl₃) δ 8.05 (d, *J* = 8.3 Hz, 1H), 7.97 (d, *J* = 8.2 Hz, 1H), 7.65 – 7.44 (m, 5H), 7.22 (d, *J* = 8.4 Hz, 1H), 6.82 (d, *J* = 7.3 Hz, 1H), 6.37 – 6.31 (m, 1H), 6.07 (ddd, *J* = 9.0, 6.4, 0.7 Hz, 1H), 3.91 (m, 2H), 1.56 – 1.38 (m, 2H), 1.06 – 0.87 (m, 6H), 0.64 (t, *J* = 6.9 Hz, 3H). ¹³C NMR (101 MHz, CDCl₃) δ 151.0, 134.1, 131.8, 131.3, 130.1, 129.1, 128.1, 127.0, 125.6, 124.3, 122.6, 121.9, 119.3, 117.1, 114.2, 110.7, 109.0, 41.7, 31.0, 29.2, 26.0, 22.2, 13.8. HRMS (ESI⁺) for C₂₃H₂₄N₂O; calculated 344.1883, found 344.1890 (error m/z = -1.9 ppm)

2-ethyl-3-(4-methoxyphenyl)imidazo[1,5-a]pyridin-2-ium-1-olate (2.2d) Green solid, 67 mg, 83%. ¹H NMR (400 MHz, CDCl₃) δ 7.51 (d, *J* = 9.0 Hz, 1H), 7.35 (d, *J* = 8.8 Hz, 2H), 7.31 (d, *J* = 7.3 Hz, 1H), 7.07 (d, *J* = 8.8 Hz, 2H), 6.39 (t, *J* = 6.2 Hz, 1H), 6.03 (dd, *J* = 8.9, 6.4 Hz, 1H), 4.03 (q, *J* = 7.2 Hz, 2H), 3.88 (s, 3H), 1.24 (t, *J* = 7.2 Hz, 4H). ¹³C NMR (101 MHz, CDCl₃) δ 160.9, 150.5, 131.1, 122.5, 119.2, 116.6, 116.5, 115.8, 115.3, 110.2, 108.8, 55.5, 36.6, 15.0. HRMS (ESI⁺) for C₁₆H₁₆N₂O₂; calculated 268.1206, found 268.1209(error m/z = -0.9 ppm)

2-benzyl-3-isopropylimidazo[1,5-a]pyridin-2-ium-1-olate (2.2e) Green solid, 64 mg, 80%. ¹H NMR (400 MHz, CDCl₃) δ 7.53 (d, *J* = 9.0 Hz, 1H), 7.30 – 7.24 (m, 3H), 7.22 (d, *J* = 7.1 Hz, 1H), 7.15 (d, *J* = 6.9 Hz, 2H), 6.45 (t, *J* = 7.5 Hz, 1H), 5.97 (dd, *J* = 8.8, 6.6 Hz, 1H), 5.30 (s, 2H), 3.31 (dt, *J* = 14.6, 7.3 Hz, 1H), 1.15 (d, *J* = 7.3 Hz, 6H). ¹³C NMR (101 MHz, CDCl₃) δ 150.3, 136.9, 128.8, 127.6, 126.9, 123.4, 120.5, 119.3, 116.9, 109.5, 107.0, 44.0, 25.6, 17.60. HRMS (ESI⁺) for C₁₇H₁₈N₂O; calculated 266.1414, found 266.1414(error m/z = -0.1 ppm)

3-cyclohexyl-2-(4-methoxyphenyl)imidazo[1,5-a]pyridin-2-ium-1-olate (2.2f) Green solid, 75 mg, 78%. ¹H NMR (400 MHz, CDCl₃) δ 7.48 (d, *J* = 8.9 Hz, 1H), 7.38 (d, *J* = 7.4 Hz, 1H), 7.20 (d, *J* = 8.7 Hz, 2H), 7.00 (d, *J* = 8.9 Hz, 2H), 6.48 (t, *J* = 6.5 Hz, 1H), 6.03 – 5.89 (m, 1H), 3.85 (s, 3H), 2.90 – 2.69 (m, 1H), 1.86 – 1.60 (m, 7H), 1.32 – 1.01 (m, 3H). ¹³C NMR (101 MHz, CDCl₃) δ 160.0, 151.4, 129.4, 126.9, 123.5, 120.7, 119.6, 116.8, 114.7, 108.7, 106.9, 55.5, 36.2, 28.2, 26.3, 25.4. HRMS (ESI⁺) for C₂₀H₂₂N₂O₂; calculated 322.1676, found 322.1670(error m/z = 1.8 ppm)

2-hexyl-3-(pyridin-3-yl)imidazo[1,5-a]pyridin-2-ium-1-olate (2.2g) Green solid, 66 mg, 75%. ¹H NMR (400 MHz, CDCl₃) δ 8.68 (dd, *J* = 4.9, 1.6 Hz, 2H), 7.79 – 7.75 (m, 1H), 7.53 – 7.47 (m, 2H), 7.43 (d, *J* = 7.3 Hz, 1H), 6.48 (t, *J* = 7.5 Hz, 1H), 6.12 (dd, *J* = 9.1, 6.2 Hz, 1H), 3.99 – 3.94 (m, 2H), 1.64 – 1.54 (m, 2H), 1.20 – 1.06 (m, 7H), 0.75 (t, *J* = 6.9 Hz, 3H). ¹³C NMR (101 MHz, CDCl₃) δ 151.2, 150.5, 150.0, 136.5, 124.3, 122.7, 121.6, 120.3, 116.0, 112.0, 111.7, 110.3, 41.7,

31.1, 29.3, 26.2, 22.3, 13.9. **HRMS** (ESI⁺) for C₁₈H₂₂N₃O⁺; calculated 296.1757, found 296.1755(error m/z = 0.6 ppm)

2-ethyl-3-(thiophen-2-yl)imidazo[1,5-a]pyridin-2-ium-1-olate (2.2h) Green solid, 58 mg, 79%. **¹H NMR** (400 MHz, CDCl₃) δ 7.59 (dt, *J* = 14.4, 4.1 Hz, 3H), 7.29 (dd, *J* = 3.6, 1.2 Hz, 1H), 7.24 (dd, *J* = 5.2, 3.7 Hz, 1H), 6.54 (t, *J* = 6.7 Hz, 1H), 6.17 (dd, *J* = 9.3, 6.8 Hz, 1H), 4.13 (q, *J* = 7.2 Hz, 2H), 1.31 (t, *J* = 7.2 Hz, 3H). **¹³C NMR** (101 MHz, CDCl₃) δ 150.8, 137.6, 130.3, 129.2, 128.1, 124.3, 122.4, 119.9, 117.6, 112.2, 110.4, 36.9, 15.1. **HRMS** (ESI⁺) for C₁₃H₁₂N₂OS; calculated 244.0665, found 244.0659(error m/z = 2.3 ppm)

2-ethyl-3-(4-(trifluoromethyl)phenyl)imidazo[1,5-a]pyridin-2-ium-1-olate (2.2i) Green solid, 81 mg, 88%. **¹H NMR** (400 MHz, CDCl₃) δ 7.81 (d, *J* = 8.2 Hz, 2H), 7.62 – 7.52 (m, 4H), 6.51 (t, *J* = 6.8 Hz, 1H), 6.16 (dd, *J* = 8.8, 6.5 Hz, 1H), 4.08 (q, *J* = 7.2 Hz, 2H), 1.27 (t, *J* = 7.2 Hz, 4H). **¹³C NMR** (101 MHz, CDCl₃) δ 151.2, 131.0, 129.1, 128.2, 126.8 (q, *J*_{CF} = 3.7 Hz), 124.9, 122.7, 120.4, 116.2, 113.6, 111.8, 110.5, 36.9, 14.9. **HRMS** (ESI⁺) for C₁₆H₁₃F₃N₂O; calculated 306.0974, found 306.0971(error m/z = 1.0 ppm)

2-ethyl-1-(p-tolyl)imidazo[1,5-a]quinolin-2-ium-3-olate (2.2j) Red-orange solid, 70 mg, 77%. **¹H NMR** (400 MHz, CDCl₃) δ 7.40 (dd, *J* = 13.6, 5.7 Hz, 4H), 7.34 (d, *J* = 8.1 Hz, 2H), 7.20 (t, *J* = 7.1 Hz, 1H), 6.94 – 6.85 (m, 2H), 6.39 (d, *J* = 9.2 Hz, 1H), 3.88 (q, *J* = 7.2 Hz, 2H), 2.51 (s, 3H), 1.20 (t, *J* = 7.2 Hz, 3H). **¹³C NMR** (101 MHz, CDCl₃) δ 150.4, 141.7, 130.66, 130.69, 130.5, 129.7, 129.6, 128.3, 126.7, 125.7, 124.5, 121.8, 119.4, 117.6, 110.9, 108.4, 36.6, 21.7, 15.0. **HRMS** (ESI⁺) for C₂₀H₁₉N₂O⁺; calculated 303.1492, found 303.1495(error m/z = -1.0 ppm)

2-octyl-1-(p-tolyl)imidazo[1,5-a]quinolin-2-ium-3-olate (2.2k) Red-orange solid, 85 mg, 73%. **¹H NMR** (400 MHz, CDCl₃) δ 7.40 (dd, *J* = 12.1, 4.9 Hz, 4H), 7.33 (d, *J* = 8.1 Hz, 2H), 7.19 (t, *J* =

8.1 Hz, 1H), 6.91 (t, $J = 7.8$ Hz, 2H), 6.39 (d, $J = 9.2$ Hz, 1H), 3.85 – 3.75 (m, 2H), 2.51 (s, 1H), 1.72 – 1.53 (m, 2H), 1.29 – 1.08 (m, 10H), 0.83 (t, $J = 7.1$ Hz, 3H). ^{13}C NMR (101 MHz, CDCl_3) δ 150.6, 141.6, 130.7, 130.6, 130.6, 129.8, 129.7, 128.2, 126.6, 125.6, 124.6, 121.9, 119.5, 117.7, 110.8, 108.3, 41.5, 31.7, 29.4, 29.0, 28.9, 26.6, 22.6, 21.6, 14.0. HRMS (ESI^+) for $\text{C}_{26}\text{H}_{30}\text{N}_2\text{O}$; calculated 386.2353, found 386.2351 (error $m/z = 0.4$ ppm)

2-hexyl-1-(naphthalen-2-yl)imidazo[1,5-a]quinolin-2-ium-3-olate (2.2l) Red-orange solid, 83 mg, 70%. ^1H NMR (400 MHz, CDCl_3) δ 8.17 (d, $J = 7.6$ Hz, 1H), 8.01 (d, $J = 8.2$ Hz, 1H), 7.70 (d, $J = 7.1$ Hz, 1H), 7.67 (d, $J = 3.1$ Hz, 1H), 7.60 – 7.55 (m, 1H), 7.52 (d, $J = 9.3$ Hz, 1H), 7.44 (d, $J = 8.2$ Hz, 1H), 7.40 (d, $J = 8.6$ Hz, 1H), 7.28 – 7.24 (m, 1H), 7.13 (t, $J = 8.1$ Hz, 1H), 6.78 – 6.59 (m, 2H), 6.48 (d, $J = 9.3$ Hz, 1H), 3.93 – 3.54 (m, 2H), 1.55 – 1.43 (m, 2H), 1.11 – 0.89 (m, 6H), 0.69 (t, $J = 7.0$ Hz, 3H). ^{13}C NMR (101 MHz, CDCl_3) δ 150.9, 133.8, 132.6, 132.0, 130.6, 130.2, 129.6, 129.0, 128.6, 128.4, 128.2, 127.4, 126.7, 126.0, 125.6, 125.1, 124.4, 119.8, 119.5, 117.2, 111.1, 41.8, 30.9, 29.3, 26.1, 22.1, 13.8. HRMS (ESI^+) for $\text{C}_{27}\text{H}_{26}\text{N}_2\text{O}$; calculated 394.2040, found 394.2042 (error $m/z = -0.4$ ppm)

2-ethyl-1-(4-methoxyphenyl)imidazo[1,5-a]quinolin-2-ium-3-olate (2.2m) Red-orange solid, 57 mg, 60%. ^1H NMR (400 MHz, CDCl_3) δ 7.44 – 7.35 (m, 4H), 7.21 (t, $J = 8.0$ Hz, 1H), 7.12 (d, $J = 8.8$ Hz, 2H), 6.99 – 6.87 (m, 2H), 6.40 (d, $J = 9.2$ Hz, 1H), 3.93 (s, 3H), 3.90 (q, $J = 7.3$ Hz, 2H), 1.22 (t, $J = 7.2$ Hz, 3H). ^{13}C NMR (101 MHz, CDCl_3) δ 161.6, 150.3, 132.2, 130.8, 129.7, 128.3, 126.6, 125.7, 121.6, 119.4, 119.3, 117.6, 115.4, 110.9, 108.4, 55.5, 36.6, 15.0. HRMS (ESI^+) for $\text{C}_{20}\text{H}_{19}\text{N}_2\text{O}_2^+$; calculated 319.1441, found 319.1438 (error $m/z = 1.0$ ppm)

2-benzyl-5-(chlorocarbonyl)-3-(p-tolyl)-2H-imidazo[1,5-a]pyridin-4-ium-1-olate (2.2n) Blue solid, 98 mg, 87%. ^1H NMR (400 MHz, CDCl_3) δ 7.95 (dd, $J = 8.0, 1.1$ Hz, 1H), 7.85 (dd, $J = 8.0, 1.0$ Hz, 1H), 7.28 – 7.21 (m, 5H), 7.11 – 7.02 (m, 4H), 6.13 (t, $J = 7.9$ Hz, 1H), 5.09 (s, 2H), 2.40

(s, 3H). ^{13}C NMR (101 MHz, CDCl_3) δ 157.5, 154.3, 141.4, 138.0, 136.2, 130.3, 130.1, 128.7, 127.8, 127.3, 126.7, 126.6, 123.9, 118.6, 117.2, 106.8, 45.3, 21.7. Crystallographically characterized.

5-(chlorocarbonyl)-2-hexyl-3-(naphthalen-2-yl)imidazo[1,5-a]pyridin-2-ium-1-olate (2.2o) Blue solid, 107 mg, 88%. ^1H NMR (400 MHz, CDCl_3) δ 8.05 (d, $J = 8.3$ Hz, 1H), 7.99 (d, $J = 8.2$ Hz, 1H), 7.94 (ddd, $J = 8.1, 4.3, 1.4$ Hz, 2H), 7.68 – 7.61 (m, 1H), 7.61 – 7.55 (m, 1H), 7.55 – 7.48 (m, 2H), 7.22 (d, $J = 8.6$ Hz, 1H), 6.20 (t, $J = 7.9$ Hz, 1H), 4.02 (ddd, $J = 13.6, 9.3, 6.0$ Hz, 1H), 3.77 (ddd, $J = 13.5, 9.3, 6.0$ Hz, 1H), 1.56 – 1.32 (m, 2H), 1.08 – 0.86 (m, 6H), 0.69 (t, $J = 7.0$ Hz, 3H). ^{13}C NMR (101 MHz, CDCl_3) δ 157.3, 153.6, 136.8, 133.7, 131.6, 129.9, 129.6, 128.2, 127.1, 126.97, 126.98, 125.5, 124.8, 124.1, 123.5, 119.4, 117.6, 106.9, 77.2, 42.5, 30.8, 28.4, 26.0, 22.1, 13.8. HRMS (ESI $^+$) for $\text{C}_{24}\text{H}_{24}\text{ClN}_2\text{O}_2^+$; calculated 407.1521, found 407.1514 (error m/z = 1.8 ppm)

2-benzyl-5-(benzylcarbamoyl)-3-(p-tolyl)-2H-imidazo[1,5-a]pyridin-4-ium-1-olate (2.2p) Orange solid, 105 mg, 78%. ^1H NMR (400 MHz, CDCl_3) δ 7.95 (t, $J = 5.6$ Hz, 1H), 7.35 (dd, $J = 8.8, 1.2$ Hz, 1H), 7.24 (dt, $J = 6.6, 5.6$ Hz, 3H), 7.18 – 7.09 (m, 7H), 7.02 (d, $J = 8.1$ Hz, 2H), 6.92 (dd, $J = 6.5, 2.9$ Hz, 2H), 6.66 (dd, $J = 6.7, 1.2$ Hz, 1H), 5.85 (dd, $J = 8.7, 6.7$ Hz, 1H), 4.91 (s, 2H), 3.94 (d, $J = 5.7$ Hz, 2H), 2.38 (s, 3H). ^{13}C NMR (101 MHz, CDCl_3) δ 162.3, 151.3, 140.3, 137.6, 136.5, 129.6, 129.0, 128.5, 128.4, 127.9, 127.6, 127.5, 127.4, 125.4, 124.1, 123.4, 122.8, 119.6, 112.3, 107.6, 44.8, 43.3, 21.6. HRMS (ESI $^+$) for $\text{C}_{29}\text{H}_{25}\text{N}_3\text{O}_2$; calculated 447.1941, found 447.1936 (error m/z = 1.3 ppm)

5-(benzylcarbamoyl)-2-hexyl-3-(naphthalen-2-yl)imidazo[1,5-a]pyridin-2-ium-1-olate (2.2q) Orange solid, 113 mg, 79%. ^1H NMR (400 MHz, cdcl_3) δ 8.01 (dd, $J = 7.7, 1.3$ Hz, 1H), 7.96 (d, $J = 8.2$ Hz, 1H), 7.59 (dd, $J = 12.2, 4.6$ Hz, 2H), 7.55 (d, $J = 7.9$ Hz, 1H), 7.53 – 7.47 (m, 1H),

7.40 (t, $J = 7.2$ Hz, 1H), 7.18 (dd, $J = 5.8, 2.4$ Hz, 4H), 6.79 (dd, $J = 6.3, 3.1$ Hz, 2H), 6.73 – 6.65 (m, 2H), 5.99 (dd, $J = 8.7, 6.7$ Hz, 1H), 3.96 – 3.83 (m, 1H), 3.74 (dd, $J = 14.6, 6.0$ Hz, 1H), 3.66 – 3.54 (m, 1H), 3.28 (dd, $J = 14.6, 5.1$ Hz, 1H), 1.49 – 1.24 (m, 3H), 1.04 – 0.86 (m, 6H), 0.66 (t, $J = 7.0$ Hz, 3H). ^{13}C NMR (101 MHz, CDCl_3) δ 162.1, 151.5, 137.1, 133.7, 130.9, 129.7, 129.1, 129.0, 128.5, 128.2, 127.7, 127.6, 127.4, 126.7, 125.7, 125.2, 124.4, 124.3, 122.4, 117.4, 113.1, 107.3, 43.2, 42.0, 30.9, 28.8, 26.0, 22.1, 13.8. **HRMS** (ESI^+) for $\text{C}_{31}\text{H}_{31}\text{N}_3\text{O}_2$; calculated 477.2411, found 477.241 (error $m/z = -0.1$ ppm)

Dimethyl 3-(p-tolyl)indolizine-1,2-dicarboxylate (2.4a)²⁴ Yellow solid, 73 mg, 75%. ^1H NMR (400 MHz, CDCl_3) δ 8.22 (d, $J = 9.1$ Hz, 1H), 8.03 (d, $J = 7.0$ Hz, 1H), 7.39 (d, $J = 7.8$ Hz, 2H), 7.30 (d, $J = 7.8$ Hz, 2H), 7.16 – 7.06 (m, 1H), 6.70 (t, $J = 6.8$ Hz, 1H), 3.90 (s, 3H), 3.81 (s, 3H), 2.42 (s, 3H). ^{13}C NMR (101 MHz, CDCl_3) δ 166.9, 164.3, 139.1, 135.2, 129.8, 129.8, 125.8, 125.2, 123.6, 123.4, 121.9, 120.3, 113.3, 101.8, 52.4, 51.3, 21.4. **HRMS** (ESI^+) for $\text{C}_{19}\text{H}_{17}\text{NO}_4\text{Na}^+$; calculated 346.10498, found 346.10410 (error $m/z = -2.54$ ppm)

1-Phenyl-3-(p-tolyl)indolizine (2.4b) Brown solid, 56 mg, 66%. ^1H NMR (400 MHz, CDCl_3) δ 8.27 (d, $J = 7.2$ Hz, 1H), 7.79 (d, $J = 9.1$ Hz, 1H), 7.66 (d, $J = 7.1$ Hz, 2H), 7.52 (d, $J = 8.0$ Hz, 2H), 7.46 (t, $J = 7.7$ Hz, 2H), 7.33 (d, $J = 7.9$ Hz, 2H), 7.27 (dd, $J = 10.0, 4.8$ Hz, 1H), 7.04 (s, 1H), 6.76 (dd, $J = 8.7, 6.8$ Hz, 1H), 6.52 (t, $J = 6.8$ Hz, 1H), 2.45 (s, 3H). ^{13}C NMR (101 MHz, CDCl_3) δ 137.2, 136.4, 130.0, 129.7, 129.3, 128.7, 128.2, 127.6, 125.8, 125.4, 122.7, 118.5, 117.9, 115.1, 113.6, 111.0, 21.3. **HRMS** (ESI^+) for $\text{C}_{21}\text{H}_{18}\text{N}^+$; calculated 284.14338, found 284.14348 (error $m/z = 0.36$ ppm)

Methyl 3-(4-methoxyphenyl)indolizine-1-carboxylate (2.4c)²⁵ Yellow solid, 58 mg, 69%. ^1H NMR (400 MHz, CDCl_3) δ 8.27 (d, $J = 9.0$ Hz, 1H), 8.23 (d, $J = 7.1$ Hz, 1H), 7.47 (d, $J = 8.8$ Hz, 2H), 7.25 (s, 1H), 7.12 – 7.01 (m, 3H), 6.71 (td, $J = 6.9, 1.2$ Hz, 1H), 3.94 (s, 3H), 3.90 (s, 3H).

^{13}C NMR (101 MHz, CDCl_3) δ 165.4, 159.5, 136.1, 130.1, 126.3, 123.5, 123.3, 122.0, 120.0, 115.5, 114.5, 112.5, 103.6, 55.4, 50.9. HRMS (ESI⁺) for $\text{C}_{17}\text{H}_{16}\text{O}_3\text{N}^+$; calculated 282.11247, found 282.11293 (error m/z = 1.63 ppm)

Dimethyl 3-isopropylindolizine-1,2-dicarboxylate (2.4d) Yellow solid, 62 mg, 75%. ^1H NMR (400 MHz, CDCl_3) δ 8.18 (d, J = 9.1 Hz, 1H), 7.93 (d, J = 7.2 Hz, 1H), 7.07 (ddd, J = 9.1, 6.6, 0.9 Hz, 1H), 6.79 (td, J = 7.0, 1.3 Hz, 1H), 3.94 (s, 3H), 3.86 (s, 3H), 3.41 – 3.28 (m, 1H), 1.39 (d, J = 7.1 Hz, 6H). ^{13}C NMR (101 MHz, CDCl_3) δ 168.2, 164.2, 134.8, 128.8, 123.2, 122.4, 120.5, 119.7, 113.1, 101.1, 52.5, 51.1, 25.7, 20.0. HRMS (ESI⁺) for $\text{C}_{15}\text{H}_{17}\text{NO}_4\text{Na}^+$; calculated 298.10498, found 298.10534 (error m/z = 1.21 ppm)

Dimethyl 3-(thiophen-2-yl)indolizine-1,2-dicarboxylate (2.4e) Brown solid, 67 mg, 71%. ^1H NMR (400 MHz, CDCl_3) δ 8.21 (dd, J = 11.7, 8.1 Hz, 2H), 7.51 (dd, J = 5.2, 1.1 Hz, 1H), 6.78 (td, J = 6.9, 1.3 Hz, 1H), 3.89 (s, 3H), 3.85 (s, 3H). ^{13}C NMR (101 MHz, CDCl_3) δ 166.5, 164.0, 135.6, 129.7, 128.7, 128.4, 128.1, 127.6, 124.0, 123.8, 120.2, 117.6, 113.8, 102.0, 52.5, 51.3. HRMS (ESI⁺) for $\text{C}_{16}\text{H}_{13}\text{NSO}_4\text{Na}^+$; calculated 338.04575, found 338.04639 (error m/z = 1.89 ppm)

Dimethyl 3-(4-nitrophenyl)indolizine-1,2-dicarboxylate (2.4f)²⁶ Orange solid, 73 mg, 69%. ^1H NMR (400 MHz, CDCl_3) δ 8.37 (d, J = 6.9 Hz, 2H), 8.27 (d, J = 9.2 Hz, 1H), 8.08 (d, J = 7.1 Hz, 1H), 7.73 (d, J = 8.9 Hz, 2H), 7.20 (dd, J = 9.2, 6.7 Hz, 1H), 6.83 (dd, J = 10.9, 4.1 Hz, 1H), 3.92 (s, 3H), 3.84 (s, 3H). ^{13}C NMR (101 MHz, CDCl_3) δ 166.3, 163.9, 147.7, 135.9, 135.6, 130.4, 129.2, 124.4, 124.3, 123.4, 123.0, 122.3, 120.8, 114.4, 52.7, 51.5. HRMS (ESI⁺) for $\text{C}_{18}\text{H}_{14}\text{N}_2\text{NaO}_4$; calculated 377.0744, found 377.0755 (error m/z = -2.9 ppm)

Dimethyl 3-cyclohexylindolizine-1,2-dicarboxylate (2.4g) Yellow solid, 64 mg, 67%. ^1H NMR (400 MHz, CDCl_3) δ 8.17 (d, J = 9.1 Hz, 1H), 7.94 (d, J = 7.1 Hz, 1H), 7.07 (dd, J = 8.9, 6.8 Hz,

1H), 6.78 (t, $J = 6.8$ Hz, 1H), 3.95 (s, 3H), 3.86 (s, 3H), 2.91 (tt, $J = 12.1, 2.9$ Hz, 1H), 1.97 (d, $J = 12.1$ Hz, 2H), 1.88 (d, $J = 12.9$ Hz, 2H), 1.78 (d, $J = 11.8$ Hz, 1H), 1.63 (m, 2H), 1.35 (m, 3H). ^{13}C NMR (101 MHz, CDCl_3) δ 168.4, 164.3, 134.7, 127.9, 123.1, 122.4, 120.5, 120.0, 113.0, 101.1, 52.5, 51.1, 36.4, 30.4, 26.8, 25.9. HRMS (ESI⁺) for $\text{C}_{18}\text{H}_{22}\text{NO}_4^+$; calculated 316.15433, found 316.15424 (error $m/z = -0.29$ ppm)

Dimethyl 3-(pyridin-3-yl)indolizine-1,2-dicarboxylate (2.4h) Brown-red solid, 80 mg, 86%. ^1H NMR (400 MHz, CDCl_3) δ 8.76 (d, $J = 1.7$ Hz, 1H), 8.68 (dd, $J = 4.9, 1.5$ Hz, 1H), 8.23 (d, $J = 9.2$ Hz, 1H), 7.97 (d, $J = 7.1$ Hz, 1H), 7.86 (dt, $J = 7.9, 1.9$ Hz, 1H), 7.45 (dd, $J = 7.8, 4.9$ Hz, 1H), 7.15 (dd, $J = 9.1, 6.7$ Hz, 1H), 6.76 (td, $J = 7.0, 1.1$ Hz, 1H), 3.90 (s, 3H), 3.80 (s, 3H). ^{13}C NMR (101 MHz, CDCl_3) δ 166.2, 164.0, 150.6, 150.0, 137.8, 135.6, 125.4, 124.0, 123.8, 123.0, 123.0, 121.5, 120.6, 114.0, 102.60, 52.5, 51.4. HRMS (ESI⁺) for $\text{C}_{17}\text{H}_{15}\text{N}_2\text{O}_4^+$; calculated 311.10263, found 311.10303 (error $m/z = 1.29$ ppm)

Dimethyl 3-(4-(trifluoromethyl)phenyl)indolizine-1,2-dicarboxylate (2.4i)²⁷ Yellow solid, 69 mg, 61%. ^1H NMR (400 MHz, CDCl_3) δ 8.24 (d, $J = 9.1$ Hz, 1H), 8.03 (d, $J = 7.1$ Hz, 1H), 7.76 (d, $J = 8.1$ Hz, 2H), 7.65 (d, $J = 8.1$ Hz, 2H), 7.15 (dd, $J = 8.6, 7.0$ Hz, 1H), 6.76 (t, $J = 6.5$ Hz, 1H), 3.90 (s, 3H), 3.82 (s, 3H). ^{13}C NMR (101 MHz, CDCl_3) δ 166.5, 164.0, 135.5, 132.7, 130.2, 126.1 (q, $J_{\text{CF}} = 3.7$ Hz), 125.2, 123.9, 123.2, 123.2, 122.8, 122.5, 120.6, 114.0, 102.5, 52.6, 51.4. HRMS (ESI⁺) for $\text{C}_{19}\text{H}_{15}\text{F}_3\text{NO}_4^+$; calculated 378.09477, found 378.09528 (error $m/z = 1.34$ ppm)

1-(methoxymethyl)-3-(p-tolyl)indolizine (2.4j) Colorless oil, 43 mg, 57%. ^1H NMR (400 MHz, CDCl_3) δ 8.21 (d, $J = 7.0$ Hz, 1H), 7.50 (d, $J = 8.9$ Hz, 1H), 7.45 (d, $J = 7.7$ Hz, 2H), 7.28 (d, $J = 7.8$ Hz, 2H), 6.85 (s, 1H), 6.74 – 6.65 (m, 1H), 6.48 (t, $J = 6.6$ Hz, 1H), 4.69 (s, 2H), 3.41 (s, 3H), 2.41 (s, 3H). ^{13}C NMR (101 MHz, CDCl_3) δ 137.0, 130.7, 129.6, 129.4, 128.9, 128.1, 122.4, 117.6,

117.0, 114.9, 110.7, 109.8, 66.7, 57.5, 21.3. **HRMS** (ESI⁺) for C₁₇H₁₇NO; calculated 251.13047, found 251.13041 (error m/z = -0.22 ppm)

3-(p-tolyl)-1-(trimethylsilyl)indolizine (2.4k) Colorless oil, 49 mg, 59%. **¹H NMR** (400 MHz, CDCl₃) δ 8.29 (d, *J* = 7.1 Hz, 1H), 7.52 (d, *J* = 9.0 Hz, 1H), 7.48 (d, *J* = 8.0 Hz, 2H), 7.30 (d, *J* = 7.8 Hz, 2H), 6.90 (s, 1H), 6.78 – 6.71 (m, 1H), 6.53 (d, *J* = 7.3 Hz, 1H), 2.43 (s, 3H), 0.39 (s, 9H). **¹³C NMR** (101 MHz, CDCl₃) δ 138.2, 136.9, 129.61, 129.58, 128.07, 128.06, 123.0, 120.4, 120.0, 117.3, 110.7, 107.6, 21.3, 0.2. **HRMS** (ESI⁺) for C₁₈H₂₁NSi; calculated 279.1438, found 279.1440 (error m/z = -0.9 ppm)

Dimethyl 1-(p-tolyl)pyrrolo[1,2-a]quinoline-2,3-dicarboxylate (2.4l) Yellow solid, 97 mg, 87%. **¹H NMR** (400 MHz, CDCl₃) δ 8.23 (d, *J* = 9.4 Hz, 1H), 7.71 (dd, *J* = 8.0, 1.2 Hz, 1H), 7.42 – 7.29 (m, 7H), 7.20 – 7.14 (m, 1H), 3.94 (s, 3H), 3.75 (s, 3H), 2.49 (s, 3H). **¹³C NMR** (101 MHz, CDCl₃) δ 166.7, 164.3, 139.2, 134.4, 133.9, 130.3, 129.6, 129.3, 128.9, 127.7, 125.5, 125.0, 124.7, 122.8, 118.4, 117.8, 104.6, 52.3, 51.5, 21.5. **HRMS** (ESI⁺) for C₂₃H₂₀NO₄⁺; calculated 374.13868, found 374.13907 (error m/z = 1.04 ppm)

Dimethyl 1-(naphthalen-2-yl)pyrrolo[1,2-a]quinoline-2,3-dicarboxylate (2.4m) Yellow solid, 99 mg, 81%. **¹H NMR** (400 MHz, CDCl₃) δ 8.30 (d, *J* = 9.5 Hz, 1H), 8.04 (d, *J* = 8.2 Hz, 1H), 7.94 (d, *J* = 8.2 Hz, 1H), 7.67 (td, *J* = 7.4, 1.3 Hz, 2H), 7.61 (dd, *J* = 8.1, 7.1 Hz, 1H), 7.47 (ddd, *J* = 8.2, 6.5, 1.5 Hz, 1H), 7.43 (d, *J* = 9.5 Hz, 1H), 7.35 – 7.27 (m, 2H), 7.20 (ddd, *J* = 8.0, 6.8, 1.4 Hz, 1H), 6.93 – 6.83 (m, 2H), 3.94 (s, 3H), 3.54 (s, 3H). **¹³C NMR** (101 MHz, CDCl₃) δ 166.3, 164.4, 134.7, 133.9, 133.5, 133.0, 130.1, 129.9, 129.5, 128.8, 128.4, 128.1, 127.4, 127.1, 126.5, 125.6, 125.5, 125.3, 125.2, 124.7, 123.5, 118.4, 117.1, 104.8, 52.1, 51.5. **HRMS** (ESI⁺) for C₂₆H₂₀NO₄⁺; calculated 410.13868, found 410.13875 (error m/z = 0.15 ppm)

Dimethyl 1-(4-methoxyphenyl)pyrrolo[1,2-a]quinoline-2,3-dicarboxylate (2.4n) Brown solid, 109 mg, 93%. $^1\text{H NMR}$ (400 MHz, CDCl_3) δ 8.19 (d, $J = 9.4$ Hz, 1H), 7.68 (dd, $J = 7.8, 1.3$ Hz, 1H), 7.39 (d, $J = 8.7$ Hz, 3H), 7.35 (d, $J = 8.1$ Hz, 1H), 7.31 (dd, $J = 8.7, 6.3$ Hz, 2H), 7.16 (ddd, $J = 8.8, 7.3, 1.6$ Hz, 1H), 7.01 (d, $J = 8.8$ Hz, 2H), 3.91 (s, 3H), 3.90 (s, 3H), 3.73 (s, 3H). $^{13}\text{C NMR}$ (101 MHz, CDCl_3) δ 166.7, 164.3, 160.2, 134.4, 134.0, 131.8, 129.1, 128.9, 127.7, 125.5, 125.0, 124.7, 124.4, 122.8, 118.4, 117.6, 114.3, 104.5, 55.3, 52.3, 51.5. **HRMS** (ESI^+) for $\text{C}_{23}\text{H}_{20}\text{NO}_5^+$; calculated 390.13360, found 390.13391 (error $m/z = 0.80$ ppm)

Methyl 1-(4-methoxyphenyl)pyrrolo[1,2-a]quinoline-3-carboxylate (2.4o) Yellow solid, 90 mg, 91%. $^1\text{H NMR}$ (400 MHz, CDCl_3) δ 8.26 (d, $J = 9.4$ Hz, 1H), 7.70 (dd, $J = 7.8, 1.4$ Hz, 1H), 7.52 (d, $J = 8.7$ Hz, 1H), 7.39 (d, $J = 8.8$ Hz, 2H), 7.33 (dd, $J = 12.4, 8.2$ Hz, 1H), 7.18 (ddd, $J = 8.7, 7.2, 1.6$ Hz, 1H), 7.07 (s, 1H), 7.01 (d, $J = 8.8$ Hz, 2H), 3.92 (s, 3H), 3.91 (s, 3H). $^{13}\text{C NMR}$ (101 MHz, CDCl_3) δ 165.4, 159.7, 135.4, 134.1, 131.0, 130.3, 128.7, 127.3, 127.1, 125.4, 124.2, 123.8, 118.6, 117.7, 117.2, 114.1, 106.4, 55.4, 51.1. **HRMS** (ESI^+) for $\text{C}_{21}\text{H}_{17}\text{NO}_3$; calculated 331.1203, found 331.1211 (error $m/z = -2.4$ ppm)

(1-(4-methoxyphenyl)pyrrolo[1,2-a]quinoline-2,3-diyl)bis(phenylmethanone) (2.4p) Yellow solid, 131 mg, 91%. $^1\text{H NMR}$ (400 MHz, CDCl_3) δ 8.05 (d, $J = 9.4$ Hz, 1H), 7.75 (dd, $J = 7.8, 1.2$ Hz, 1H), 7.49 – 7.28 (m, 11H), 7.22 (dt, $J = 15.5, 4.7$ Hz, 3H), 7.14 (t, $J = 7.8$ Hz, 2H), 6.98 (d, $J = 8.7$ Hz, 2H), 3.87 (s, 3H). $^{13}\text{C NMR}$ (101 MHz, CDCl_3) δ 193.0, 191.7, 160.2, 140.8, 139.5, 134.5, 134.0, 132.4, 132.1, 131.5, 131.2, 129.0, 128.9, 128.8, 128.7, 128.0, 127.94, 127.87, 126.0, 125.7, 124.9, 124.4, 118.5, 118.1, 115.5, 114.2, 55.3. **HRMS** (ESI^+) for $\text{C}_{33}\text{H}_{24}\text{NO}_3^+$; calculated 482.17507, found 482.17467 (error $m/z = -0.83$ ppm)

Dimethyl 5-(benzylcarbamoyl)-3-(p-tolyl)indolizine-1,2-dicarboxylate (2.4q) Yellow-green solid, 115 mg, 84%. $^1\text{H NMR}$ (400 MHz, CDCl_3) δ 8.16 (d, $J = 9.0$ Hz, 1H), 7.34 – 7.24 (m, 3H), 7.17

(dd, $J = 12.7, 4.1$ Hz, 6H), 6.92 (dd, $J = 9.0, 6.8$ Hz, 1H), 6.79 (d, $J = 8.0$ Hz, 1H), 6.58 (t, $J = 5.3$ Hz, 1H), 3.84 (d, $J = 5.2$ Hz, 2H), 3.77 (s, 3H), 3.73 (s, 3H), 2.39 (d, $J = 6.6$ Hz, 3H). ^{13}C NMR (101 MHz, CDCl_3) δ 166.7, 164.2, 162.3, 138.6, 136.8, 135.9, 132.6, 129.1, 128.8, 128.7, 128.1, 127.8, 127.7, 126.5, 123.9, 122.0, 121.6, 115.8, 103.1, 52.4, 51.4, 43.8, 21.5. **HRMS** (ESI^+) for $\text{C}_{27}\text{H}_{24}\text{N}_2\text{NaO}_5^+$; calculated 479.1577, found 479.1584 (error $m/z = -1.4$ ppm)

Methyl 5-(benzylcarbamoyl)-3-(p-tolyl)indolizine-1-carboxylate (2.4r) Yellow solid, 62 mg, 52%. ^1H NMR (400 MHz, CDCl_3) δ 8.33 (dd, $J = 8.6, 1.6$ Hz, 1H), 7.30 (dd, $J = 15.4, 7.4$ Hz, 5H), 7.23 (t, $J = 3.9$ Hz, 3H), 7.14 (d, $J = 6.3$ Hz, 2H), 7.01 – 6.91 (m, 2H), 6.09 (t, $J = 5.0$ Hz, 1H), 3.91 (d, $J = 5.2$ Hz, 2H), 3.86 (s, 3H), 2.42 (s, 3H). ^{13}C NMR (101 MHz, CDCl_3) δ 165.2, 162.7, 137.7, 137.2, 136.8, 132.1, 130.5, 129.3, 128.8, 128.2, 128.1, 127.8, 127.1, 122.0, 120.7, 118.5, 115.6, 105.7, 51.1, 44.0, 21.4. **HRMS** (ESI^+) for $\text{C}_{25}\text{H}_{22}\text{N}_2\text{O}_3$; calculated 398.16249, found 397.16176 (error $m/z = -1.85$ ppm)

Dimethyl 5-(benzylcarbamoyl)-3-(naphthalen-2-yl)indolizine-1,2-dicarboxylate (2.4s) Yellow solid, 99 mg, 67%. ^1H NMR (500 MHz, CDCl_3) δ 8.43 (dd, $J = 9.2, 1.2$ Hz, 1H), 7.97 (dd, $J = 12.5, 8.2$ Hz, 2H), 7.70 – 7.57 (m, 2H), 7.51 (t, $J = 7.5$ Hz, 1H), 7.33 (t, $J = 7.6$ Hz, 1H), 7.22 (dd, $J = 7.9, 5.4$ Hz, 4H), 7.13 – 7.07 (m, 1H), 6.84 (dd, $J = 6.5, 2.8$ Hz, 2H), 6.79 (dd, $J = 6.7, 1.2$ Hz, 1H), 5.39 – 5.32 (m, 1H), 3.92 (s, 3H), 3.75 (dd, $J = 14.4, 6.7$ Hz, 2H), 3.60 (s, 3H). ^{13}C NMR (126 MHz, CDCl_3) δ 166.3, 164.1, 161.9, 136.4, 136.2, 133.5, 132.9, 132.3, 130.0, 129.6, 128.8, 128.6, 127.9, 127.73, 127.70, 126.7, 126.1, 125.9, 125.1, 125.0, 124.8, 122.1, 122.0, 115.3, 103.5, 52.3, 51.5, 43.4. **HRMS** (ESI^+) for $\text{C}_{30}\text{H}_{25}\text{N}_2\text{O}_5^+$; calculated 493.17580, found 493.17636 (error $m/z = 1.14$ ppm)

N-benzyl-1-phenyl-3-(p-tolyl)indolizine-5-carboxamide (2.4t) Yellow solid, 59 mg, 47%. ^1H NMR (400 MHz, CDCl_3) δ 7.84 (dd, $J = 9.0, 1.1$ Hz, 1H), 7.61 (d, $J = 7.1$ Hz, 2H), 7.47 (t, $J = 7.7$

Hz, 2H), 7.39 (d, $J = 8.0$ Hz, 2H), 7.35 – 7.25 (m, 5H), 7.20 – 7.11 (m, 2H), 7.04 (s, 1H), 6.95 (dd, $J = 6.6, 1.0$ Hz, 1H), 6.76 (dd, $J = 9.0, 6.7$ Hz, 1H), 5.90 (t, $J = 5.1$ Hz, 1H), 3.95 (d, $J = 5.3$ Hz, 2H), 2.46 (s, 3H). ^{13}C NMR (126 MHz, CDCl_3) δ 163.3, 137.2, 137.0, 135.6, 131.6, 131.3, 131.1, 129.4, 128.8, 128.7, 128.2, 128.1, 127.7, 127.6, 126.4, 126.0, 121.0, 117.7, 116.5, 116.5, 115.3, 43.8, 21.4. HRMS (ESI⁺) for $\text{C}_{29}\text{H}_{24}\text{N}_2\text{O}$; calculated 416.18831, found 416.18848 (error $m/z = 0.39$ ppm)

Methyl 3-(p-tolyl)indolizine-1-carboxylate (2.5)²⁴ Yellow-green solid, 59 mg, 74%. ^1H NMR (400 MHz, CDCl_3) δ 8.28 – 8.23 (m, 2H), 7.42 (d, $J = 8.1$ Hz, 2H), 7.30 (d, $J = 7.9$ Hz, 2H), 7.25 (s, 1H), 7.06 (dd, $J = 10.0, 6.6$ Hz, 1H), 6.69 (t, $J = 6.3$ Hz, 1H), 3.91 (s, 3H), 2.42 (s, 3H). ^{13}C NMR (101 MHz, CDCl_3) δ 165.4, 138.0, 136.3, 129.8, 128.6, 128.3, 126.6, 123.4, 122.2, 120.1, 115.7, 112.5, 103.7, 50.9, 21.3. HRMS (ESI⁺) for $\text{C}_{17}\text{H}_{16}\text{O}_2\text{N}^+$; calculated 266.11756, found 266.11697 (error $m/z = -2.20$ ppm)

2.5 References

- (1) This chapter is a copy of a published communication and is reproduced with permission from Huseyin Erguven, David C. Leitch, Evan N. Keyzer and Bruce A. Arndtsen, “Development and Cycloaddition Reactivity of a New Class of Pyridine-Based Mesoionic 1,3-Dipole” *Angew. Chem.* **2017**, *129*, 6174. Copyright 2017 Wiley-VCH Verlag GmbH & Co. KGaA, Weinheim.
- (2) For reviews: a) Padwa, A., *1,3-dipolar cycloaddition chemistry*. Wiley: 1984. b) Reissig, H.-U.; Zimmer, R., *Angew. Chem. Int. Ed.* **2014**, *53*, 9708-9710. c) Reissig, H.-U.; Zimmer, R., *Angew. Chem. Int. Ed.* **2014**, *53*, 9708-9710. d) Singh, M. S.; Chowdhury, S.; Koley, S., *Tetrahedron* **2016**, *72*, 1603-1644.

- (3) a) Kolb, H. C.; Finn, M. G.; Sharpless, K. B., *Angew. Chem. Int. Ed.* **2001**, *40*, 2004-2021; *Angew. Chem.* **2001**, *113*, 2056-2075. b) Moses, J. E.; Moorhouse, A. D., *Chem. Soc. Rev.* **2007**, *36*, 1249-1262.
- (4) Reviews: a) Narayan, R.; Potowski, M.; Jia, Z.-J.; Antonchick, A. P.; Waldmann, H., *Acc. Chem. Res.* **2014**, *47*, 1296-1310. b) Sletten, E. M.; Bertozzi, C. R., *Acc. Chem. Res.* **2011**, *44*, 666-676. c) Lutz, J.-F.; Zarafshani, Z., *Adv. Drug Delivery Rev.* **2008**, *60*, 958-970. d) Kolb, H. C.; Sharpless, K. B., *Drug Discovery Today* **2003**, *8*, 1128-1137.
- (5) For a review: a) Delaittre, G.; Guimard, N. K.; Barner-Kowollik, C., *Acc. Chem. Res.* **2015**, *48*, 1296-1307. For representative examples: b) Vretik, L.; Ritter, H., *Macromolecules* **2003**, *36*, 6340-6345. c) Lee, I.-H.; Kim, H.; Choi, T.-L., *J. Am. Chem. Soc.* **2013**, *135*, 3760-3763. d) Handa, N. V.; Li, S.; Gerbec, J. A.; Sumitani, N.; Hawker, C. J.; Klinger, D., *J. Am. Chem. Soc.* **2016**, *138*, 6400-6403. e) Leitch, D. C.; Kayser, L. V.; Han, Z.-Y.; Siamaki, A. R.; Keyzer, E. N.; Gefen, A.; Arndtsen, B. A., *Nat. Comm.* **2015**, *6*, 7411.
- (6) Reviews: a) Xi, W.; Scott, T. F.; Kloxin, C. J.; Bowman, C. N., *Adv. Funct. Mater.* **2014**, *24*, 2572-2590. b) Yan, W.; Seifermann, S. M.; Pierrat, P.; Bräse, S., *Org. Biomol. Chem.* **2015**, *13*, 25-54.
- (7) Huisgen, R., *Angew. Chem. Int. Ed Engl.* **1963**, *2*, 633-645; *Angew. Chem.* **1963**, *75*, 742-754.
- (8) For an overview of mesoionic heterocycles in cycloaddition: a) Gribble, G. W., Mesoionic Ring Systems. In *Synthetic Applications of 1,3-Dipolar Cycloaddition Chemistry Toward Heterocycles and Natural Products*, **2003**, pp 681-753; For recent reviews, see: b) Mgnchnones: see Ref. [2b]; c) Sydnones: Browne, D. L.; Harrity, J. P. A., *Tetrahedron* **2010**, *66*, 553-568. d) Carbenes: Crabtree, R. H., *Coord. Chem. Rev.* **2013**, *257*, 755-766. e) Tetrazoles: Moderhack, D., *Heterocycles* **2016**, *92*, 185– 233.
- (9) a) Morin, M. S. T.; St-Cyr, D. J.; Arndtsen, B. A.; Krenske, E. H.; Houk, K. N., *J. Am. Chem. Soc.* **2013**, *135*, 17349-17358. b) Morin, M. S. T.; Arndtsen, B. A., *Org. Lett.* **2014**, *16*, 1056-1059. c) St-Cyr, D. J.; Morin, M. S. T.; Bélanger-Gariépy, F.; Arndtsen, B. A.; Krenske, E. H.; Houk, K. N., *J. Org. Chem.* **2010**, *75*, 4261-4273.

- (10) a) Besthorn, E.; Jaeglé, G., *Ber. Dtsch. Chem. Ges.* **1894**, *27*, 907-914. b) Besthorn, E.; Ibele, J., *Ber. Dtsch. Chem. Ges.* **1904**, *37*, 1236-1243.
- (11) a) Krollpfeiffer, F.; Schneider, K., *Justus Liebigs Ann. Chem.* **1937**, *530*, 34-50. b) Brown, B. R.; Wild, E. H., *J. Chem. Soc.* **1956**, 1158-1163.
- (12) For reviews: a) Sharma, V.; Kumar, V., *Med. Chem. Res.* **2014**, *23*, 3593-3606. b) Singh, G. S.; Mmatli, E. E., *Eur. J. Med. Chem.* **2011**, *46*, 5237-5257. c) Han, W. B.; Zhang, A. H.; Deng, X. Z.; Lei, X.; Tan, R. X., *Org. Lett.* **2016**, *18*, 1816-1819.
- (13) Allen, F.; Kennard, O.; Watson, D.; Brammer, L.; Orpen, A.; Taylor, R., *International Tables for Crystallography, Vol. C*, edited by AJC Wilson. Dordrecht: Kluwer Academic Publishers: **1992**. pp. 685– 706.
- (14) The rates of cycloaddition with **2.2** are comparable to that observed with Münchnones (Ref. [8]), although slower than with unstabilized azomethine ylides, where the formation of the dipole is often rate determining: a) Harwood, L.M., Vickers R. J. in *The Chemistry of Heterocyclic Compounds*, Vol. 59A (Eds.: Padwa, A., Person, W. H.), Wiley, New York, **2002**, pp. 169–252; b) Mantelingu, K.; Lin, Y.; Seidel, D., *Org. Lett.* **2014**, *16*, 5910-5913.
- (15) For review: Jan, J.; Eva Van, H.; Sven, C.; Norbert De, K., *Curr. Org. Chem.* **2011**, *15*, 1340-1362.
- (16) For review: a) Kim, E.; Lee, Y.; Lee, S.; Park, S. B., *Acc. Chem. Res.* **2015**, *48*, 538-547; For representative examples: b) Huckaba, A. J.; Yella, A.; McNamara, L. E.; Steen, A. E.; Murphy, J. S.; Carpenter, C. A.; Punecky, G. D.; Hammer, N. I.; Nazeeruddin, M. K.; Grätzel, M., *Chem. Eur. J.* **2016**, *22*, 15536-15542. c) Mitsumori, T.; Bendikov, M.; Dautel, O.; Wudl, F.; Shioya, T.; Sato, H.; Sato, Y., *J. Am. Chem. Soc.* **2004**, *126*, 16793-16803. d) Kim, E.; Koh, M.; Lim, B. J.; Park, S. B., *J. Am. Chem. Soc.* **2011**, *133*, 6642-6649.
- (17) For reviews: a) Sadowski, B.; Klajn, J.; Gryko, D. T., *Org. Biomol Chem.* **2016**, *14*, 7804-7828. b) Dudnik, A.; Gevorgyan, V., *Catalysed Carbon–Heteroatom Bond Formation*; Yudin, AK, Ed. Wiley-VCH: Weinheim: 2010, pp. 317– 410; c) Uchida, T.; Matsumoto, K., *Synthesis* **1976**, *1976*, 209-236.

- (18) Representative recent examples from substituted pyridines: a) Seregin, I. V.; Gevorgyan, V., *J. Am. Chem. Soc.* **2006**, *128*, 12050-12051. b) Chen, X.; Hu, X.; Deng, Y.; Jiang, H.; Zeng, W., *Org. Lett.* **2016**, *18*, 4742-4745. c) Zhao, B.; Yu, M.; Liu, H.; Chen, Y.; Yuan, Y.; Xie, X., *Adv. Synth. Catal.* **2014**, *356*, 3295-3301. d) Rogness, D. C.; Markina, N. A.; Waldo, J. P.; Larock, R. C., *J. Org. Chem.* **2012**, *77*, 2743-2755. e) Liu, R.-R.; Lu, C.-J.; Zhang, M.-D.; Gao, J.-R.; Jia, Y.-X., *Chem. Eur. J.* **2015**, *21*, 7057-7060. f) Oh, K. H.; Kim, S. M.; Park, S. Y.; Park, J. K., *Org. Lett.* **2016**, *18*, 2204-2207. g) Barluenga, J.; Lonzi, G.; Riesgo, L.; Lopez, L. A.; Tomas, M., *J. Am. Chem. Soc.* **2010**, *132*, 13200-13202. h) Gao, M.; Tian, J.; Lei, A., *Chem. Asian J.* **2014**, *9*, 2068-2071. i) Sahoo, B.; Hopkinson, M. N.; Glorius, F., *Angew. Chem. Int. Ed.* **2015**, *54*, 15545-15549; *Angew. Chem.* **2015**, *127*, 15766-15770.
- (19) Representative recent examples from substituted pyrroles: a) Li, X.; Xie, X.; Liu, Y., *J. Org. Chem.* **2016**, *81*, 3688-3699. b) Lee, J. H.; Kim, I., *J. Org. Chem.* **2013**, *78*, 1283-1288. c) Park, S.; Kim, I., *Tetrahedron* **2015**, *71*, 1982-1991. d) Outlaw, V. K.; d'Andrea, F. B.; Townsend, C. A., *Org. Lett.* **2015**, *17*, 1822-1825. e) Hao, W.; Wang, H.; Ye, Q.; Zhang, W.-X.; Xi, Z., *Org. Lett.* **2015**, *17*, 5674-5677.
- (20) For examples: a) Liu, B.; Wang, Z.; Wu, N.; Li, M.; You, J.; Lan, J., *Chem. Eur. J.* **2012**, *18*, 1599-1603. b) Liegault, B.; Lapointe, D.; Caron, L.; Vlassova, A.; Fagnou, K., *J. Org. Chem.* **2009**, *74*, 1826-1834.
- (21) For examples of involving cycloaddition to pyridinium salts, including multicomponent methods: a) Day, J.; McKeever-Abbas, B.; Dowden, J., *Angew. Chem. Int. Ed.* **2016**, *55*, 5809-5813; *Angew. Chem.* **2016**, *128*, 5903-5907. b) Rotaru, A. V.; Druta, I. D.; Oeser, T.; Mueller, T. J., *Helv. Chim. Acta* **2005**, *88*, 1798-1812. c) Katritzky, A. R.; Qiu, G.; Yang, B.; He, H.-Y., *J. Org. Chem.* **1999**, *64*, 7618-7621. d) Bora, U.; Saikia, A.; Boruah, R. C., *Org. Lett.* **2003**, *5*, 435-438. e) Shang, Y.; Zhang, M.; Yu, S.; Ju, K.; Wang, C.; He, X., *Tetrahedron Lett.* **2009**, *50*, 6981-6984. f) Briocche, J.; Meyer, C.; Cossy, J., *Org. Lett.* **2015**, *17*, 2800-2803. g) Li, F.; Chen, J.; Hou, Y.; Li, Y.; Wu, X.-Y.; Tong, X., *Org. Lett.* **2015**, *17*, 5376-5379. h) Bayazit, M. K.; Coleman, K. S., *Arkivoc* **2014**, *4*, 362-371.
- (22) This section was published as the supporting information.

- (23) Layer, R. W., *Chem. Rev.* **1963**, *63*, 489-510.
- (24) Liu, B.; Wang, Z.; Wu, N.; Li, M.; You, J.; Lan, J., *Chem. Euro. J.* **2012**, *18*, 1599-1603.
- (25) Liu, J.-L.; Liang, Y.; Wang, H.-S.; Pan, Y.-M., *Synlett* **2015**, *26*, 2024-2028.
- (26) Bayazit, M. K.; Coleman, K. S., *Arkivoc* **2014**, *4*, 362-371.
- (27) Hu, H.; Liu, Y.; Xu, J.; Kan, Y.; Wang, C.; Ji, M., *RSC Advances* **2014**, *4*, 24389-24393.

CHAPTER 3

Multicomponent Synthesis of Furans via a New Class of Phosphorus-Based 1,3-Dipole

3.0 Preface

We described in Chapter 2 how a new class of pyridine-based mesoionic heterocycle can be generated and used in the synthesis of indolizines. In this chapter, we turn our attention to the assembly of another new 1,3-dipole: a carbonyl-ylide version of phosphamünchnones (section 1.2.3.2). These phosphorus-based substrates are generated *in situ* via the one pot reaction of aldehydes, acyl chlorides and the phosphonite PhP(catechyl), and undergo cycloaddition with electron deficient alkynes or alkenes to generate furans. The formation of these 1,3-dipoles, and their ability to offer a modular approach to furan synthesis, is described below.

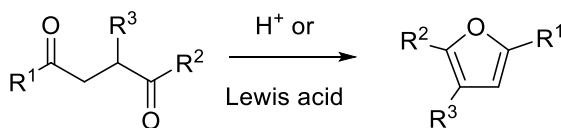
3.1 Introduction

Polysubstituted furans are valuable heterocyclic motifs, and can be found in a wide variety of natural products¹ and related pharmaceutically relevant products.² Furans have also been exploited as components in optoelectronic devices,³ and serve as useful building blocks in organic synthesis.⁴ Classical synthetic methods employed to assemble furans include the Paal-Knorr and Feist-Benary reactions (Scheme 3.1a),⁵ or substitution reactions on the furan ring (Scheme 3.1b).⁶ In addition, a number of more recent methods have been reported, including many that involve metal catalyzed cyclization or coupling reactions (e.g Scheme 3.1c).^{7,8} Phosphines have been

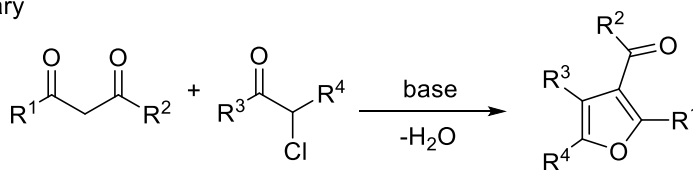
employed in furan synthesis as well, either as catalysts or stoichiometric reagents (Scheme 3.1d).⁹ Interestingly, a study by He have demonstrated the use of readily available aldehydes, acyl chlorides and alkynes in furan synthesis.^{9b} However, the proposed mechanism of this reaction requires an initial coupling between tributylphosphine and an electron deficient alkyne, which limits the substrate scope of this synthesis. While each of these syntheses are effective, they either require the initial synthesis of one or more substrates incorporating the correct substituents, which both creates waste and can limit their ease of generalization; or work with limited substrates or substitution patterns.

a) Classical furan synthesis

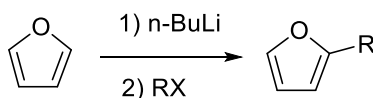
Paal-Knorr



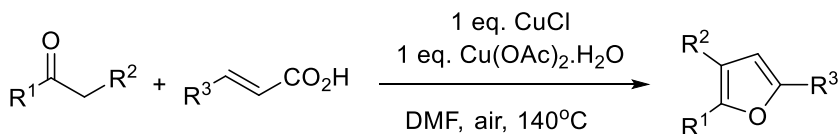
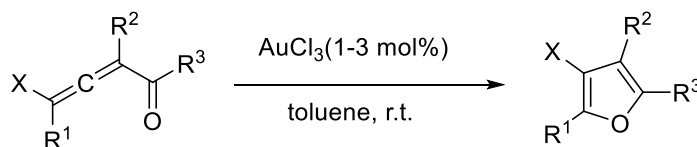
Feist-Benary



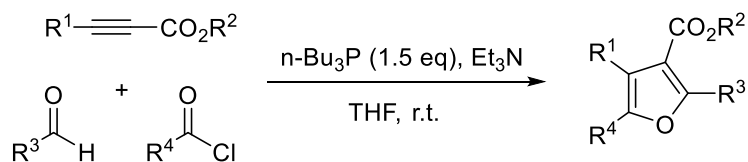
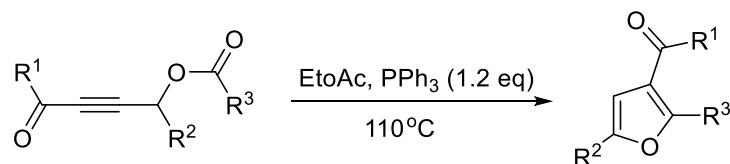
b) Furan derivatization



c) Metal catalyzed examples



d) Phosphine-mediated furan synthesis

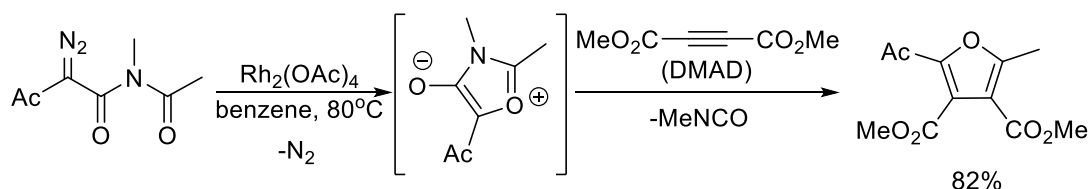


Scheme 3.1 Common approaches to furan synthesis

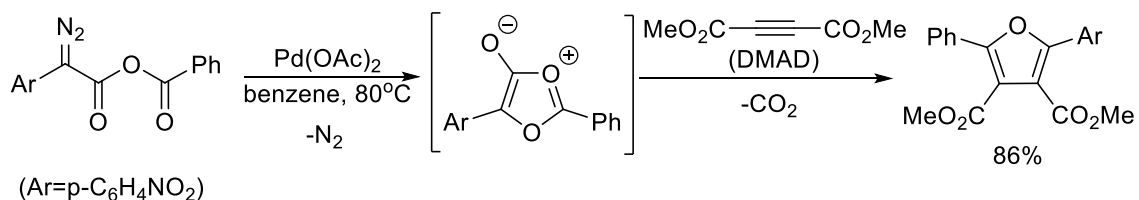
An alternative approach to furans is via 1,3-dipolar cycloaddition reactions with mesoionic heterocycles. Mesoionic heterocycles such as münchnones have been heavily exploited for the assembly nitrogen-containing heterocycles.¹⁰ Unfortunately, the use of similar approaches to synthesize oxygen-based furans are much less common. A variant of münchnones, isomünchnones

have been shown to generate furans upon cycloaddition with alkynes.¹¹ Despite the good yields of furan products, this method is not widely applicable due to involved synthesis of the precursor to this 1,3-dipole (α -diazo imides, Scheme 3.2a). Alternatively, early studies¹² by Nagai and Hamaguchi show that highly unstable oxygen variant of münchnones, 1,3-dioxolium-4-oxides, can also be coupled with alkynes to access furans (Scheme 3.2b). However, the scope of this reaction is limited to very electron poor alkynes and phenyl substituents on both C2-C5, and in this case requires the initial synthesis of an α -diazo-benzoic anhydride precursor to the 1,3-dipole, which limits its accessibility.

a) Isomünchnones



b) 1,3-dioxolium-4-oxides



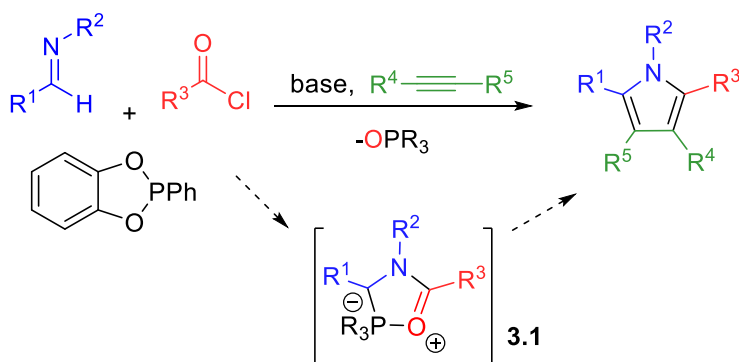
Scheme 3.2 Furan synthesis via mesoionic 1,3-dipoles

We have been interested in the development of more modular methods to assemble 1,3-dipoles for use in cycloaddition reactions.^{13,14} One such system are phospho-münchnones **3.1** (Scheme 3.3a). These 1,3-dipoles can be considered as a phosphorus analogue to münchnones, and is generated from imines, acyl chlorides and phosphonites. Moreover, they participate in cycloaddition reactions to provide an overall synthesis of nitrogen-containing heterocycles,

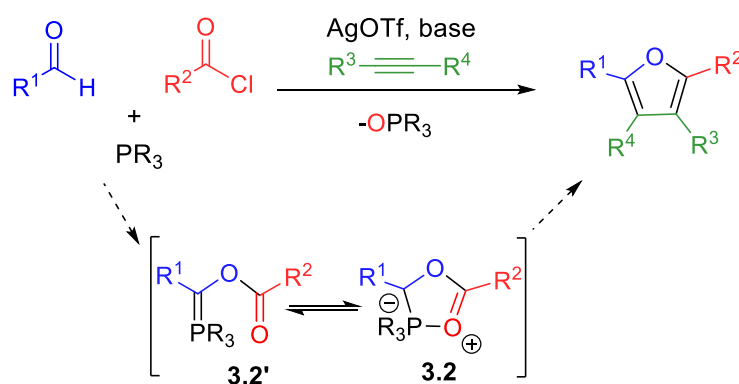
including pyrroles^{14a,16} and imidazoles.¹⁵ In considering the synthesis of **3.1**, we questioned if a similar method might offer a route to generate oxygen-containing dipoles **3.2** (Scheme 3.3b). In principle, this could be accomplished by replacing the imine used in this reaction with an even more accessible aldehyde. While appearing straightforward, aldehydes are much less nucleophilic than imines, and do not classically react with acyl chlorides: a key step in the assembly of **3.1** with imines (*vide infra*). In addition, the ester in this product is less strongly chelating than an amide, which would presumably also inhibit the cyclization of the Wittig reagent **3.2'** to form the 1,3-dipole **3.2**. Nevertheless, our previous studies on **3.1** have shown that the angle strain at phosphorus center caused by the catechyl unit can be effective in favoring cyclization to generate a five-coordinate phosphorus, which led us to question if such a system might also allow the generation of **3.2**.

We describe here our studies towards developing an oxygen-variant of phosphamünchnones. These demonstrate that the creation of potent acylating agents *in situ*, such as acyl iodides and acyl triflates, can indeed allow the coupling of aldehydes, acylating agents and PhP(catechyl) to form a new class of 1,3-dipole: **3.2**. Combining the formation of **3.2** with subsequent cycloaddition opens a modular and regioselective route to synthesis of furans in one pot from three broadly available and easily modulated reagents: aldehydes, acyl chlorides and alkynes.

a) *Pyrrole synthesis via phosphamünchnones*



b) *This work: modular synthesis of furans via 1,3-dipolar cycloaddition*



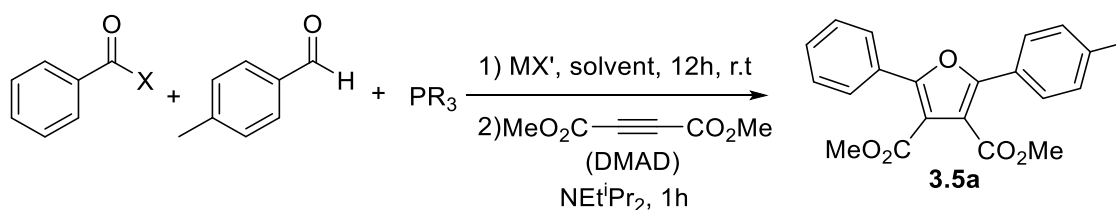
Scheme 3.3 1,3-Dipolar cycloaddition routes to furans.

3.2 Results and Discussion

Our postulated pathway for the formation of 1,3-dipole **3.2** is shown in Scheme. 3.4. In this, the reaction of an acyl chloride, or an acyl chloride analogue, with aldehyde would generate a α -haloester. Such products have been shown to be accessible via aldehyde acylation, although this typically require the use of Lewis acid catalysts such as $ZnCl_2$ or $Zn(OTf)_2$ to activate the acyl chloride to nucleophilic attack.^{17,18} The formation of the ester would ideally be followed by nucleophilic attack of the phosphonite to obtain a phosphonium salt **3.4**. Subsequent deprotonation generates **3.2'**, a Wittig reagent, which has the potential to cyclize to form 1,3-dipole **3.2**, in

followed by the addition of first PhP(catechyl) and then DMAD and base, the formation of furan **3.5a** could now be observed, albeit in low yield (entries 7, 8). The direct use of benzoyl bromide or iodide further improves the yield of furan (entries 9, 10).

Table 3.1 Synthesis of furan **3.5a** via cycloaddition^a



entry	X	MX'	PR ₃	solvent	3.5a (%) ^c
1	Cl	-	PhP(catechyl)	CD ₃ CN	-
2	Br	-	PhP(catechyl)	CD ₃ CN	-
3	I	-	PhP(catechyl)	CD ₃ CN	-
4	Cl	TMSBr	PhP(catechyl)	CD ₃ CN	-
5	Cl	TMSI	PhP(catechyl)	CD ₃ CN	-
6	Cl	NaI	PhP(catechyl)	CD ₃ CN	-
7 ^b	Cl	TMSI	PhP(catechyl)	CD ₃ CN	25
8 ^b	Cl	NaI	PhP(catechyl)	CD ₃ CN	32
9 ^b	Br	-	PhP(catechyl)	CD ₃ CN	45
10 ^b	I	-	PhP(catechyl)	CD ₃ CN	70
11	Cl	AgOTf	PhP(catechyl)	DCE	80
12	Cl	AgOTf	PPh ₃	DCE	-
13	Cl	AgOTf	PCy ₃	DCE	-
14	Cl	AgOTf	P(OCH ₂ CF ₃) ₃	DCE	-
15	Cl	AgOTf	P(OPh) ₃	DCE	20

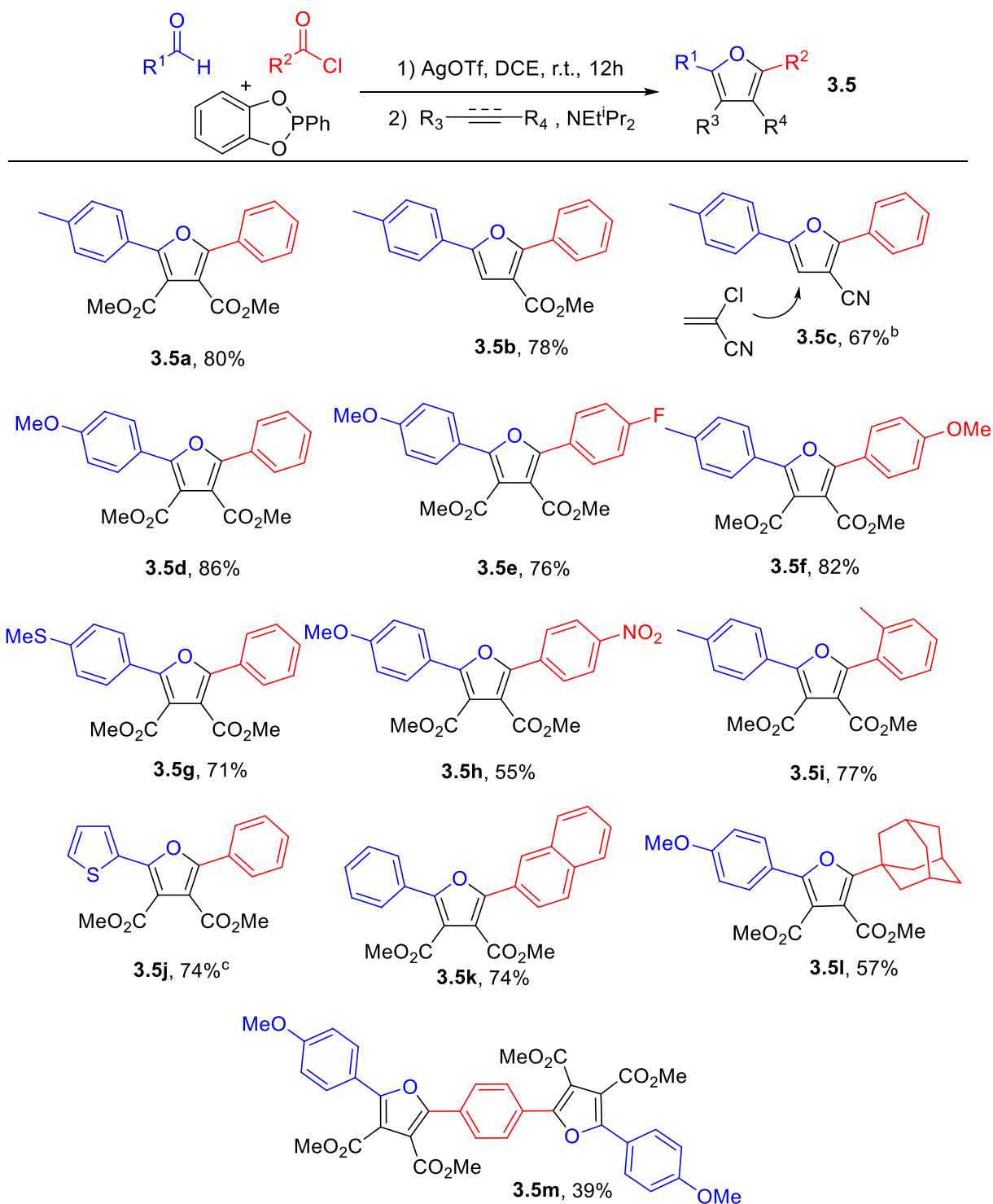
^a0.12 mmol acyl halide, 0.1 mmol aldehyde and 0.12 mmol phosphine in 1 ml of solvent, followed by 0.15 mmol MX', stir for 12 h, followed by the addition of DMAD (21 mg, 0.15 mmol) and NEt₂Pr₂ (19 mg, 0.15 mmol) and stir for 1 h. ^bacyl halide, MX' (if needed) and aldehyde first mixed in 1 ml CD₃CN for 12 h, followed by addition of phosphine and stir for 6 h. ^cNMR yields vs an internal standard ((CH₃)₂SO₂)

While these results were encouraging, the stepwise addition of reagents adds a layer of complexity to the overall synthesis. In addition, the procedure was found to be highly sensitive to substrates and reaction times, where any small change in the acyl halide or aldehyde (*vide infra*)

led to drastically different results. Therefore, we probed alternative ways to access **3.2**. One option is to generate an even more potent acylating agent, which can react with the aldehyde more readily than the phosphonite. After examining various conditions, we were pleased to find that this can be accomplished by the simple addition of AgOTf. Thus, the one pot reaction of benzoyl chloride, aldehyde and PhP(catechyl) in the presence of AgOTf, which presumably reacts rapidly with the acyl chloride to form an electrophilic acyl triflate intermediate,²¹ can allow the formation of furan **3.5a** in good yield upon DMAD and base addition (entry 11). A variety of solvents and triflate salts were tested, but optimal conditions were found to involve use of 1,2-dichloroethane (DCE) and AgOTf. The use of more electron rich phosphines (entries 12, 13) or electron deficient phosphites (entries 14, 15) all lead to either diminished product yields or inhibit the reaction altogether, which is consistent with the previously postulated role of the catechyl unit angle strain favoring the formation of the five-coordinate phosphorus in **3.1**.

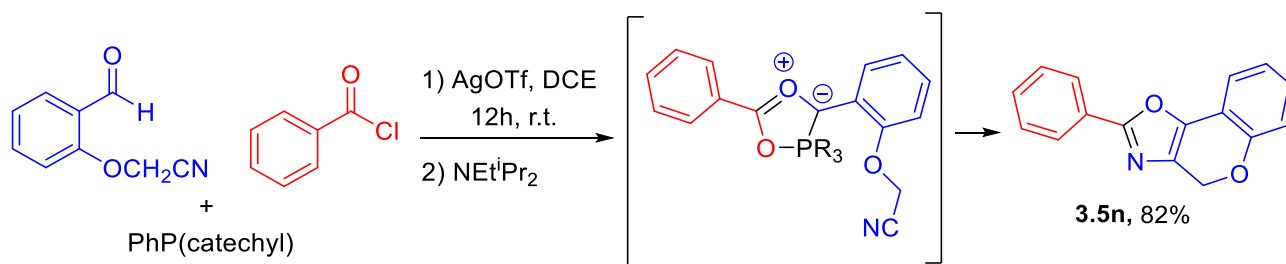
Combining these optimized conditions with the wide availability of acyl chlorides, aldehydes and alkynes opens a simple pathway to build-up a range of furan products (Table 3.2). For example, other dipolarophiles can be used in cycloaddition with **3.2** as a route to modulate the 3,4-substituents on the furan core (**3.5b**, **3.5c**). Of note, these unsymmetrical dipolarophiles lead to a single product, where the electron withdrawing unit is directed away from the former aldehyde carbon. The latter is consistent with the results observed with phosphamünchnones, wherein the localization of negative charge on this carbon, together with the large PR₃ unit, direct cycloaddition selectivity.²² However, more electron rich alkynes, such as 1-hexyne or phenyl acetylene, do not react with **3.2**. A variety of aromatic aldehydes and acyl chlorides can be employed in the reaction, including those with either electron donating or withdrawing groups, and even ortho-substitution (**3.5d-i**). In addition to aromatic units, a thiophene-based aldehyde can also be used as a substrate

(3.5j), as can the large adamantyl acyl chloride **(3.5l)**. This reaction can also be extended to the assembly of bis-1,3-dipoles by the use of broadly available terephthaloyl chloride as a reagent, offering here a route to prepare an oligomer containing alternating arene and furan rings in a single pot reaction **(3.5m)**.

Table 3.2 Substrate diversity of tetrasubstituted furan synthesis^a

^a0.24 mmol acyl halide, 0.2 mmol aldehyde and PhP(catechyl) (52 mg, 0.24 mmol) in 1 ml of 1,2-dichloroethane, followed by $AgOTf$ (62 mg, 0.24 mmol), stir for 12 h, followed by the addition of DMAD (43 mg, 0.30 mmol) and NEt^iPr_2 (39 mg, 0.30 mmol) and stir for 1 h. ^b NEt^iPr_2 (65 mg, 0.50 mmol), stir for 8°C at 12 h. ^c stir for 1 h after $AgOTf$.

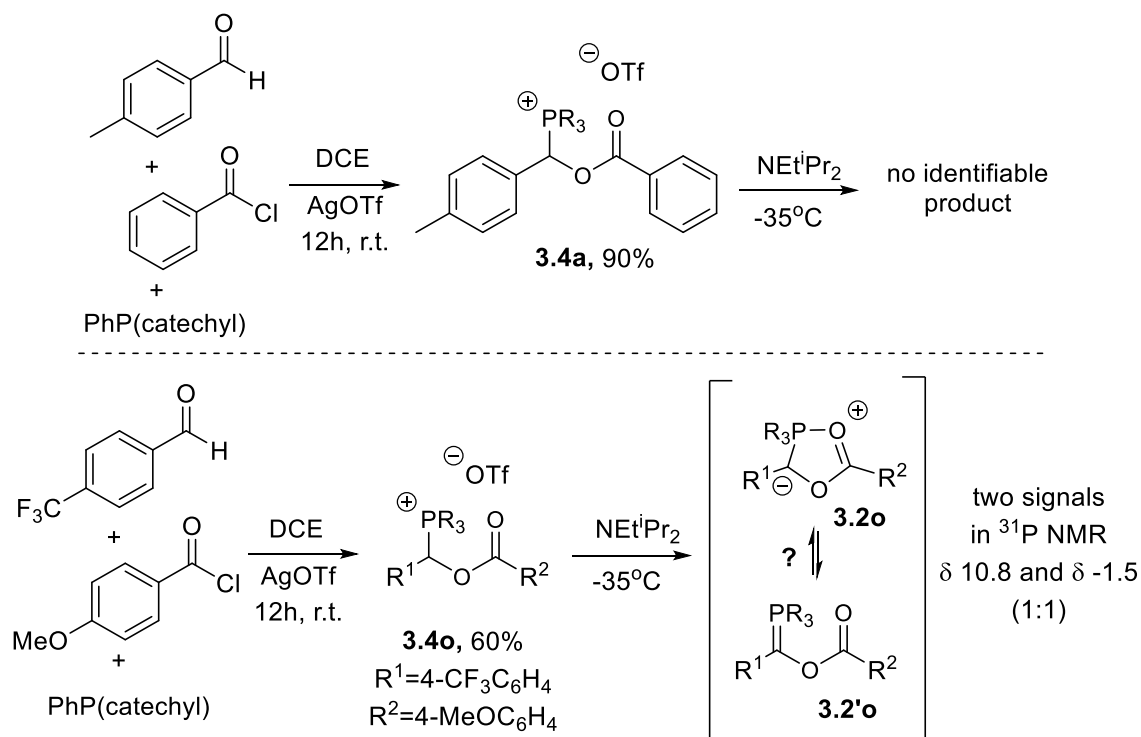
As an alternative to furan synthesis, we also investigated the use of other classes of dipolarophiles in cycloaddition. In principle, trapping of this 1,3-dipole with a nitrile or electron poor imine can lead to formation of oxazoles. Our attempts to use ethyl cyanoformate or electron poor *N*-tosyl or *N*-nosyl imines in cycloadditions resulted in no observable oxazole formation. In contrast, the use of the nitrile-tethered aromatic aldehyde in this reaction led to rapid cycloaddition to form the fused-ring oxazole **3.5n** in high yield (Scheme 3.5). This is, to our knowledge, the first example of oxazole synthesis using mesoionic heterocycles.



Scheme 3.5 Synthesis of fused-ring oxazole **3.5n** via intramolecular cycloaddition

Finally, we turned our attention to explore how precisely this transformation proceeds. Monitoring the initial reaction of benzoyl chloride, *p*-tolualdehyde and PhP(catechyl) in the presence of AgOTf by NMR analysis shows the immediate formation of a new product in near quantitative yield. This product can be precipitated from the mixture by addition of pentane, and has been preliminarily characterized in situ by ¹H and ³¹P NMR analysis to be the phosphonium salt **3.4a** (Scheme 3.6). Of note, ¹H NMR analysis shows the expected resonances for aromatic residues and the methine hydrogen coupled to phosphorus (δ 6.82 ppm, d, *J* = 4.5 Hz), as well as the expected phosphonium signal (δ 24.3 ppm). However, this compound was formed with other impurities, and the addition of EtNⁱPr₂ base -35°C without a dipolarophile present led in the formation of a complex mixture of unidentifiable products, including Ph(catechyl)P=O, suggesting that the putative 1,3-dipole generated here was unstable.

In order to improve the stability of **3.2**, we paired an electron donating acyl chloride (p-methoxy benzoyl chloride) and electron withdrawing aldehyde (4-trifluoromethyl benzaldehyde), which could presumably stabilize the positive and negative charges on the two respective carbons. The reaction of these reagents with PhP(catechyl) followed by the addition of base to this mixture at -35°C led to the formation of two major products by ^{31}P NMR analysis, with signals at δ 10.8 and δ -1.5 in a ca. 1:1 ratio (Scheme 3.6). Of note here, the former is in the region expected for Wittig-type reagents,²³ while the upfield signal is in a similar region to that noted for the five-coordinate phosphorus in **3.1** (δ -16.9 ppm),¹⁹ suggesting this may be the new oxygen-based 1,3-dipole **3.2o**. Unfortunately, the ^1H NMR spectra of this mixture is complex and other impurities are observed. Further characterization of the putative 1,3-dipole is needed.



Scheme 3.6. ^{31}P NMR analysis of **3.2o**

3.3 Conclusion

In conclusion, we have described a phosphonite mediated new method to construct substituted furans from readily available aldehydes, acyl chlorides and alkynes. This transformation is postulated to proceed via the one pot assembly of a new class of 1,3-dipole, **3.2**. These 1,3-dipoles demonstrate cycloaddition reactivity towards alkynes, alkenes and nitriles. Studies toward the characterization of this new phosphorus-based 1,3-dipolar cycloaddition substrate are currently underway.

3.4 Experimental Section

3.4.1 General Procedures

All manipulations were conducted in a glovebox under a nitrogen atmosphere. Unless otherwise noted, all reagents were purchased from commercial sources and used without purification. Solvents were dried by using a solvent purifier system. Solvents were stored over activated 3Å molecular sieves inside the glovebox. Deuterated acetonitrile was stirred over calcium hydride, vacuum transferred, degassed, and stored over 4Å molecular sieves. 2-phenylbenzo[1,3,2]dioxaphosphole ((catechyl)PPh) was prepared as indicated in our previous studies.^{14a} The nitrile-tethered aldehyde was prepared using standard literature procedures.²⁴ Nuclear magnetic resonance (NMR) characterization was performed on 400 MHz spectrometers for proton, 101 MHz for carbon and 162 MHz for phosphorus. ¹H, and ¹³C NMR chemical shifts were referenced to residual solvent. ¹H and ¹³C NMR spectra to show the purity are available in Appendix II. Mass spectra were recorded on a high-resolution electrospray ionization quadrupole mass spectrometer.

3.4.2 Experimental Procedures

Procedure a for screening reactions (Table 3.1) In a glovebox, p-tolualdehyde (12 mg, 0.10 mmol), benzoyl halide (0.12 mmol), phosphine (0.12 mmol) and (CH₃)₂SO₂ internal standard (5 mg, 0.05 mmol) were dissolved in 1 ml of solvent, followed by additive (0.12 mmol). This mixture was allowed to stir for 12 hours at room temperature, and dimethylacetylene dicarboxylate (21 mg, 0.15 mmol) and diisopropylethylamine (19 mg, 0.15 mmol) were added. This mixture was stirred for 1 h at room temperature. Yield of furan **3.5a** was determined by ¹H NMR relative to the (CH₃)₂SO₂ internal standard.

Procedure b for screening reactions (Table 3.1) In a glovebox, p-tolualdehyde (12 mg, 0.10 mmol), benzoyl halide (0.12 mmol) and (CH₃)₂SO₂ internal standard (5 mg, 0.05 mmol) were dissolved in 1 ml of solvent, followed by additive (0.12 mmol). This mixture was allowed to stir for 12 hours at room temperature. Phosphine (0.12 mmol) was added and the mixture was stirred for another 6 hours. Finally, dimethylacetylene dicarboxylate (21 mg, 0.15 mmol) and diisopropylethylamine (19 mg, 0.15 mmol) were added. This mixture was stirred for 1 h at room temperature. Yield of furan **3.5a** was determined by ¹H NMR relative to the (CH₃)₂SO₂ internal standard.

Typical formation of furans 3.5 In a glovebox, p-tolualdehyde (24 mg, 0.20 mmol), benzoyl chloride (34 mg, 0.24 mmol) and (catechyl)PPh (52 mg, 0.24 mmol) were dissolved in 1 ml of dichloroethane, followed by addition of silver triflate (62 mg, 0.24 mmol). This mixture was allowed to stir for 12 hours at room temperature, and dimethylacetylene dicarboxylate (43 mg, 0.30 mmol) and diisopropylethylamine (39 mg, 0.30 mmol) were added. This mixture was stirred for 30 min at room temperature. The solvent was removed in vacuo, and the furan product **3.5a** was isolated by column chromatography using ethyl acetate-hexanes as a colorless liquid. (80%, 56 mg, 0.160 mmol).

Formation of furan 3.5c In a glovebox, p-tolualdehyde (24 mg, 0.20 mmol), benzoyl chloride (34 mg, 0.24 mmol) and (catechyl)PPh (52 mg, 0.24 mmol) were dissolved in 1 ml of dichloroethane, followed by additon of silver triflate (62 mg, 0.24 mmol). This mixture was allowed to stir for 12 hours at room temperature, and 2-chloroacrylonitrile (35 mg, 0.40 mmol) and diisopropylethylamine (65 mg, 0.50 mmol) were added. This mixture was transferred to a sealed vessel and taken out of the glovebox to be heated in an oil bath at 80°C for 12 hours. The solvent was removed in vacuo, and the furan product **3.5c** was isolated by column chromatography using ethyl acetate-hexanes as a pale-yellow liquid. (67%, 35 mg, 0.134 mmol).

Formation of fused-ring oxazole 3.5n In a glovebox, 2-(2-formylphenoxy)acetonitrile (32 mg, 0.20 mmol), benzoyl chloride (34 mg, 0.24 mmol) and (catechyl)PPh (52 mg, 0.24 mmol) were dissolved in 1 ml of dichloroethane, followed by additon of silver triflate (62 mg, 0.24 mmol). This mixture was allowed to stir for 12 hours at room temperature, and diisopropylethylamine (39 mg, 0.30 mmol) was added. This mixture was stirred for 30 min at room temperature. The solvent was removed in vacuo, and the furan product **3.5n** was isolated by column chromatography using ethyl acetate-hexanes as a white solid. (82%, 41 mg, 0.164 mmol).

Formation of phosphonium salt 3.4a In a glovebox, p-tolualdehyde (24 mg, 0.20 mmol), benzoyl chloride (34 mg, 0.24 mmol) and (catechyl)PPh (52 mg, 0.24 mmol) were dissolved in 1 ml of dichloroethane, followed by additon of silver triflate (62 mg, 0.24 mmol). This mixture was allowed to stir for 12 hours at room temperature. Solvent was removed in vacuo, and resulting oil was washed with 2 ml of pentane to result in a brown precipitate containing **3.4a** along with impurities: ¹H NMR (400 MHz, CD₃CN) δ 8.42 (d, *J* = 7.3 Hz, 2H), 8.07 (t, *J* = 7.6 Hz, 1H), 7.86 – 7.74 (m, 3H), 7.61 (m, 3H), 7.43 (dd, *J* = 8.4, 2.5 Hz, 2H), 7.24 (d, *J* = 8.1 Hz, 2H), 7.21 – 7.14

(m, 2H), 7.11 – 7.03 (m, 3H), 6.82 (d, $J = 4.5$ Hz, 1H), 2.34 (d, $J = 2.6$ Hz, 3H). ^{31}P NMR (162 MHz, CD_3CN) δ 24.3.

Formation and deprotonation of phosphonium salt **3.4o** In a glovebox, p-trifluoromethyl benzaldehyde (35 mg, 0.20 mmol), anisoyl chloride (41 mg, 0.24 mmol) and (catechyl)PPh (52 mg, 0.24 mmol) were dissolved in 1 ml of dichloroethane, followed by addition of silver triflate (62 mg, 0.24 mmol). This mixture was allowed to stir for 12 hours at room temperature. Solvent was removed in vacuo, and resulting oil was washed with 2 ml of pentane to result in a yellow precipitate containing **3.4o** with significant amount of impurities.: ^{31}P NMR (162 MHz, CD_3CN) δ 15.1. This salt was dissolved in CD_3CN , kept at -35°C for 2 hours followed by addition of diisopropylethylamine (26 mg, 0.20 mmol). ^{31}P NMR was quickly taken at 0°C . Analysis of the spectra reveals formation of 2 new peaks at nearly 1:1 ratio: ^{31}P NMR (162 MHz, CD_3CN) δ 10.8, -1.5. Spectra taken at later times indicate mostly decomposition.

3.4.3 Characterization Data

Dimethyl 2-phenyl-5-(p-tolyl)furan-3,4-dicarboxylate (**3.5a**) Colorless liquid, 56 mg, 80%. ^1H NMR (500 MHz, CDCl_3) δ 7.87 (d, $J = 7.0$ Hz, 2H), 7.78 (d, $J = 8.2$ Hz, 2H), 7.46 (m, 3H), 7.29 (d, $J = 8.0$ Hz, 2H), 3.91 (s, 3H), 3.90 (s, 3H), 2.43 (s, 3H). ^{13}C NMR (126 MHz, CDCl_3) δ 164.4, 164.2, 154.0, 153.1, 139.9, 129.5, 129.2, 128.9, 128.5, 127.4, 127.3, 126.0, 115.2, 114.6, 52.4, 52.3, 21.5. HRMS (ESI⁺) for $\text{C}_{21}\text{H}_{18}\text{NaO}_5$; calculated 373.1046, found 373.1049 (error m/z = 0.7 ppm)

Methyl 2-phenyl-5-(p-tolyl)furan-3-carboxylate (**3.5b**) Pale yellow liquid, 45 mg, 78%. ^1H NMR (500 MHz, CDCl_3) δ 8.09 (d, $J = 7.2$ Hz, 2H), 7.64 (d, $J = 8.2$ Hz, 2H), 7.48 (t, $J = 7.4$ Hz, 2H),

7.42 (t, $J = 7.3$ Hz, 1H), 7.24 (d, $J = 8.0$ Hz, 2H), 7.04 (s, 1H), 3.88 (s, 3H), 2.40 (s, 3H). ^{13}C NMR (126 MHz, CDCl_3) δ 164.1, 156.3, 152.7, 138.1, 129.8, 129.5, 129.3, 128.3, 128.2, 127.1, 124.0, 115.3, 107.1, 51.7, 21.4. HRMS (ESI⁺) for $\text{C}_{19}\text{H}_{17}\text{O}_3$; calculated 293.1172, found 293.1173 (error $m/z = 0.2$ ppm)

2-phenyl-5-(p-tolyl)furan-3-carbonitrile (3.5c) Pale yellow liquid, 35 mg, 67%. ^1H NMR (500 MHz, CDCl_3) δ 8.08 (d, $J = 7.2$ Hz, 2H), 7.63 (d, $J = 8.2$ Hz, 2H), 7.53 (t, $J = 8.0$ Hz, 2H), 7.47 (t, $J = 7.4$ Hz, 1H), 7.28 (d, $J = 7.6$ Hz, 2H), 6.83 (s, 1H), 2.42 (s, 3H). ^{13}C NMR (126 MHz, CDCl_3) δ 158.4, 153.9, 139.1, 130.0, 129.7, 129.1, 128.2, 126.1, 125.3, 124.2, 115.1, 107.0, 93.4, 21.4. HRMS (ESI⁺) for $\text{C}_{18}\text{H}_{14}\text{ON}$; calculated 260.1070, found 260.1080 (error $m/z = 4.1$ ppm)

Dimethyl 2-(4-methoxyphenyl)-5-phenylfuran-3,4-dicarboxylate (3.4d) White solid, 63 mg, 86%. ^1H NMR (500 MHz, CDCl_3) δ 7.91 – 7.82 (m, 4H), 7.52 – 7.38 (m, 3H), 7.00 (d, $J = 9.0$ Hz, 2H), 3.91 (s, 3H), 3.89 (s, 3H), 3.89 (s, 3H). ^{13}C NMR (126 MHz, CDCl_3) δ 164.6, 164.2, 160.7, 154.4, 152.4, 129.4, 129.3, 128.9, 128.6, 127.1, 121.5, 115.3, 113.9, 113.8, 55.4, 52.4, 52.3. HRMS (ESI⁺) for $\text{C}_{21}\text{H}_{19}\text{O}_6$; calculated 367.1176, found 367.1188 (error $m/z = 3.1$ ppm)

Dimethyl 2-(4-fluorophenyl)-5-(4-methoxyphenyl)furan-3,4-dicarboxylate (3.5e) Brown liquid, 58 mg, 76%. ^1H NMR (500 MHz, CDCl_3) δ 7.88 (dd, $J = 9.0, 5.3$ Hz, 2H), 7.84 (d, $J = 9.0$ Hz, 2H), 7.16 (t, $J = 8.7$ Hz, 2H), 7.00 (d, $J = 9.0$ Hz, 2H), 3.90 (s, 3H), 3.89 (s, 3H), 3.88 (s, 3H). ^{13}C NMR (126 MHz, CDCl_3) δ 164.3, 164.2, 162.3, 160.8, 154.0, 129.5, 129.1, 125.2, 121.3, 115.8, 115.6, 115.0, 114.0, 113.9, 55.4, 52.4, 52.3. ^{19}F NMR (471 MHz, CDCl_3) δ -110.6. HRMS (ESI⁺) for $\text{C}_{21}\text{H}_{18}\text{O}_6\text{F}$; calculated 385.1082, found 385.1089 (error $m/z = 1.8$ ppm)

Dimethyl 2-(4-methoxyphenyl)-5-(p-tolyl)furan-3,4-dicarboxylate (3.5f) Pale yellow liquid, 62 mg, 82%. ^1H NMR (500 MHz, CDCl_3) δ 7.86 (d, $J = 9.0$ Hz, 2H), 7.75 (d, $J = 8.2$ Hz, 2H), 7.27 (d, $J = 8.0$ Hz, 2H), 7.00 (d, $J = 9.0$ Hz, 2H), 3.90 (s, 3H), 3.89 (s, 3H), 3.88 (s, 3H), 2.42 (s, 3H).

^{13}C NMR (126 MHz, CDCl_3) δ 164.6, 164.3, 160.7, 153.9, 153.0, 139.7, 129.3, 129.2, 127.1, 126.1, 121.6, 114.7, 113.9, 113.8, 55.4, 52.4, 52.3, 21.5. **HRMS** (ESI^+) for $\text{C}_{22}\text{H}_{21}\text{O}_6$; calculated 381.1333, found 381.1342 (error m/z = 2.5 ppm)

Dimethyl 2-(4-(methylthio)phenyl)-5-phenylfuran-3,4-dicarboxylate (3.5g) White solid, 54 mg, 71%. ^1H NMR (500 MHz, CDCl_3) δ 7.86 (d, J = 8.0 Hz, 2H), 7.83 (d, J = 8.6 Hz, 2H), 7.52 – 7.41 (m, 3H), 7.32 (d, J = 8.6 Hz, 2H), 3.91 (s, 3H), 3.90 (s, 3H), 2.54 (s, 3H). ^{13}C NMR (126 MHz, CDCl_3) δ 164.4, 164.1, 153.6, 153.0, 141.1, 129.6, 128.8, 128.6, 127.8, 127.2, 125.8, 125.2, 115.4, 114.7, 52.4, 52.4, 15.2. **HRMS** (ESI^+) for $\text{C}_{21}\text{H}_{18}\text{NaO}_5\text{S}$; calculated 405.0767, found 405.0767 (error m/z = 0.0 ppm)

Dimethyl 2-(4-methoxyphenyl)-5-(4-nitrophenyl)furan-3,4-dicarboxylate (3.5h) Yellow solid, 45 mg, 55%. ^1H NMR (500 MHz, CDCl_3) δ 8.31 (d, J = 9.0 Hz, 2H), 8.04 (d, J = 9.0 Hz, 2H), 7.87 (d, J = 8.9 Hz, 2H), 7.02 (d, J = 8.9 Hz, 2H), 3.95 (s, 3H), 3.90 (s, 6H). ^{13}C NMR (126 MHz, CDCl_3) δ 164.1, 163.6, 161.2, 155.9, 149.3, 147.6, 134.6, 129.5, 127.4, 124.0, 120.8, 118.3, 114.3, 114.1, 55.4, 52.8, 52.4. **HRMS** (ESI^+) for $\text{C}_{21}\text{H}_{17}\text{NaO}_8\text{N}$; calculated 434.0846, found 434.0858 (error m/z = 2.6 ppm)

Dimethyl 2-(o-tolyl)-5-(p-tolyl)furan-3,4-dicarboxylate (3.5i) White solid, 56 mg, 77%. ^1H NMR (500 MHz, CDCl_3) δ 7.69 (d, J = 8.3 Hz, 2H), 7.49 (dd, J = 7.6, 1.2 Hz, 1H), 7.39 (td, J = 7.5, 1.4 Hz, 1H), 7.34 – 7.23 (m, 4H), 3.94 (s, 3H), 3.76 (s, 3H), 2.41 (s, 3H), 2.39 (s, 3H). ^{13}C NMR (126 MHz, CDCl_3) δ 165.0, 163.3, 155.8, 153.1, 139.6, 137.9, 130.8, 130.5, 130.0, 129.4, 128.7, 126.7, 126.1, 125.4, 116.3, 113.9, 52.6, 52.0, 21.4, 20.3. **HRMS** (ESI^+) for $\text{C}_{22}\text{H}_{20}\text{NaO}_5$; calculated 387.1203, found 387.1218 (error m/z = 3.9 ppm)

Dimethyl 2-phenyl-5-(thiophen-2-yl)furan-3,4-dicarboxylate (3.5j) Pale yellow liquid, 51 mg, 74%. ^1H NMR (500 MHz, CDCl_3) δ 7.95 (dd, J = 3.8, 1.2 Hz, 1H), 7.82 (d, J = 7.0 Hz, 2H), 7.52

– 7.40 (m, 4H), 7.16 (dd, $J = 5.0, 3.8$ Hz, 1H), 3.93 (s, 3H), 3.93 (s, 3H). ^{13}C NMR (126 MHz, CDCl_3) δ 164.7, 163.2, 151.4, 150.6, 130.4, 129.5, 129.0, 129.0, 128.7, 128.5, 127.6, 126.7, 115.6, 113.1, 52.6, 52.2. HRMS (ESI^+) for $\text{C}_{18}\text{H}_{14}\text{NaO}_5\text{S}$; calculated 365.0454, found 365.0462 (error $m/z = 2.2$ ppm)

Dimethyl 2-(naphthalen-2-yl)-5-phenylfuran-3,4-dicarboxylate (3.5k) White solid, 57 mg, 74%. ^1H NMR (500 MHz, CDCl_3) δ 8.42 (s, 1H), 7.98 – 7.91 (m, 5H), 7.90 – 7.87 (m, 1H), 7.59 – 7.54 (m, 2H), 7.53 – 7.45 (m, 3H), 3.95 (s, 3H), 3.94 (s, 3H). ^{13}C NMR (126 MHz, CDCl_3) δ 164.3, 164.2, 153.7, 153.6, 133.6, 133.0, 129.7, 128.9, 128.8, 128.6, 128.2, 127.8, 127.5, 127.3, 127.2, 126.7, 126.1, 124.3, 115.6, 115.4, 52.5, 52.5. HRMS (ESI^+) for $\text{C}_{21}\text{H}_{18}\text{NaO}_5$; calculated 409.1046, found 409.1056 (error $m/z = 2.2$ ppm)

Dimethyl 2-((3*r*,5*r*,7*r*)-adamantan-1-yl)-5-(4-methoxyphenyl)furan-3,4-dicarboxylate (3.5l) White solid, 48 mg, 57%. ^1H NMR (500 MHz, CDCl_3) δ 7.79 (d, $J = 8.9$ Hz, 2H), 6.97 (d, $J = 8.9$ Hz, 2H), 3.90 (s, 3H), 3.87 (s, 3H), 3.81 (s, 3H), 2.08 (s, 9H), 1.79 (s, 6H). ^{13}C NMR (126 MHz, CDCl_3) δ 166.0, 163.8, 160.5, 160.3, 153.9, 129.6, 122.0, 113.9, 113.7, 112.0, 55.4, 52.4, 51.9, 40.0, 36.5, 36.3, 28.2. HRMS (ESI^+) for $\text{C}_{25}\text{H}_{28}\text{NaO}_6$; calculated 447.1778, found 447.1781 (error $m/z = 0.7$ ppm)

Tetramethyl 5,5'-(1,4-phenylene)bis(2-(4-methoxyphenyl)furan-3,4-dicarboxylate) (3.5m) White solid, 51 mg, 39%. ^1H NMR (500 MHz, CDCl_3) δ 7.94 (s, 4H), 7.88 (d, $J = 8.9$ Hz, 4H), 7.01 (d, $J = 8.9$ Hz, 4H), 3.94 (s, 6H), 3.90 (s, 12H). ^{13}C NMR (126 MHz, CDCl_3) δ 164.5, 164.0, 160.9, 154.7, 151.4, 129.4, 129.3, 129.1, 127.0, 121.3, 116.1, 114.0, 55.4, 52.6, 52.3. HRMS (ESI^+) for $\text{C}_{36}\text{H}_{30}\text{NaO}_{12}$; calculated 677.1654, found 677.1645 (error $m/z = -1.3$ ppm)

2-phenyl-4H-chromeno[3,4-d]oxazole (3.5n) White solid, 41 mg, 82%. ^1H NMR (500 MHz, CDCl_3) δ 8.11 (d, $J = 9.7$ Hz, 2H), 7.60 – 7.48 (m, 3H), 7.43 (dd, $J = 7.5, 1.6$ Hz, 1H), 7.23 – 7.14

(m, 1H), 7.01 (td, $J = 7.5, 1.0$ Hz, 1H), 6.94 (dd, $J = 8.2, 0.8$ Hz, 1H), 5.55 (s, 2H). ^{13}C NMR (126 MHz, CDCl_3) δ 161.8, 153.0, 142.5, 130.9, 130.6, 129.3, 128.9, 127.2, 126.3, 121.7, 119.9, 116.5, 115.1, 66.4. HRMS (ESI^+) for $\text{C}_{16}\text{H}_{12}\text{NO}_2$; calculated 250.0863, found 250.0865 (error $m/z = 1.1$ ppm)

3.5 References

- (1) a) Boto, A. and Alvarez, L. Furan and Its Derivatives. In *Heterocycles in Natural Product Synthesis* (eds K.C. Majumdar and S.K. Chattopadhyay), **2011**. b) Keay, B. A.; Hopkins, J. M.; Dibble, P. W., Furans and their Benzo Derivatives: Applications. In *Comprehensive Heterocyclic Chemistry III*, Katritzky, A. R.; Ramsden, C. A.; Scriven, E. F. V.; Taylor, R. J. K., Eds. Elsevier: Oxford, **2008**; pp 571-623. c) Pozharskii, A.F., Soldatenkov, A.T. and Katritzky, A.R. *Heterocycles in Life and Society* (eds A.F. Pozharskii, A.T. Soldatenkov and A.R. Katritzky), **2011**. d) Saleem, M.; Kim, H. J.; Ali, M. S.; Lee, Y. S., *Nat. Prod. Rep.* **2005**, *22*, 696-716.
- (2) a) Sperry, J. B.; Wright, D. L., *Curr. Opin. Drug Discovery Dev.* **2005**, *8*, 723-740. b) Zanatta, N.; Alves, S. H.; Coelho, H. S.; Borchhardt, D. M.; Machado, P.; Flores, K. M.; da Silva, F. M.; Spader, T. B.; Santurio, J. M.; Bonacorso, H. G.; Martins, M. A. P., *Biorg. Med. Chem.* **2007**, *15*, 1947-1958. c) Mortensen, D. S.; Rodriguez, A. L.; Carlson, K. E.; Sun, J.; Katzenellenbogen, B. S.; Katzenellenbogen, J. A., *J. Med. Chem.* **2001**, *44*, 3838-3848. d) Wu, Y.-J., *Prog. Heterocycl. Chem.* **2012**, *24*, 1-53. e) Hasegawa, F.; Niidome, K.; Migihashi, C.; Murata, M.; Negoro, T.; Matsumoto, T.; Kato, K.; Fujii, A., *Bioorg. Med. Chem. Lett.* **2014**, *24*, 4266-4270.
- (3) a) Tsuji, H.; Nakamura, E., *Acc. Chem. Res.* **2017**, *50*, 396-406. b) Glenis, S.; Benz, M.; LeGoff, E.; Schindler, J. L.; Kannewurf, C. R.; Kanatzidis, M. G., *J. Am. Chem. Soc.* **1993**, *115*, 12519-12525. c) Bunz, U. H. F., *Angew. Chem. Int. Ed.* **2010**, *49*, 5037-5040. d) Woo, C. H.; Beaujuge, P. M.; Holcombe, T. W.; Lee, O. P.; Fréchet, J. M. J., *J. Am. Chem. Soc.* **2010**, *132*, 15547-15549. e) Lin, J. T.; Chen, P.-C.; Yen, Y.-S.; Hsu, Y.-C.; Chou, H.-H.; Yeh, M.-C. P., *Org. Lett.* **2009**, *11*, 97-100.
- (4) a) Lee, H.-K.; Chan, K.-F.; Hui, C.-W.; Yim, H.-K.; Wu, X.-W.; Wong Henry, N. C., *Pure Appl. Chem.* **2005**, *77*, 139. b) Lipshutz, B. H., *Chem. Rev.* **1986**, *86*, 795-819. c) Montagnon, T.; Tofi, M.; Vassilikogiannakis, G., *Acc. Chem. Res.* **2008**, *41*, 1001-1011. d) Pedro, M.; Tomas, T.; Delso, J. I.; Rosa, M., *Curr. Org. Chem.* **2007**, *11*, 1076-1091.

- (5) a) Amarnath, V.; Amarnath, K., *J. Org. Chem.* **1995**, *60*, 301-307. b) Feist, F., *Ber. Dtsch. Chem. Ges.* 1902, *35*, 1537-1544. c) Benary, E., *Ber. Dtsch. Chem. Ges.* **1911**, *44*, 489-493.
- (6) a) Wong, H.N.C., Hou, X.-L., Yeung, K.-S. and Huang, H. Five-Membered Heterocycles: Furan. *In Modern Heterocyclic Chemistry*, **2011**, pp: 533-592. b) Ila, H.; Baron, O.; Wagner, A. J.; Knochel, P., *Chem. Comm.* **2006**, *6*, 583-593. c) Melzig, L.; Rauhut, C. B.; Knochel, P., *Chem. Comm.* **2009**, (24), 3536-3538. d) Chadwick, D. J.; Willbe, C., *J. Chem. Soc., Perkin Trans. 1* **1977**, *8*, 887-893. e) Pinhey, J. T.; Roche, E. G., *J. Chem. Soc., Perkin Trans. 1* **1988**, *8*, 2415-2421.
- (7) For reviews, see: a) Donnelly, D. M. X.; Meegan, M. J., Furans and their Benzo Derivatives: (iii) Synthesis and Applications. In *Comprehensive Heterocyclic Chemistry*, Katritzky, A. R.; Rees, C. W., Eds. Pergamon: Oxford, **1984**; pp 657-712. b) A. Keay, B., *Chem. Soc. Rev.* **1999**, *28*, 209-215. c) Hou, X. L.; Cheung, H. Y.; Hon, T. Y.; Kwan, P. L.; Lo, T. H.; Tong, S. Y.; Wong, H. N. C., *Tetrahedron* **1998**, *54*, 1955-2020. d) Brown, R. C. D., *Angew. Chem. Int. Ed.* **2005**, *44*, 850-852. e) Krasnoslobodskaya, L. D.; Gol'dfarb, Y. L., *Russ. Chem. Rev.* 1969, *38* (5), 389-406. f) Moran, W. J.; Rodríguez, A., *Org. Prep. Proced. Int.* **2012**, *44*, 103-130. g) Gulevich, A. V.; Dudnik, A. S.; Chernyak, N.; Gevorgyan, V., *Chem. Rev.* 2013, *113* (5), 3084-3213.
- (8) For selected recent examples, see a) Sromek, A. W.; Rubina, M.; Gevorgyan, V., *J. Am. Chem. Soc.* **2005**, *127*, 10500-10501. b) Yang, Y.; Yao, J.; Zhang, Y., *Org. Lett.* **2013**, *15*, 3206-3209. c) Barluenga, J.; Riesgo, L.; Vicente, R.; López, L. A.; Tomás, M., *J. Am. Chem. Soc.* **2008**, *130*, 13528-13529. d) He, C.; Guo, S.; Ke, J.; Hao, J.; Xu, H.; Chen, H.; Lei, A., *J. Am. Chem. Soc.* **2012**, *134*, 5766-5769. e) Dey, A.; Ali, M. A.; Jana, S.; Hajra, A., *J. Org. Chem.* **2017**, *82*, 4812-4818. f) Wu, J.; Yoshikai, N., *Angew. Chem. Int. Ed.* **2015**, *54* 11107-11111. g) Raut, V. S.; Jean, M.; Vanthuynne, N.; Roussel, C.; Constantieux, T.; Bressy, C.; Bugaut, X.; Bonne, D.; Rodriguez, J., *J. Am. Chem. Soc.* **2017**, *139*, 2140-2143.
- (9) a) Jung, C.-K.; Wang, J.-C.; Krische, M. J., *J. Am. Chem. Soc.* **2004**, *126*, 4118-4119. b) Zou W., He Z.-R., He Z., *Chin. J. Org. Chem.*, **2015**, *35*, 1739-1745. c) Kao, T.-T.; Syu, S.-e.; Jhang, Y.-W.; Lin, W., *Org. Lett.* **2010**, *12*, 3066-3069.

- (10) a) Gribble, G. W., Mesoionic Ring Systems. In *Synthetic Applications of 1,3-Dipolar Cycloaddition Chemistry Toward Heterocycles and Natural Products*, **2002**, pp 681-753. b) Gingrich, H.L. and Baum, J.S. Mesoionic Oxazoles. In *Chemistry of Heterocyclic Compounds*, **2008**, pp 731-961
- (11) a) Hamaguchi, M.; Ibata, T., *Tetrahedron Lett.* **1974**, *15*, 4475-4476. b) Padwa, A.; Hertzog, D. L.; Chinn, R. L., *Tetrahedron Lett.* **1989**, *30*, 4077-4080. c) Gowravaram, M. R.; Gallop, M. A., *Tetrahedron Lett.* **1997**, *38*, 6973-6976.
- (12) a) Hamaguchi, M.; Nagai, T., *J. Chem. Soc., Chem. Commun.* **1985**, *4*, 190-191. b) Hamaguchi, M.; Nagai, T., *J. Chem. Soc., Chem. Commun.* **1985**, *19*, 1319-1321.
- (13) a) Dhawan, R.; Dghaym, R. D.; Arndtsen, B. A., *J. Am. Chem. Soc.* **2003**, *125*, 1474-1475. b) St. Cyr, D. J.; Martin, N.; Arndtsen, B. A., *Org. Lett.* **2007**, *9*, 449-452.
- (14) a) St. Cyr, D. J.; Arndtsen, B. A., *J. Am. Chem. Soc.* **2007**, *129*, 12366-12367. b) Erguven, H.; Leitch, D. C.; Keyzer, E. N.; Arndtsen, B. A., *Angew. Chem.* **2017**, *129*, 6174-6178
- (15) Aly, S.; Romashko, M.; Arndtsen, B. A., *J. Org. Chem.* **2015**, *80*, 2709-2714.
- (16) a) Kayser, L. V.; Vollmer, M.; Welnhof, M.; Krikeziokat, H.; Meerholz, K.; Arndtsen, B. A., *J. Am. Chem. Soc.* **2016**, *138*, 10516-10521. b) Kayser, L. V.; Hartigan, E. M.; Arndtsen, B. A., *ACS Sustainable Chem. Eng.* **2016**, *4*, 6263-6267. c) Moquin, A.; Hanna, R.; Liang, T.; Erguven, H.; Gran, E. R.; Arndtsen, B. A.; Maysinger, D.; Kakkar, A., *Chem. Comm.* **2019**, *55*, 9829-9832.
- (17) a) Su, W.; Can, J., *J. Chem. Res.* **2005**, *2005*, 88-90. b) Ishino, Y.; Mihara, M.; Takeuchi, T.; Takemoto, M., *Tetrahedron Lett.* **2004**, *45*, 3503-3506. c) Chou, T. S.; Knochel, P., *J. Org. Chem.* **1990**, *55*, 4791-4793.
- (18) Adams, R.; Vollweiler, E. H., *J. Am. Chem. Soc.* **1918**, *40*, 1732-1746.
- (19) St-Cyr, D. J.; Morin, M. S. T.; Bélanger-Gariépy, F.; Arndtsen, B. A.; Krenske, E. H.; Houk, K. N., *J. Org. Chem.* **2010**, *75*, 4261-4273.
- (20) Engel, R. Phosphorus Addition at sp^2 Carbon. In *Organic Reactions*, **2004**, pp 175-248.

- (21) Boa, A.N. and Jenkins, P.R. Benzoyl Trifluoromethanesulfonate. In *Encyclopedia of Reagents for Organic Synthesis*, **2001**.
- (22) Morin, M. S. T.; St-Cyr, D. J.; Arndtsen, B. A.; Krenske, E. H.; Houk, K. N., *J. Am. Chem. Soc.* **2013**, *135*, 17349-17358.
- (23) Tebby, J. C., *Handbook of Phosphorus-31 Nuclear Magnetic Resonance Data (1990)*. CRC press: **2017**.
- (24) Vedachalam, S.; Zeng, J.; Gorityala, B. K.; Antonio, M.; Liu, X.-W., *Org. Lett.* **2010**, *12*, 352-355.

CHAPTER 4

A Versatile Approach to Dynamic Amide Bond Formation with Imine Nucleophiles¹

4.0 Preface

In Chapters 2 and 3, we exploited the ability of imines or aldehydes to react with acyl chlorides to form electrophilic *N*-acyl iminium salts or oxonium salts, respectively, as intermediates in the assembly of new 1,3-dipoles. In this chapter, we turn to use this chemistry with imines in another direction: dynamic covalent chemistry (DCvC), and the controlled formation of amides. Amides are typically generated in an irreversible fashion from carboxylic acid derivatives and amines, and their high C-N bond strength prevents their use in dynamic chemistry, except under specific conditions (Section 1.3.3). We show here how this can be addressed by replacing amines with imines in reaction with acyl chlorides. In contrast to classical amides, the formation of α -chloroamides is found to be highly reversible at ambient temperature, and without the need for catalysts. This chapter details this investigation, including equilibrium constants for the formation of α -chloroamides, the influence of structure and conditions on this equilibrium, as well as the ability of these systems to undergo exchange and be trapped to robust amides. This work has been submitted for publication (Erguven, H.; Keyzer, E. N.; Arndtsen, B. A. *Chem. Eur. J.* doi: 10.1002/chem.202001140).

4.1 Introduction

The use of reversible bonding interactions to control product formation is central to self-assembly and supramolecular chemistry.² While these efforts have traditionally relied upon weak bonding forces such as metal coordination, hydrogen bonding, or related van der Waals interactions, there has been significant recent interest in exploiting covalent organic bonds in these platforms, i.e. dynamic covalent chemistry (DCvC).³ Such dynamic covalent systems can form more robust products, and have seen growing use in applications ranging from covalent organic frameworks,⁴ adaptive materials,⁵ polymerizations,⁶ drug discovery,⁷ or catalyst design.⁸ However, it is notable that the functional groups commonly generated in DCvC (imines, disulfides, boronic acid derivatives, etc.)⁹ are often not those that have found widespread use in synthetic materials. This distinction is due in large part to the moderate strength and reversible nature of many the bonds generated by these reactions, which can present a problem in the many areas where structural integrity is critical. The use of catalysis to create dynamic bond forming reactions has provided a solution to these limitations in a number of systems (e.g. olefin metathesis),¹⁰ as has post-synthesis modification.¹¹ Nevertheless, coupling dynamic bond formation with the generation of robust and relevant functional groups remains a challenge.

One particularly attractive bond for dynamic formation are amides. Amides represent the core functional units in a tremendous array of useful compounds, including polymers (Nylons, Kevlar), biomolecules, or pharmaceuticals (>54% of marketed drugs).¹² A useful feature of amides is their high carbonyl-nitrogen bond strength of up to 90-100 kcal/mol,¹³ together with accessibility from available reagents: amines and carboxylic acid derivatives (Figure 4.1a). Unfortunately, the strength of the amide bond has limited its direct use in dynamic covalent chemistry. Important exceptions include the work by Gellman, Stahl and others on catalysts for amide exchange

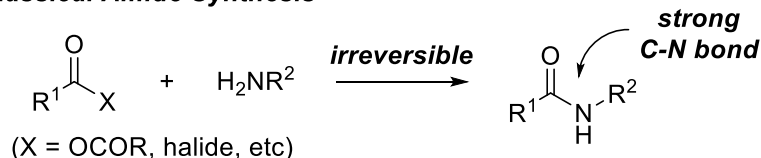
reactions,¹⁴ or the use of thiol-tethered amides in peptide-based dynamic covalent chemistry (Figure 4.1b).^{15,16} The conversion of dynamically generated imines by oxidation has also been shown by Yaghi to allow access amide structures in COFs.¹⁷ However, the scope, specific substrates or conditions required in these systems can be limiting for many applications.

In light of these features, the design of an accessible and general route to form amides in a dynamic fashion could prove of utility. One possible approach is via a change to the substrate. In contrast to the primary or secondary amines commonly employed in amidations, imines are weak nucleophiles that are easily generated from primary amines and aldehydes, and couple with acyl chlorides to form reactive products: α -chloroamides. The latter are established precursors to *N*-acyl iminium salt electrophiles that have been exploited in a broad range of synthetic transformations.¹⁸ Importantly here, as *N*-R substituted imines lack a leaving proton, their products with acyl chlorides are also less stable than classical amides. During the course of our studies using α -chloroamides in catalysis,¹⁹ we have noted that the generation of these substrates from imines and acyl chlorides, while rapid, is often incomplete, suggesting that this may be a reversible reaction. The latter has been alluded to as well in other reports focusing on exploiting their reactivity,^{18,20} but has not been probed for its dynamic nature. This led us to question if the simple reaction of imines and acyl chlorides could be a previously unexploited dynamic covalent reaction that can be used to generate amides.

In order to use this reaction in dynamic covalent chemistry, it is important that the system is able to: a) undergo reversible C-N bond formation, b) be readily modulated to control the equilibrium, c) access thermodynamically favored products via exchange, and ideally d) be used to generate robust amide products. We describe herein our systematic studies of these factors. These demonstrate that the surprisingly simple use of imines rather than amines in the well-known

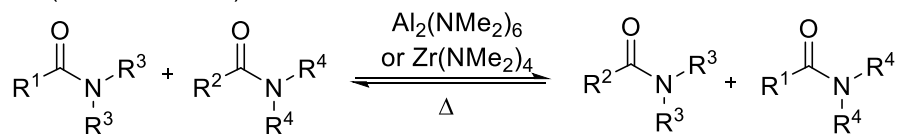
reaction with acyl chlorides can offer what is to our knowledge the first general platform to generate amides in a dynamic fashion (Figure 4.1c). The transformation occurs at ambient temperature, without catalysts, can be broadly diversified, and the reactivity of the iminium salt can allow it to be converted into various classes of amide-containing products.

a) Classical Amide Synthesis

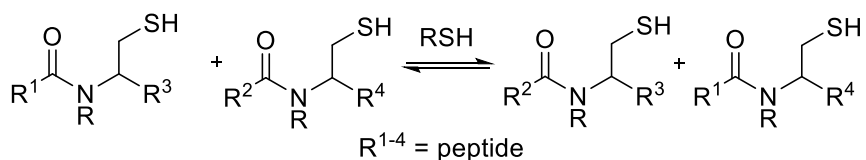


b) Reversible Amides with Catalysts/Thiol Tethered Peptides

(Stahl, Gellman)



(Giuseppone)



c) This work: Dynamic Amide Formation with Imines

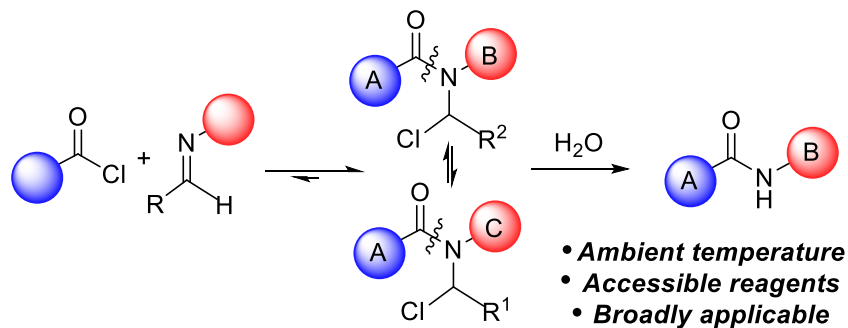


Figure 4.1 Dynamic covalent approaches to amides

4.2 Results and Discussion

4.2.1. Reversibility of Imine/Acyl Chloride Reaction

Our initial studies on this system probed the reversibility in the reaction of *N*-benzyl substituted imine **4.1a** with benzoyl chloride (**4.2a**). As has been previously noted, mixing these in CDCl₃ leads to the rapid build-up of amide **4.3aa** within minutes at ambient temperature, as determined by ¹H NMR analysis (Figure 4.2a, b). This reaction reaches a maximum conversion of 94% after 2 h together with remaining imine and acyl chloride. While this is suggestive of the reaction reaching equilibrium, it is also possible that low concentrations of **4.1a** and **4.2a** slow the chemistry and inhibit complete **4.3aa** formation. One way to probe the reaction is truly at equilibrium is to isolate **4.3aa** and examine its chemistry. **4.3aa** can be isolated as a white solid by precipitation with pentane, and NMR analysis shows it is stable in CDCl₃ at low temperatures (5°C). However, warming **4.3aa** to ambient temperature leads to that rapid re-formation of imine/acyl chloride in the same ratios as noted above (Figure 4.2b), clearly demonstrating that the formation of amide **4.3** is indeed dynamic, and establishes this equilibrium within minutes at ambient conditions. Performing the reaction in both the forward and reverse direction allowed the accurate assessment of K_{eq} , which show it has a high association constant ($K_{eq} = 1.54 \pm 0.03 \times 10^3 \text{ M}^{-1}$), and the formation of **4.3aa** is essentially quantitative at high concentrations (>0.40 M).

4.2.2. Control of Equilibrium

We next examined our ability to control this equilibrium. The formation of **4.3** shows a moderate dependence upon solvent. For example, the reaction of **4.1a** and **4.2a** in the higher dielectric constant solvent acetonitrile leads to a faster establishment of the equilibrium, but a similar equilibrium constant ($1.80 \pm 0.02 \times 10^3 \text{ M}^{-1}$). The equilibrium constant is more

significantly lowered in benzene solvent ($9.9 \pm 0.2 \times 10^2 \text{ M}^{-1}$). However, the solvent polarity influence on K_{eq} is not large, implying that **4.3aa** exists in the predominately non-ionic α -chloroamide form shown. The latter is supported by ^1H and ^{13}C NMR analysis, which show an upfield shift in the former imine hydrogen of **4.3aa** (from 8.44 to 7.33 ppm) and carbon (from 161.6 to 78.0 ppm), and consistent with previous reports on these structures.^{19b,21} Variation of the reaction temperature can also favor the formation of **4.3aa** ($K_{\text{eq}} = 6100$ at 8°C), and show its generation is exothermic ($\Delta H = -54.0 \pm 0.7 \text{ kJ/mol}$) and entropically disfavored ($\Delta S = -119 \pm 2.2 \text{ J/mol}\cdot\text{K}$, Figure 4.2c).

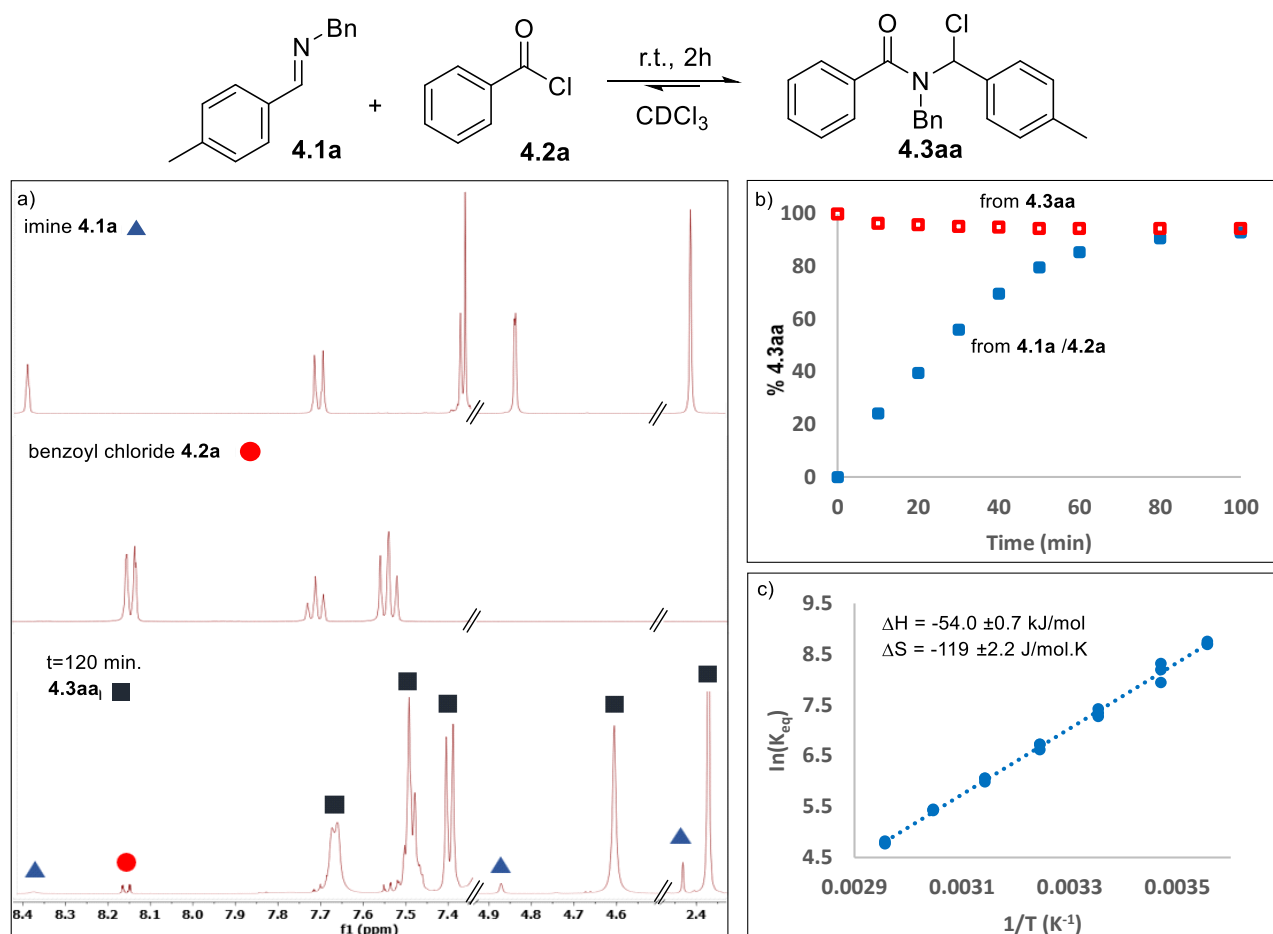
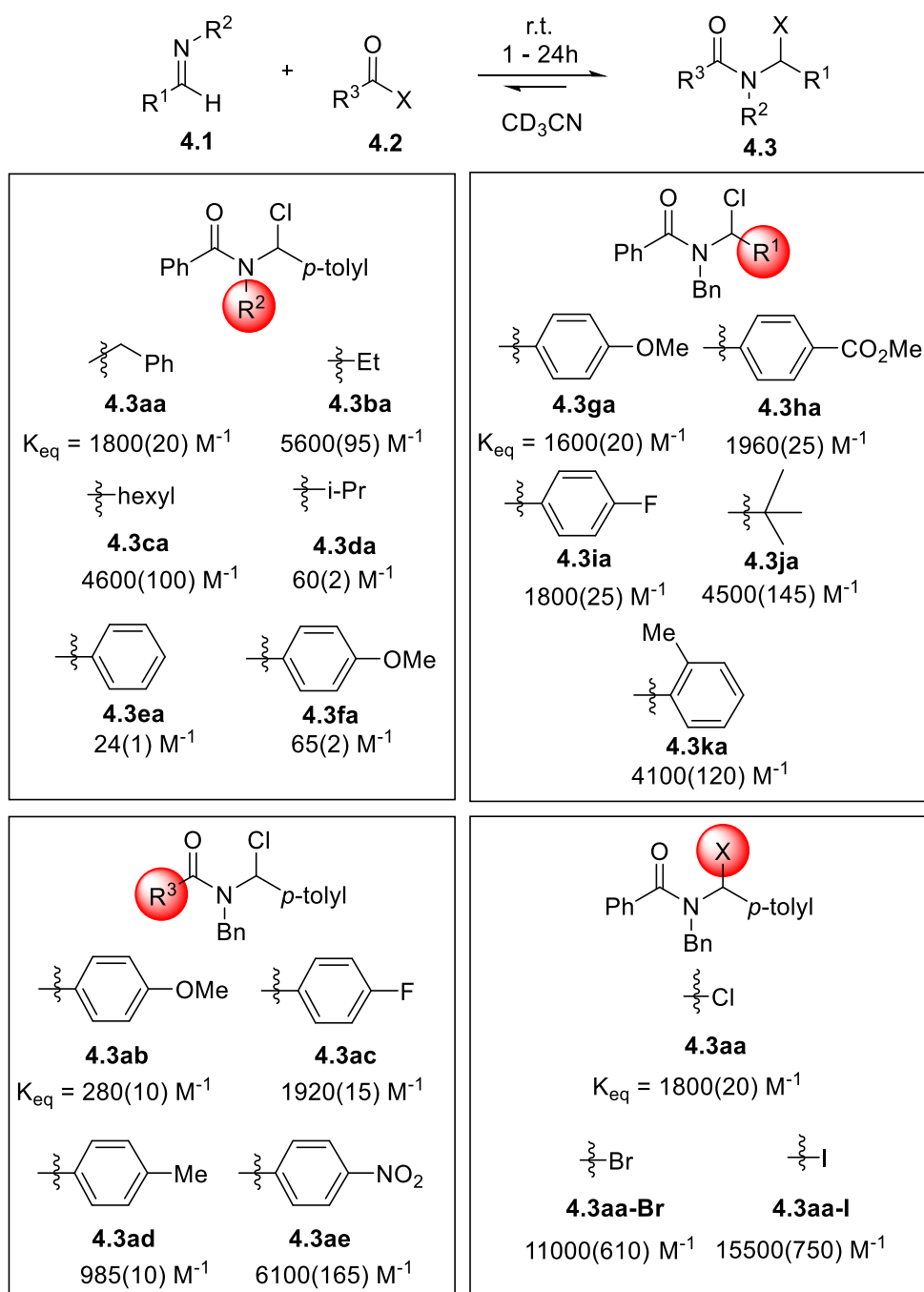


Figure 4.2 Reaction of **4.1a** and **4.2a** (0.20 mmol) in 1.0 mL CDCl_3 . a) ^1H NMR spectra of components **4.1a**, **4.2a**, and reaction at 120 min. b) Reaction progression vs. time from **4.1a** + **4.2a** (filled) or from isolated **4.3aa** (open). c) van't Hoff plot, $\ln(K_{\text{eq}})$ vs. temperature $^{-1}$ in CD_3CN .

In addition to manipulation of the physical parameters, the availability of the imine (from amines/aldehydes) and acyl chloride substrates can be employed to tune the structure of **4.3** to further modulate the equilibrium (Table 4.1). For example, the incorporation of electron donor alkyl groups onto the imine nitrogen shifts the reaction toward **4.3**, but retains the ability to rapidly establish an equilibrium at ambient temperature (e.g. **4.3ba**: $K_{\text{eq}} = 5600 \text{ M}^{-1}$; **4.3ca**: $K_{\text{eq}} = 4600 \text{ M}^{-1}$). Alternatively, electron withdrawing groups suppress the reaction ($K_{\text{eq}} = 24 \text{ M}^{-1}$ for **4.3ea**). There is less electronic influence of the imine carbon substituent, where *p*-Me- (**4.1a**), *p*-MeO- (**4.1g**) and *p*-MeO₂C- (**4.1h**) substituted *C*-aryl imines lead to comparable equilibrium constants. The latter may arise from the decreased conjugation of this aromatic substituent in the covalent form of **4.3**, limiting its influence on stability. Consistent with this postulate, the *C*-^tBu imine (**4.1j**), which lacks conjugation in **4.1**, display increased association constants ($K_{\text{eq}} = 4500 \text{ M}^{-1}$), as does the *o*-tolyl imine (**4.1k**, $K_{\text{eq}} = 4100 \text{ M}^{-1}$), where the sterically encumbered aryl unit may diminish conjugation with the C=N bond and favors acylation.

The acyl chloride unit can similarly influence K_{eq} , wherein electron deficient reagents favor reaction, while electron donating groups lead to lower equilibrium constants (**4.3ab-4.3ae**). The halide anion itself offers a further tool of reaction control. Thus, exchange of chloride for bromide or iodide leads to a further favored formation of **4.3aa** ($K_{\text{eq}} = 1.1 \times 10^4 \text{ M}^{-1}$ and $1.5 \times 10^4 \text{ M}^{-1}$ for X = Br and I, respectively). The latter presumably reflects the enhanced electrophilicity of the acyl halide.²² Overall, between temperature, concentration, anion, and the structure of the three substituents, the equilibrium with **4.3** can be finely modulated to generate libraries of products in anywhere from the near quantitative yield to those where the reaction is disfavored.

Table 4.1. Influence of imine, acyl chloride and halide on dynamic formation of amides **4.3**.^a



^aEquilibrium constants determined by ¹H NMR analysis, average of three experiments. Error in brackets.

4.2.3. Dynamic Exchange

An important feature for the use of amide **4.3** in dynamic chemistry is its ability to undergo exchange reactions to access thermodynamically favored products. To test this potential, the *N*-benzyl substituted imine **4.1a** was added to **4.3ee**. Monitoring this reaction by *in situ* NMR analysis shows the rapid incorporation of **4.1a** to generate **4.3ae** (Figure 4.3a). Within 2 h at ambient temperature, the equilibrium is fully established, and the equilibrium constant ($K_{\text{eq}} = 25$) reflects the more stable amide generated with imine **4.1a** (e.g. Table 4.1).

A similar reaction was examined with the more stable amide **4.3aa** and the imine **4.11** (Figure 4.3b). Once again, exchange is observed, although here the reaction takes ca. 48 h to achieve equilibrium. This slower equilibration presumably arises from the greater stability of **4.3aa**, which has a less favored dissociation to free imine and acyl chloride. This reaction once again leads to the favored formation of the more robust product **4.3la**, with a $K_{\text{eq}} = 8.0$ relative to **4.3aa**.

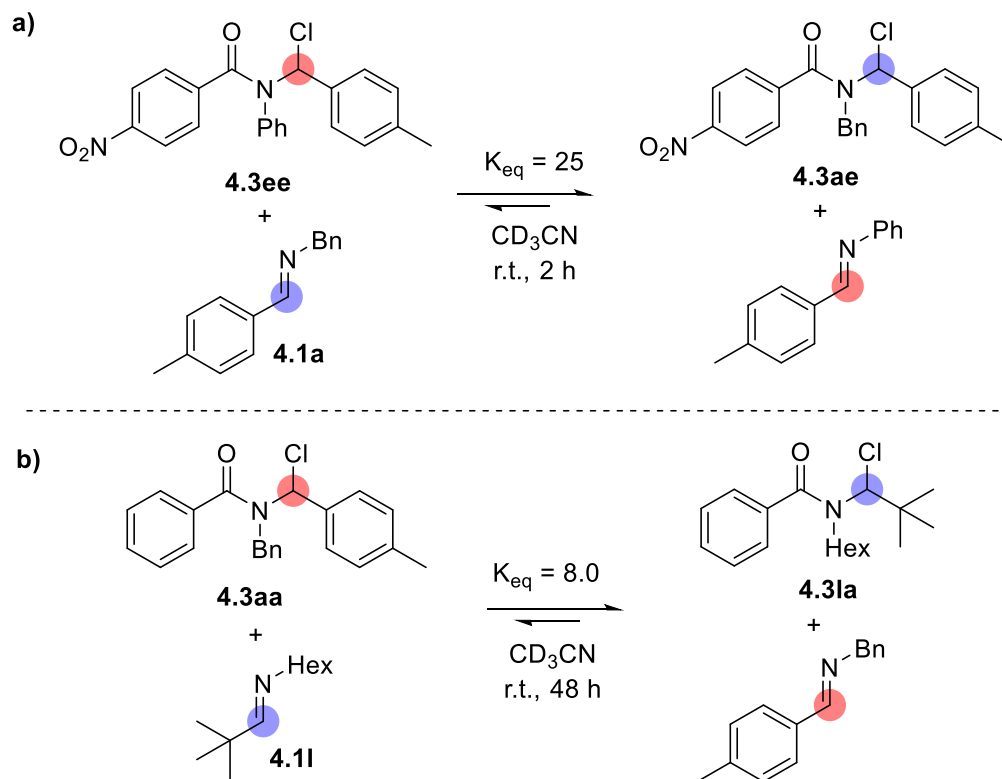


Figure 4.3 Dynamic exchange of **4.3** with imines

While the above data suggests a free imine can exchange with **4.3**, a more critical feature for the ultimate use of this transformation in DCvC is the ability of **4.3** to undergo self-exchange. The latter is necessary in order to design amide forming transformations that cycle into thermodynamically favoured products, but has also not been shown to be viable with α -chloroamides. Nevertheless, the rapid rate of equilibration between **4.3** and free imine (Figure 4.3) suggests such a reaction should be viable.

This potential was assessed in the reaction between two different α -chloroamides, **4.3ma** and **4.3ie**. These substrates were chosen since they both have *N*-alkyl substituents and therefore high association constants, which would therefore not bias the system towards free imine and acyl chloride and favor exchange. Moreover, the fluoro-substituent on the aromatic unit can be used to

easily monitor the equilibrium by ^{19}F NMR analysis. As shown in Figure 4.4, despite their favoured association, the amides begin to scramble within 1 h at ambient temperature. After ca. 30 h, a near statistical mixture of all four expected amide products is observed, and can be quantified by ^1H and ^{19}F NMR analysis. Of note, the overall equilibrium constant for this exchange ($K_{\text{eq}} = 1.1$) is slightly biased toward interaction of the more nucleophilic imine with the more electrophilic acyl chloride fragment (**4.3me**). The latter is reflected as well in the individual association constants of the four products (values given in Figure 4.4). Moreover, the overall equilibrium constant of this scrambling is a composite of the four individual equilibrium reactions, suggesting that the exchange has reached equilibrium at ambient temperature.

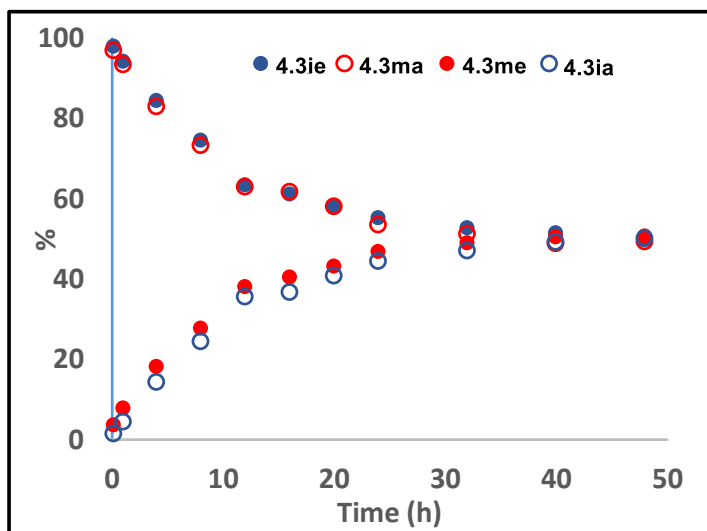
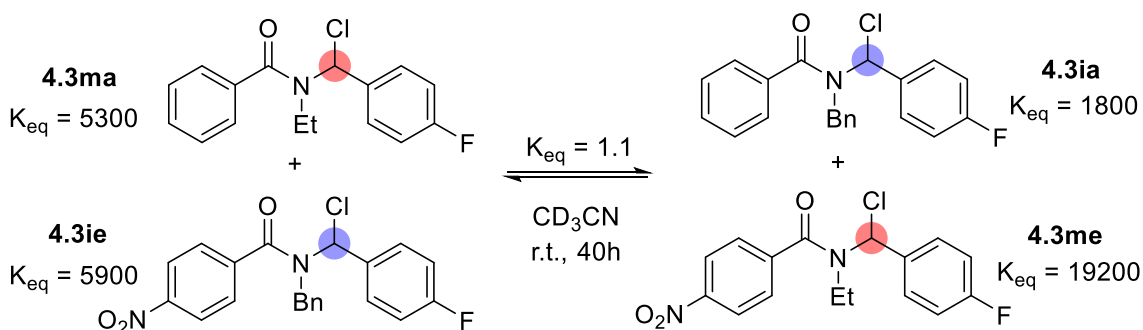
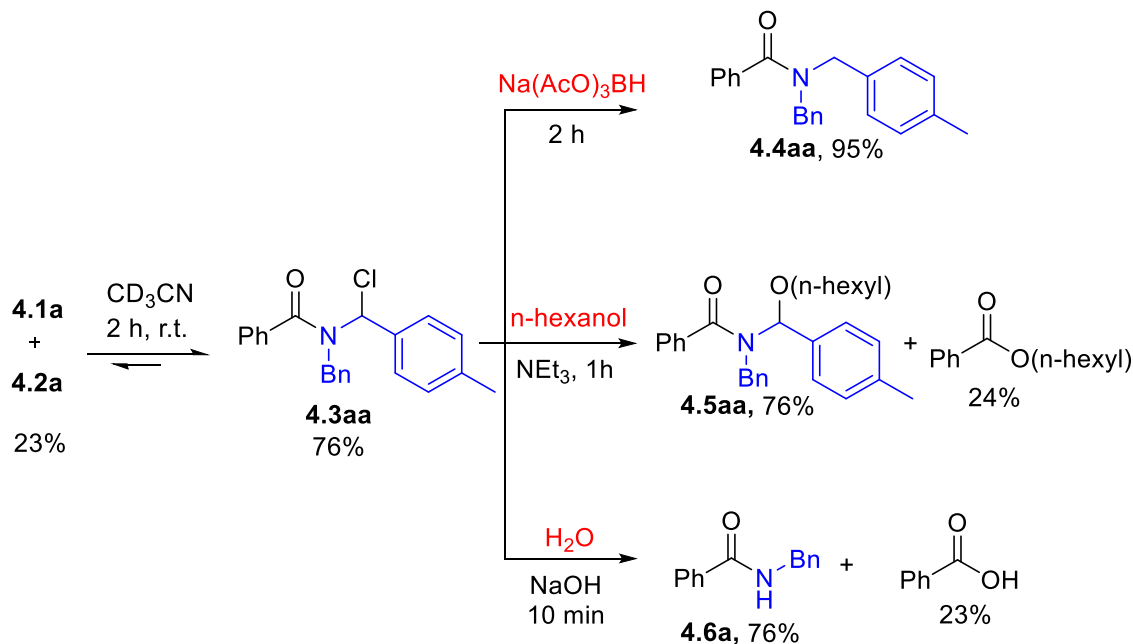


Figure 4.4 Dynamic exchange between amides **4.3**.

4.2.4. Controlled Generation of Secondary and Tertiary Amide Products

The above results demonstrate that the formation of amide **4.3** is dynamic, these amide products can undergo exchange, and each of the equilibrium is established within minutes or hours without the need for catalysts or high temperatures. Moreover, the reagents needed for the reaction are not synthetically elaborate, and instead either commercial (acyl chlorides) or generated from amines and aldehydes (imines) that are inexpensive and available in many forms. However, one limitation of this reaction is that this reversibility of **4.3** is obtained through the lability of the C-N bond. Thus, these are not the robust amides found in many products, and, much as with many dynamic reactions, **4.3** can easily dissociate or react. Another notable feature of **4.3** is that it is an *N*-acyl iminium salt precursor, and capable of rapidly reacting with nucleophiles to generate robust secondary and tertiary amide products.¹⁹ We therefore next questioned if this reactivity could be coupled with the dynamic formation of **4.3** to access stable materials.

In order to exploit this reactivity of **4.3**, the nucleophile would need to efficiently couple with **4.3** but not influence the equilibrium reaction between different amides or the reagents. Since the equilibrium between **4.3** and imine/acyl chloride occurs at ambient temperature, if the nucleophile does not efficiently trap both **4.3** and the acyl chloride at the same time, this equilibrium will shift away from the thermodynamically favored product. This was explored by generating **4.3aa** at low concentration to allow it to form in only moderate yield (76%) together with significant remaining imine and acyl chloride (ca. 23%), meaning that any perturbation on the equilibrium mixture should be easily observed. As shown in Scheme 4.1, the addition of the hydride donor sodium triacetoxyborohydride to this mixture effectively reacts with **4.3aa** but not acyl chloride **4.1a**, and results in the formation of tertiary amide **4.4aa** in near quantitative yield, rather than freezing the equilibrium mixture.²³



Scheme 4.1 Efficient Trapping of the Dynamically Formed **4.3** to Access Secondary and Tertiary Amides.

In contrast to the soft hydride nucleophile, we were pleased to find that the addition of simple alcohols (e.g. hexanol) to **4.3aa** forms **4.5aa** within 1 h at ambient temperature in a yield (76%) that reflects the initial concentration of **4.3aa**. More importantly, the residual acyl chloride formed in the equilibrium is rapidly converted to ester under these conditions (24%). This suggests that the alcohol quantitatively traps the amide structure originally present in solution. The trapping can also be performed with water. The simple hydrolysis of **4.3aa** with 1M NaOH results in a rapid and quantitative reaction to generate amide **4.6a** and carboxylic acid in yields (76% and 23% respectively) that also reflect the equilibrium concentration of **4.3aa**. The latter offers a route to access robust secondary amide products after exchange.

4.2.5. Coupling Exchange and Hydrolysis

A final test of this transformation is if trapping can effectively freeze systems where dynamic exchange is possible. The latter was examined with the coupling of two different imines, **4.1g** and **4.1l**, and benzoyl chloride. The reaction of the two parent amines with substoichiometric benzoyl chloride under these conditions leads to a 1:1 mixture of amide products. In contrast, the reaction of imines **4.1g** and **4.1l** with 0.25 equiv. benzoyl chloride leads to the rapid, preferred formation of **4.3ga**. Moreover, immediate quenching by hydrolysis after 10 min generates amide **4.6a** in 78% yield (Figure 4.5). The latter presumably arises from the faster reaction of the benzaldimine **4.1g** compared to the more sterically hindered **4.1l**. However, if instead this imine/acyl chloride mixture is allowed to reach equilibrium (45 °C, 2h), the more thermodynamically stable **4.3la** forms (e.g. Figure 4.3b), and hydrolysis results instead in the high yield formation of amide **4.6c** (81%). The coupling of equilibration of **4.3** with hydrolysis can therefore be directed towards either secondary amide product, where in this case the imine *C*-substituent modulates selectivity.

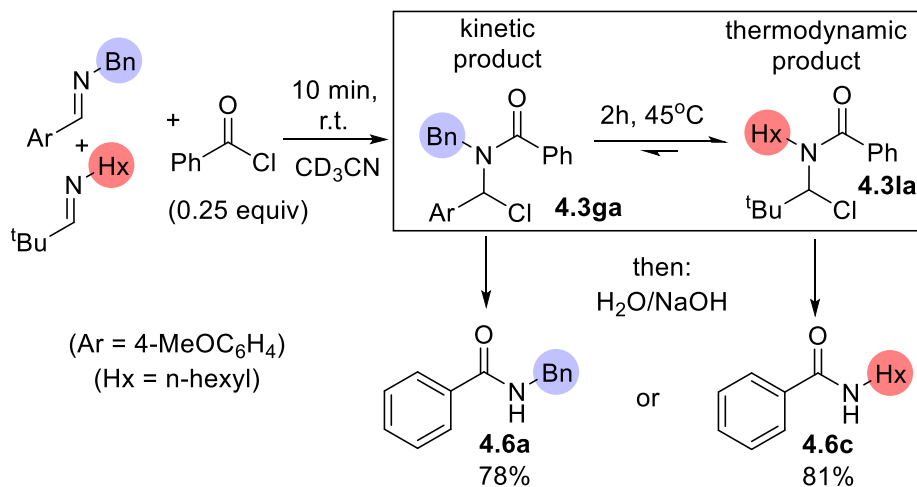


Figure 4.5 Kinetical and Thermodynamic Controlled Generation and Trapping of Secondary Amides via **4.3**.

4.2.6. Utility in Macrocyclizations

The above data suggests that the reaction of imines/acyl chlorides offers a new avenue to access amides in a dynamic fashion, as well as one that can be readily controlled. As a preliminary illustration of how this system could prove useful, we explored its application to the formation of amide polymers and macrocycles. Polyamides, such as commodity nylons, are classically prepared from diamines and diacyl chlorides.²⁴ However, the control of this reaction between polymers and macrocycles can prove a challenge, since the irreversibility of amide formation often limits factors that might be modulated to reagent ratios and concentration. This has proven particularly difficult in amide macrocyclizations, which have found utility in areas ranging from drug design and supramolecular chemistry,²⁵ but commonly require ultra-high dilution (< 0.005 M) and slow addition to form products in mixtures with polymers.²⁶ These features can often make many amide macrocyclizations impractical for large scale synthesis, or require the use of specifically designed products or templates to favor cyclization, limiting their generality.^{27,28}

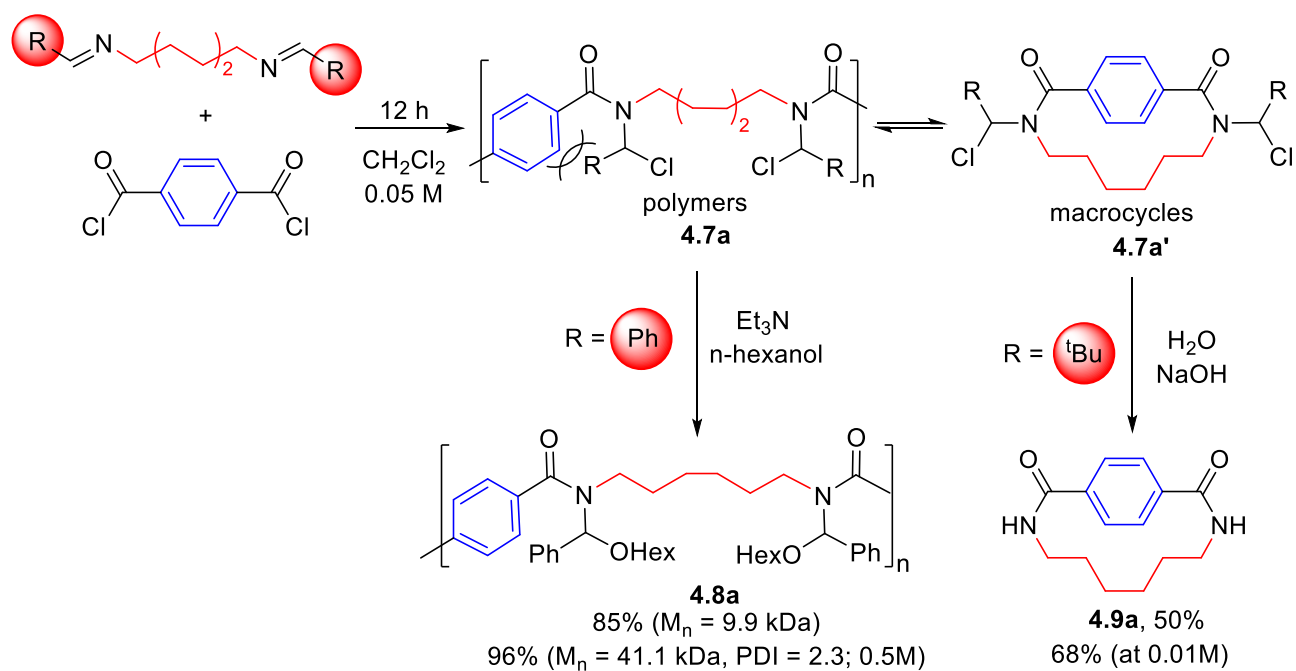
As an alternative, the dynamic formation of **4.3** can offer a method to access these structures in a controlled fashion at ambient conditions. For example, the reaction of the benzaldehyde-derived imine of 1,6-diaminohexane with terephthaloyl chloride forms polyamide **4.7a**, which can be trapped with alcohols to afford polyamide **4.8a** (85%, Figure 4.6). Performing the reaction at higher concentrations to more strongly favor the equilibrium formation of the α -chloroamide leads to the assembly of **4.8a** in high molecular weight ($M_n = 44$ kDa at 0.5 M). In addition to molecular weight, the thermodynamic features of the structure of **4.7** can be used to influence the structure generated. Thus, the replacement of the phenyl in the aldehyde component with a ^tBu unit leads to the now favored formation of macrocycle **4.9a**. Of note, the generation of **4.9a** does not require the high dilution typically required for the analogous macrocyclization, and can instead be performed at the same concentration as the polymerization. For comparison, the

reaction of the parent 1,6-hexanediamine and terephthaloyl chloride under these conditions leads to polymer and <2% of **4.9a**.

The preferred formation of macrocycles with R = ^tBu appears to result from the ability of the amide in this system to equilibrate to the more cis-structure in cyclic **4.7a'**. In this, the large ^tBu substituent is directed away from the aromatic unit. ¹H NMR analysis of **4.7a'** (R = ^tBu) is consistent with this structure, and shows a strongly deshielded ^tBu(H)C methyne hydrogen relative to **4.7a** (R = Ph), suggesting close interactions with the amide oxygen. Moreover, nOe studies show no contacts between the ^tBu(H)C unit and aromatic fragment.

This macrocyclization with pivaldehyde-derived imines can be generalized to access a variety of products **4.9b-g**, and do so in concentrated solutions (Figure 4.6b). Warming the reaction system to 75°C leads to an increase in macrocycle yield (up to 77%) that is retained upon cooling, which is consistent with high selectivity resulting from the generation of **4.7'** under thermodynamic control. The latter corresponds to a macrocyclization efficiency factor (E_{mac}) of 7.3, which is among the highest of which we are aware for a non-templated and bimolecular amide macrocyclization.²⁹ While simple structures, these products have been shown to have utility as monomers for ring-opening polymerization and supramolecular guest binding.³⁰ Overall, this offers a unique avenue to generate amide macrocycles in high yield, in a controlled fashion, with structurally flexible reagents, and one that could in principle be applied to the assembly of many amide products.

a. Control of Polymerization vs. Macrocyclization



b. Dynamic Assembly of Macrocycles

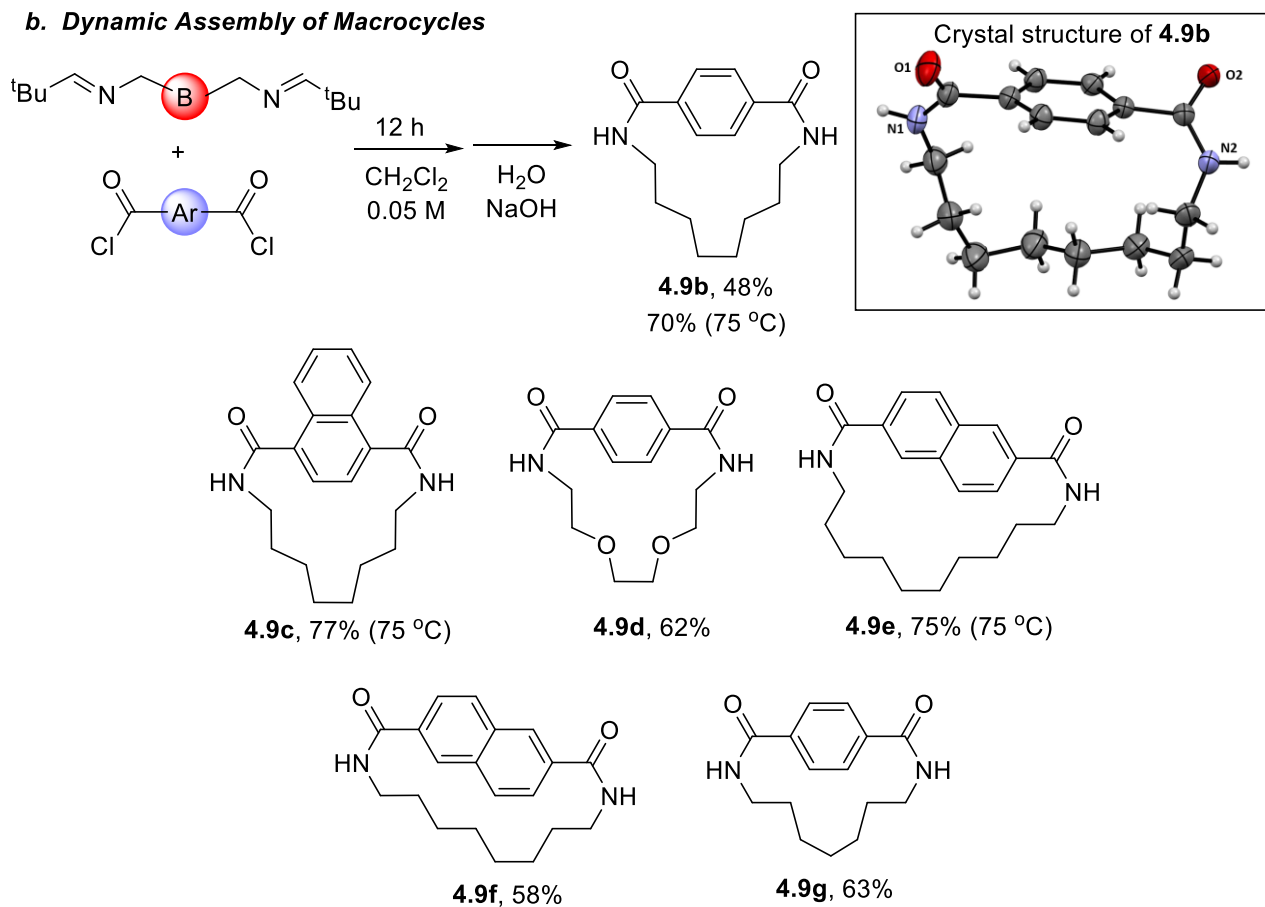


Figure 4.6 Controlled generation of amide macrocycles or polymers.

4.3 Conclusion

In conclusion, we have described a straightforward and broadly applicable approach to the dynamic formation of amides. The reaction exploits reagents that are accessible (imines/acyl chlorides), occurs at ambient temperature, and the equilibrium can be readily tuned by substrate, solvent, temperature or anion. Coupling this with hydrolysis has opened a route to generate robust secondary amide products, with structures ranging from amide-macrocycles to polymers, in a controlled fashion. Considering the broad utility of amides as products, the ability to access these structures in a controlled fashion via dynamic covalent chemistry and from available substrates could prove relevant in a range of applications. Efforts directed towards the latter are currently underway.

4.4 Experimental Section

4.4.1. General Procedures

All manipulations were conducted in a glovebox under a nitrogen atmosphere. Unless otherwise noted, all reagents were purchased from commercial sources and used without purification. Solvents were dried by using a solvent purifier system, then stored over activated 3Å molecular sieves inside the glovebox. Deuterated acetonitrile, chloroform and benzene were stirred over calcium hydride, vacuum transferred, degassed, and stored over 4Å molecular sieves. Naphthalene-2,6-dicarbonyl dichloride and naphthalene-1,4-dicarbonyl dichloride were prepared according to literature procedures.³¹ In order to ensure the clean formation of N-acyl iminium salts, acyl chlorides were purified by careful distillation (if liquids) or crystallization from pentane in a glovebox (if solids) and stored in the glovebox. Imines were prepared from commercially available amines and aldehydes using standard literature procedures and dried with excess

magnesium sulfate.³² For N-benzyl imines, the reactions were performed with a 1:1 mixture of amine:aldehyde, and any remaining aldehyde/amine was carefully removed by vacuum distillation. For N-alkyl imines, a slight excess of amine was used in the synthesis, then removed by evaporation, and the product then dried with sodium sulfate. For N-aryl imines, the products were purified in a glovebox by crystallization from pentane. For diimines, a 1:3 mixture of diamine:aldehyde was refluxed in toluene, the excess aldehyde was removed *in vacuo*, and the product then dried with sodium sulfate. In all cases, imines were stored in a glovebox, and their purity tested by mixing with benzoyl chloride to see if any hydrolysis occurs. Nuclear magnetic resonance (NMR) characterization was performed on 400 MHz spectrometers for proton, 101 MHz for carbon, and 377 MHz for fluorine. ¹H, ¹³C and ¹⁹F NMR chemical shifts were referenced to residual solvent. Mass spectra were recorded on a high-resolution electrospray ionization quadrupole mass spectrometer. GPC analysis were performed in THF using a cross-linked styrene-divinylbenzene column.

4.4.2 Experimental Procedures

Typical procedure for determination of K_{eq} for formation of **4.3aa** in CD_3CN : In a glovebox, (p-tolyl)HC=NBn (8.4 mg, 0.040 mmol) and benzoyl chloride (5.6 mg, 0.040 mmol) were dissolved in 1.0 ml of CD_3CN and then transferred into a J-Young NMR tube and allowed to reach equilibrium by 24 hours at room temperature, after which no change in the relative concentrations of **4.1a**, **4.2a**, and **4.3aa** was noted. This was repeated for several initial concentrations of **4.1a**, **4.2a**, or from **4.3aa**, and a plot of $[4.1a] \cdot [4.2a]$ vs $[4.3aa]$ was used to determine K_{eq} . A similar procedure was done with $CDCl_3$ and C_6D_6 .

Run	Initial [4.1a] (mM)	Initial [4.2a] (mM)	Initial [4.3aa] (mM)	Final [4.1a] (mM)	Final [4.2a] (mM)	Final [4.3aa] (mM)
1	40.0	42.7	0	3.4	6.1	36.6
2	41.5	40.8	0	4.8	4.2	36.7
3	41.1	40.9	0	4.5	4.5	36.6
4	0	0	41.2	4.6	4.5	36.7
5	30.6	30.3	0	4.0	3.6	26.5
6	29.5	32.4	0	2.7	5.6	27.1
7	30.1	30.2	0	3.8	3.9	26.4
8	19.0	20.0	0	2.5	3.6	16.5
9	20.1	20.0	0	3.1	3.0	16.9
10	22.0	21.0	0	3.7	2.8	18.7

Table 4.2 Equilibrium data for **4.3aa** in CD₃CN

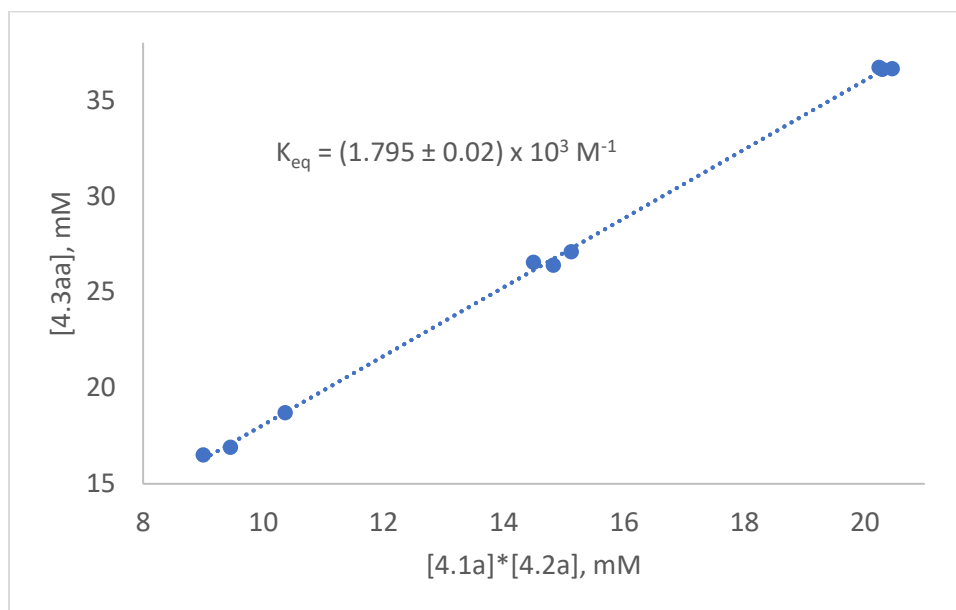


Figure 4.7 [4.1a]*[4.2a] vs [4.3aa] plot used to determine the K_{eq} value of **4.3aa** in CD₃CN

Typical procedure for determination of K_{eq} for other **4.3** in CD₃CN: The following example procedure was employed for determining K_{eq} for all **4.3** in CD₃CN. In a glovebox, imine **4.1d** (7.6 mg, 0.05 mmol) and **4.2a** (7.0 mg, 0.05 mmol) were dissolved in 1.0 ml of CD₃CN and then transferred into a J-Young NMR tube and allowed to reach equilibrium. The concentration of each compound at equilibrium was determined from the ¹H NMR integrations. In order to prevent

integration errors due to relaxation delay differences, spectra was taken with a one-scan method with a fixed gain. K_{eq} was calculated according to the formula $[4.3xy]/[4.1x][4.2y]$. This procedure was repeated for at two other initial concentrations of **4.1/4.2** and overall average was reported.

van't Hoff plot for formation of **4.3aa**: In a glovebox, (p-tolyl)HC=NBn (8.4 mg, 0.040 mmol) and benzoyl chloride (5.6 mg, 0.040 mmol) were dissolved in 1.0 ml of CD₃CN and then transferred into a J-Young NMR tube and allowed to reach equilibrium at different temperatures. For 25 °C and below, mixture was allowed to reach equilibrium for a day, whereas this time was 2 h for higher temperatures. ¹H NMR analysis was performed by first bringing the NMR probe to the desired temperature before starting data acquisition. Equilibrium constants at different temperatures were calculated from the relative concentrations of **4.1a**, **4.2a**, and **4.3aa**. For each temperature, the experiment was repeated 3 times at differing initial concentrations of **4.1a/4.2a** (20 mM, 30mM, and 40mM), and the values were plotted against 1/T with a linear fit.

T (°C)	T(K)	1/T	ln(K_{eq}) @- 20mM	ln(K_{eq}) @- 30mM	ln(K_{eq}) @- 40mM
8	281	0.00356	8.75	8.70	8.69
15	288	0.00347	8.19	7.94	8.31
25	298	0.00335	7.34	7.42	7.27
35	308	0.00325	6.72	6.72	6.62
45	318	0.00314	6.06	6.05	5.98
55	328	0.00305	5.43	5.42	5.44
65	338	0.00296	4.78	4.81	4.76

Table 4.3 Data for van't Hoff plot for formation of **4.3aa** in CD₃CN

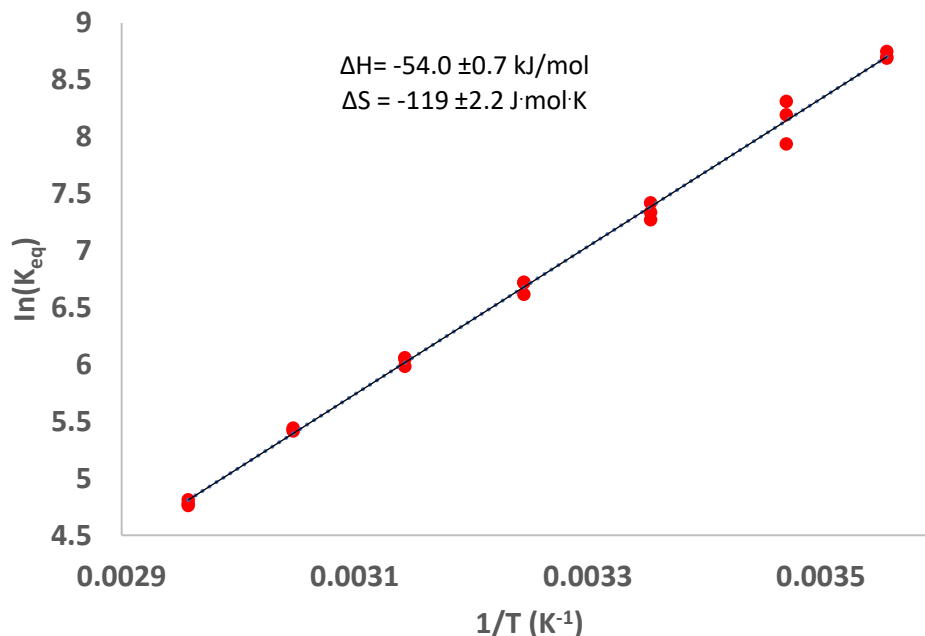


Figure 4.8 van't Hoff plot for formation of **4.3aa** in CD₃CN

Typical procedure for the isolation of **4.3**: In a glovebox, (p-tolyl)HC=NBn (84.0 mg, 0.40 mmol) and benzoyl chloride (56.1 mg, 0.40 mmol) were dissolved in 1 ml of CH₃CN and then stirred in a vial for 2 hours. Removal of solvent in vacuo results in a colorless oil. Addition of 3 ml pentane and allowing the mixture to cool down at -35°C for 20 minutes leads to precipitation of **4.3aa** as a white solid. Pure **4.3aa** was obtained after decanting the pentane and removing remaining solvent in vacuo (128 mg, 92%). In order to prevent re-equilibration before characterization, NMR analysis was performed by dissolving **4.3aa** in NMR solvent pre-cooled -35°C, and taking the NMR spectra immediately at 5°C. **4.3ba**, **4.3ca**, **4.3la** and **4.3ma** do not precipitate with this procedure, and were instead characterized in situ from concentrated 1:1 solutions of the corresponding imines and acyl chlorides. While **4.3ea**, **4.3fa** and **4.3ee** do precipitate, they reestablish a partial equilibrium even at low temperatures, and were also characterized in situ from 1:1 solutions of the corresponding imines and acyl chlorides.

Dynamic Exchange of 4.3ee with 4.1a: In a glovebox, (p-tolyl)HC=NPh (19.5 mg, 0.10 mmol) and p-nitrobenzoyl chloride (18.6 mg, 0.10 mmol) and were dissolved in 1 ml of CD₃CN together with (CH₃)₂SO₂ (4.3 mg, 0.045 mmol) as an internal standard, and then transferred into a J-Young NMR tube. After 2h, this reaction reached equilibrium with the formation of **4.3ee** in 83% yield ([**4.1e**] = 17.1 mM, [**4.2e**] =16.9 mM, [**4.3ee**] = 83.0 mM; K_{eq} =290 M⁻¹; see ¹H NMR spectra below). This solution was brought into the glovebox, and (p-tolyl)HC=NBn (20.9 mg, 0.10 mmol) was added to the solution. The loss of **4.3ee** and build-up of **4.3ae** were monitored by ¹H NMR analysis, which reached an equilibrium at 2 h. The final concentrations of reagents by ¹H NMR analysis are: [**4.1e**] = 86.4 mM, [**4.2e**] =0 mM, [**4.1a**]=16.5 mM, [**4.3ee**] = 18.1 mM, [**4.3ae**]=86.4 Mm, K_{eq} =25.

Dynamic Exchange of 4.3aa with 4.1l: In a glovebox, (p-tolyl)HC=NBn (20.9 mg, 0.10 mmol) and p-nitrobenzoyl chloride (18.6 mg, 0.10 mmol) and were dissolved in 1 ml of CD₃CN together with (CH₃)₂SO₂ (3.4 mg, 0.036 mmol) as an internal standard, and then transferred into a J-Young NMR tube. After 2h, this reaction reached equilibrium with the formation of **4.3aa** in 95 % yield ([**4.1a**] = 5.4 mM, [**4.2a**] =8.3 mM, [**4.3aa**] = 94.6 mM) This solution was brought into the glovebox, and (t-Bu)HC=NH_{hexyl} (16.9 mg, 0.10 mmol) was added to the solution. The loss of **4.3aa** and build-up of **4.3la** were monitored by ¹H NMR analysis, which reached an equilibrium at 48 h. The final concentrations of reagents by ¹H NMR analysis are: [**4.1a**] = 76.9 mM, [**4.2a**] =0 mM, [**4.3aa**] = 23.1 mM, [**4.1l**] = 30.0 mM, [**4.3la**] = 72.3, K_{eq} =8.0.

Dynamic Exchange of 4.3ie and 4.3ma: In a glovebox, (p-FC₆H₄)HC=NBn (21.3 mg, 0.10 mmol) and p-nitrobenzoyl chloride (18.6 mg, 0.10 mmol) were dissolved in 0.5 ml of CD₃CN together with (CH₃)₂SO₂ (1.0 mg, 0.010 mmol) and then transferred into a J-Young NMR tube. In another J-Young NMR tube; (p-FC₆H₄)HC=NEt (15.1 mg, 0.10 mmol) and benzoyl chloride (14.1 mg,

0.10 mmol) were dissolved in 0.5 ml of CD₃CN together with (CH₃)₂SO₂ (3.4 mg, 0.036 mmol). These two reactions containing **4.3ie** and **4.3ma** were allowed to stand for a day, and then mixed together. The loss of **4.3ie** and **4.3ma**, along with build-up of **4.3me** and **4.3ia** was monitored by ¹H and ¹⁹F NMR analysis. Final concentrations and individual K_{eq}'s of formation of each amide based on ¹H and ¹⁹F NMR analysis are: [**4.3ie**]=24.7 mM; [**4.3ma**]=24 mM; [**4.3me**]=25.9 mM, [**4.3ia**]=25.4 mM,. Overall K_{eq} of the exchange is 1.10. By comparison, the individual K_{eq} for the 4 amides are: **4.3ie**: K_{eq} =5900 M⁻¹ **4.3ma**: K_{eq} =5300 M⁻¹ **4.3me**: K_{eq} =19200 M⁻¹ **4.3ia**: K_{eq} =1800 M⁻¹ , and have a composite K_{eq} = 1.1.

Reduction of **4.3aa** with sodium triacetoxyborohydride: In a glovebox, **4.3aa** (3.5 mg, 0.010 mmol) and (CH₃)₂SO₂ (0.5 mg, 0.005 mmol) standard were dissolved in 1 ml of CD₃CN and mixture allowed to reach the equilibrium for 2 hours at room temperature. ¹H NMR analysis reveals the presence of **4.3aa** (76%), **4.1a** (24%), and **4.2a** (21%). The solution was brought back into the glovebox, and sodium triacetoxyborohydride (3.2 mg, 0.015 mmol) was added. After 2 h, ¹H NMR analysis shows the formation of **4.4aa** in 95% yield.

Synthesis of **4.4aa**: In a glovebox, (p-tolyl)HC=NBn (83.8 mg, 0.40 mmol) and benzoyl chloride (56.5 mg, 0.40 mmol) were dissolved in 1 ml of CH₃CN and then stirred in a vial for 2 hours. Sodium triacetoxyborohydride (127.2 mg, 0.60 mmol) was added to the solution and stirred for 12 hours. Amide product **4.4aa** can be isolated by column chromatography with ethyl acetate/hexane as a white solid (124.7 mg, 99%).

Reaction of **4.3aa** with Hexanol/Et₃N: In a glovebox, **4.3aa** (3.5 mg, 0.010 mmol) and (CH₃)₂SO₂ (1.2 mg, 0.013 mmol) standard were dissolved in 1 ml of CD₃CN and mixture allowed to reach the equilibrium for 2 hours at room temperature. ¹H NMR analysis shows the following in

solution: **4.3aa** (76%), **4.1a** (24%) and **4.2a** (22%). The NMR tube was brought back into the glovebox and Et₃N (4.0 mg, 0.040 mmol) followed by n-C₆H₁₃OH (4.1 mg, 0.040 mmol) was added. ¹H NMR analysis after 3 h shows the formation of **4.5aa** (76%) and PhCO₂hexyl³³ (24%).

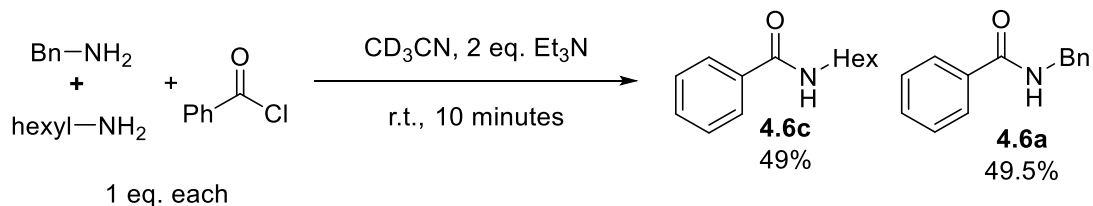
Synthesis of **4.5aa**: In a glovebox, (p-tolyl)HC=NBn (83.5 mg, 0.40 mmol) and benzoyl chloride (56.2 mg, 0.40 mmol) were dissolved in 1 ml of CH₃CN and then stirred in a vial for 2 hours. Et₃N (121 mg, 1.2 mmol) was added, followed by addition of n-hexanol (122 mg, 1.2 mmol). The mixture was allowed to stir in a vial for another 2 hours. **4.5aa** can be isolated by column chromatography with ethyl acetate/hexane as a white solid (154.4 mg, 93%).

Reaction of **4.3aa** with H₂O/NaOH: In a glovebox, **4.3aa** (34.9 mg, 0.10 mmol) and benzyl benzoate (8.5 mg, 0.04 mmol) were dissolved in 10 ml of CH₃CN and mixture allowed to reach the equilibrium for 2 hours at room temperature. ¹H NMR analysis of a portion of this solution shows the presence of **4.3aa** in 76% with imine **4.1a** benzoyl chloride **4.2a** (24% each). The solution was removed from the glovebox, and 2.0 ml of aqueous 1.0 M NaOH was added. After 10 min, 2.5 ml of aqueous 1.0 M HCl was added to neutralize the aqueous layer. The organic phase was collected, and the aqueous layer washed with 10 ml dichloromethane. The organic phases were combined, dried with sodium sulfate, filtered, and solvent removed in vacuo. ¹H NMR analysis of the resultant mixture in CD₃CN shows the formation of amide **4.6a** (76%) together with benzoic acid (23%). The latter ¹H NMR signals (δ 7.64, 8.02 ppm) can be clearly distinguished from benzoyl chloride (δ 7.81, 8.16 ppm).

Synthesis of **4.6a**: In a glovebox, (p-tolyl)HC=NBn (83.0 mg, 0.40 mmol) and benzoyl chloride (56.3 mg, 0.40 mmol) were dissolved in 1 ml of CH₃CN and then stirred in a vial for 2 hours. The mixture was taken outside the glovebox, mixed with 1 ml of aqueous 1M NaOH, and stirred for 30 minutes. Organic phase was collected with 5 ml of dichloromethane, dried with sodium sulfate,

filtered, and the solvent removed in vacuo. Aldehyde and remaining starting materials were washed away with cold pentane to obtain N-benzyl benzamide (**4.6a**) as a white solid (80.2 mg, 95%).

Reaction of Amine Mixture with Benzoyl Chloride



In a glovebox, benzoyl chloride (14.1 mg, 0.10 mmol) and $(\text{CH}_3)_2\text{SO}_2$ (2.6 mg, 0.028 mmol) standard were dissolved in 0.5 ml of CD_3CN . ^1H NMR analysis provided the ratio of benzoyl chloride to the standard. A 0.5 ml of CD_3CN solution containing benzylamine (10.7 mg, 0.10 mmol), n-hexylamine (10.1 mg, 0.10 mmol) and triethylamine (20.2 mg, 0.20 mmol) was added to the benzoyl chloride solution. ^1H NMR analysis after 10 min shows the formation of amides **4.6a** (49.5%) and **4.6c**³⁴ (49%).

Controlled Formation of Amides via 4.3: In a glovebox, benzoyl chloride (7.0 mg, 0.050 mmol) and $(\text{CH}_3)_2\text{SO}_2$ (1.3 mg, 0.014 mmol) standard were dissolved in 0.5 ml of CD_3CN . ^1H NMR analysis provided the ratio of benzoyl chloride to the standard. A 0.5 ml CD_3CN solution containing $(p\text{-MeOC}_6\text{H}_4)\text{HC}=\text{NBn}$ (45.0 mg, 0.20 mmol) and $(t\text{Bu})\text{HC}=\text{N-hexyl}$ (33.6 mg, 0.20 mmol) was mixed with benzoyl chloride solution. This mixture was split into two equal parts.

a. One portion of the solution above was removed from the glovebox after 10 min and immediately hydrolyzed with 0.5 ml aqueous 1M NaOH solution. After 1 h, the aqueous layer was removed,

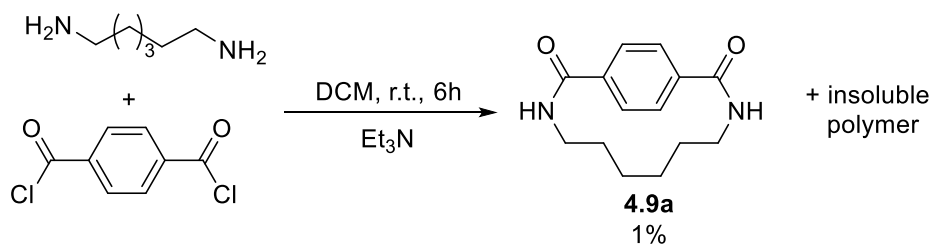
and organic layer was dried with sodium sulfate then filtered. ^1H NMR analysis of the CD_3CN solution shows the formation of amides **4.6a** (78%) and **4.6c** (21%).

b. The second portion of this solution was heated for 2 hours at 45°C and then hydrolyzed with 0.5 ml aqueous 1M NaOH solution. After 1 h, the aqueous layer was removed, and organic layer was dried with sodium sulfate. ^1H NMR analysis of the CD_3CN solutions show the formation of amides **4.6a** (18%) and **4.6c** (81%).

Synthesis of Polymer **4.8a**: In a glovebox, terephthaloyl chloride (101 mg, 0.50 mmol) and hexane-1,6-bis(1-phenylmethanimine) (146 mg, 0.50 mmol) were dissolved in 1 ml of dichloromethane and stirred for 12 h at room temperature. To this solution was added triethylamine (202 mg, 2.0 mmol) and then n-hexanol (204 mg, 2.0 mmol) and the mixture was stirred for 5 h. The solvent was removed in vacuo and mixture was dissolved in 2 ml of toluene. The amine salt precipitate was removed by filtration, and solvent was removed in vacuo, affording **4.8a** as a white solid (300 mg, 96%, $M_n=41.1\text{kDa}$, $M_w=96.3\text{kDa}$, PDI=2.3).

Typical procedure for synthesis of Macrocycles **4.9**: In a glovebox, terephthaloyl chloride (40.6 mg, 0.20 mmol) and hexane-1,6-bis(2,2-dimethylpropan-1-imine) (50.4 mg, 0.20 mmol) were dissolved in 4 ml of dichloromethane and stirred for 6 h at room temperature. (For macrocycles **4.9b**, **4.9c** and **4.9e**, higher yields were obtained by instead transferring the mixture into a sealed vessel, which was removed from the glovebox and heated for 6 h at 75°C in an oil bath.) The solution was removed from the glovebox, and 2 ml aqueous 1 M NaOH was added and stirred for 30 minutes. The organic phase was collected, and the aqueous solution was washed with dichloromethane (3x10 ml). The organic fractions were combined, filtered to remove any precipitate, and the solvent was removed in vacuo to afford **4.9a** as a white solid (24.6 mg, 50%).

Reaction between 1,6-Hexanediamine and Terephthaloyl Chloride:



A solution of terephthaloyl chloride (101.5 mg, 0.50 mmol) in 5 ml of dichloromethane was added to another solution containing 1,6-hexanediamine (58.0 mg, 0.50 mmol) and triethylamine (151.5 mg, 1.50 mmol) in 5 ml of dichloromethane and stirred for 6 h at room temperature. Precipitate was filtered off and washed with dichloromethane (3x25 ml). Filtrates were combined, and solvent was removed in vacuo to afford 136.5 mg of white solid. ¹H NMR analysis of this solid in deuterated dimethylsulfoxide with (CH₃)₂SO₂ as external standard reveals presence of 1% **4.9a** (along with Et₃NHCl) relative to starting materials.

X-ray Crystal Structure Analysis of **4.9b**: A colorless crystal of macrocyclic amide **4.9b** suitable for X-ray analysis was obtained by recrystallization from a dimethyl sulfoxide/hexane mixture. Single crystal X-ray diffraction was measured on a Bruker D8 Advance diffractometer equipped with a Photon 200 CMOS area detector, and an I μ S microfocus X-ray source (Bruker AXS, CuK α source). The measurement was carried out at 298(2) K on crystals coated with a thin layer of amorphous oil. Structure solution was carried out using the SHELXTL package from Bruker. The parameters were refined for all data by full-matrix-least-squares on F² using SHELXL. All the non-hydrogen atoms were refined with anisotropic thermal parameters. All other hydrogen atoms were placed in calculated positions and allowed to ride on the carrier atoms.

4.4.3 Characterization Data

N-benzyl-N-(chloro(p-tolyl)methyl)benzamide (4.3aa) White solid, 128 mg, 92% $^1\text{H NMR}$ (500 MHz, CDCl_3) δ 7.63 (s, 2H), 7.47 (m, 3H), 7.35 (d, $J = 8.0$ Hz, 2H), 7.25 (s, 1H), 7.13 (m, 7H), 4.55 (s, 2H), 2.34 (s, 3H). $^{13}\text{C NMR}$ (126 MHz, CDCl_3) δ 172.5, 139.1, 137.4, 135.2, 133.7, 130.5, 129.2, 128.8, 128.0, 127.8, 127.3, 126.9, 126.8, 77.7, 46.9, 21.1. **HRMS** (ESI^+) for $\text{C}_{22}\text{H}_{20}\text{NO}^+$ (M-Cl) calculated 314.1539, found 314.1541 (error $m/z = -0.4$ ppm)

N-(chloro(p-tolyl)methyl)-N-ethylbenzamide (4.3ba) Clear liquid, 110 mg, 96% $^1\text{H NMR}$ (500 MHz, CDCl_3) δ 7.62 (m, 2H), 7.49 (m, 3H), 7.41 (d, $J = 8.0$ Hz, 2H), 7.22 (m, 3H), 3.43 (q, $J = 7.2$ Hz, 2H), 2.39 (s, 3H), 1.06 (t, $J = 7.2$ Hz, 3H). $^{13}\text{C NMR}$ (126 MHz, CDCl_3) δ 171.8, 139.0, 135.5, 134.0, 130.2, 129.3, 128.8, 127.1, 126.6, 77.6, 38.8, 21.1, 14.0. **HRMS** (ESI^+) for $\text{C}_{17}\text{H}_{18}\text{NO}^+$ (M-Cl) calculated 252.1383, found 252.1378 (error $m/z = 1.8$ ppm)

N-(chloro(p-tolyl)methyl)-N-hexylbenzamide (4.3ca) Clear liquid, 133 mg, 97% $^1\text{H NMR}$ (500 MHz, CDCl_3) δ 7.62 (m, 2H), 7.49 (m, 3H), 7.40 (d, $J = 8.0$ Hz, 2H), 7.22 (m, 3H). 3.53 – 3.04 (bs, 2H), 2.39 (s, 3H), 1.69 – 1.12 (m, 8H), 0.84 (t, $J = 7.1$ Hz, 3H). $^{13}\text{C NMR}$ (126 MHz, CDCl_3) δ 172.0, 139.0, 135.6, 134.1, 130.2, 129.2, 128.8, 127.2, 126.7, 77.4, 43.9, 31.1, 28.3, 26.7, 22.4, 21.1, 13.9. **HRMS** (ESI^+) for $\text{C}_{21}\text{H}_{26}\text{NO}^+$ (M-Cl) calculated 308.2009, found 308.2011 (error $m/z = -0.7$ ppm)

N-(chloro(p-tolyl)methyl)-N-isopropylbenzamide (4.3da) White solid, 86 mg, 71% $^1\text{H NMR}$ (500 MHz, CDCl_3) δ 7.63 (m, 2H), 7.50 – 7.45 (m, 3H), 7.37 (d, $J = 8.2$ Hz, 2H), 7.18 (d, $J = 8.1$ Hz, 2H), 6.91 (s, 1H), 3.63 (hept, $J = 6.8$ Hz, 1H), 2.36 (s, 3H), 1.38 (bs, 6H). $^{13}\text{C NMR}$ (126 MHz, CDCl_3) δ 171.5, 138.9, 136.6, 133.8, 130.0, 129.1, 128.9, 127.1, 126.2, 79.0, 49.3, 21.1, 20.2. **HRMS** (ESI^+) for $\text{C}_{18}\text{H}_{20}\text{NO}^+$ (M-Cl) calculated 266.1539, found 266.1538 (error $m/z = 0.5$ ppm)

N-(chloro(p-tolyl)methyl)-N-phenylbenzamide (4.3ea) White solid, 121 mg, 90% $^1\text{H NMR}$ (400 MHz, CDCl_3) δ 8.02 (s, 1H), 7.35 (d, $J = 7.2$ Hz, 2H), 7.26 – 6.97 (m, 10H), 6.80 (bs, 2H), 2.31 (s, 3H). $^{13}\text{C NMR}$ (101 MHz, CDCl_3) δ 170.9, 138.8, 135.0, 134.0, 130.9, 130.1, 128.7, 128.6, 128.3, 128.1, 128.0, 127.8, 120.9, 72.9, 21.2. **HRMS** (ESI^+) for $\text{C}_{21}\text{H}_{18}\text{NO}^+$ (M-Cl) calculated 300.1383, found 300.1378 (error $m/z = 1.5$ ppm)

N-(chloro(p-tolyl)methyl)-N-(4-methoxyphenyl)benzamide (4.3fa) White solid, 138 mg, 95% $^1\text{H NMR}$ (400 MHz, CDCl_3) δ 7.98 (s, 1H), 7.34 (d, $J = 7.3$ Hz, 2H), 7.28 – 7.10 (m, 5H), 7.06 (d, $J = 8.0$ Hz, 2H), 6.67 (bs, 1H), 6.56 (d, $J = 8.3$ Hz, 2H), 3.66 (s, 3H), 2.32 (s, 3H). $^{13}\text{C NMR}$ (101 MHz, CDCl_3) δ 171.1, 158.9, 138.8, 135.2, 134.1, 132.0, 130.3, 130.0, 128.7, 128.5, 128.1, 127.8, 113.5, 73.0, 55.2, 21.2. **HRMS** (ESI^+) for $\text{C}_{22}\text{H}_{20}\text{NO}_2^+$ (M-Cl) calculated 330.1489, found 330.1483 (error $m/z = 1.7$ ppm)

N-benzyl-N-(chloro(4-methoxyphenyl)methyl)benzamide (4.3ga) White solid, 131 mg, 90% $^1\text{H NMR}$ (500 MHz, CDCl_3) δ 7.65 (d, $J = 6.4$ Hz, 2H), 7.48 (m, 3H), 7.41 (d, $J = 8.7$ Hz, 2H), 7.30 (bs, 1H), 7.25 – 7.15 (m, 3H), 7.12 (d, $J = 6.9$ Hz, 2H), 6.86 (d, $J = 8.8$ Hz, 2H), 4.61 (s, 3H), 3.81 (s, 3H). $^{13}\text{C NMR}$ (126 MHz, CDCl_3) δ 172.5, 160.1, 137.4, 135.2, 131.5, 130.5, 128.8, 128.8, 128.6, 128.1, 127.8, 126.8, 113.8, 77.5, 55.4, 46.8. **HRMS** (ESI^+) for $\text{C}_{22}\text{H}_{20}\text{NO}^+$ (M-Cl) calculated 330.1489, found 330.1482 (error $m/z = 1.9$ ppm)

Methyl 4-((N-benzylbenzamido)chloromethyl)benzoate (4.3ha) White solid, 151 mg, 96% $^1\text{H NMR}$ (500 MHz, CDCl_3) δ 7.99 (d, $J = 8.5$ Hz, 2H), 7.64 (d, $J = 6.5$ Hz, 2H), 7.56 (d, $J = 8.3$ Hz, 2H), 7.48 (m, 3H), 7.36 (bs, 1H), 7.16 (m, 3H), 7.07 (d, $J = 7.1$ Hz, 2H), 4.65 (d, $J = 15.4$ Hz, 1H), 4.51 (d, $J = 15.4$ Hz, 1H), 3.94 (s, 3H). $^{13}\text{C NMR}$ (126 MHz, CDCl_3) δ 172.5, 166.2, 141.1, 136.9, 134.8, 130.8, 130.7, 129.8, 128.9, 128.2, 127.7, 127.6, 127.0, 126.8, 77.3, 52.3, 47.2. **HRMS** (ESI^+) for $\text{C}_{23}\text{H}_{20}\text{NO}_3^+$ (M-Cl) calculated 358.1438, found 358.1453 (error $m/z = -4.3$ ppm)

N-benzyl-N-(chloro(4-fluorophenyl)methyl)benzamide (4.3ia) White solid, 131 mg, 93% ^1H NMR (500 MHz, CDCl_3) δ 7.65 (d, $J = 6.4$ Hz, 2H), 7.54 – 7.41 (m, 4H), 7.32 (s, 1H), 7.19 (d, $J = 7.0$ Hz, 2H), 7.08 (d, $J = 7.2$ Hz, 2H), 7.00 (t, $J = 8.6$ Hz, 2H), 4.62 (d, $J = 86.0$ Hz, 2H). ^{13}C NMR (126 MHz, CDCl_3) δ 172.5, 163.9, 161.9, 137.2, 135.0, 132.3, 130.6, 129.4, 128.9, 128.1, 127.7, 127.0, 126.8, 115.3, 76.7, 46.9. ^{19}F NMR (377 MHz, CD_3CN) δ -114.5. HRMS (ESI $^+$) for $\text{C}_{21}\text{H}_{17}\text{FNO}^+$ (M-Cl) calculated 318.1289, found 318.1281 (error $m/z = 2.4$ ppm)

N-benzyl-N-(1-chloro-2,2-dimethylpropyl)benzamide (4.3ja) Colorless oil, 120 mg, 95% ^1H NMR (400 MHz, CDCl_3) δ 7.39 (m, Hz, 10H), 6.00 (bs, 1H), 4.78 (dd, $J = 116.0, 14.6$ Hz, 2H), 1.12 (s, 9H). ^{13}C NMR (126 MHz, CDCl_3) δ 172.5, 137.8, 135.9, 130.2, 128.6, 128.2, 127.5, 126.8, 126.7, 85.9, 47.8, 40.8, 27.3. HRMS (ESI $^+$) for $\text{C}_{19}\text{H}_{22}\text{NO}^+$ (M-Cl) calculated 280.1696, found 280.1691 (error $m/z = 1.8$ ppm)

N-benzyl-N-(chloro(o-tolyl)methyl)benzamide (4.3ka) White solid, 135 mg, 97% ^1H NMR (500 MHz, CDCl_3) δ 7.97 (d, $J = 7.8$ Hz, 1H), 7.69 (d, $J = 5.3$ Hz, 2H), 7.54 – 7.44 (m, 3H), 7.43 – 7.32 (m, 1H), 7.28 (t, $J = 7.4$ Hz, 1H), 7.21 (t, $J = 7.4$ Hz, 1H), 7.12 (m, 3H), 7.00 (d, $J = 7.4$ Hz, 1H), 6.96 – 6.92 (m, 2H), 4.62 (bs, 2H), 2.07 (s, 3H). ^{13}C NMR (126 MHz, CDCl_3) δ 172.4, 137.0, 135.5, 135.3, 134.2, 130.6, 130.4, 129.3, 129.2, 128.5, 127.9, 127.8, 126.8, 126.8, 126.3, 75.4, 46.7, 19.4. HRMS (ESI $^+$) for $\text{C}_{22}\text{H}_{20}\text{NO}^+$ (M-Cl) calculated 314.1539, found 314.1529 (error $m/z = 3.3$ ppm)

N-benzyl-N-(chloro(p-tolyl)methyl)-4-methoxybenzamide (4.3ab) White solid, 127 mg, 84% ^1H NMR (500 MHz, CDCl_3) δ 7.68 (d, $J = 8.4$ Hz, 2H), 7.39 (m, 3H), 7.15 (m, 6H), 6.97 (d, $J = 8.7$ Hz, 2H), 4.55 (s, 2H), 3.85 (s, 3H), 2.36 (s, 3H). ^{13}C NMR (126 MHz, CDCl_3) δ 172.4, 161.6, 139.0, 137.5, 134.0, 133.9, 129.2, 129.1, 128.0, 127.8, 127.3, 127.1, 126.8, 114.1, 78.4, 55.4, 47.1,

21.1. **HRMS** (ESI⁺) for C₂₃H₂₂NO₂⁺ (M-Cl) calculated 344.1645, found 344.1653 (error m/z = -2.3 ppm)

N-benzyl-N-(chloro(p-tolyl)methyl)-4-fluorobenzamide (4.3ac) White solid, 138 mg, 94% ¹H NMR (500 MHz, CDCl₃) δ 7.64 (s, 2H), 7.35 (d, *J* = 8.0 Hz, 4H), 7.29 – 6.86 (m, 8H), 4.52 (s, 2H), 2.35 (s, 3H). ¹³C NMR (126 MHz, CDCl₃) δ 171.5, 164.9, 139.2, 137.2, 133.5, 131.2, 129.3, 129.3, 128.1, 127.8, 127.3, 126.9, 115.8, 77.5, 47.2, 21.1. ¹⁹F NMR (471 MHz, CDCl₃) δ -108.7.

HRMS (ESI⁺) for C₂₂H₁₉FNO⁺ (M-Cl) calculated 332.1445, found 332.1434 (error m/z = 3.3 ppm)

N-benzyl-N-(chloro(p-tolyl)methyl)-4-methylbenzamide (4.3ad) White solid, 131 mg, 90% ¹H NMR (500 MHz, CDCl₃) δ 7.58 (d, *J* = 7.9 Hz, 2H), 7.38 (d, *J* = 8.1 Hz, 2H), 7.33 (s, 1H), 7.29 (d, *J* = 7.9 Hz, 2H), 7.17 (m, 7H), 4.58 (s, 2H), 2.42 (s, 3H), 2.36 (s, 3H). ¹³C NMR (126 MHz, CDCl₃) δ 172.7, 140.9, 139.0, 137.5, 133.8, 132.2, 129.2, 128.0, 127.8, 127.3, 127.0, 126.8, 78.1, 46.8, 21.5, 21.1. **HRMS** (ESI⁺) for C₂₃H₂₂NO⁺ (M-Cl) calculated 328.1696, found 328.1696 (error m/z = 0.1 ppm)

N-benzyl-N-(chloro(p-tolyl)methyl)-4-nitrobenzamide (4.3ae) Yellow solid, 153 mg, 97% ¹H NMR (500 MHz, CDCl₃) δ 8.29 (d, *J* = 6.9 Hz, 2H), 7.71 (s, 2H), 7.36 (m, 3H), 7.17 (d, *J* = 7.0 Hz, 5H), 7.02 (s, 2H), 4.54 (t, *J* = 13.2 Hz, 2H), 2.37 (s, 3H). ¹³C NMR (126 MHz, CDCl₃) δ 170.3, 148.7, 141.3, 139.5, 136.7, 132.9, 129.4, 128.2, 127.9, 127.8, 127.3, 127.2, 124.0, 77.9, 47.2,

21.1. **HRMS** (ESI⁺) for C₂₂H₁₉N₂O₃⁺ (M-Cl) calculated 359.1390, found 359.1382 (error m/z = 2.2 ppm)

N-benzyl-N-(bromo(p-tolyl)methyl)benzamide (4.3aa-Br) White solid, 143 mg, 91% ¹H NMR (500 MHz, CDCl₃) δ 7.65 (m, 2H), 7.57 (s, 1H), 7.53 – 7.46 (m, 3H), 7.42 (d, *J* = 8.2 Hz, 2H), 7.21 – 7.16 (m, 3H), 7.12 (d, *J* = 8.0 Hz, 2H), 7.07 (m, 2H), 4.67 (s, 2H), 2.35 (s, 3H). ¹³C NMR

(126 MHz, CDCl₃) δ 172.6, 139.2, 136.9, 135.1, 133.8, 130.6, 129.1, 128.8, 128.3, 128.1, 127.7, 126.8, 126.8, 72.5, 47.9, 21.0.

N-benzyl-N-(iodo(p-tolyl)methyl)benzamide (4.3aa-I) Orange oil, 159 mg, 90% ¹H NMR (500 MHz, CDCl₃) δ 7.91 (s, 1H), 7.60 (m, 2H), 7.53 – 7.44 (m, 3H), 7.42 (d, *J* = 8.2 Hz, 2H), 7.17 (m, 3H), 7.10 – 6.98 (m, 4H), 4.65 (s, 2H), 2.33 (s, 3H). ¹³C NMR (126 MHz, CDCl₃) δ 172.3, 139.2, 136.1, 135.3, 134.8, 130.7, 129.3, 129.0, 128.8, 128.1, 127.6, 126.9, 126.7, 55.9, 50.2, 21.0.

N-(chloro(p-tolyl)methyl)-4-nitro-N-phenylbenzamide (4.3ee) Yellow solid, 137 mg, 90% ¹H NMR (500 MHz CDCl₃) δ 8.02 (d, *J* = 8.6 Hz, 2H), 7.48 (d, *J* = 8.5 Hz, 2H), 7.35 – 6.91 (m, 8H), 6.75 (s, 2H), 2.34 (s, 3H). ¹³C NMR (101 MHz, CDCl₃) δ 168.7, 139.2, 136.8, 133.3, 132.2, 130.9, 129.5, 129.4, 129.1, 128.8, 128.7, 128.0, 123.0, 71.9, 21.2. HRMS (ESI⁺) for C₂₁H₁₇N₂O₃⁺ (M-Cl) calculated 345.1234, found 345.1220 (error m/z = 4.0 ppm)

N-(1-chloro-2,2-dimethylpropyl)-N-hexylbenzamide (4.3la) Clear liquid, 122 mg, 99% ¹H NMR (500 MHz, CDCl₃) δ 7.41 (m, 5H), 5.59 (bs, 1H), 3.44 (d, *J* = 53.9 Hz, 2H), 2.25 – 0.39 (m, 20H). ¹³C NMR (126 MHz, CDCl₃) δ 172.3, 136.2, 129.9, 128.6, 126.5, 85.7, 44.6, 40.2, 31.3, 28.2, 27.3, 26.8, 22.5, 14.0. HRMS (ESI⁺) for C₁₈H₂₈NO⁺ (M-Cl) calculated 274.2165, found 274.2157 (error m/z = 3.0 ppm)

N-benzyl-N-(chloro(4-fluorophenyl)methyl)-4-nitrobenzamide (4.3ie) Yellow solid, 156 mg, 98% ¹H NMR (500 MHz, CDCl₃) δ 8.28 (s, 2H), 7.71 (s, 2H), 7.43 (s, 3H), 7.15 (s, 3H), 7.01 (m, 4H), 4.93 – 4.16 (m, 2H). ¹³C NMR (126 MHz, CDCl₃) δ 170.4, 164.0, 148.7, 141.1, 136.4, 131.6, 129.4, 128.3, 127.7, 127.6, 127.3, 124.0, 115.7, 75.4, 47.2. ¹⁹F NMR (377 MHz, CD₃CN) δ -114.2. HRMS (ESI⁺) for C₂₁H₁₆FN₂O₃⁺ (M-Cl) calculated 363.1139, found 363.1140 (error m/z = -0.1 ppm)

N-(chloro(4-fluorophenyl)methyl)-N-ethylbenzamide (4.3ma) Clear liquid, 115 mg, 99% ^1H NMR (500 MHz, CDCl_3) δ 7.59 (s, 2H), 7.64 – 7.40 (m, 5H), 7.08 (t, $J = 8.6$ Hz, 3H), 3.39 (s, 2H), 1.01 (s, 3H). ^{13}C NMR (126 MHz, CDCl_3) δ 171.8, 163.8, 135.3, 132.9, 130.4, 129.2, 128.9, 126.6, 115.5, 76.3, 38.8, 14.0. ^{19}F NMR (377 MHz, CD_3CN) δ -114.6. HRMS (ESI $^+$) for $\text{C}_{16}\text{H}_{15}\text{FNO}^+$ (M-Cl) calculated 256.1132, found 256.1125 (error $m/z = 2.8$ ppm)

N-(chloro(4-fluorophenyl)methyl)-N-ethyl-4-nitrobenzamide (4.3me) White solid, 131 mg, 97% ^1H NMR (500 MHz, CDCl_3) δ 8.37 (d, $J = 8.3$ Hz, 2H), 7.79 (s, 2H), 7.48 (s, 2H), 7.13 (t, $J = 8.4$ Hz, 2H), 6.77 (bs, 1H), 3.43 (s, 2H), 1.04 (s, 3H). ^{13}C NMR (126 MHz, CDCl_3) δ 169.6, 164.0, 148.8, 141.3, 132.0, 129.2, 127.7, 124.2, 115.7, 82.1, 39.0, 14.1. ^{19}F NMR (377 MHz, CD_3CN) δ -114.3. HRMS (ESI $^+$) for $\text{C}_{16}\text{H}_{14}\text{FN}_2\text{O}_3^+$ (M-Cl) calculated 301.0983, found 301.0982 (error $m/z = 0.3$ ppm)

N-benzyl-N-(4-methylbenzyl)benzamide (4.4aa) White solid, 124.7mg, 99% ^1H NMR (500 MHz, CDCl_3) δ 7.53 (bs, 2H), 7.48 – 7.33 (m, 5H), 7.33 (t, $J = 7.1$ Hz, 2H), 7.20 (m, 4H), 7.07 (bs, 1H), 4.72 (d, $J = 15.1$ Hz, 2H), 4.41 (d, $J = 12.5$ Hz, 2H), 2.40 (s, 3H). ^{13}C NMR (126 MHz, CDCl_3) δ 172.2, 137.3, 136.6, 136.3, 133.9, 129.6, 129.5, 128.7, 128.5, 128.5, 127.5, 127.0, 126.7, 51.4, 46.7, 21.1. HRMS (ESI $^+$) for $\text{C}_{22}\text{H}_{21}\text{NONa}^+$ (M+Na $^+$) calculated 338.1515, found 338.1520 (error $m/z = -1.5$ ppm)

N-benzyl-N-((hexyloxy)(p-tolyl)methyl)benzamide (4.5aa) White solid, 154.4 mg, 93% ^1H NMR (100 $^\circ\text{C}$, 500 MHz, CDCl_3) δ 7.48 (d, $J = 5.3$ Hz, 2H), 7.47 – 7.22 (m, 5H), 7.14 (d, $J = 8.0$ Hz, 7H), 6.33 (bs, 1H), 4.48 (dd, $J = 158.0, 15.2$ Hz, 2H), 3.44 (dd, $J = 69.7, 7.0$ Hz, 2H), 2.36 (s, 3H), 1.70 – 1.45 (m, 2H), 1.33 (m, 6H), 0.92 (t, $J = 6.8$ Hz, 3H). ^{13}C NMR (126 MHz, CDCl_3) δ 172.9, 138.9, 138.1, 136.7, 134.9, 129.7, 129.1, 128.8, 128.6, 127.9, 126.9, 126.6, 126.5, 88.97, 67.9,

45.0, 31.6, 29.1, 25.8, 22.6, 21.1, 14.0. **HRMS** (ESI⁺) for C₂₈H₃₃NO₂Na⁺ (M+Na⁺) calculated 438.2404, found 438.2419 (error m/z = -3.6 ppm)

N-benzylbenzamide (4.6a) White solid, 80.2 mg, 95% **¹H NMR** (500 MHz, CDCl₃) δ 7.82 (d, *J* = 8.5 Hz, 2H), 7.52 (t, *J* = 7.4 Hz, 1H), 7.45 (t, *J* = 7.5 Hz, 2H), 7.38 (d, *J* = 4.4 Hz, 4H), 7.35 – 7.29 (m, 1H), 6.48 (bs, 1H), 4.67 (d, *J* = 5.6 Hz, 2H). **¹³C NMR** (126 MHz, CDCl₃) δ 167.3, 138.2, 134.4, 131.5, 128.8, 128.6, 127.9, 127.6, 127.0, 44.2. **HRMS** (ESI⁺) for C₁₄H₁₃NONa⁺ (M+Na⁺) calculated 234.0889, found 234.0881 (error m/z = 3.5 ppm)

Polyamide 4.8a Molar mass of the polymers were determined by gel permeation chromatography (GPC). Measurements were carried out with THF as the eluent (flow rate: 1.0 mL/min) with RI detectors. Samples were analyzed versus monodispersed polystyrene standards.

4.8a (from 0.05 M monomers): White solid, 50.7 mg, 85%, (¹H NMR: n=15), M_n=9.9 kDa, PDI = 1.5

4.8a (from 0.5 M monomers): White solid, 300.5 mg, 96%, (¹H NMR: n=66), M_n=41.1 kDa, PDI = 2.3

¹H NMR (100°C, 500 MHz, CDCl₃) δ 8.03 – 7.16 (m, 14H), 6.15 (bs, 2H), 3.59 (s, 2H), 3.39 (s, 2H), 3.22 (s, 2H), 3.03 (s, 2H), 1.63 (s, 4H), 1.38 (m, 16H), 0.92 (s, 10H). **¹³C NMR** (50°C, 126 MHz, CDCl₃) δ 171.5, 138.0, 137.7, 128.5, 128.3, 127.2, 126.3, 88.8, 67.9, 42.3 31.6, 29.4, 28.5, 27.1, 25.9, 22.6, 14.0.

3,10-diaza-1(1,4)-benzenacycloundecaphane-2,11-dione (4.9a) White solid, 25mg, 50% **¹H NMR** (500 MHz, DMSO-*d*₆) δ 7.84 (t, *J* = 5.9 Hz, 2H), 7.51 (s, 4H), 2.85 – 2.65 (m, 4H), 0.87 (bs, 4H), 0.55 (bs, 4H). **¹³C NMR** (126 MHz, DMSO) δ 171.9, 137.4, 126.8, 42.2, 25.7, 23.3. **HRMS** (APCI⁺) for C₁₄H₁₈N₂NaO₂⁺ (M+Na⁺) calculated 269.1260, found 269.1268 (error m/z = -2.9 ppm)

3,12-diaza-1(1,4)-benzenacyclotridecaphane-2,13-dione (4.9b) White solid, 38 mg, 70%, ^1H NMR (500 MHz, DMSO- d_6) δ 7.87 (t, J = 6.8 Hz, 2H), 7.49 (s, 4H), 2.97 (q, J = 7.1 Hz, 4H), 1.16 (s, 4H), 0.98 (s, 4H), 0.53 (s, 4H). ^{13}C NMR (126 MHz, DMSO) δ 171.9, 137.0, 127.1, 41.5, 29.8, 27.0, 25.1. HRMS (APCI $^+$) for $\text{C}_{16}\text{H}_{23}\text{N}_2\text{O}_2^+$ (M+1) calculated 275.1754, found 275.1753 (error m/z = 0.4 ppm)

3,12-diaza-1(1,4)-naphthalenacyclotridecaphane-2,13-dione (4.9c) White solid, 50 mg, 77%, ^1H NMR (500 MHz, DMSO- d_6) δ 8.25 (t, J = 6.8 Hz, 2H), 7.88 (dd, J = 6.4, 3.3 Hz, 2H), 7.67 (dd, J = 6.4, 3.3 Hz, 2H), 7.55 (s, 2H), 2.80 (m, 2H), 2.56 – 2.46 (m, 2H), 1.15 (m, 4H), 0.90 (m, 4H), 0.35 (m, 4H). ^{13}C NMR (126 MHz, DMSO) δ 171.1, 135.3, 129.3, 127.9, 125.6, 123.8, 42.2, 30.1, 26.8, 24.9. HRMS (APCI $^+$) for $\text{C}_{20}\text{H}_{24}\text{N}_2\text{NaO}_2^+$ (M+Na $^+$) calculated 347.1730, found 347.1720 (error m/z = 2.8 ppm)

6,9-dioxa-3,12-diaza-1(1,4)-benzenacyclotridecaphane-2,13-dione (4.9d) White solid, 35mg, 62% ^1H NMR (400 MHz, DMSO- d_6) δ 7.82 (s, 2H), 7.54 (s, 4H), 3.11 (s, 8H), 2.90 (s, 4H). ^{13}C NMR (126 MHz, DMSO) δ 172.0, 136.9, 127.1, 70.3, 68.2, 41.7. HRMS (APCI $^+$) for $\text{C}_{14}\text{H}_{29}\text{N}_2\text{O}_4^+$ (M+1) calculated 279.1339, found 275.1338 (error m/z = -0.6 ppm)

3,14-diaza-1(2,6)-naphthalenacyclopentadecaphane-2,15-dione (4.9e) White solid, 53mg, 75% ^1H NMR (500 MHz, DMSO- d_6) δ 8.09 (d, J = 8.3 Hz, 2H), 8.06 (s, 2H), 7.89 (t, J = 6.7 Hz, 2H), 7.58 (d, J = 8.2 Hz, 2H), 3.07 – 2.88 (m, 4H), 1.24 (bs, 4H), 0.94 (bs, 4H), 0.31 (m, 8H). ^{13}C NMR (126 MHz, DMSO) δ 172.3, 134.7, 132.7, 128.8, 126.5, 125.3, 41.5, 30.4, 29.9, 27.5, 25.3. HRMS (APCI $^+$) for $\text{C}_{22}\text{H}_{28}\text{N}_2\text{NaO}_2^+$ (M+Na $^+$) calculated 375.2042, found 375.2045 (error m/z = -0.4 ppm)

3,12-diaza-1(2,6)-naphthalenacyclotridecaphane-2,13-dione (4.9f) White solid, 37mg, 58% ^1H NMR (500 MHz, DMSO- d_6) δ 8.10 (d, J = 8.3 Hz, 2H), 8.04 (s, 2H), 7.93 (t, J = 6.2 Hz, 2H), 7.55

(d, $J = 8.4$ Hz, 2H), 3.00 – 2.75 (m, 2H), 2.71 – 2.58 (m, 2H), 0.88 – 0.54 (m, 8H), 0.18 – 0.06 (m, 4H). ^{13}C NMR (126 MHz, DMSO) δ 172.4, 134.9, 132.8, 128.8, 125.8, 125.0, 42.6, 29.3, 27.7, 26.6. HRMS (APCI⁺) for $\text{C}_{20}\text{H}_{24}\text{N}_2\text{NaO}_2^+$ (M+Na⁺) calculated 347.1730, found 347.1729 (error $m/z = 0.3$ ppm)

3,11-diaza-1(1,4)-benzenacyclododecaphane-2,12-dione (4.9g) White solid, 33mg, 63% ^1H NMR (500 MHz, DMSO- d_6) δ 7.93 (t, $J = 6.6$ Hz, 2H), 7.48 (s, 4H), 2.90 (m, 4H), 1.02 (m, 4H), 0.72 (m, 4H), 0.60 (m, 2H). ^{13}C NMR (126 MHz, DMSO) δ 172.1, 137.3, 127.0, 41.7, 30.2, 26.3, 24.8. HRMS (APCI⁺) for $\text{C}_{15}\text{H}_{30}\text{N}_2\text{NaO}_2^+$ (M+Na⁺) calculated 283.1417, found 283.1418 (error $m/z = -0.5$ ppm)

4.5 References

- (1) This chapter is a copy of an article which has been submitted for publication. Spectroscopic data as proof of purity and regiochemistry is provided in Appendix III.
- (2) a) Atwood, J.; Steed, J. *Supramolecular Chemistry*, Wiley, Hoboken, N.J., **2013** b) Lehn, J. -M. *Science* **2002**, 295, 2400-2403. c) Savyasachi, A. J.; Kotova, O.; Shanmugaraju, S.; Bradberry, S. J.; Ó'Máille, G. M.; Gunnlaugsson, T. *Chem* **2017**, 3, 764-811.
- (3) a) Lehn, J.-M. *Chem. Eur. J.* **1999**, 5, 2455-2463. b) Rowan, S. J.; Cantrill, S. J.; Cousins, G. R. L.; Sanders, J. K. M.; Stoddart, J. F. *Angew. Chem. Int. Ed.* **2002**, 41, 898-952. c) Zhang, W.; Jin, Y. *Dynamic Covalent Chemistry: Principles, Reactions, and Applications*, John Wiley & Sons, Hoboken, **2018**.
- (4) a) Diercks, C. S.; Yaghi, O. M. *Science* **2017**, 355, 923 b) Feng, X.; Ding, X.; Jiang, D. *Chem. Soc. Rev.* **2012**, 41, 6010-6022. c) Ding, S.-Y.; Wang, W. *Chem. Soc. Rev.* **2013**, 42, 548-568. d) Lohse, M. S.; Bein, T. *Adv. Funct. Mater.* **2018**, 28, 1705553.
- (5) a) Moulin, E.; Cormos, G.; Giuseppone, N. *Chem. Soc. Rev.* **2012**, 41, 1031-1049. b) Kloxin, C. J.; Bowman, C. N. *Chem. Soc. Rev.* **2013**, 42, 7161-7173. c) Mukherjee, S.;

- Cash, J.J.; Sumerlin, B.S. *Responsive Dynamic Covalent Polymers. In Dynamic Covalent Chemistry*, John Wiley & Sons, Inc, **2017**
- (6) a) Zhang, Y.; Barboiu, M. *Chem. Rev.* **2016**, *116*, 809-834. b) Roy, N.; Bruchmann, B.; Lehn, J.-M. *Chem. Soc. Rev.* **2015**, *44*, 3786-3807. c) Moulin, E.; Cormos, G.; Giuseppone, N. *Chem. Soc. Rev.* **2012**, *41*, 1031-1049.
- (7) a) Miller, B.L. *Dynamic Combinatorial Chemistry: In Drug Discovery, Bioorganic Chemistry, and Materials Science*; Wiley: Hoboken, N.J., **2010**. b) Corbett, P. T.; Leclaire, J.; Vial, L.; West, K. R.; Wietor, J.-L.; Sanders, J. K. M.; Otto, S. *Chem. Rev.* **2006**, *106*, 3652-3711. c) Ulrich, S. *Acc. Chem. Res.* **2019**, *52*, 510-519. d) Ramström, O.; Lehn, J.-M. *Nat. Rev. Drug Discov.* **2002**, *1*, 26-36.
- (8) Dydio, P.; Breuil, P.-A. R.; Reek, J. N. H. *Isr. J. Chem.* **2013**, *53*, 61-74.
- (9) a) Jin, Y.; Yu, C.; Denman, R. J.; Zhang, W. *Chem. Soc. Rev.* **2013**, *42*, 6634-6654. b) Belowich, M. E.; Stoddart, J. F. *Chem. Soc. Rev.* **2012**, *41*, 2003-2024. c) Black, S. P.; Sanders, J. K. M.; Stefankiewicz, A. R. *Chem. Soc. Rev.* **2014**, *43*, 1861-1872. d) Bull, S. D.; Davidson, M. G.; van den Elsen, J. M. H.; Fossey, J. S.; Jenkins, A. T. A.; Jiang, Y.-B.; Kubo, Y.; Marken, F.; Sakurai, K.; Zhao, J.; James, T. D. *Acc. Chem. Res.* **2013**, *46*, 312-326.
- (10) a) Vougioukalakis, G. C.; Grubbs, R. H. *Chem. Rev.* **2010**, *110*, 1746-1787. b) Fürstner, A. *Angew. Chem. Int. Ed.* **2013**, *52*, 2794-2819. c) Jin, Y.; Wang, Q.; Taynton, P.; Zhang, W. *Acc. Chem. Res.* **2014**, *47*, 1575-1586. d) White, S. R.; Sottos, N. R.; Geubelle, P. H.; Moore, J. S.; Kessler, M. R.; Sriram, S. R.; Brown, E. N.; Viswanathan, S. *Nature* **2001**, *409*, 794-797.
- (11) For examples with imines: a) Hartley, C. S.; Moore, J. S. *J. Am. Chem. Soc.* **2007**, *129*, 11682-11683. b) Li, X.; Zhang, C.; Cai, S.; Lei, X.; Alton, V.; Hong, F.; Urban, J. J.; Ciston, J.; Chan, E. M.; Liu, Y. *Nat. Commun.* **2018**, *9*, 2998. c) Osowska, K.; Miljanić, O. Š. *J. Am. Chem. Soc.* **2011**, *133*, 724-727. d) Seo, J.-M.; Noh, H.-J.; Jeong, H. Y.; Baek, J.-B. *J. Am. Chem. Soc.* **2019**, *141*, 11786-11790.
- (12) Roughley, S. D.; Jordan, A. M. *J. Med. Chem.* **2011**, *54*, 3451-3479.

- (13) Luo, Y.R. *Comprehensive handbook of chemical bond energies*; Taylor & Francis: Boca Raton, Fla., **2007**.
- (14) a) Stephenson, N. A.; Zhu, J.; Gellman, S. H.; Stahl, S. S. *J. Am. Chem. Soc.* **2009**, *131*, 10003-10008. For related reactions: b) Nguyen, T. B.; Sorres, J.; Tran, M. Q.; Ermolenko, L.; Al-Mourabit, A. *Org. Lett.* **2012**, *14*, 3202-3205. c) Zhang, M.; Imm, S.; Bähn, S.; Neubert, L.; Neumann, H.; Beller, M. *Angew. Chem. Int. Ed.* **2012**, *51*, 3905-3909. d) Becerra-Figueroa, L.; Ojeda-Porras, A.; Gamba-Sánchez, D. *J. Org. Chem.* **2014**, *79*, 4544-4552.
- (15) a) Ruff, Y.; Garavini, V.; Giuseppone, N. *J. Am. Chem. Soc.* **2014**, *136*, 6333-6339. For related examples: b) Swann, P. G.; Casanova, R. A.; Desai, A.; Frauenhoff, M. M.; Urbancic, M.; Slomczynska, U.; Hopfinger, A. J.; Le Breton, G. C.; Venton, D. L. *Pept. Sci.* **1996**, *40*, 617-625. c) Sadownik, J. W.; Ulijn, R. V. *Curr. Opin. Biotechnol.* **2010**, *21*, 401-411.
- (16) For an alternative approach using metallated *N,O*-acetals, see: You, L.; Berman, J. S.; Anslyn, E. V. *Nat. Chem.* **2011**, *3*, 943.
- (17) a) Waller, P. J.; AlFaraj, Y. S.; Diercks, C. S.; Jarenwattananon, N. N.; Yaghi, O. M. *J. Am. Chem. Soc.* **2018**, *140*, 9099-9103. b) Waller, P. J.; Lyle, S. J.; Osborn Popp, T. M.; Diercks, C. S.; Reimer, J. A.; Yaghi, O. M. *J. Am. Chem. Soc.* **2016**, *138*, 15519-15522.
- (18) a) Wu, P.; Nielsen, T. E. *Chem. Rev.* **2017**, *117*, 7811-7856. b) Speckamp, W. N.; Hiemstra, H.; *Tetrahedron* **1985**, *41*, 4367-4416. c) Hiemstra, H.; Speckamp, W. N. in *The Alkaloids: Chemistry and Pharmacology, Vol. 32* (Ed.: Brossi A.), Academic Press, **1988**, pp. 271-339. d) Maryanoff, B. E.; Zhang, H.-C.; Cohen, J. H.; Turchi, I. J.; Maryanoff, C. A. *Chem. Rev.* **2004**, *104*, 1431-1628.
- (19) a) Tjutrins, J.; Dhawan, R.; Lu, Y.; Arndtsen, B. A. *Chem. Eur. J.* **2016**, *22*, 15945-15954. b) Kayser, L. V.; Vollmer, M.; Welnhöfer, M.; Kriekciokat, H.; Meerholz, K.; Arndtsen, B. A. *J. Am. Chem. Soc.* **2016**, *138*, 10516-10521.
- (20) a) Böhme, H.; Hartke, K. *Chem. Ber.* **1963**, *96*, 600-603. b) Bose, A. K.; Spiegelman, G.; Manhas, M. S. *Tetrahedron Lett.* **1971**, *12*, 3167-3170.

- (21) Uray, G. ; Ziegler, E. in *Z. Naturforsch. B, Vol. 30*, **1975**, p. 245.
- (22) This enhanced electrophilicity is also reflected on the product, which results in side products over time.
- (23) It is equally possible that the increased yield of **4.4aa** results from reduction of the imine for subsequent reaction with acyl chloride.
- (24) a) Richards, A. F. *Nylon Fibres in Synthetic Fibres: Nylon, Polyester, Acrylic, Polyolefin* (Ed.: McIntyre, J. E.), Woodhead Publishing, **2005**, pp. 20-94. b) Kohan, M. I. *Nylon Plastics Handbook*, Hanser/Gardner Publications, **1995**.
- (25) a) Yudin, A. K. *Chemical Science* **2015**, *6*, 30-49. b) Newman, D. J.; Cragg, G. M. in *Macrocycles in Drug Discovery*, The Royal Society of Chemistry, **2015**, pp. 1-36. c) Marsault, E.; Peterson, M. L. *J. Med. Chem.* **2011**, *54*, 1961-2004. d) Webber, M. J.; Langer, R. *Chem. Soc. Rev.* **2017**, *46*, 6600-6620. e) Luis, S. V.; Alfonso, I. *Acc. Chem. Res.* **2014**, *47*, 112-124. f) Chmielewski, M. J.; Jurczak, J. *Chem. Eur. J.* **2005**, *11*, 6080-6094.
- (26) a) Rossa, L.; Vögtle, F. in *Cyclophanes I* (Ed.: Vögtle, F.), Springer, Berlin, Heidelberg, **1983**, pp. 1-86. b) Stetter, H.; Marx-Moll, L.; Rutzen, H. *Chem. Ber.* **1958**, *91*, 1775-1781. c) Rodgers, S. J.; Ng, C. Y.; Raymond, K. N. *J. Am. Chem. Soc.* **1985**, *107*, 4094-4095.
- (27) a) Zhang, D.-W.; Zhao, X.; Hou, J.-L.; Li, Z.-T. *Chem. Rev.* **2012**, *112*, 5271-5316. b) Gong, B. *Acc. Chem. Res.* **2008**, *41*, 1376-1386. c) Zaretsky, S.; Yudin, A. K. *Contemporary Macrocyclization Technologies. In Practical Medicinal Chemistry with Macrocycles: Design, Synthesis, and Case Studies, 1st ed.* (Ed.: Marsault, E. and Peterson, M. L.), John Wiley & Sons, Inc., **2017**.
- (28) a) Johnston, A. G.; Leigh, D. A.; Murphy, A.; Smart, J. P.; Deegan, M. D. *J. Am. Chem. Soc.* **1996**, *118*, 10662-10663. b) Leigh, D. A.; Marcos, V.; Nalbantoglu, T.; Vitorica-Yrezabal, I. J.; Yasar, F. T.; Zhu, X. *J. Am. Chem. Soc.* **2017**, *139*, 7104-7109. c) Martí-Centelles, V.; Burguete, M. I.; Luis, S. V. *J. Org. Chem.* **2016**, *81*, 2143-2147. d) Schalley, C. A.; Weilandt, T.; Brüggemann, J.; Vögtle, F. in *Templates in Chemistry I* (Eds.:

- Schalley, C. A.; Vögtle, F.; Dötz, K. H.), Springer Berlin Heidelberg, Berlin, Heidelberg, **2004**, pp. 141-200.
- (29) Collins, J. C.; James, K. *MedChemComm* **2012**, *3*, 1489-1495.
- (30) a) Glans, J. H.; Akkapeddi, M. K. *Macromolecules* **1992**, *25*, 5526-5527. b) Glans, J. H.; Akkapeddi, M. K. (Allied Signal Inc.), 5276131, **1994**. c) Katoono, R.; Kawai, H.; Fujiwara, K.; Suzuki, T. *Tetrahedron Lett.* **2004**, *45*, 8455-8459.
- (31) Siamaki, A. R.; Sakalauskas, M.; Arndtsen, B. A. *Angew. Chem. Int. Ed.* **2011**, *50*, 6552-6556.
- (32) Layer, R. W. *Chem. Rev.* **1963**, *63*, 489-510.
- (33) Ohshima, T.; Iwasaki, T.; Maegawa, Y.; Yoshiyama, A.; Mashima, K. *J. Am. Chem. Soc.* **2008**, *130*, 2944-2945.
- (34) Dam, J. H.; Osztrovszky, G.; Nordstrøm, L. U.; Madsen, R. *Chem. Eur. J.* **2010**, *16*, 6820-6827.

CHAPTER 5

Summary, Conclusions and Future Work

This chapter provides a summary of important results, conclusions and contributions to original knowledge in this thesis. Suggestions for future work are also described.

5.1 Conclusions and Contributions to Original Knowledge

Chapters 2-3 of this thesis described the development of new classes of 1,3-dipoles and investigation of their cycloaddition reactivity. As mentioned in Chapter 1, 1,3-dipolar cycloaddition offers an efficient approach to access five-membered heterocycles. Although this chemistry is commonly utilized, the synthesis of 1,3-dipoles is still a challenge that limits their wider applications, since most substituted 1,3-dipoles are generated via a multistep synthesis. Previous studies in our group have demonstrated modular ways to access 1,3-dipoles, and their corresponding cycloaddition products, from readily available materials. However, these efforts have covered a limited number of heterocyclic motifs.

We described in Chapter 2 the discovery of a new class of 1,3-dipole. These pyridine-based mesoionic heterocycles can be accessed from 2-pyridyl acyl chlorides and imines. This 1,3-dipole was inspired by Besthorn's red, an early example of mesoionic heterocycles, which does not undergo cycloaddition due to its extended conjugation. Instead of using quinoline-based starting materials, we introduced less conjugated components such as pyridines and imines into the 1,3-dipolar core. This indeed induced cycloaddition reactivity to these molecules, generating indolizines upon cycloaddition with alkynes. Although these 1,3-dipoles are reactive, they can still

be isolated and characterized, unlike many mesoionic heterocycles. Overall, this approach offers modular and regioselective route to synthesize substituted indolizines from commercially available 2-pyridyl acyl chlorides, alkynes, and easily generated imines.

In Chapter 3, we presented our efforts to design another class of 1,3-dipole; a carbonyl ylide version of a phosphamünchnone. Simply replacing the imine substrate in phosphamünchnones with an aldehyde did not result in the formation of 1,3-dipole, presumably due to the weak nucleophilicity of aldehydes. To address this, we generated more potent acyl triflate electrophiles *in situ* from acyl chlorides and silver triflate. As we hoped, this led to the acylation of aldehyde and following nucleophilic attack of the phosphonite PhP(catechyl) generated the precursor to the targeted 1,3-dipole. Although deprotonation was observed upon addition of base, we were not able isolate and characterize this 1,3-dipole. Instead, the latter was conveniently trapped by 1,3-dipolar cycloaddition with alkynes to generate furans. In contrast to many common methods employed to synthesize furans, this has opened a modular route to generate families of these heterocycles from commercially available acyl chlorides, aldehydes and alkynes. In addition, polycyclic oxazoles can also be obtained via the intramolecular cycloaddition of nitriles.

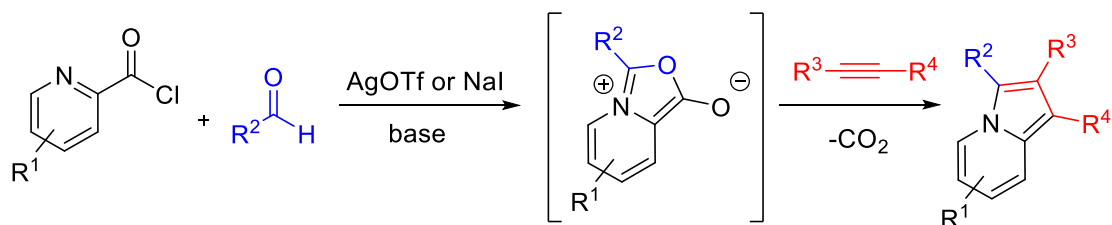
Finally, in Chapter 4, we described a new method for dynamic amide bond formation. Amides are often formed via irreversible reactions between amines and carboxylic acid derivatives. Our studies focused on the reversible coupling of imines and acyl chlorides to form α -chloroamides. This reaction is a well-known method to generate *N*-acyl iminium salts. However, the dynamic features of this transformation have not been investigated in the context of dynamic covalent chemistry (DCvC). We demonstrated the dynamic nature of imine-acyl chloride coupling through a series of systematic studies, and used this to perform exchange and scrambling reactions. Of note, the reaction was found to be dynamic under ambient conditions, without a catalyst, and

using easily generated components. In addition, stable secondary and tertiary amide products can be obtained by trapping the dynamically generated α -chloroamides by hydrolysis or nucleophilic attack. Ultimately, we demonstrated a utility of this approach to access polymers and macrocycles. The latter is a particularly challenging target, since macrocyclic amide formation from irreversible reactions usually occurs under kinetic control using ultrahigh dilutions or specialized substrates. Instead, our approach allows the formation of macrocyclic amides under thermodynamic control, in a general fashion, from simple diimines and diacyl chlorides, and at normal concentrations. Importantly, thermodynamic control can also be utilized to switch between macrocyclic and polymeric products.

5.2 Suggestions for Future Work

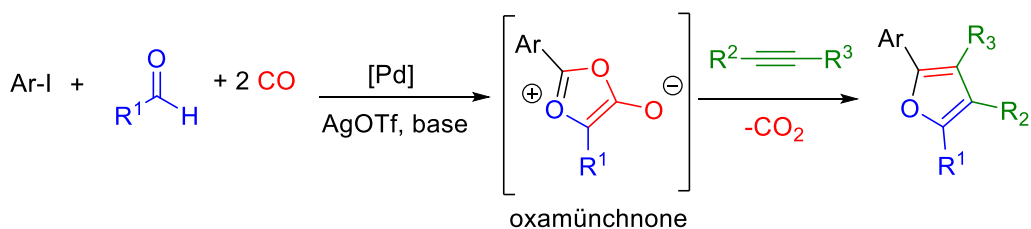
In Chapter 2, a new method to access indolizines from 2-pyridyl acyl chlorides, imines and alkynes is demonstrated. Although efficient, this method suffers in two features. Firstly, the imine starting materials must be generated from amines and aldehydes. More importantly, the cycloaddition of these dipoles with alkynes and alkenes leads to the generation of a stoichiometric isocyanate by-product. The latter are highly toxic, and requires quenching with amines. In principle, this can be addressed by applying our findings in Chapter 3, and replacing imines in this reaction with aldehydes. Although an aldehyde is a weak nucleophile and does not react by itself with acyl chlorides, the *in situ* conversion of pyridyl acyl chlorides to acyl triflates can allow formation of the oxygen-containing pyridine-based 1,3-dipole (Scheme 5.1). Combined with the cycloaddition, the same indolizine products can be obtained. This would require stoichiometric amount of a halide-exchange reagent, such as silver triflate; but it provides two advantages. Firstly,

initial synthesis of imine would no longer be needed and instead the transformation could be carried out directly from inexpensive and broadly available aldehydes. Secondly, the by-product of cycloaddition would be non-toxic CO₂.



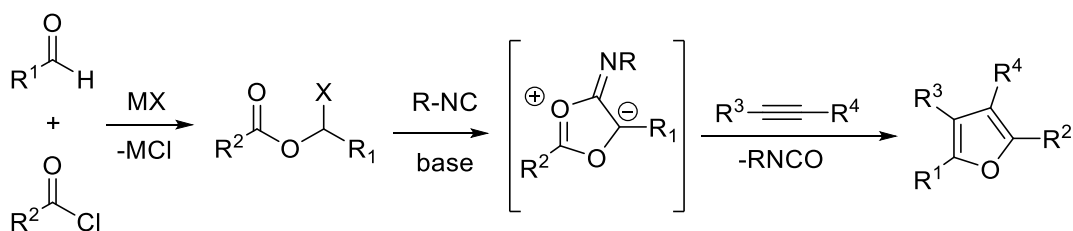
Scheme 5.1 Synthesis of pyridine-based münchnones

In Chapter 3, we demonstrated the synthesis of a new class of oxygen-based 1,3-dipole from aldehydes, acyl chlorides and a phosphonite. One limitation of this approach is the need for the PhP(catechyl) reagent, which must be generated, and forms a stoichiometric amount of phosphonate waste. As an alternative, our previously reported, palladium catalyzed multicomponent synthesis of münchnones (section 1.2.3.1)¹ might be modified to accommodate aldehydes as substrates. The *in situ* formation of potent acyl triflate electrophiles from aryl iodides was achieved in a recent study from our group.² The combination of these two approaches could potentially lead to synthesis of oxamünchnones (Section 1.2.3.5). This 1,3-dipole has not been isolated, but their intermediacy is proposed in the formation of furans upon cycloaddition with alkynes.³ Overall, this could offer a modular method to access oxamünchnones and their cycloaddition products from aryl iodides, aldehydes, CO and alkynes (Scheme 5.2).



Scheme 5.2 Palladium-catalyzed carbonylative synthesis of oxamünchnones

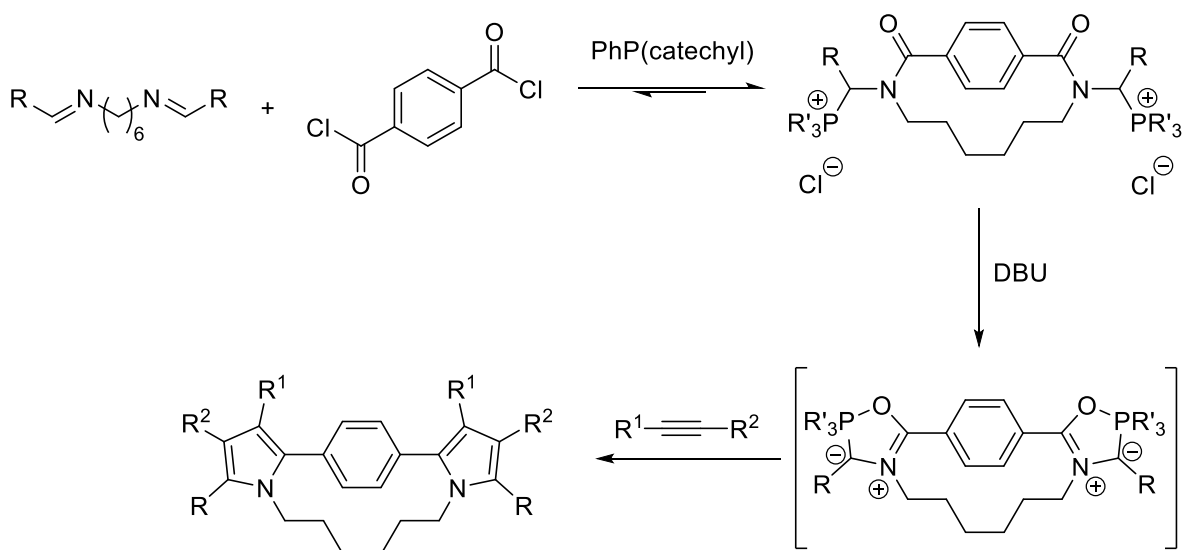
Alternatively, the phosphonites in this chemistry might instead be replaced with isocyanides. Our group has developed an isocyanide-mediated synthesis of pyrroles, through the generation of münchnone-imines from acyl chlorides, imines and isocyanides.⁴ Performing the analogous reaction of an acyl chloride, aldehyde and isocyanide would generate a new, carbonyl-ylide version of this mesoionic heterocycle, an “oxamünchnone-imine” for use in furan synthesis. One potential limitation of this approach is the reactivity of isocyanides towards acyl halides. This might be prevented by step-wise addition of reagents. This overall sequence is shown in Scheme 5.3.



Scheme 5.3 Isocyanide-mediated synthesis of furans

Finally, the dynamic formation of amides (Chapter 4) is a general synthetic platform with many potential applications, since amides are broadly employed products. As one possible

application, this chemistry might be used to not just generate amides, but instead be combined with the 1,3-dipolar cycloaddition to offer a controlled method to access heterocycle-containing macrocycles. This could be accomplished by combining macrocyclic α -chloroamide formation with the addition of PhP(catechyl) and base to form a macrocyclic phosphamünchnone. The corresponding macrocyclic pyrrole would be formed after cycloaddition (Scheme 5.4). It is notable that the conjugated system in these products would be twisted due to ring strain, which may offer an interesting avenue to modulate their electronic properties.⁵



Scheme 5.4 Synthesis of macrocyclic phosphamünchnones and pyrroles

5.3 References

- (1) a) Dhawan, R.; Dghaym, R. D.; Arndtsen, B. A., *J. Am. Chem. Soc.* **2003**, *125*, 1474-1475.
 b) Torres, G. M.; Quesnel, J. S.; Bijou, D.; Arndtsen, B. A., *J. Am. Chem. Soc.* **2016**, *138*, 7315-7324.

- (2) Kinney, R.G.; Tjutrins, J.; Torres, G. M.; Liu, N. J.; Kulkarni, O.; Arndtsen, B. A., *Nat. Chem.* **2018**, *10*, 193-199.
- (3) Hamaguchi, M.; Nagai, T., *J. Chem. Soc., Chem. Commun.* **1985**, *4*, 190-191.
- (4) St. Cyr, D. J.; Martin, N.; Arndtsen, B. A., *Org. Lett.* **2007**, *9*, 449-452.
- (5) a) Herges, R., *Nature* **2007**, *450*, 36-37. b) Xiao, S.; Myers, M.; Miao, Q.; Sanaur, S.; Pang, K.; Steigerwald, M. L.; Nuckolls, C., *Angew. Chem. Int. Ed.* **2005**, *44*, 7390-7394.

Appendix I

Copyright waiver for Chapter 2

TERMS AND CONDITIONS

This copyrighted material is owned by or exclusively licensed to John Wiley & Sons, Inc. or one of its group companies (each a "Wiley Company") or handled on behalf of a society with which a Wiley Company has exclusive publishing rights in relation to a particular work (collectively "WILEY"). By clicking "accept" in connection with completing this licensing transaction, you agree that the following terms and conditions apply to this transaction (along with the billing and payment terms and conditions established by the Copyright Clearance Center Inc., ("CCC's Billing and Payment terms and conditions"), at the time that you opened your RightsLink account (these are available at any time at <http://myaccount.copyright.com>).

Terms and Conditions

- The materials you have requested permission to reproduce or reuse (the "Wiley Materials") are protected by copyright.
- You are hereby granted a personal, non-exclusive, non-sub licensable (on a stand-alone basis), non-transferable, worldwide, limited license to reproduce the Wiley Materials for the purpose specified in the licensing process. This license, **and any CONTENT (PDF or image file) purchased as part of your order**, is for a one-time use only and limited to any maximum distribution number specified in the license. The first instance of republication or reuse granted by this license must be completed within two years of the date of the grant of this license (although copies prepared before the end date may be distributed thereafter). The Wiley Materials shall not be used in any other manner or for any other purpose, beyond what is granted in the license. Permission is granted subject to an appropriate acknowledgement given to the author, title of the material/book/journal and the publisher. You shall also duplicate the copyright notice that appears in the Wiley publication in your use of the Wiley Material. Permission is also granted on the understanding that nowhere in the text is a previously published source acknowledged for all or part of this Wiley Material. Any third party content is expressly excluded from this permission.

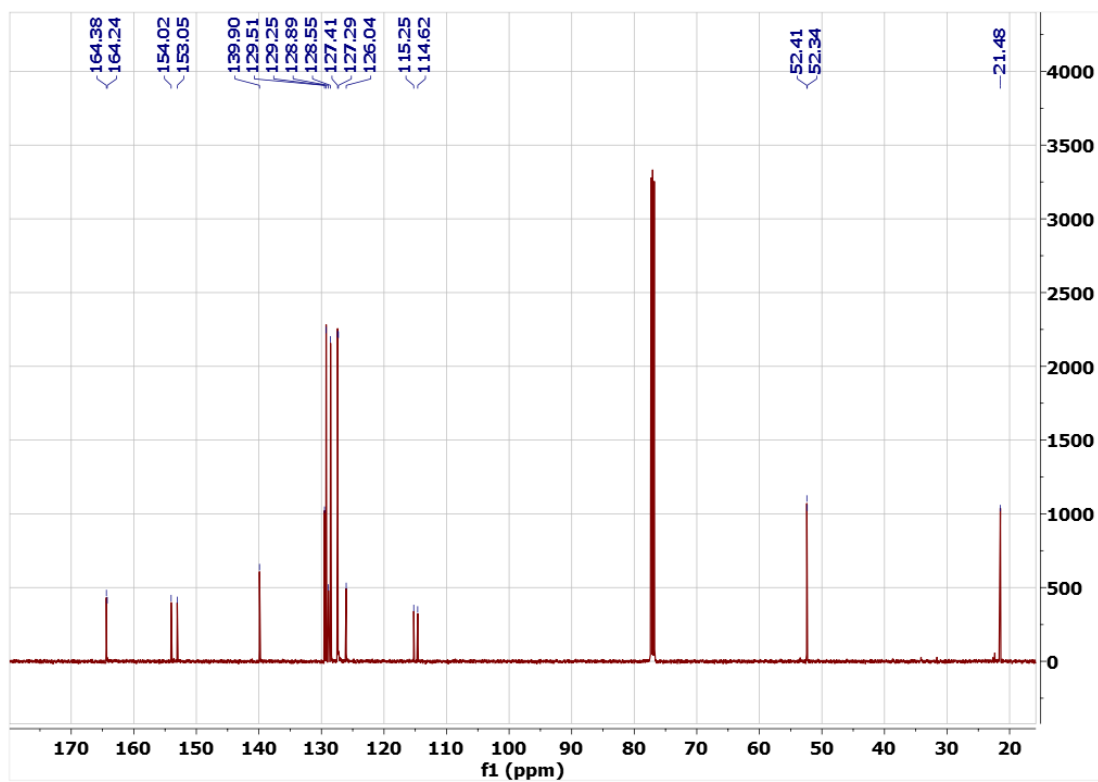
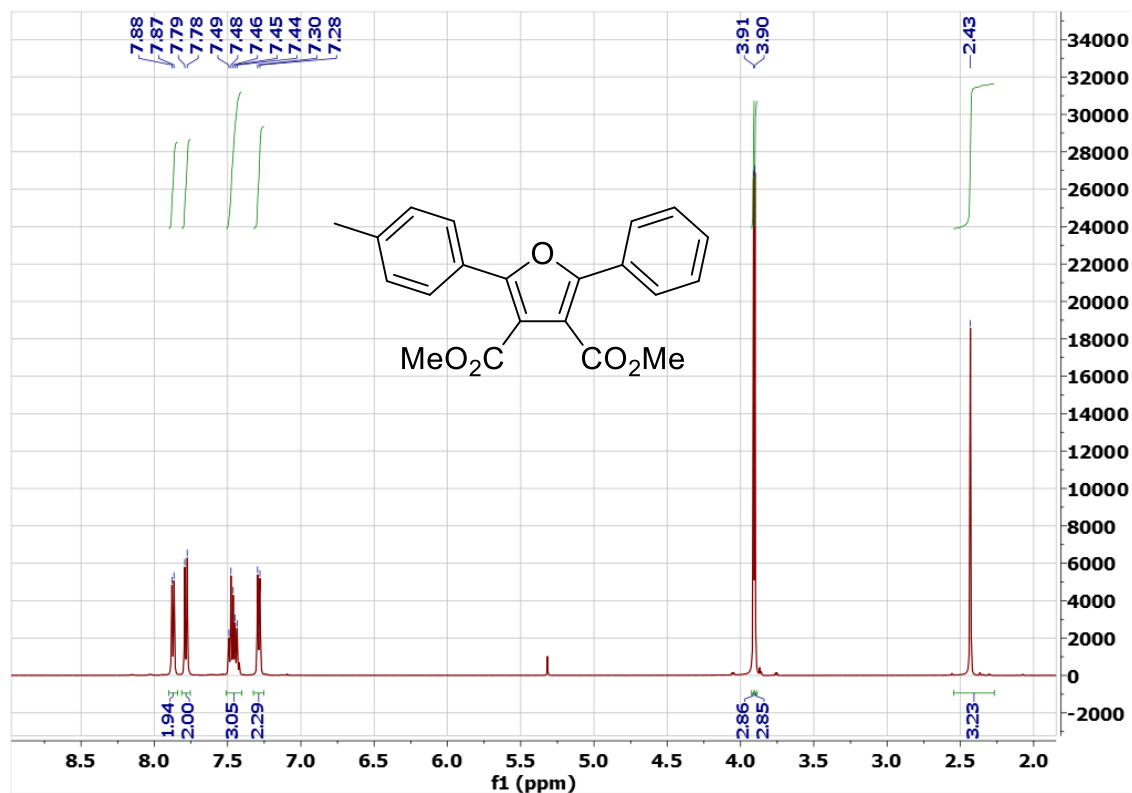
Appendix II

^1H , ^{13}C , ^{19}F and 2D NMR spectroscopic data as proof of purity and regiochemistry, for unpublished Chapter 3 is provided below.

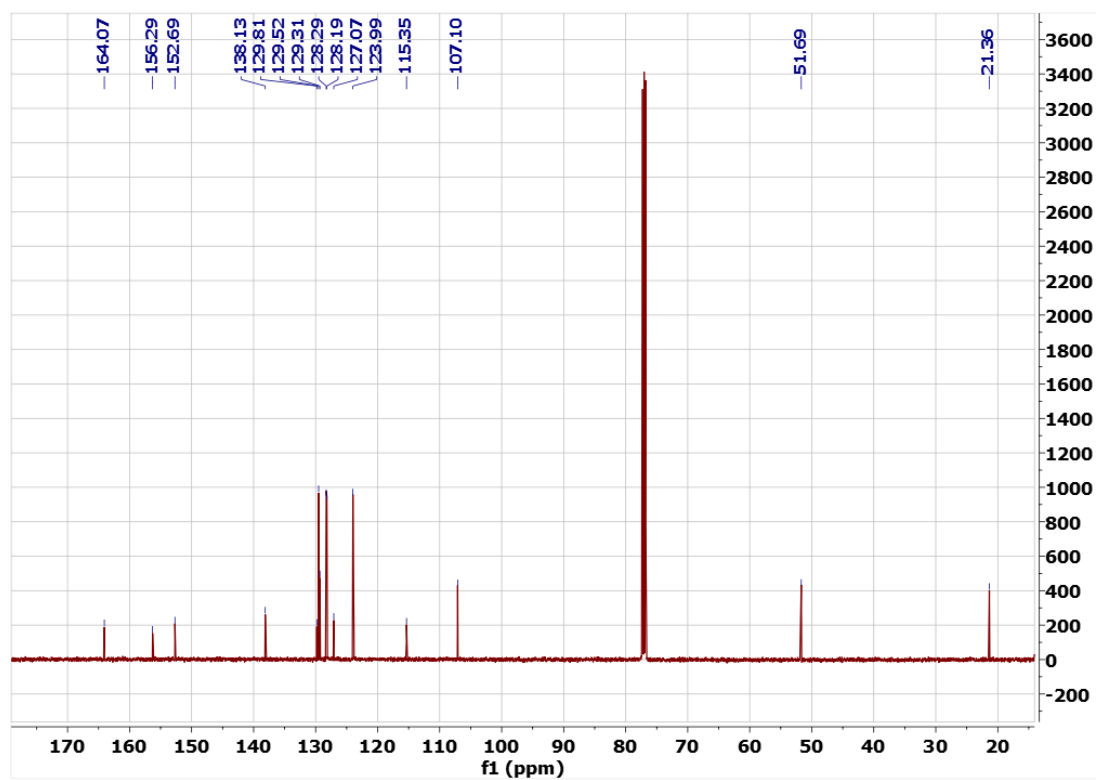
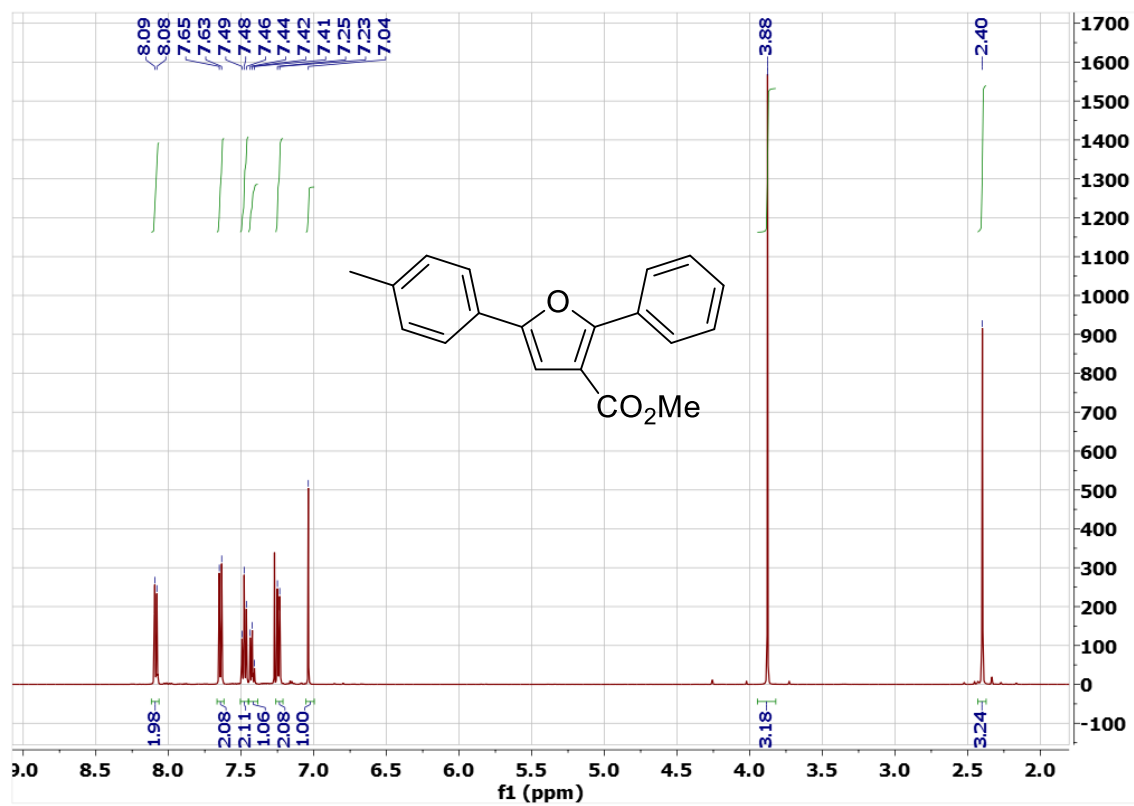
Table of Contents

^1H and ^{13}C NMR Spectra of 3.5a.....	3
^1H and ^{13}C NMR Spectra of 3.5b.....	4
2D-NOE Spectra of 3.5b.....	5
^1H and ^{13}C NMR Spectra of 3.5c.....	6
2D-NOE Spectra of 3.5c.....	7
^1H and ^{13}C NMR Spectra of 3.5d.....	8
^1H , ^{13}C and ^{19}F NMR Spectra of 3.5e.....	9
^1H and ^{13}C NMR Spectra of 3.5f.....	11
^1H and ^{13}C NMR Spectra of 3.5g.....	12
^1H and ^{13}C NMR Spectra of 3.5h.....	13
^1H and ^{13}C NMR Spectra of 3.5i.....	14
^1H and ^{13}C NMR Spectra of 3.5j.....	15
^1H and ^{13}C NMR Spectra of 3.5k.....	16
^1H and ^{13}C NMR Spectra of 3.5l.....	17
^1H and ^{13}C NMR Spectra of 3.5m.....	18
^1H and ^{13}C NMR Spectra of 3.5n.....	19
^1H and ^{31}P NMR Spectra of 3.4a.....	20
^{31}P NMR Spectra of 3.4o before and after base addition.....	21

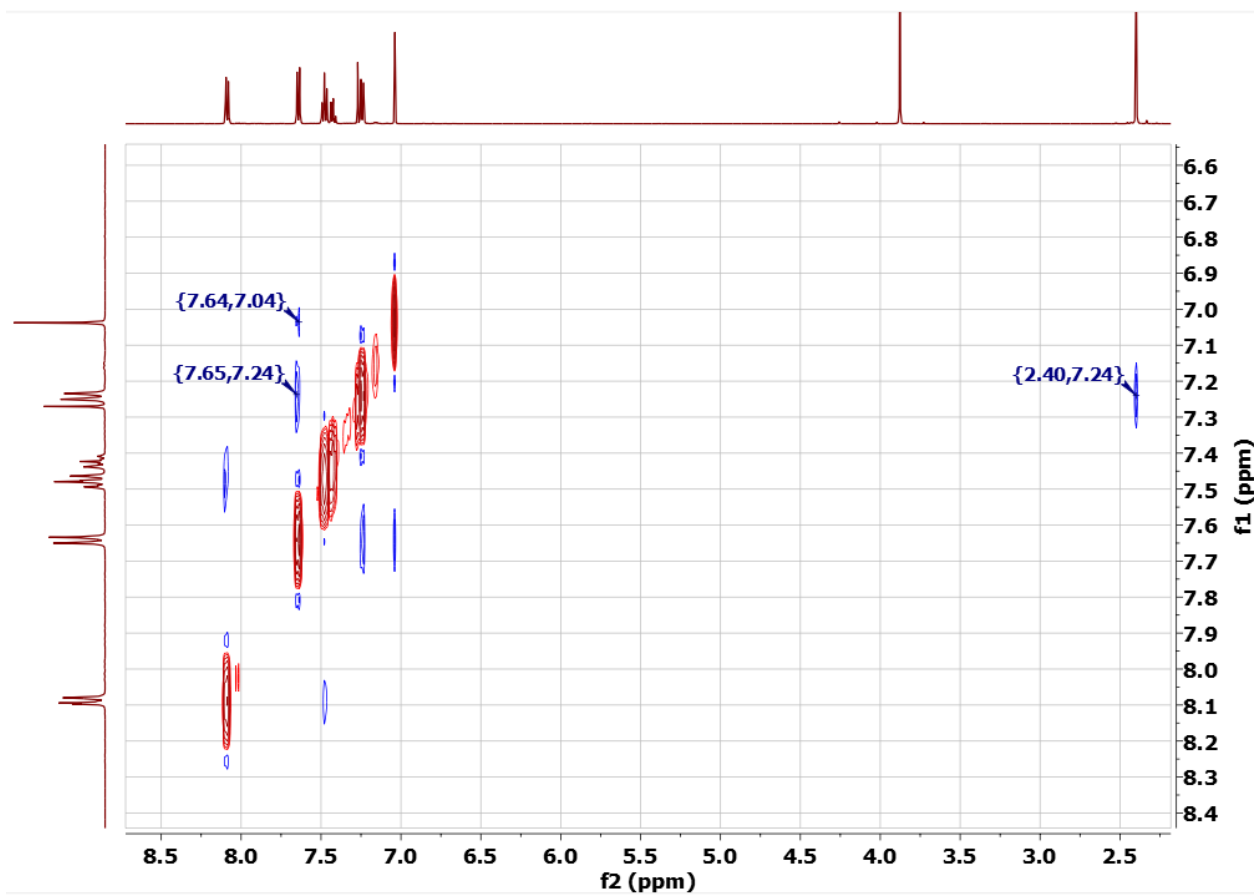
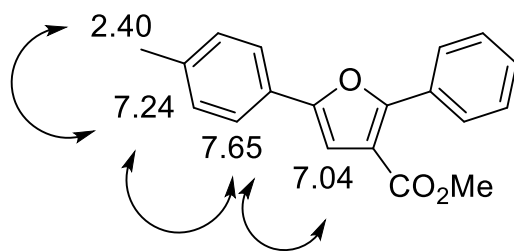
^1H and ^{13}C NMR Spectra of 3.5a (CDCl_3)



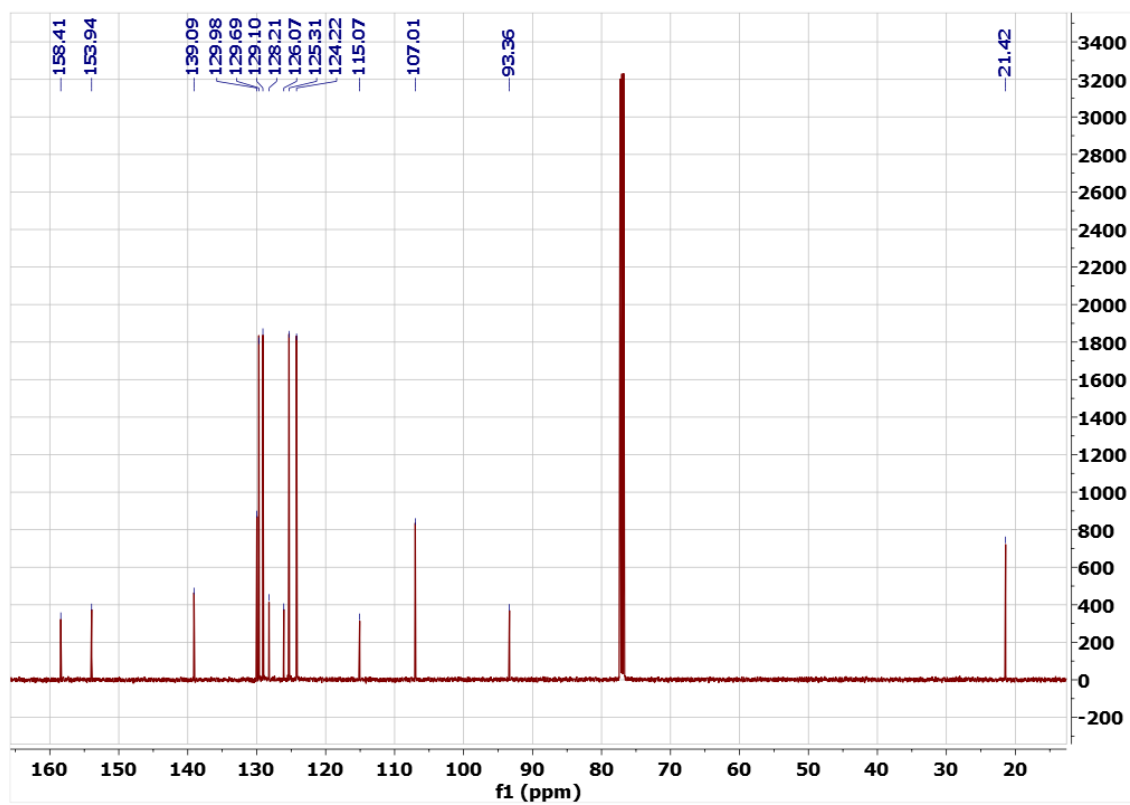
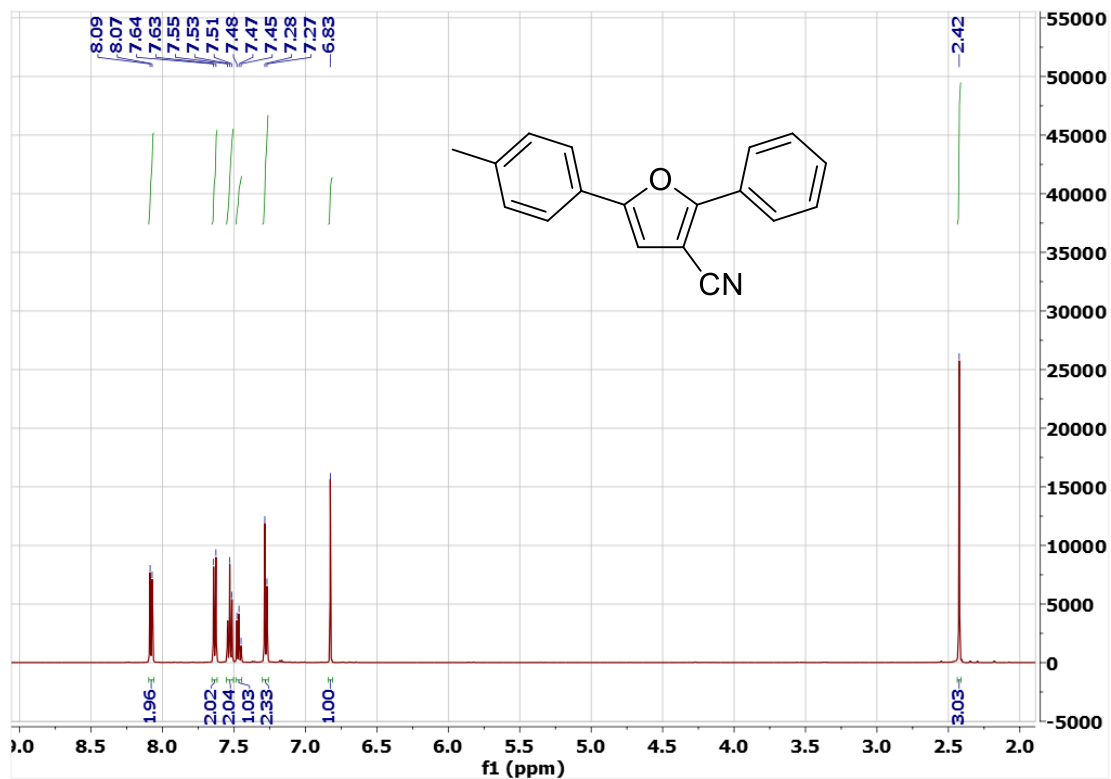
^1H and ^{13}C NMR Spectra of 3.5b (CDCl_3)



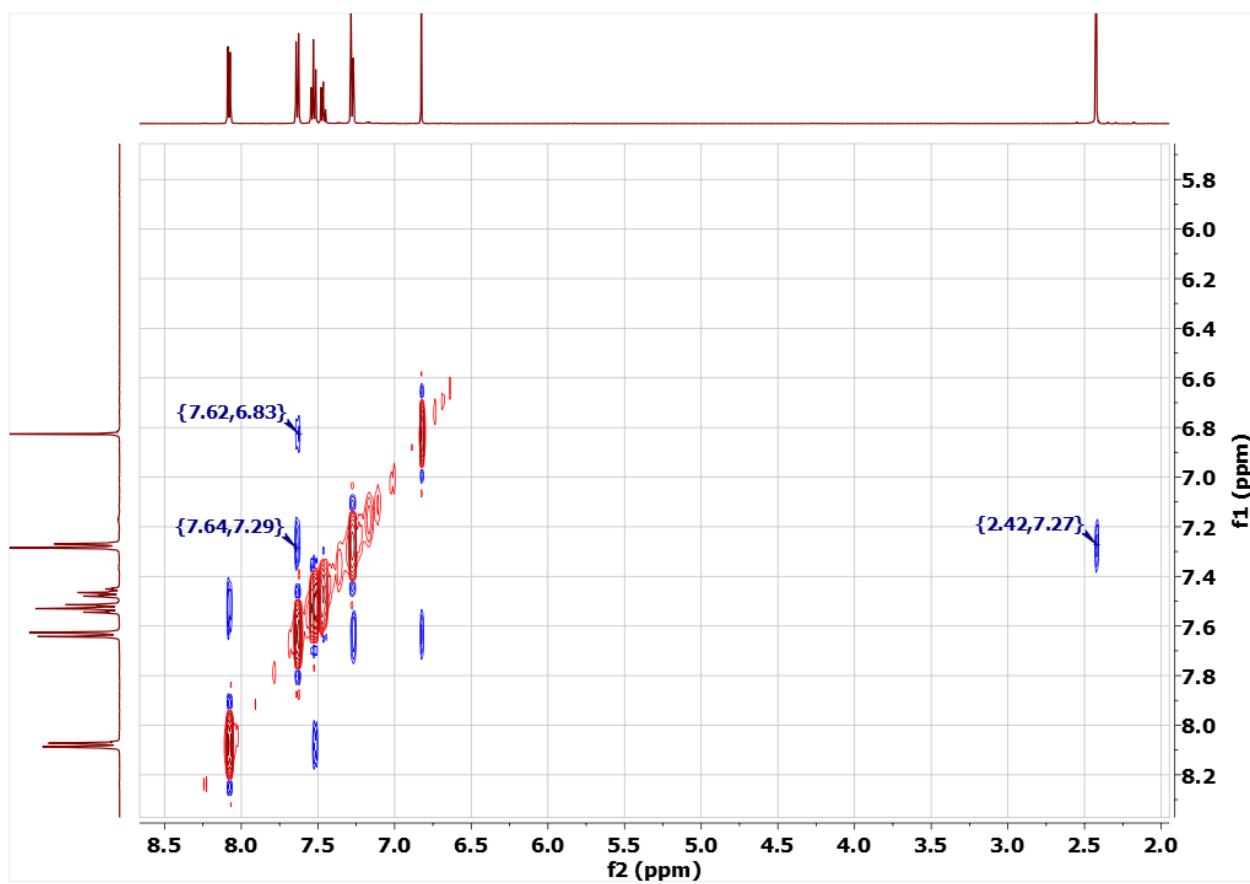
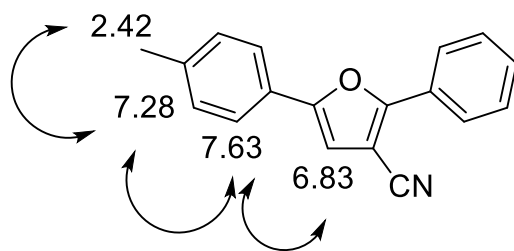
2D-NOE Spectra of 3.5b (CDCl₃)



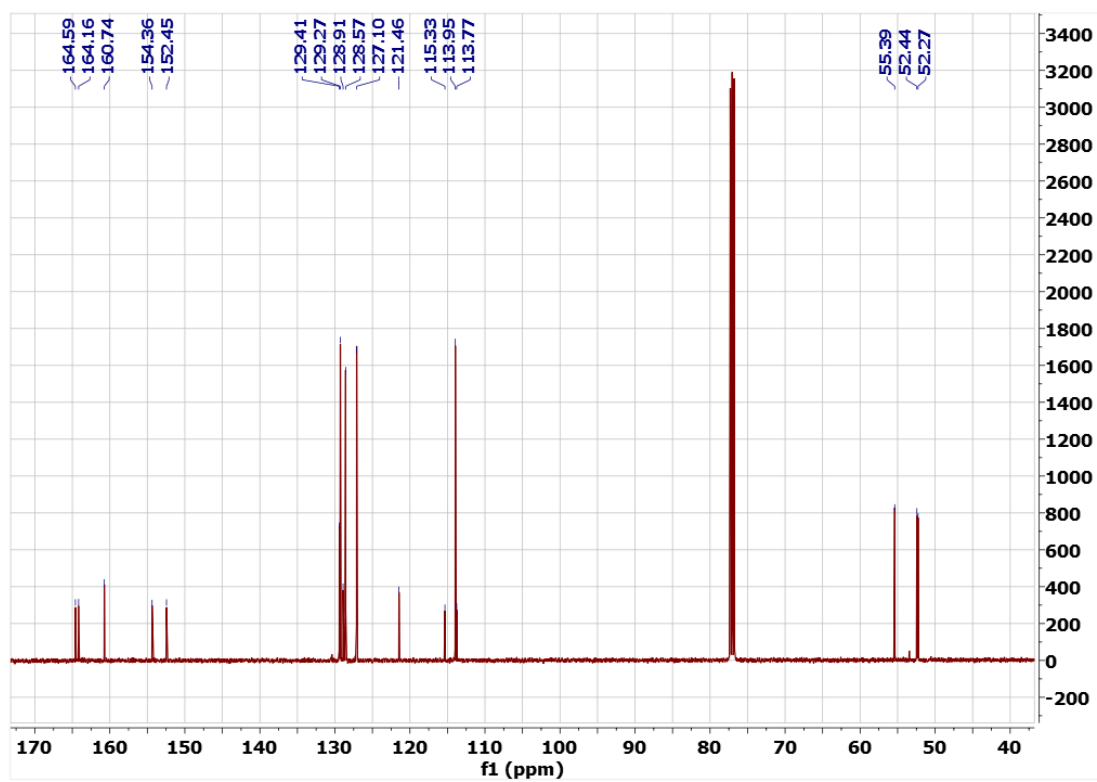
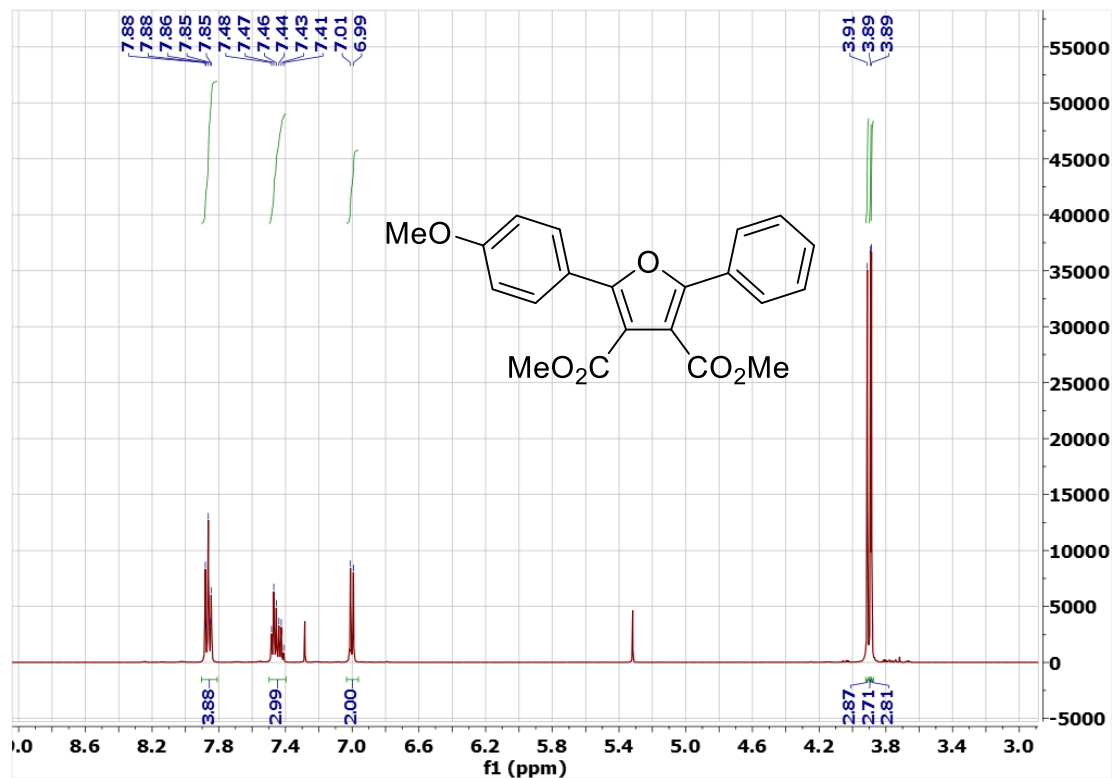
¹H and ¹³C NMR Spectra of 3.5c (CDCl₃)



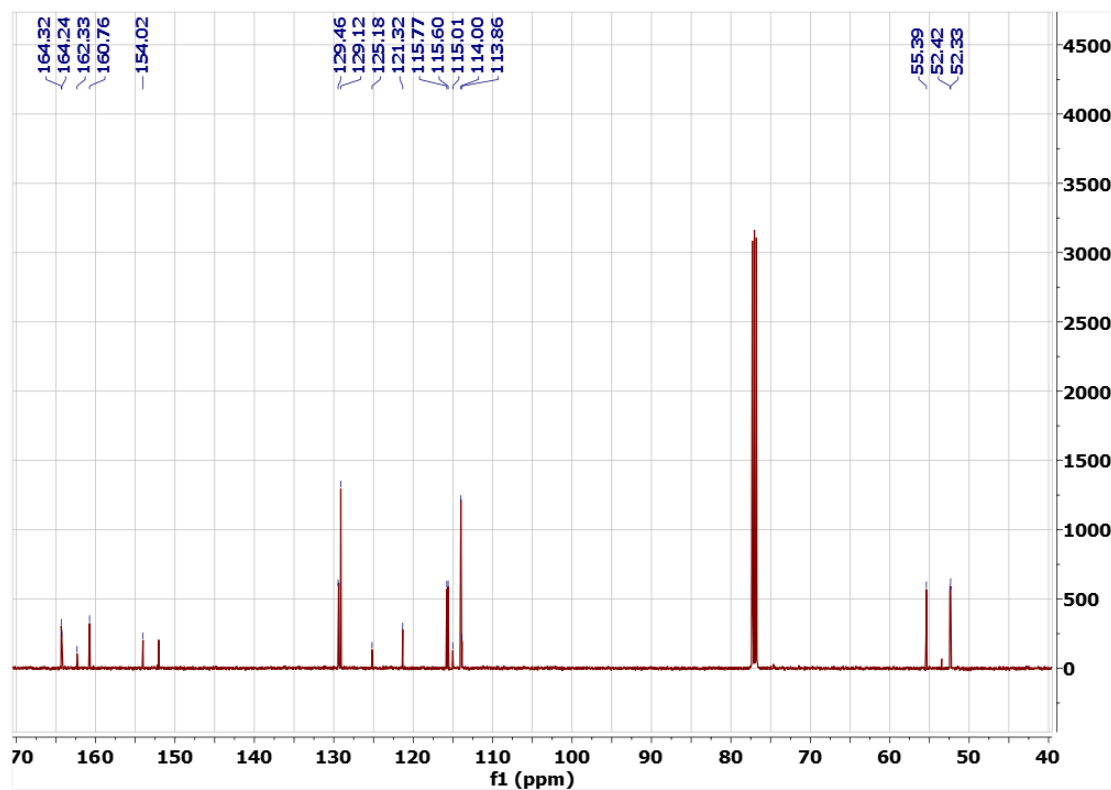
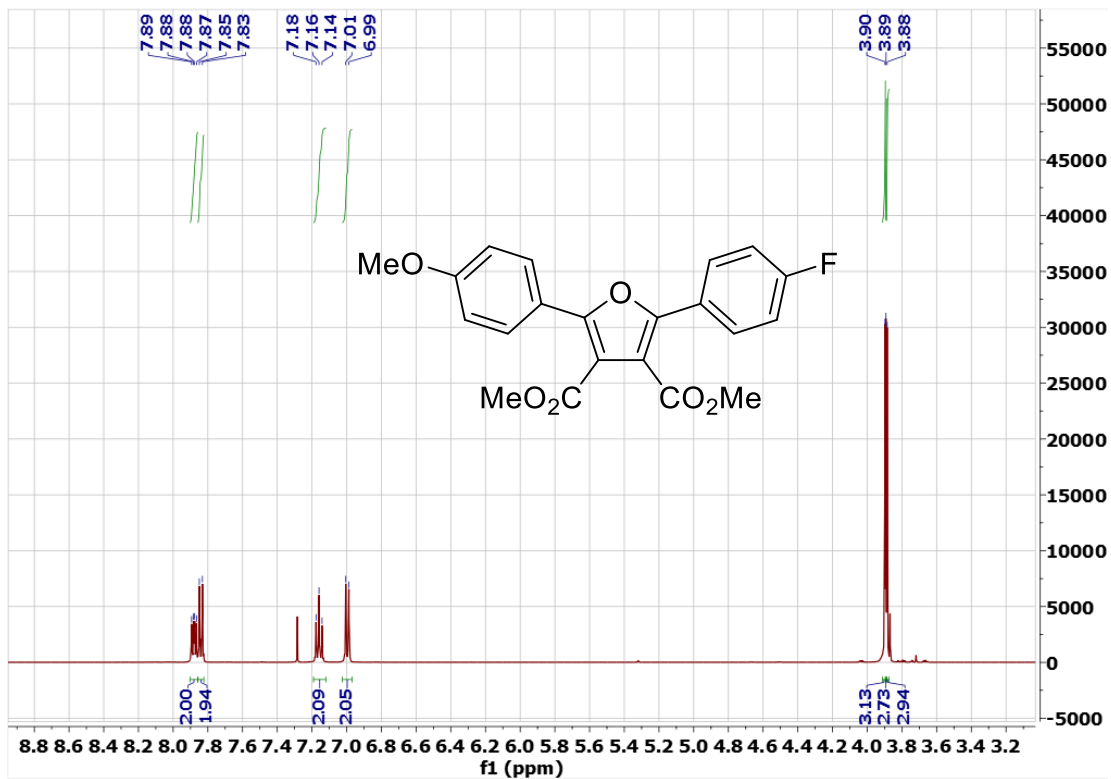
2D-NOE Spectra of 3.5c (CDCl₃)

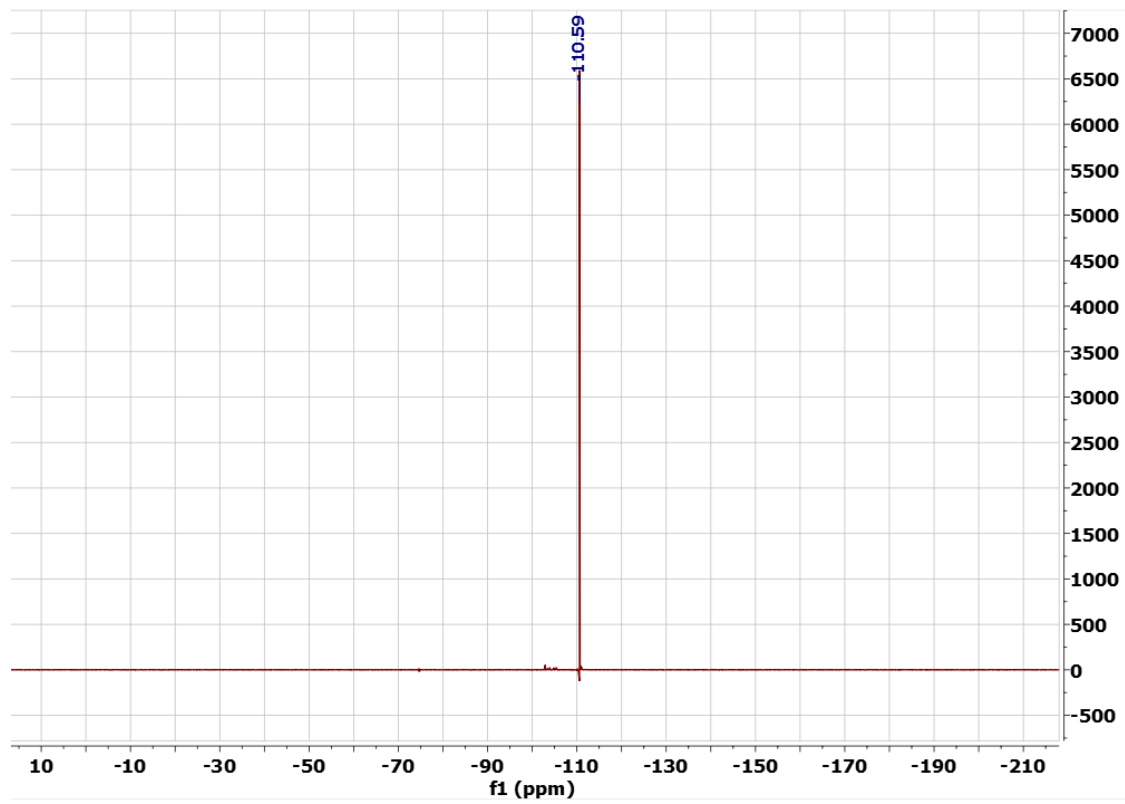


¹H and ¹³C NMR Spectra of 3.5d (CDCl₃)

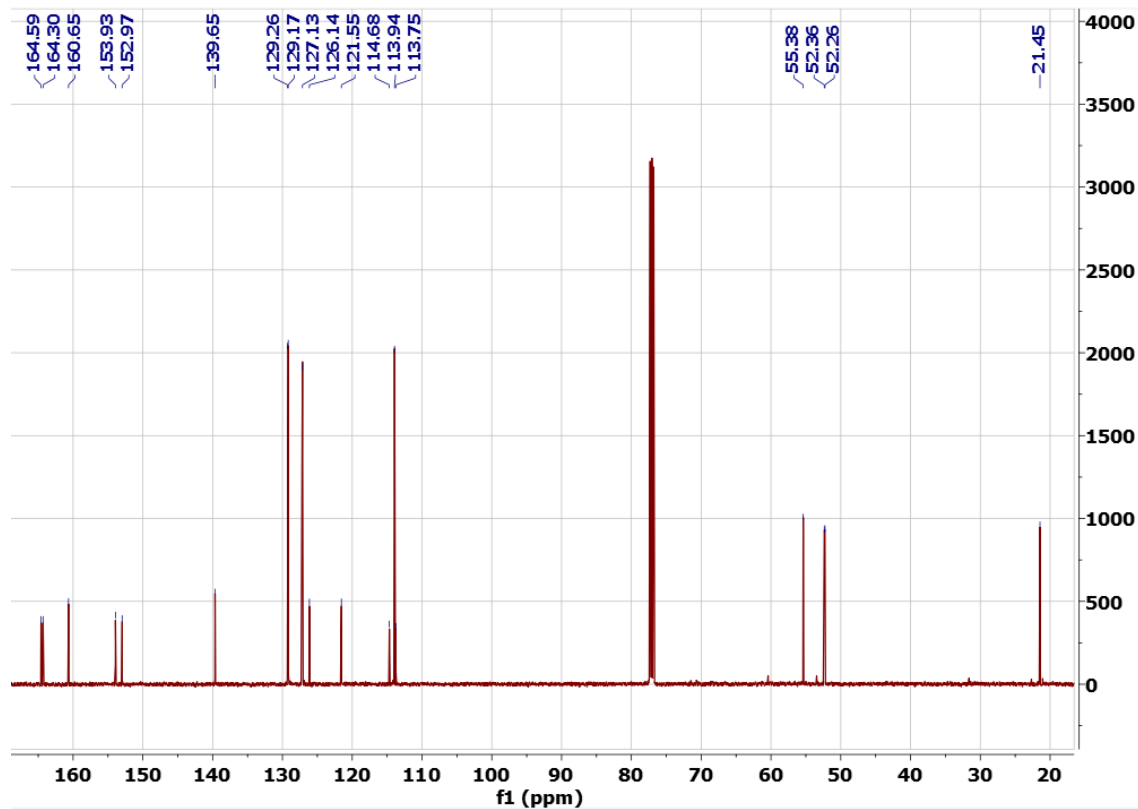
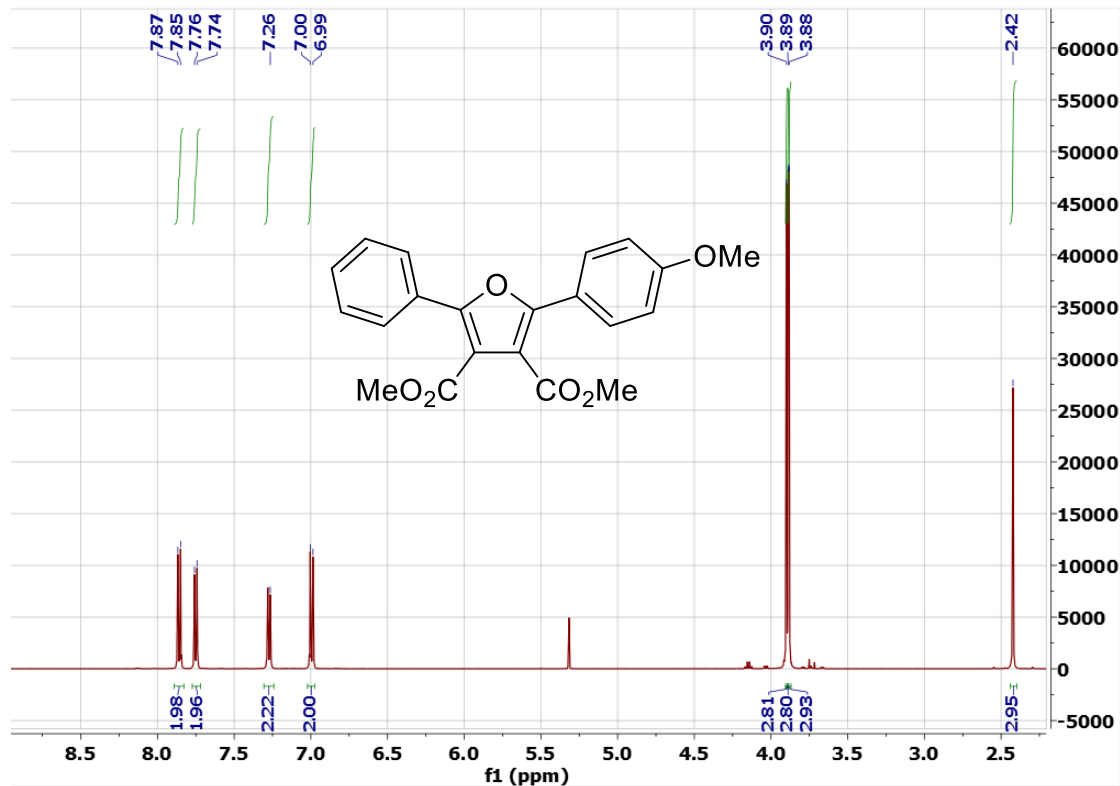


^1H , ^{13}C and ^{19}F NMR Spectra of 3.5e (CDCl_3)

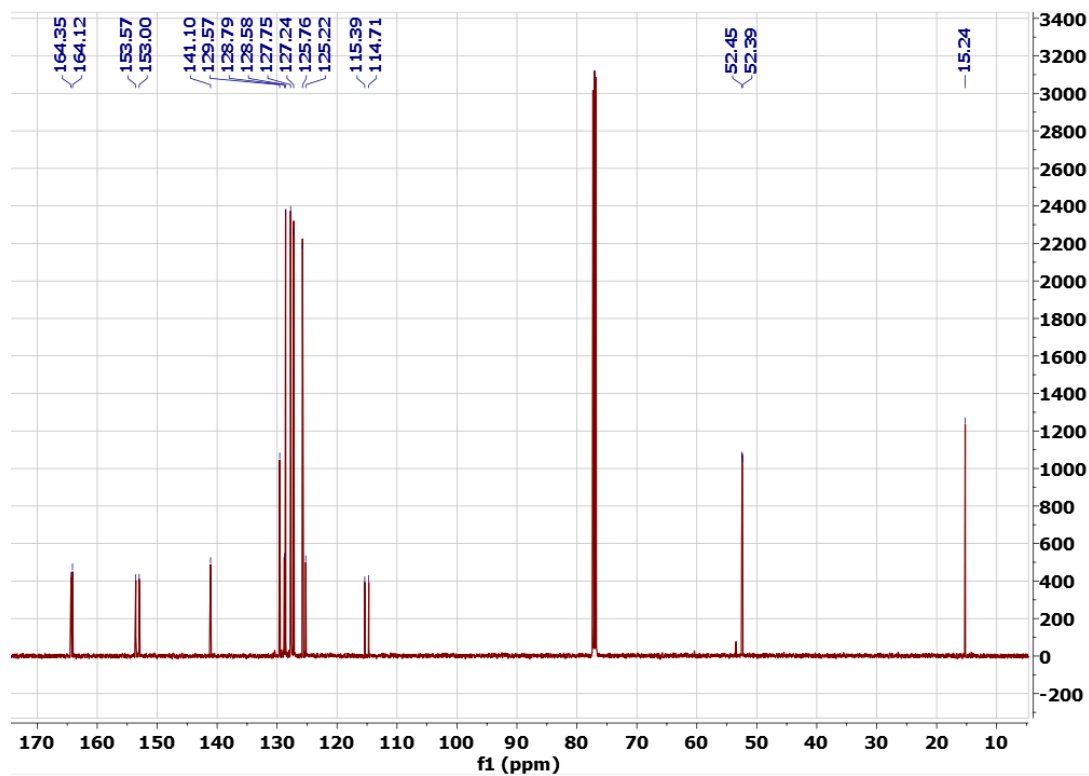
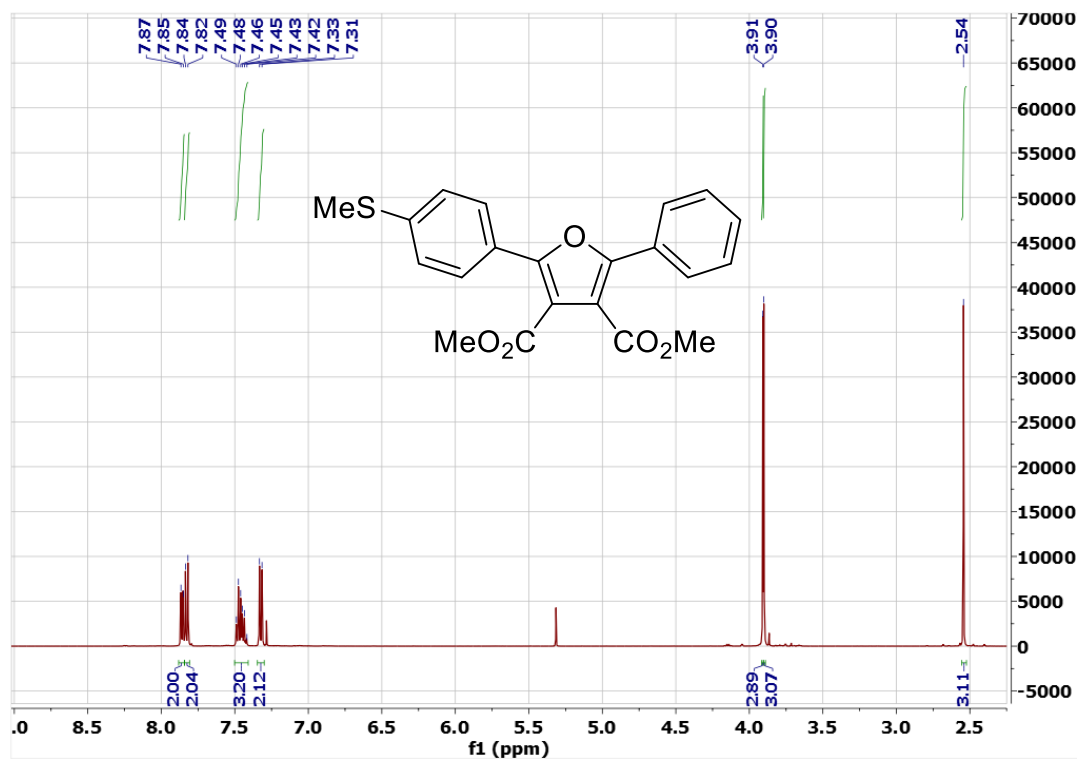




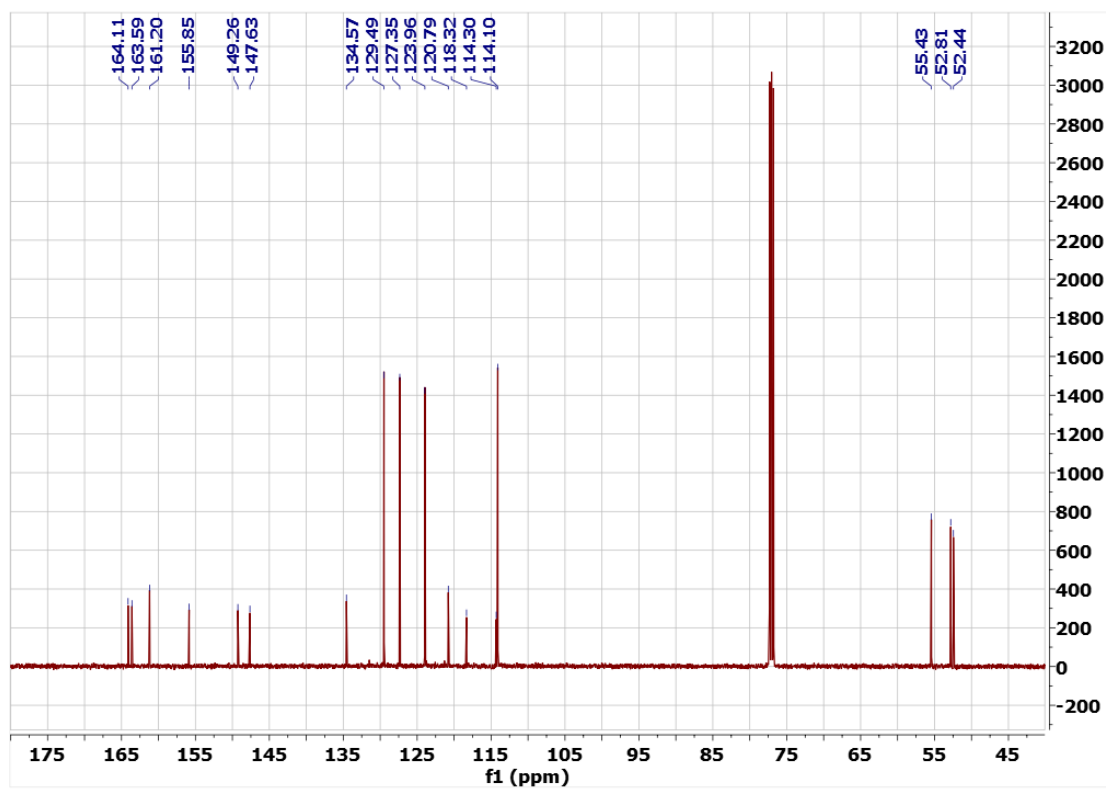
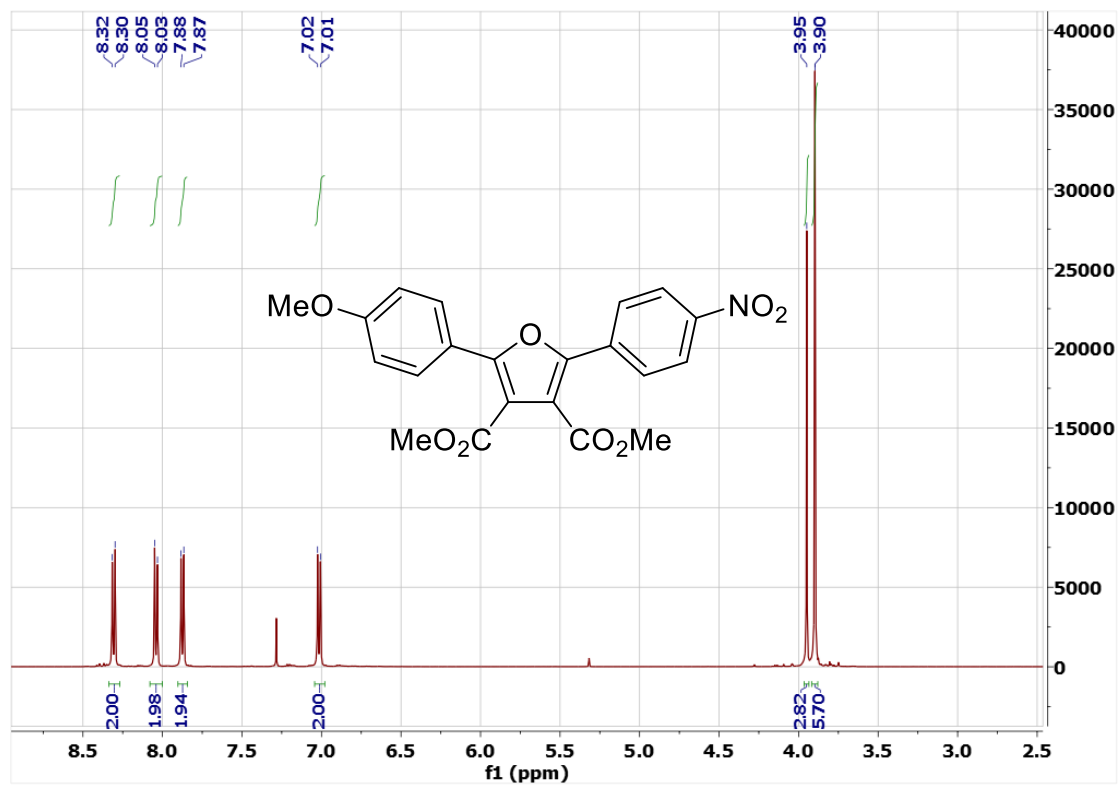
^1H and ^{13}C NMR Spectra of 3.5f (CDCl_3)



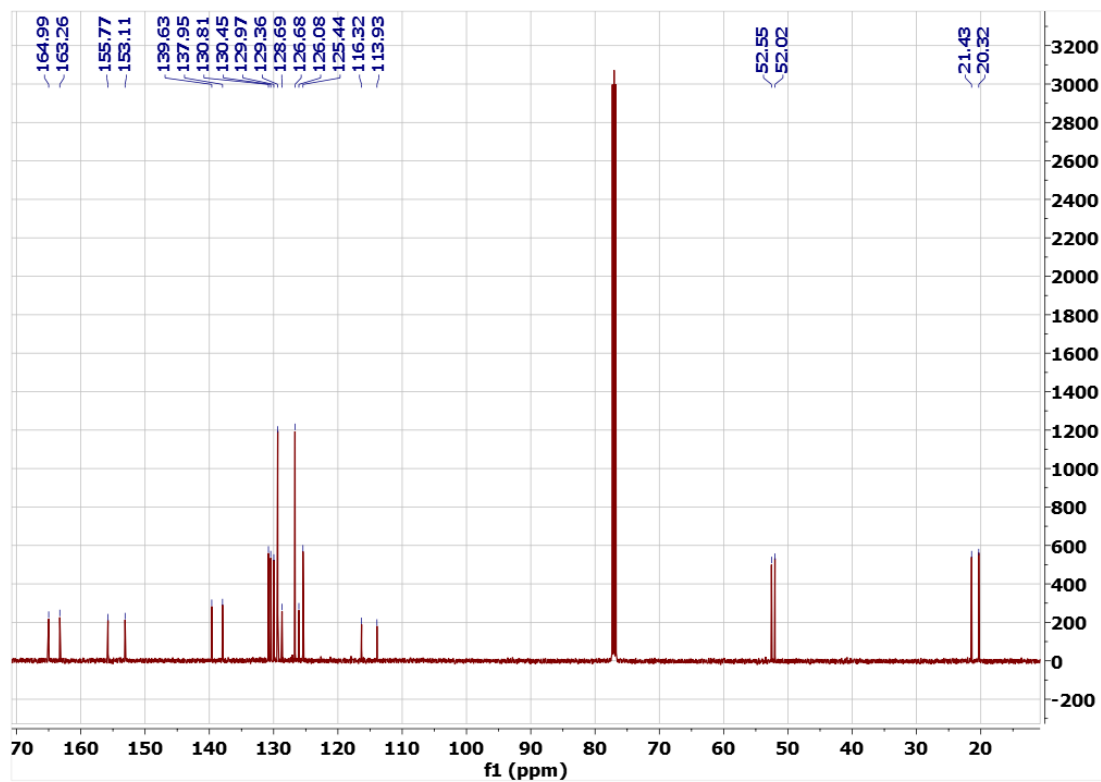
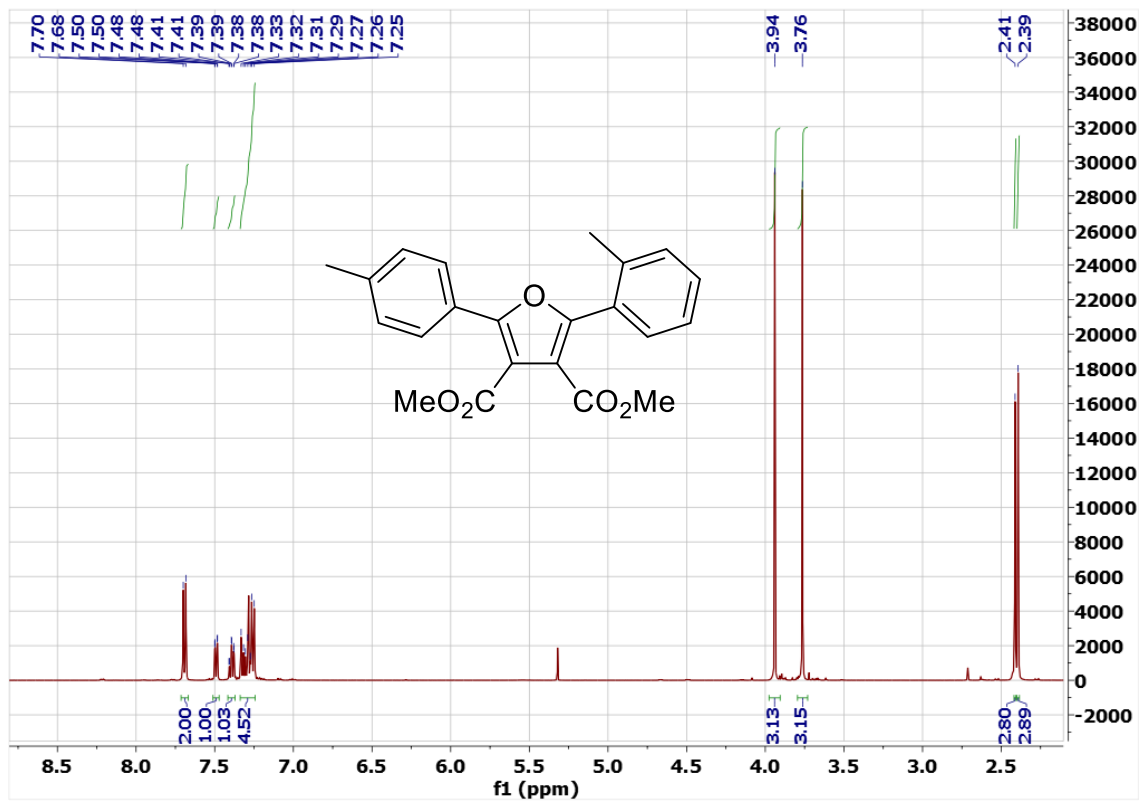
^1H and ^{13}C NMR Spectra of 3.5g (CDCl_3)



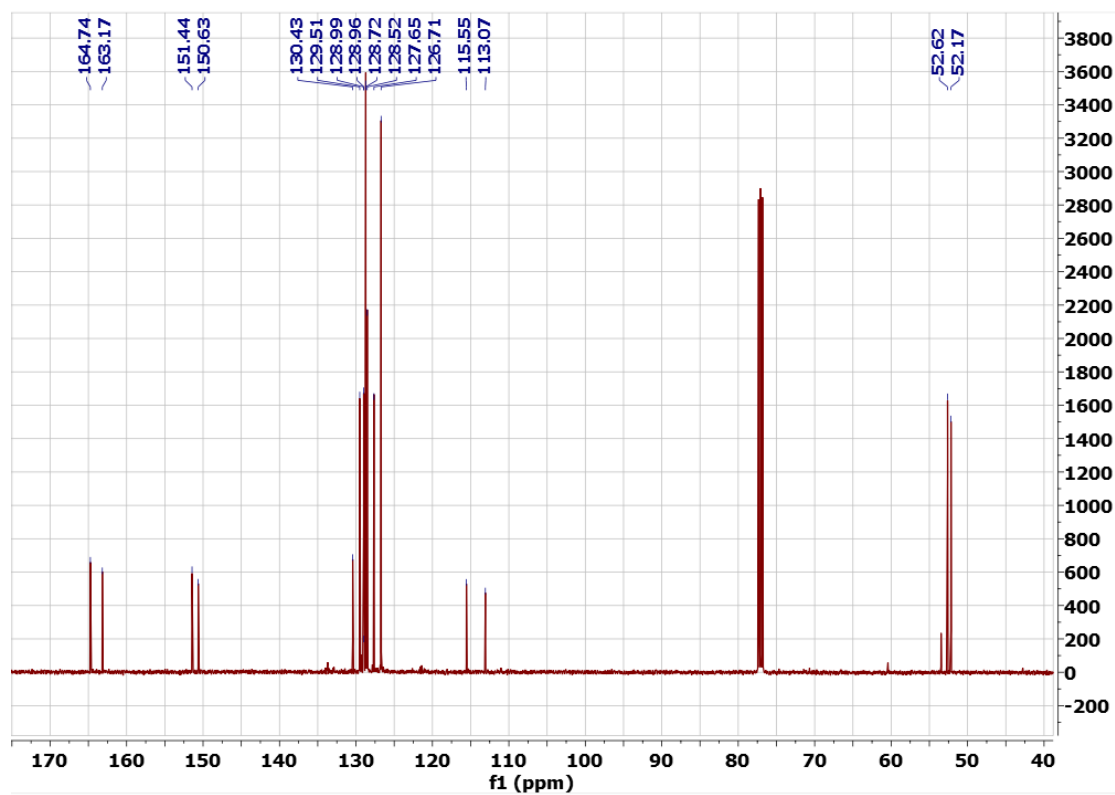
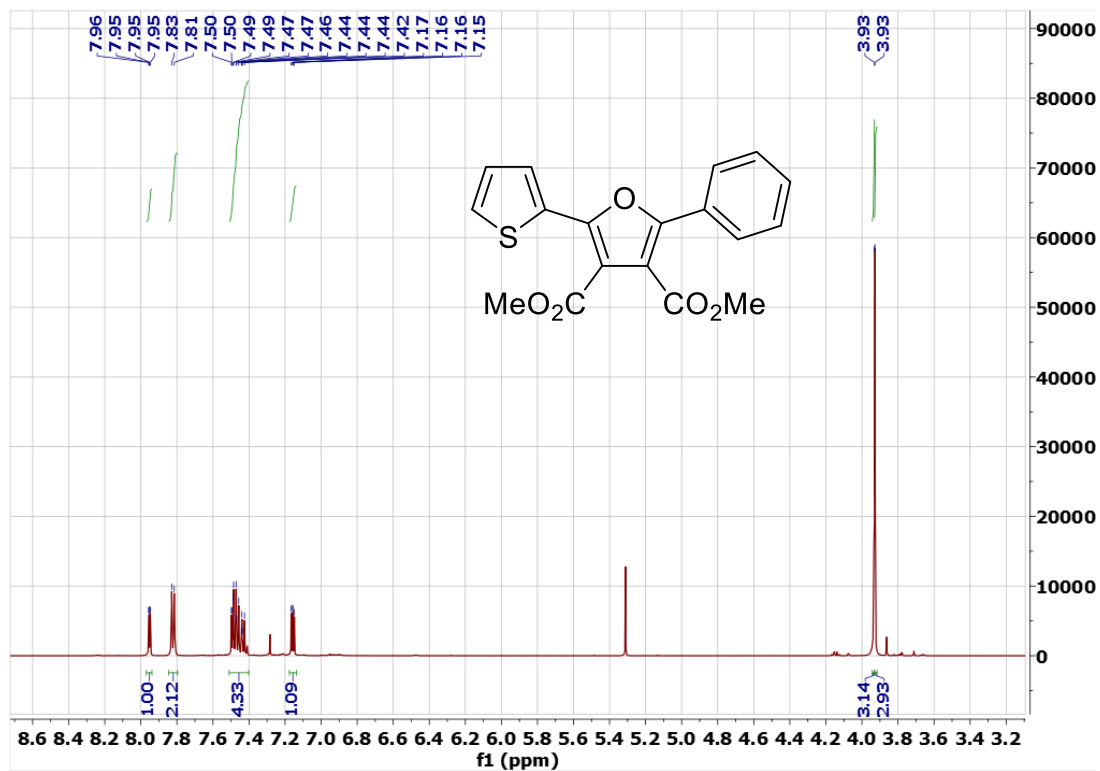
^1H and ^{13}C NMR Spectra of 3.5h (CDCl_3)



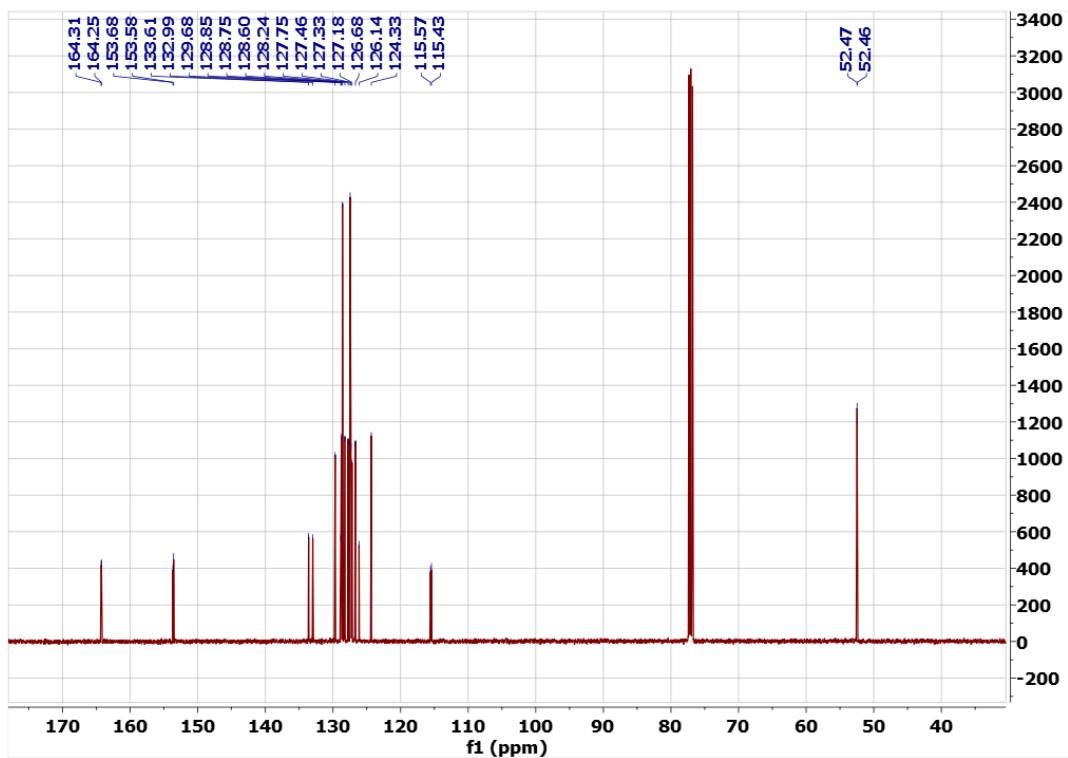
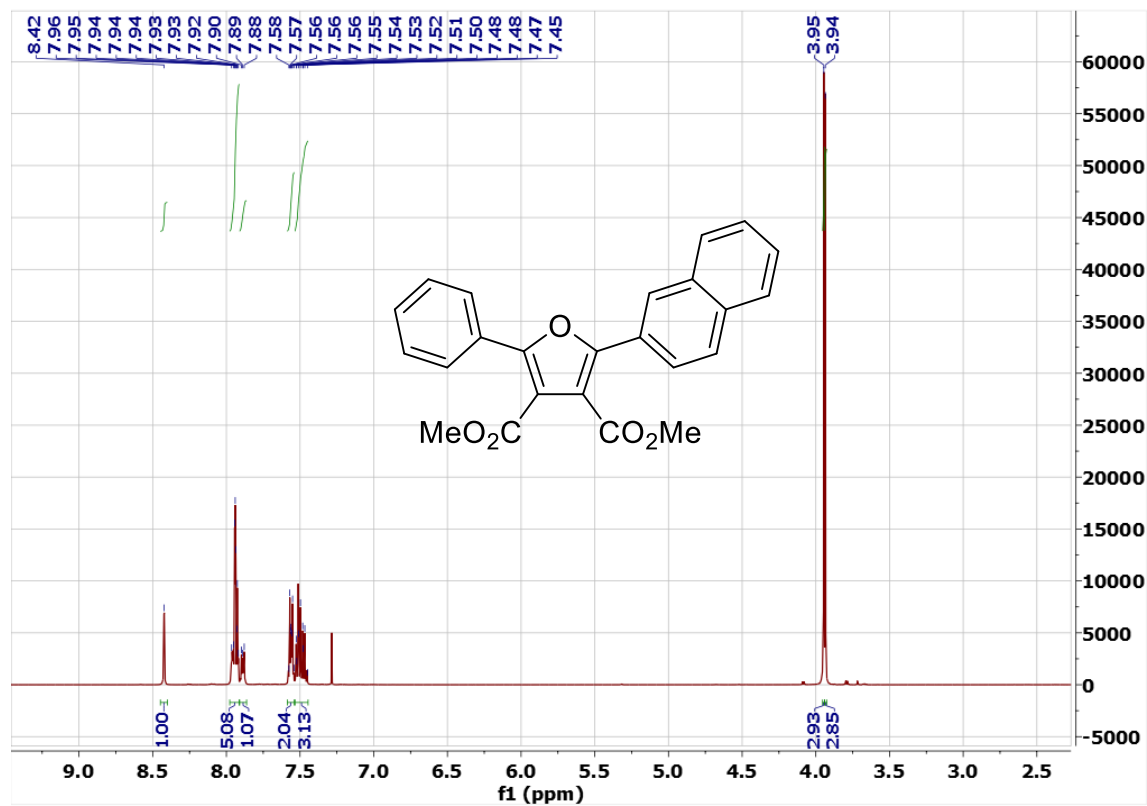
^1H and ^{13}C NMR Spectra of 3.5i (CDCl_3)



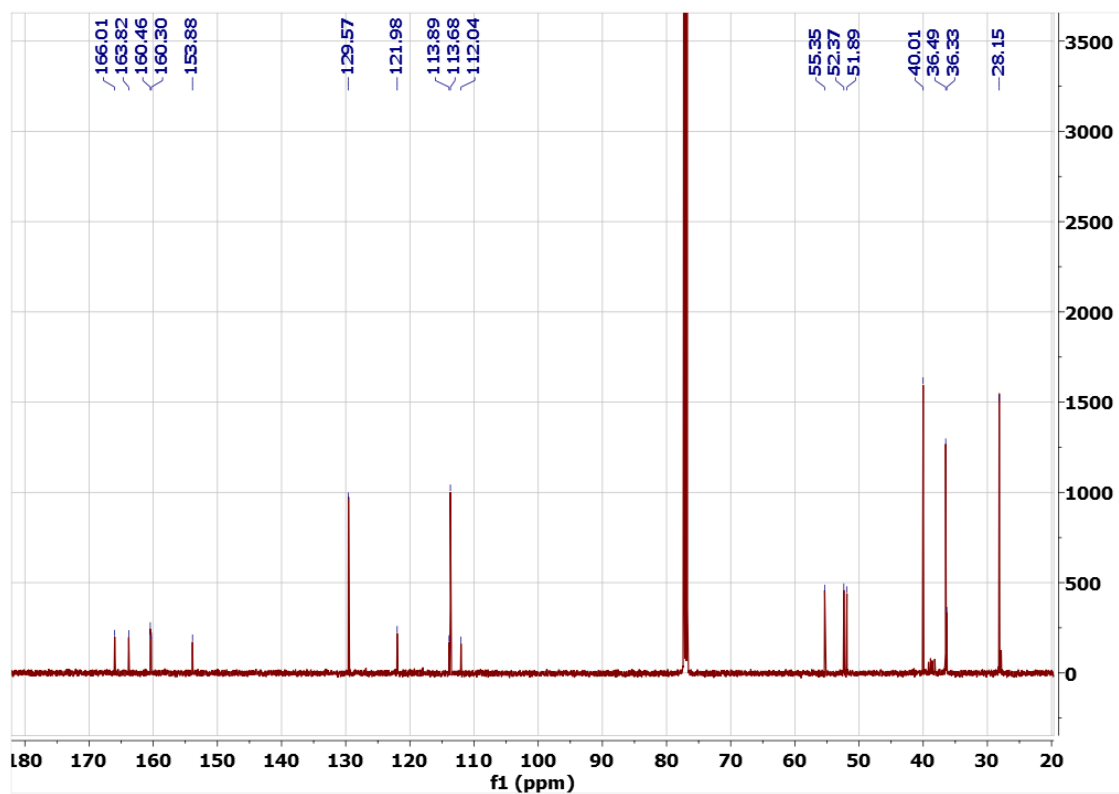
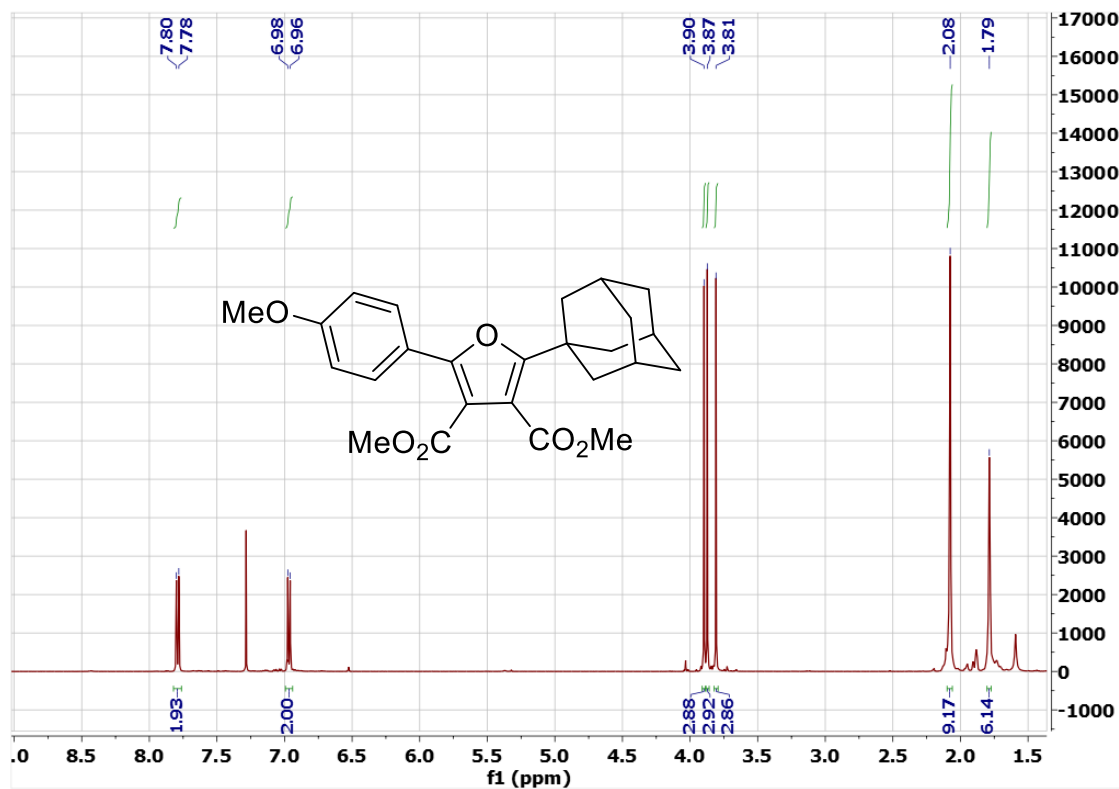
¹H and ¹³C NMR Spectra of 3.5j (CDCl₃)



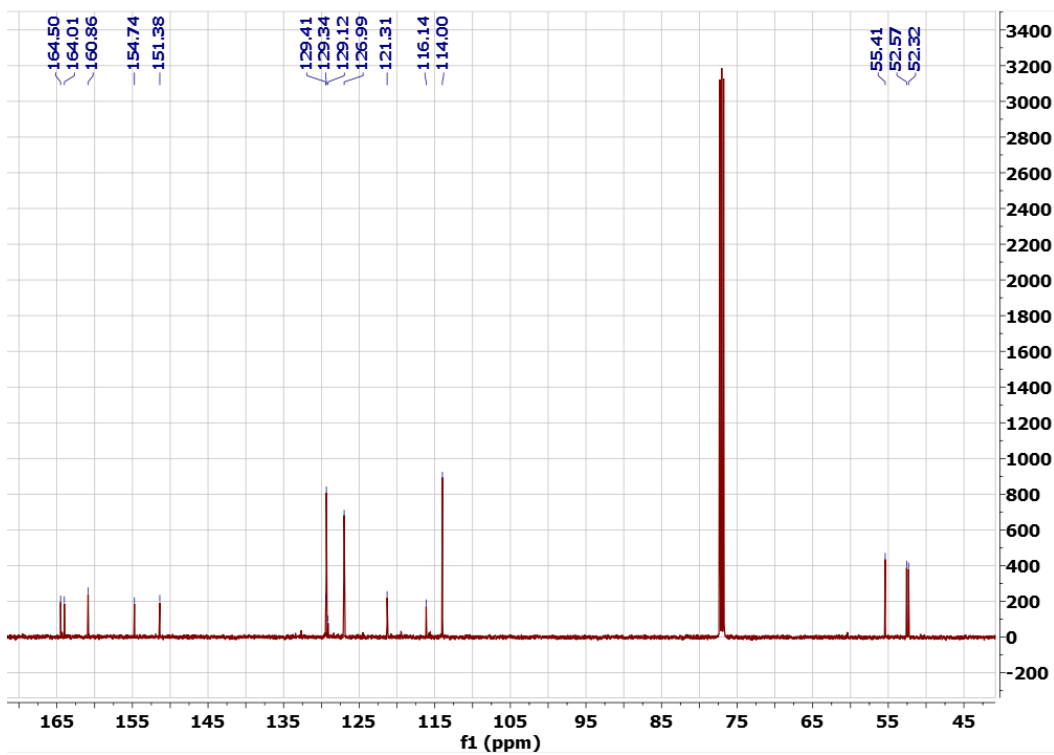
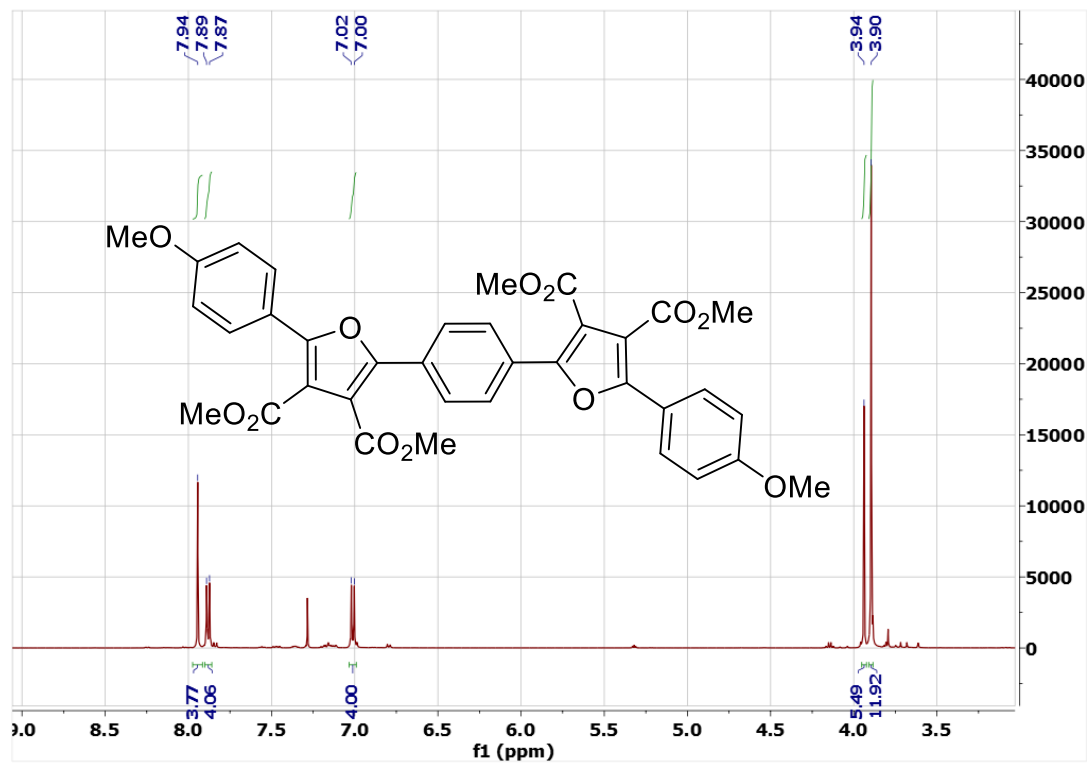
¹H and ¹³C NMR Spectra of 3.5k (CDCl₃)



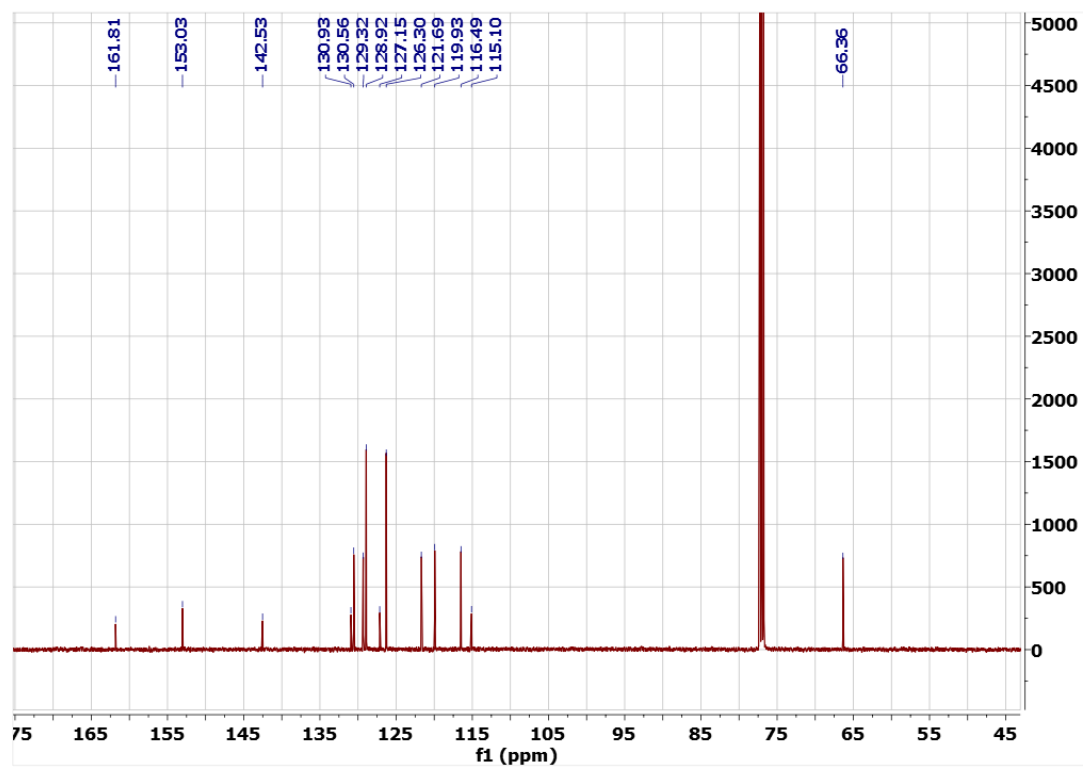
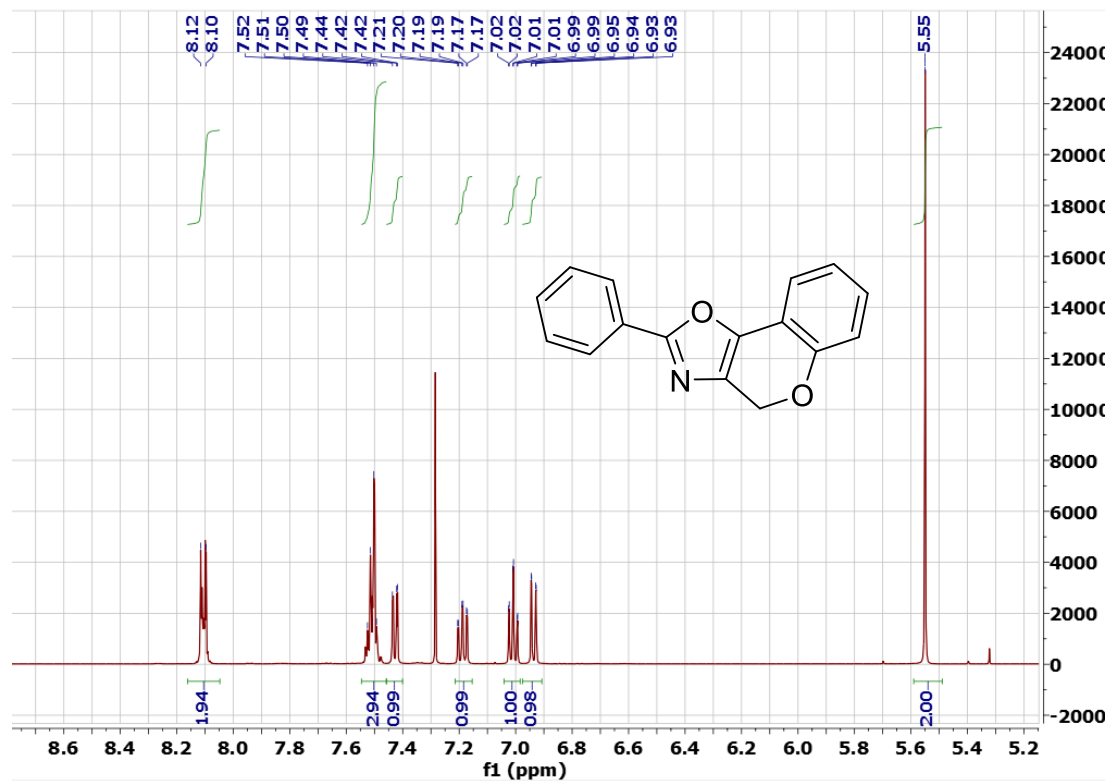
^1H and ^{13}C NMR Spectra of 3.5l (CDCl_3)



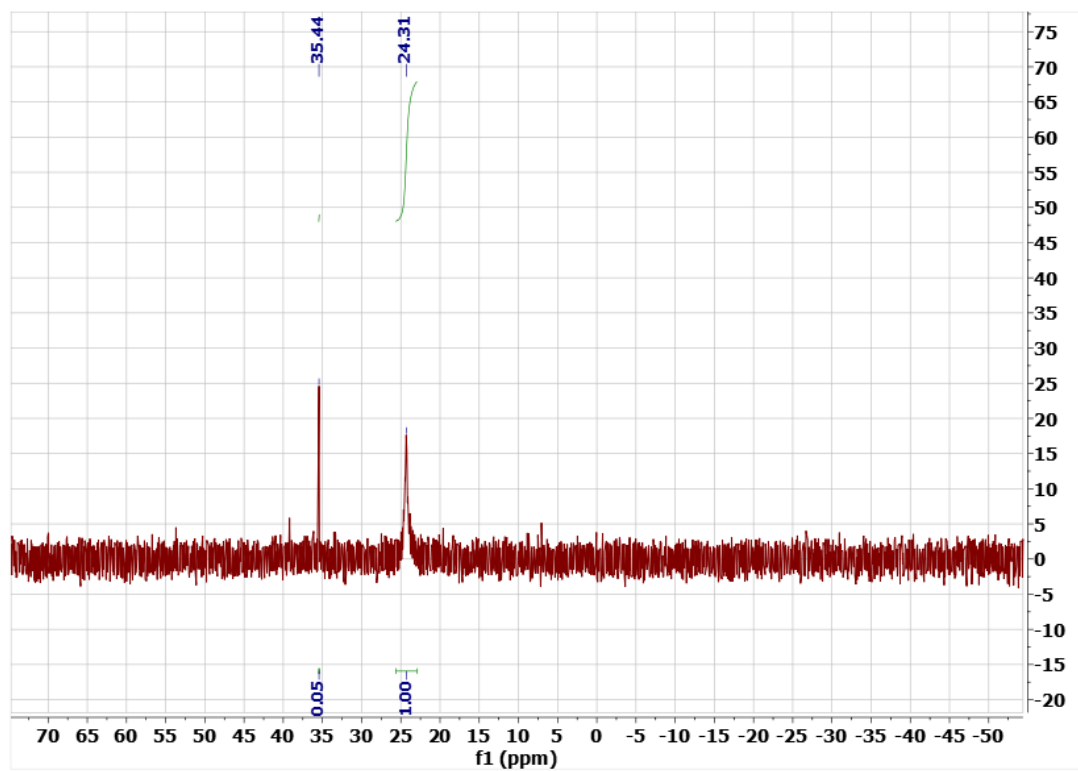
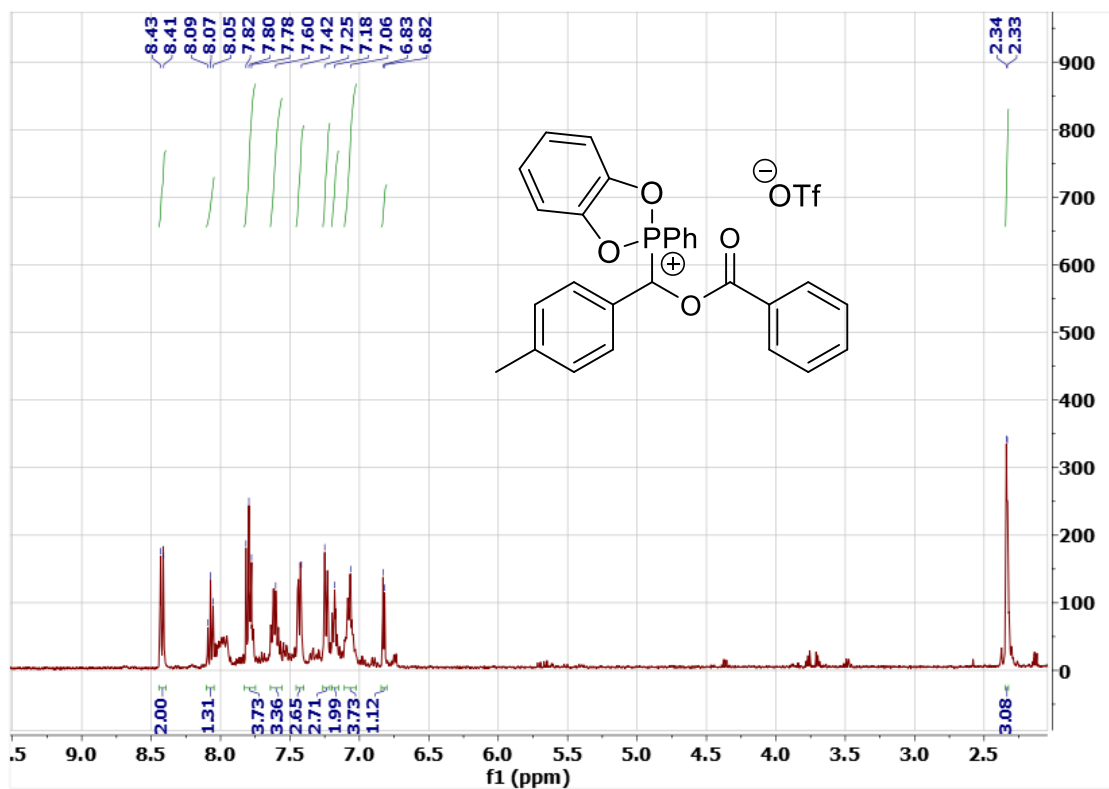
^1H and ^{13}C NMR Spectra of 3.5m (CDCl_3)



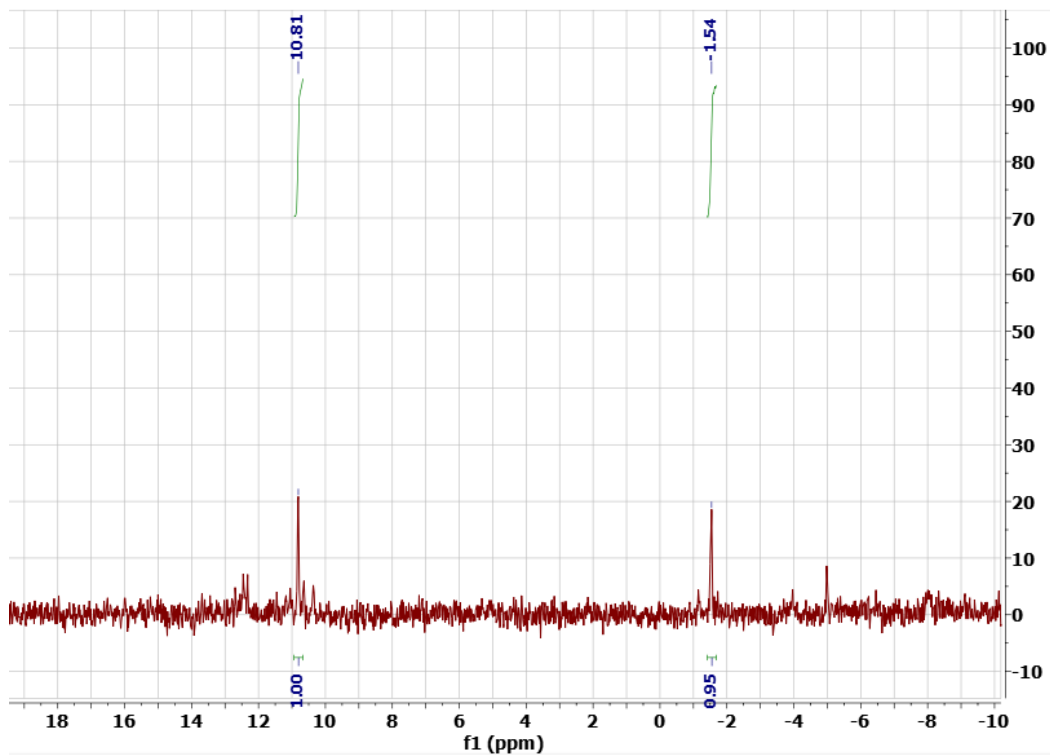
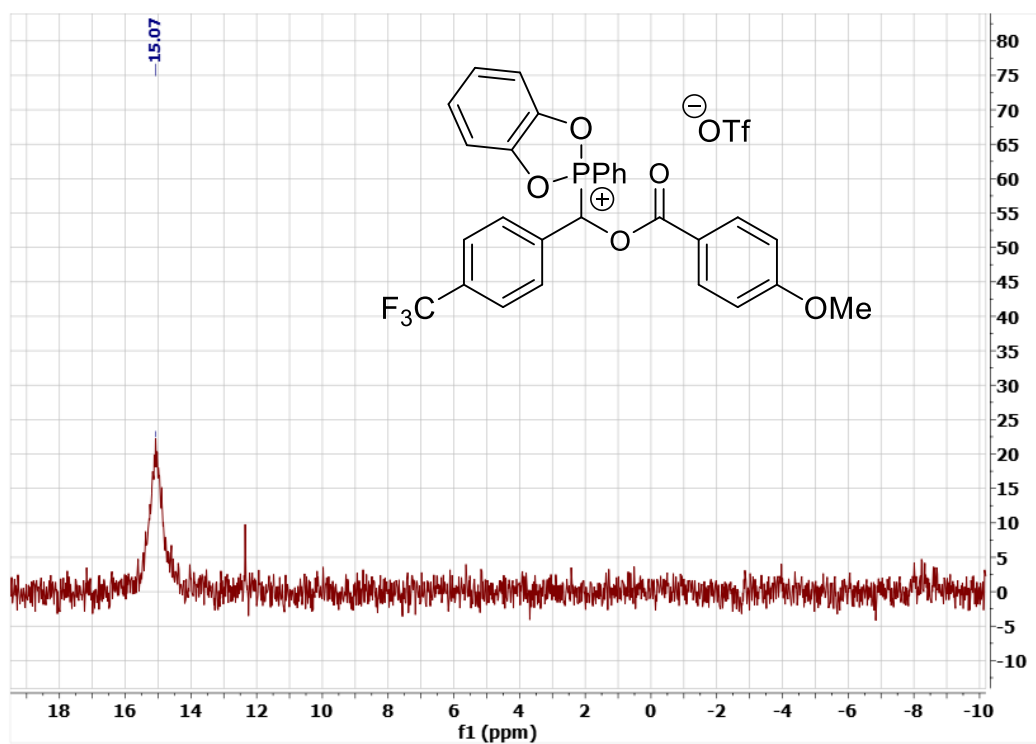
^1H and ^{13}C NMR Spectra of 3.5n (CDCl_3)



¹H and ³¹P NMR Spectra of 3.4a (CD₃CN)



^{31}P NMR Spectra of 3.4o before and after base addition (CD_3CN)



Appendix III

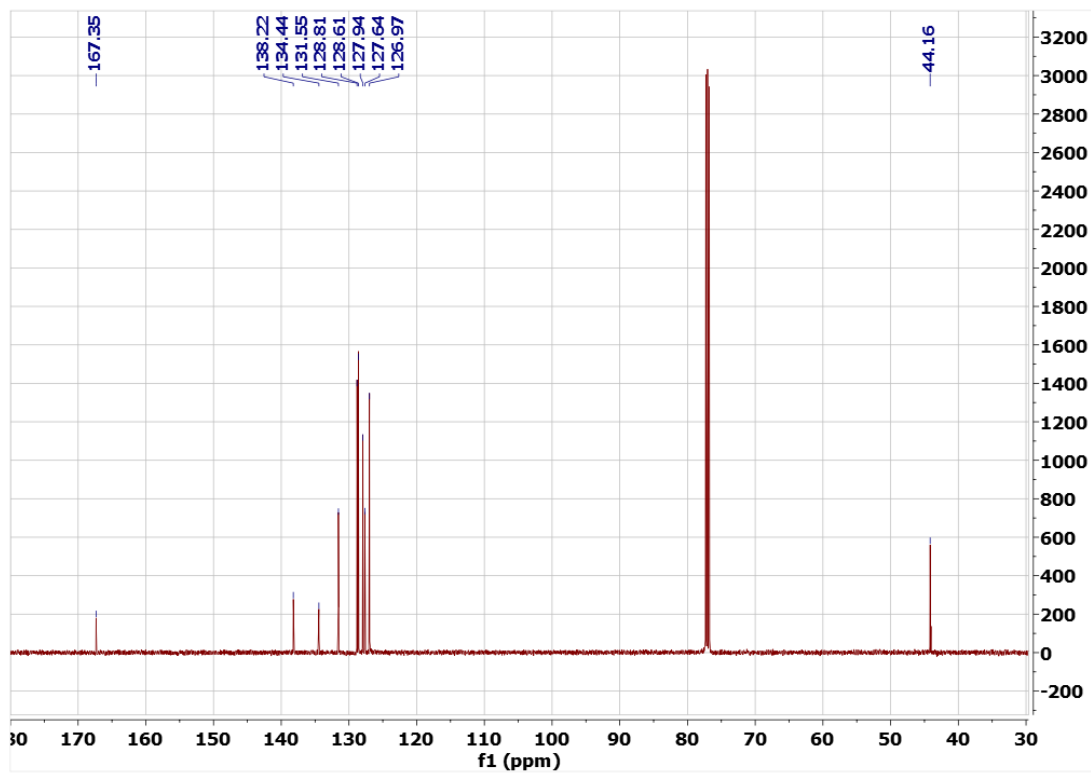
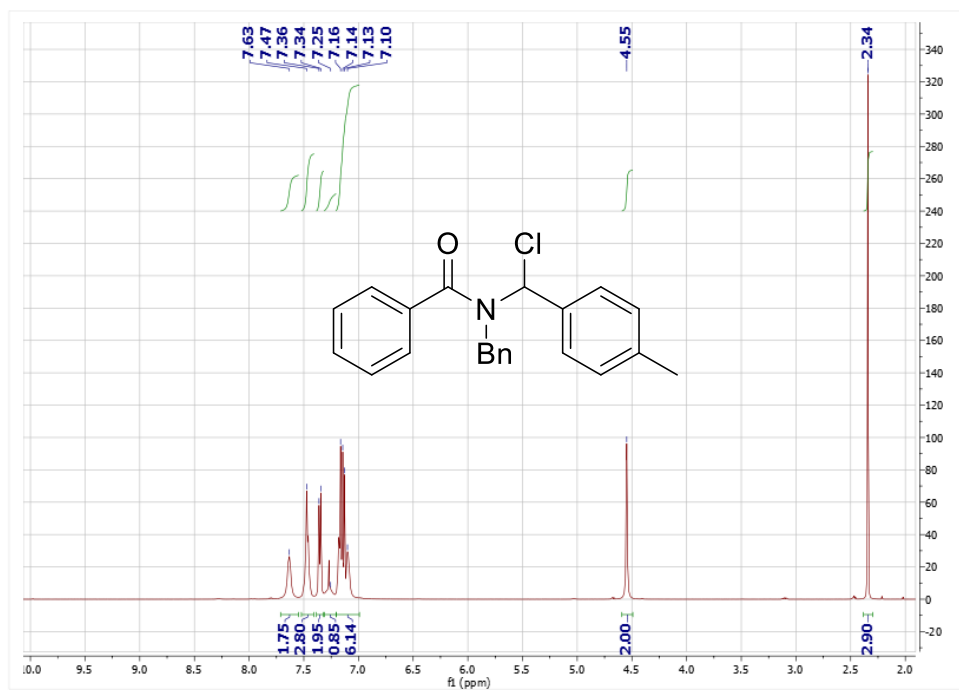
^1H , ^{13}C ^{19}F and 2D NMR spectroscopic data as proof of purity and regiochemistry, as well as crystallographic data for unpublished Chapter 4 is provided below.

Table of Contents

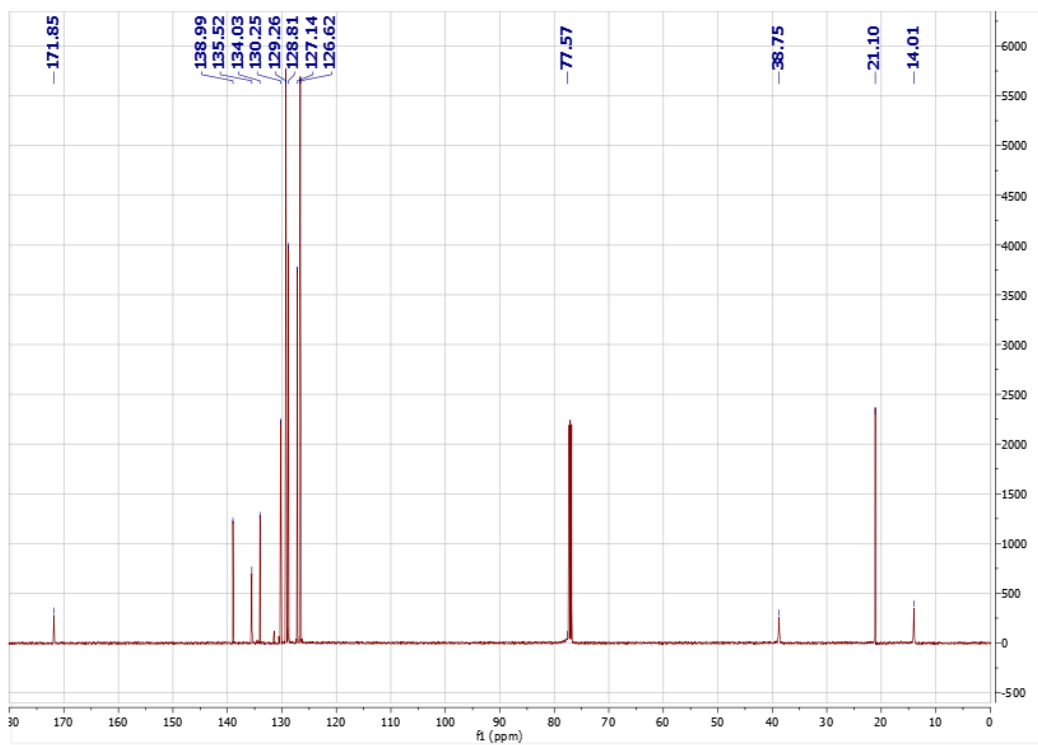
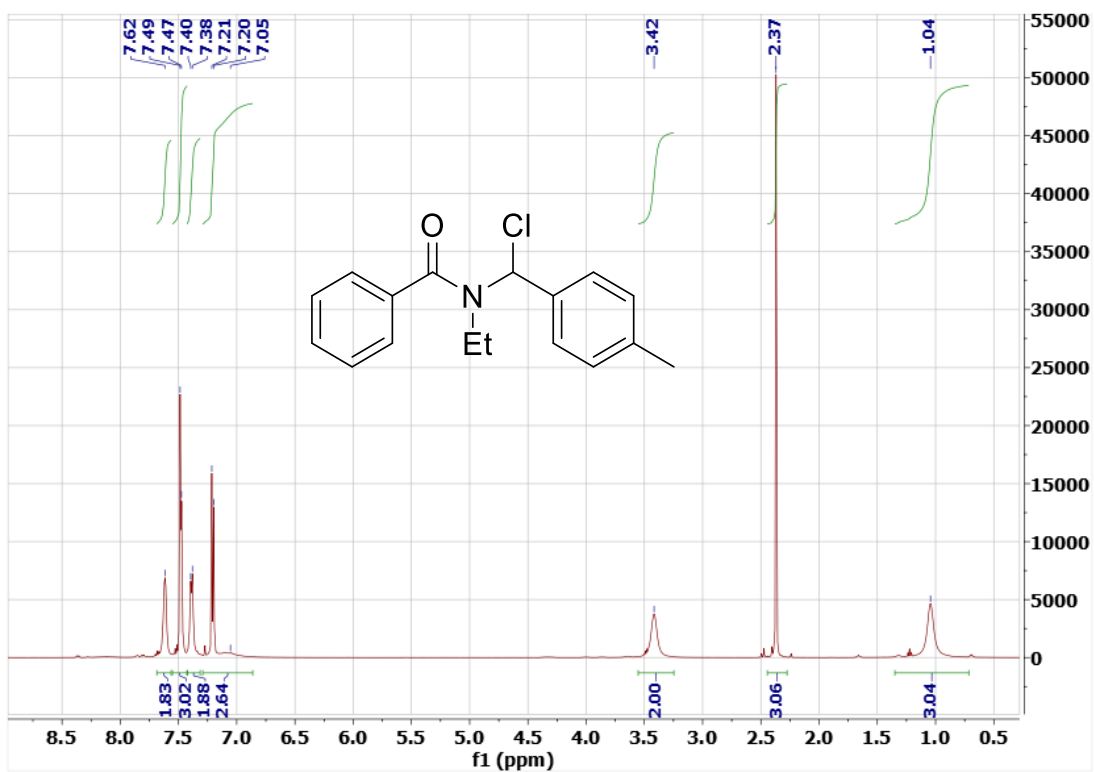
^1H and ^{13}C NMR Spectra of 4.3aa	24
^1H and ^{13}C NMR Spectra of 4.3ba	25
^1H and ^{13}C NMR Spectra of 4.3ca	26
^1H and ^{13}C NMR Spectra of 4.3da	27
^1H and ^{13}C NMR Spectra of 4.3ea	28
^1H and ^{13}C NMR Spectra of 4.3fa	29
^1H and ^{13}C NMR Spectra of 4.3ga	30
^1H and ^{13}C NMR Spectra of 4.3ha	31
^1H , ^{13}C and ^{19}F NMR Spectra of 4.3ia	32
^1H and ^{13}C NMR Spectra of 4.3ja	34
^1H and ^{13}C NMR Spectra of 4.3ka	35
^1H and ^{13}C NMR Spectra of 4.3ab	36
^1H , ^{13}C and ^{19}F NMR Spectra of 4.3ac	37
^1H and ^{13}C NMR Spectra of 4.3ad	39
^1H and ^{13}C NMR Spectra of 4.3ae	40
^1H and ^{13}C NMR Spectra of 4.3aa-Br	41
^1H and ^{13}C NMR Spectra of 4.3aa-I	42
^1H and ^{13}C NMR Spectra of 4.3ee	43
^1H and ^{13}C NMR Spectra of 4.3la	44
^1H , ^{13}C and ^{19}F NMR Spectra of 4.3ie	45
^1H , ^{13}C and ^{19}F NMR Spectra of 4.3ma	47
^1H , ^{13}C and ^{19}F NMR Spectra of 4.3me	49
^1H and ^{13}C NMR Spectra of 4.4aa	51

^1H and ^{13}C NMR Spectra of 4.5aa	52
^1H and ^{13}C NMR Spectra of 4.6a	53
^1H and ^{13}C NMR Spectra of 4.8	54
^1H and ^{13}C NMR Spectra of 4.9a	55
^1H and ^{13}C NMR Spectra of 4.9b	56
^1H and ^{13}C NMR Spectra of 4.9c	57
^1H and ^{13}C NMR Spectra of 4.9d	58
^1H and ^{13}C NMR Spectra of 4.9e	59
^1H and ^{13}C NMR Spectra of 4.9f	60
^1H and ^{13}C NMR Spectra of 4.9g	61
^1H NMR Spectra of 4.7-4.7' mixture	62
2D-NOE Spectra of 4.7'	63
X-Ray crystallography data for 4.9b	64

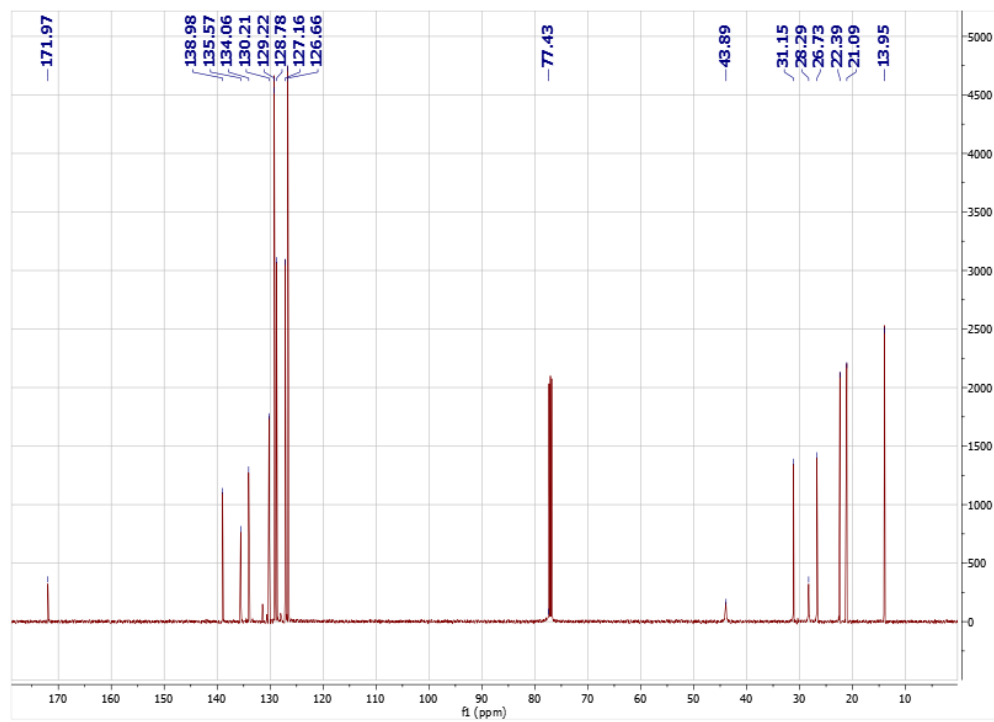
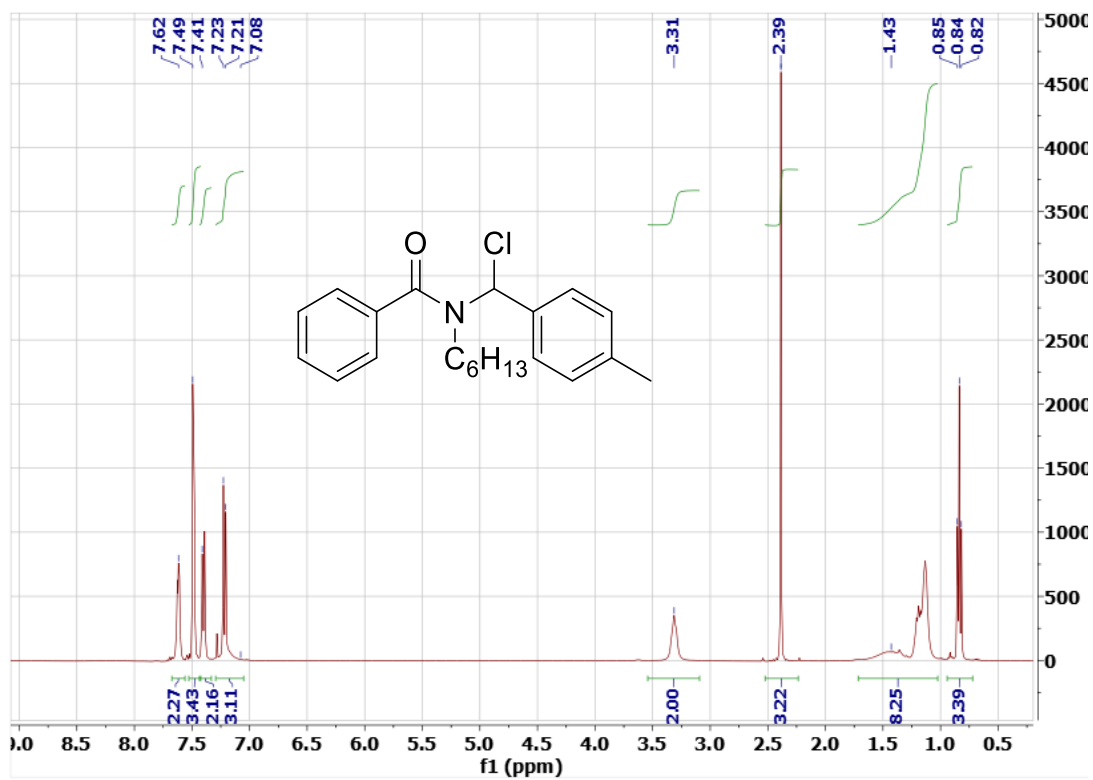
^1H and ^{13}C NMR Spectra of 4. 3aa (CDCl_3) at 5°C



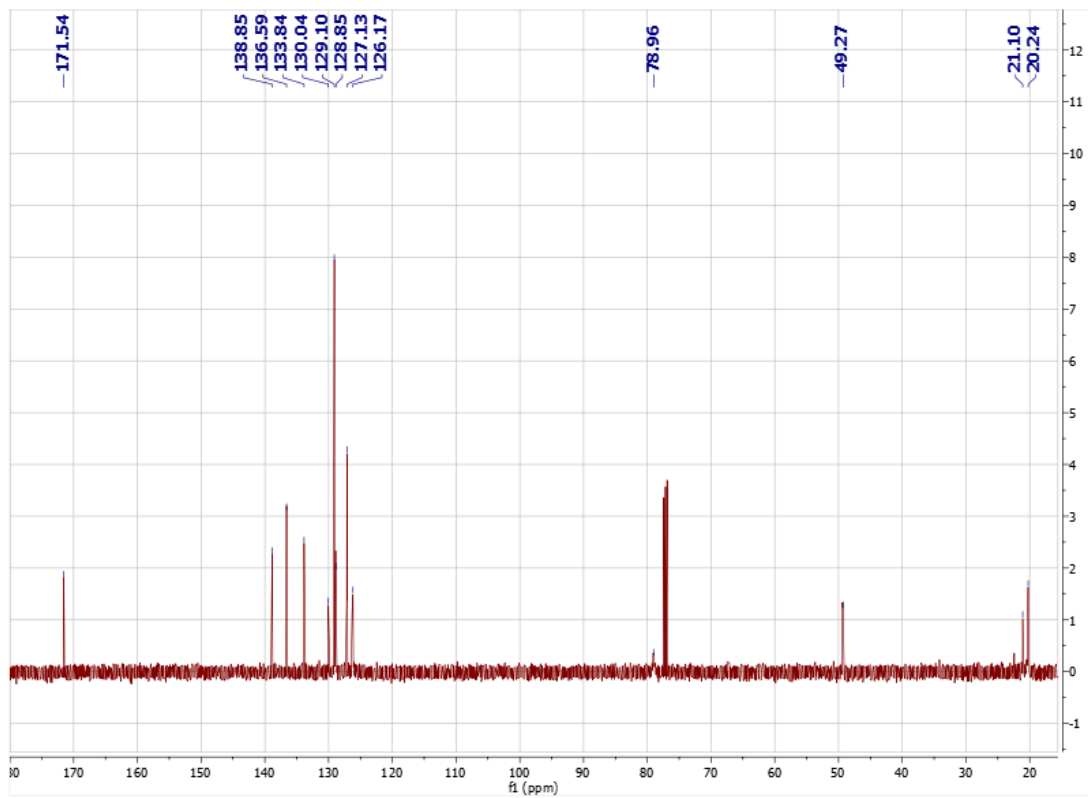
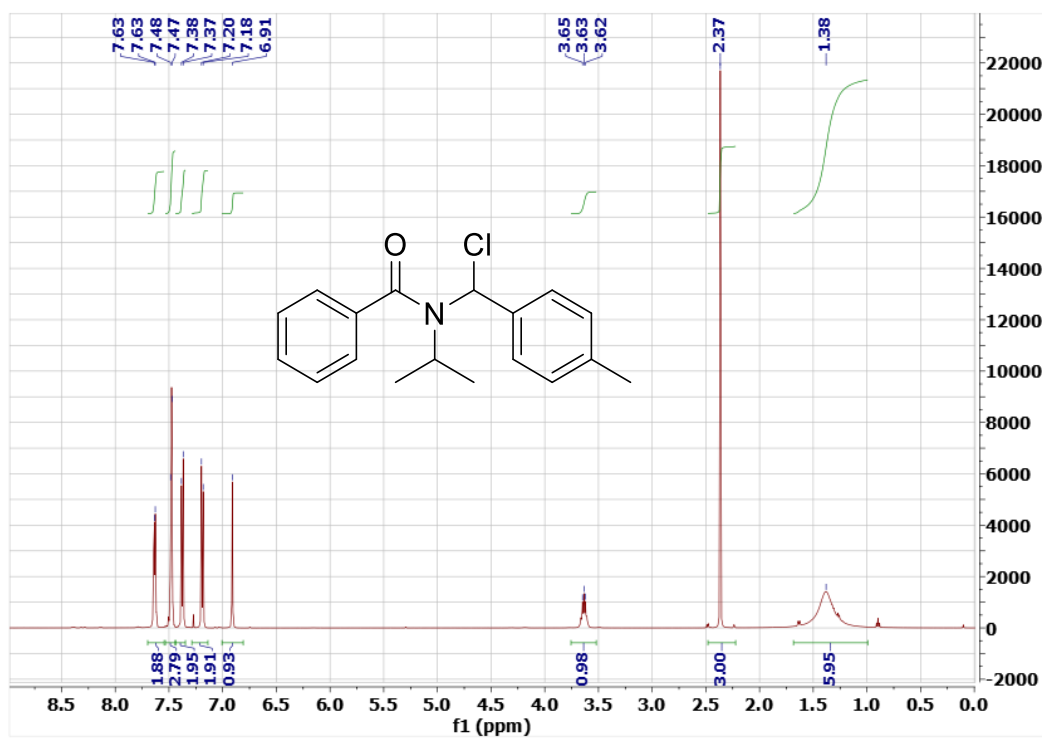
^1H and ^{13}C NMR Spectra of 4.3ba (CDCl_3) at 5°C



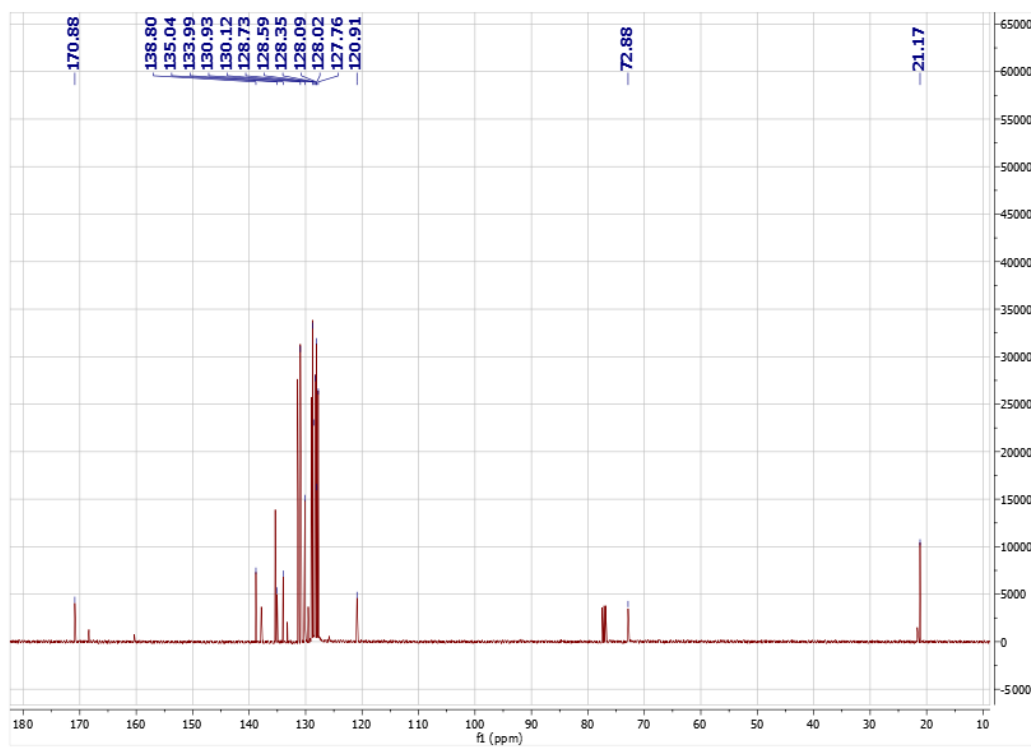
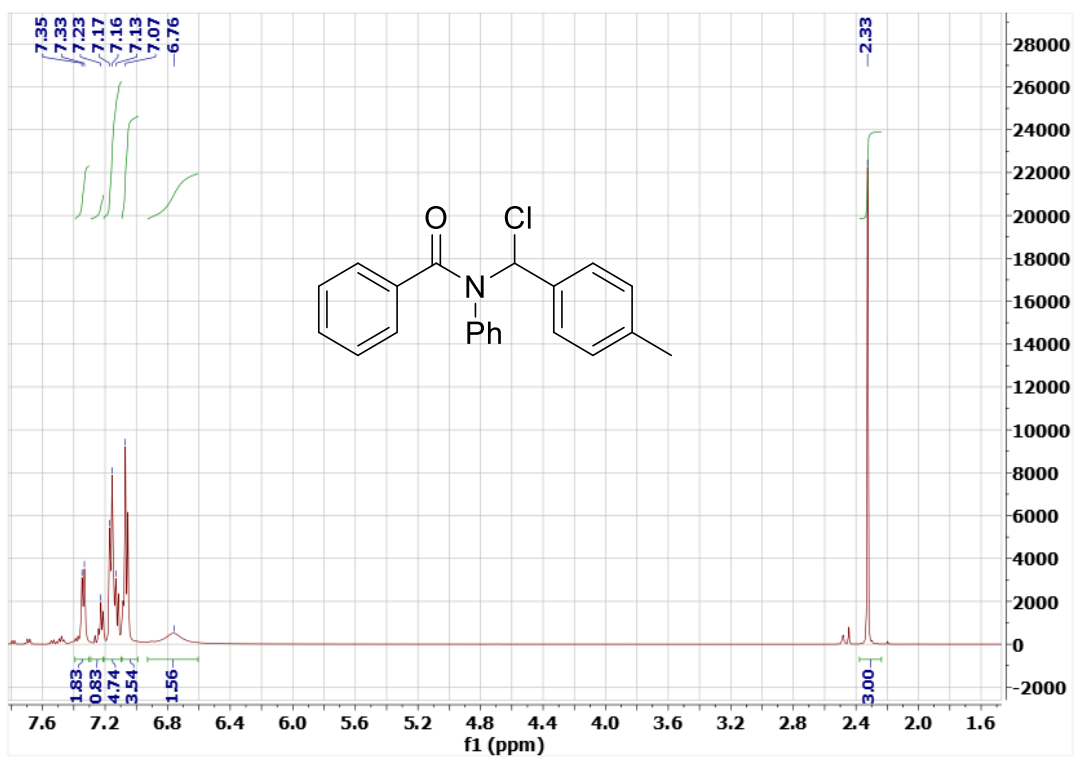
^1H and ^{13}C NMR Spectra of 4.3ca (CDCl_3) at 5°C



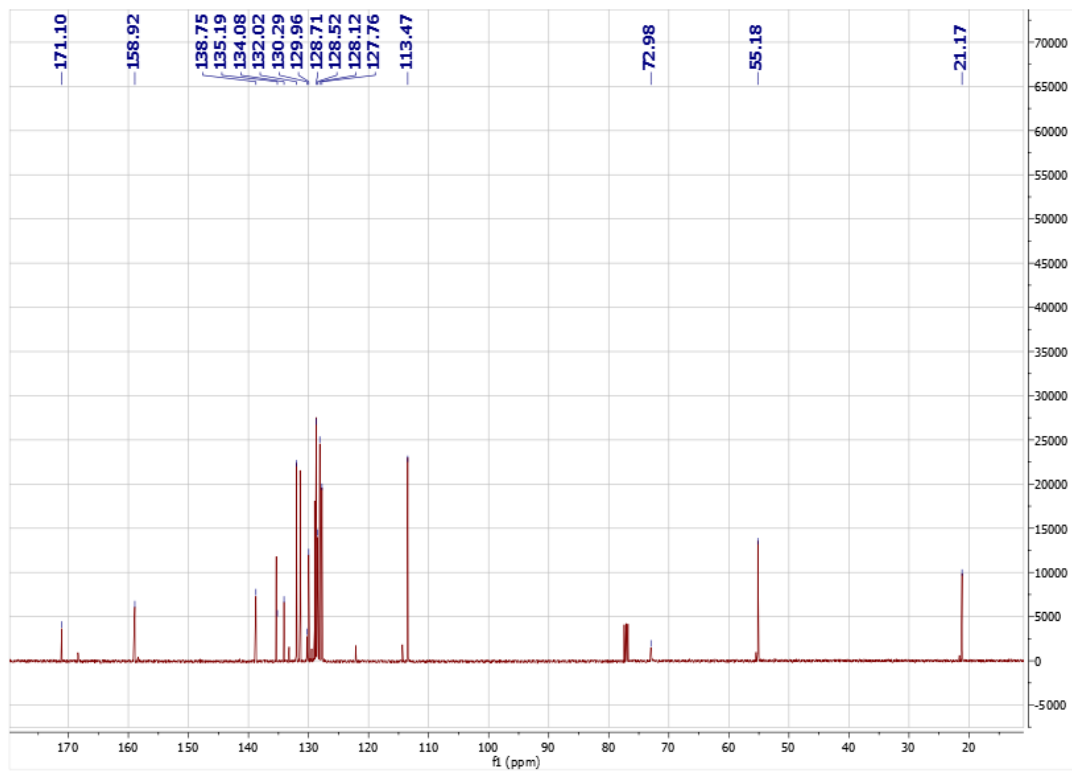
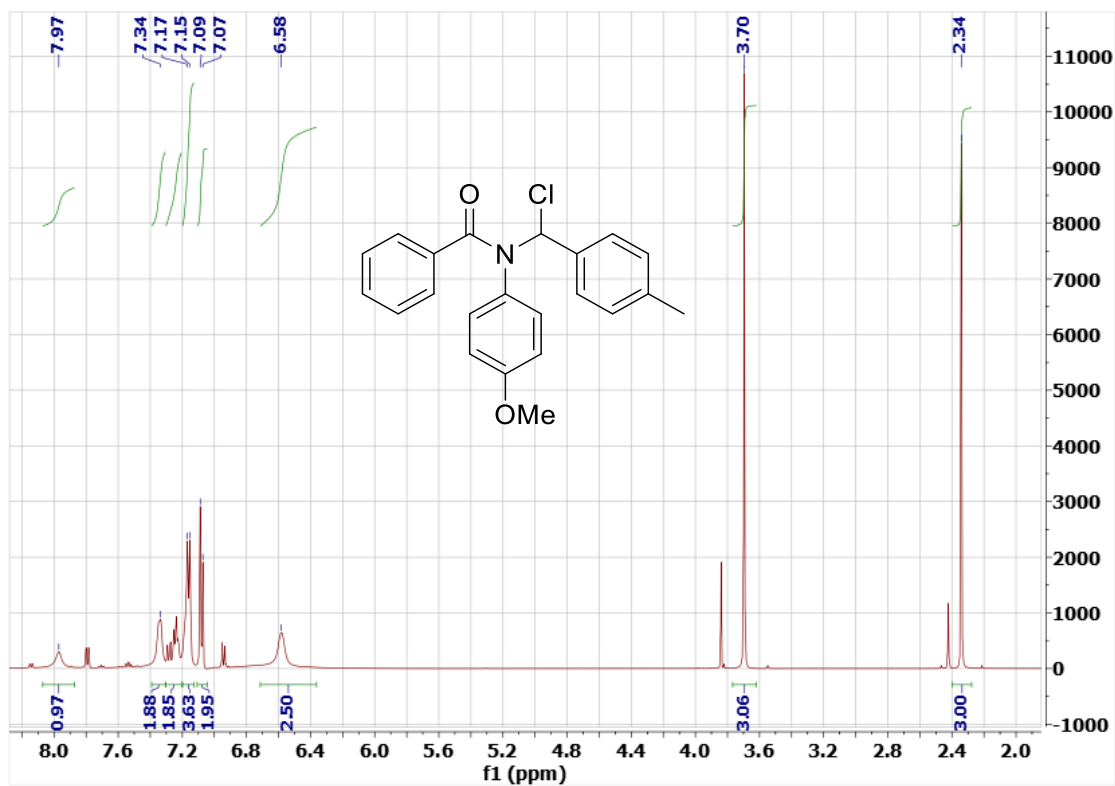
^1H and ^{13}C NMR Spectra of 4.3da (CDCl_3) at 5°C



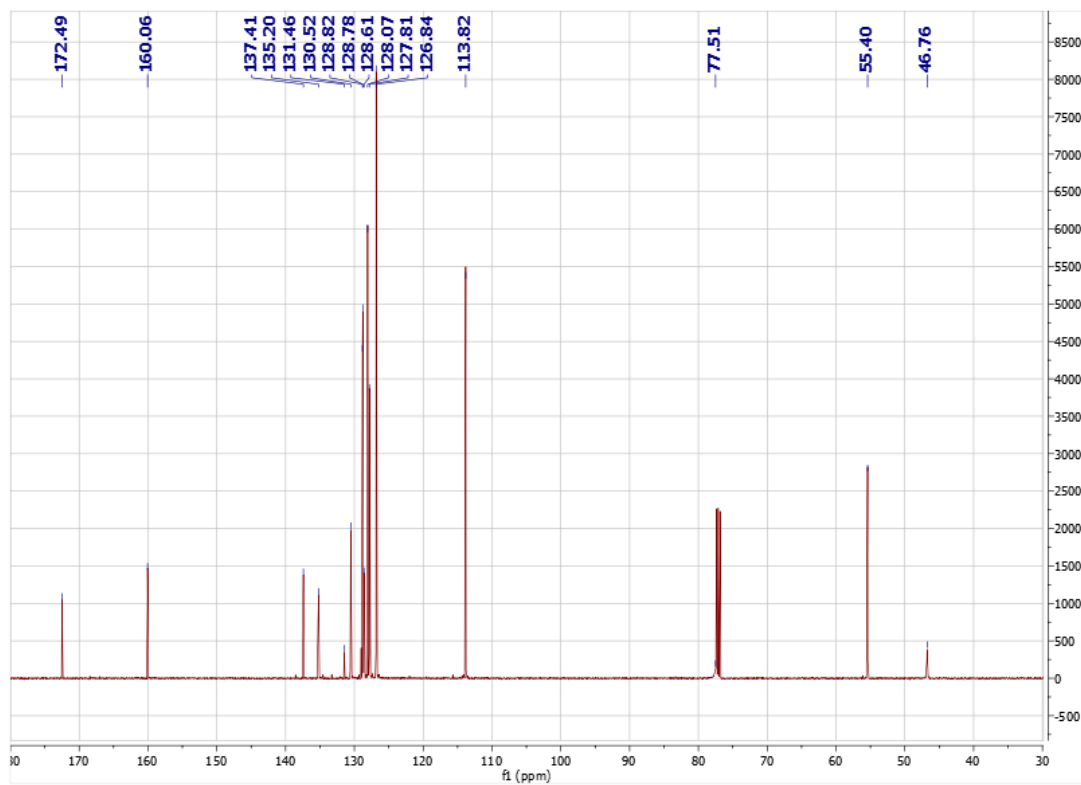
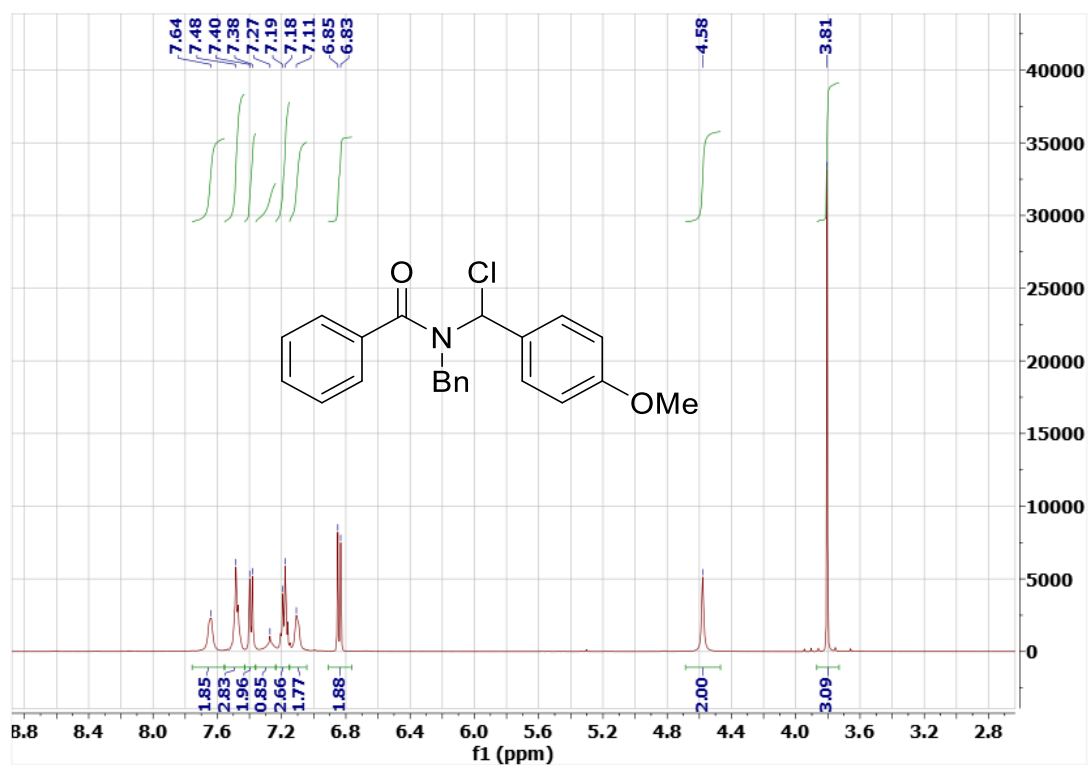
¹H and ¹³C NMR Spectra of 4.3ea (CDCl₃) at 5°C



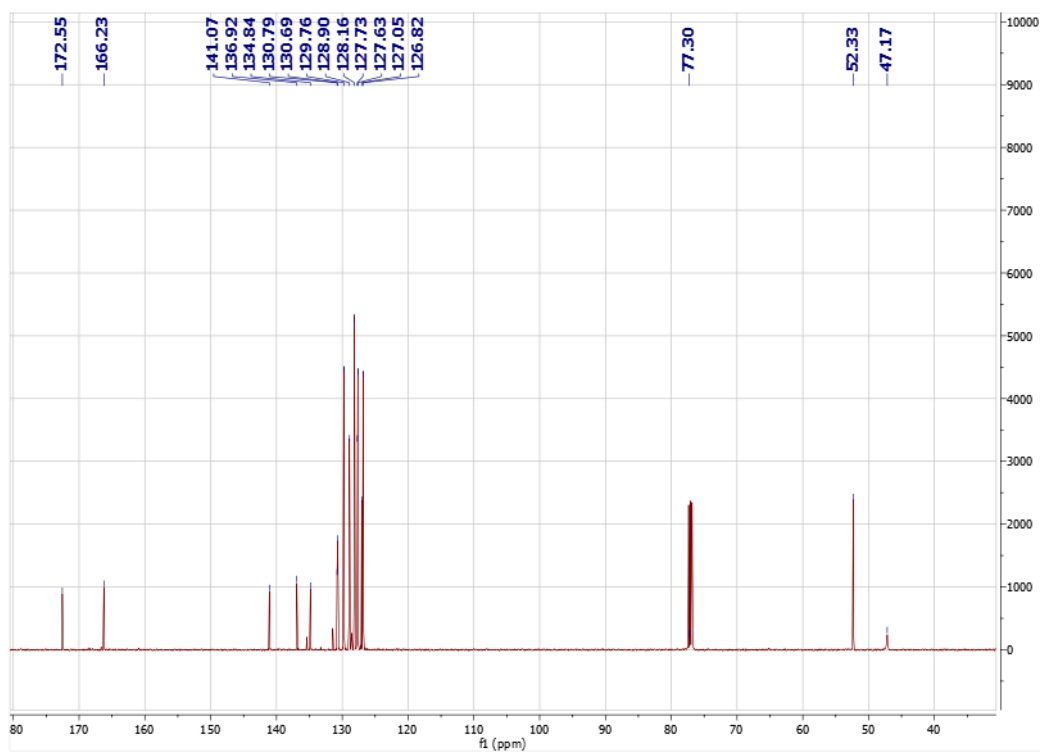
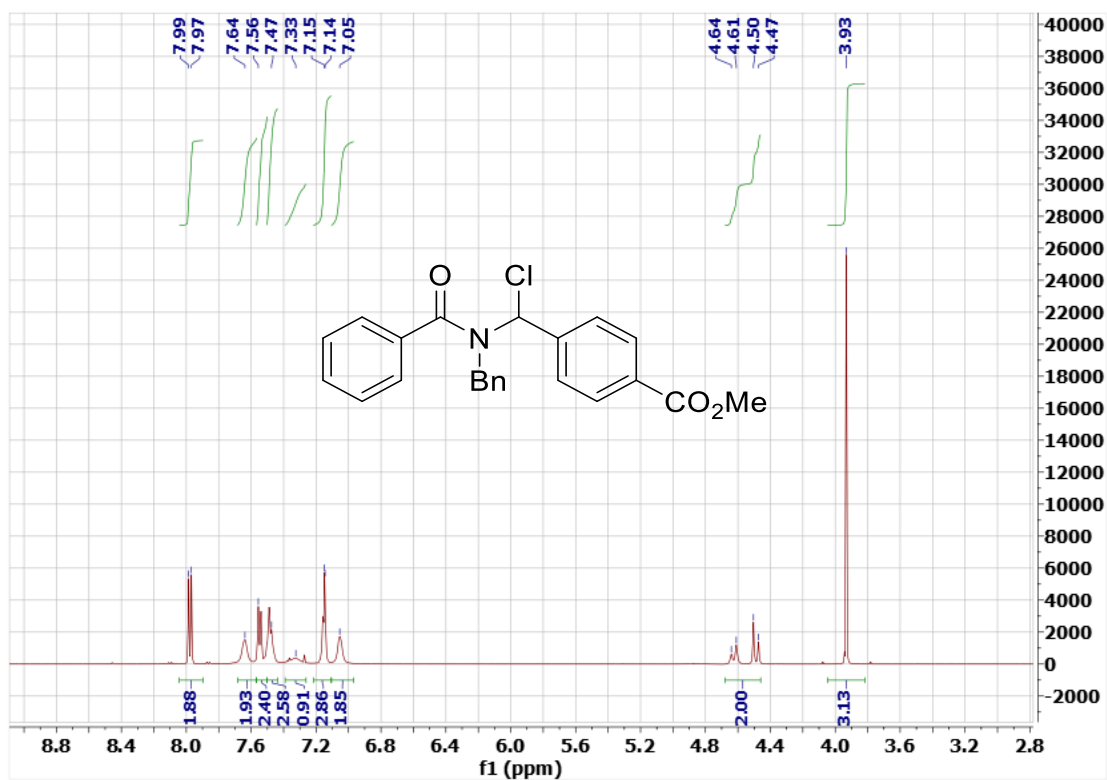
^1H and ^{13}C NMR Spectra of 4.3fa (CDCl_3) at 5°C



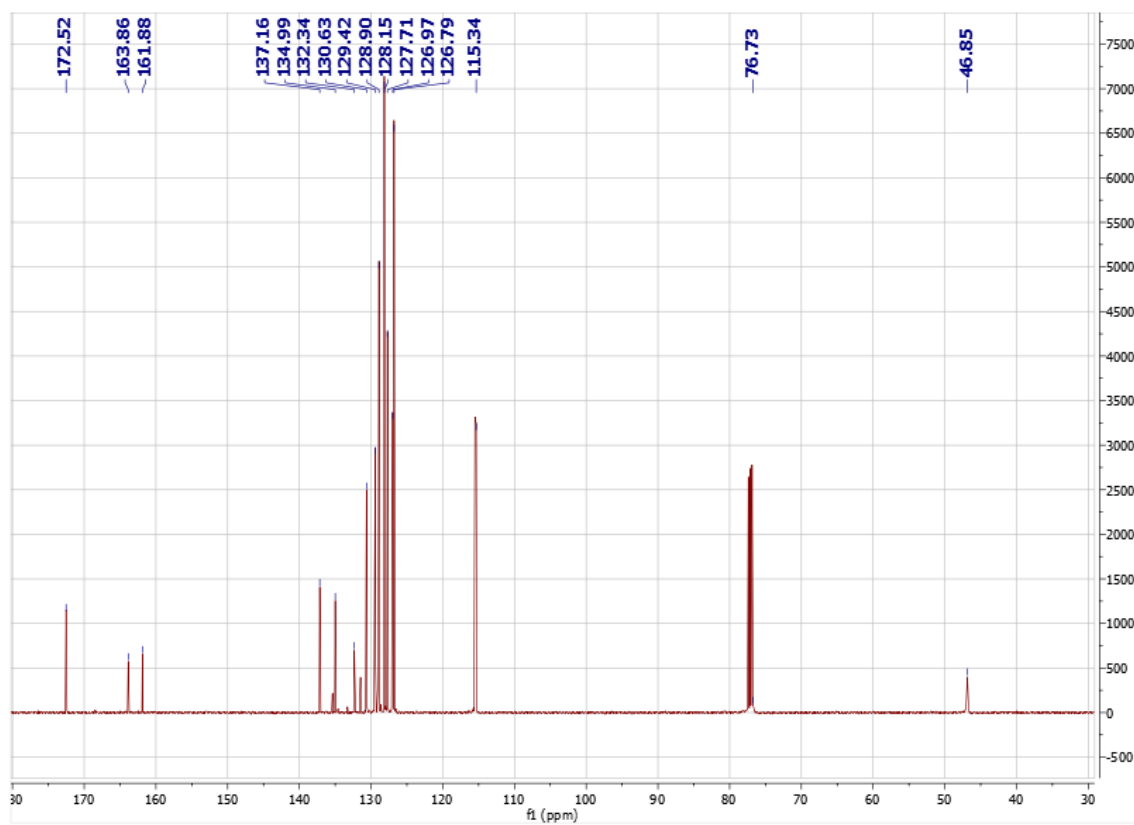
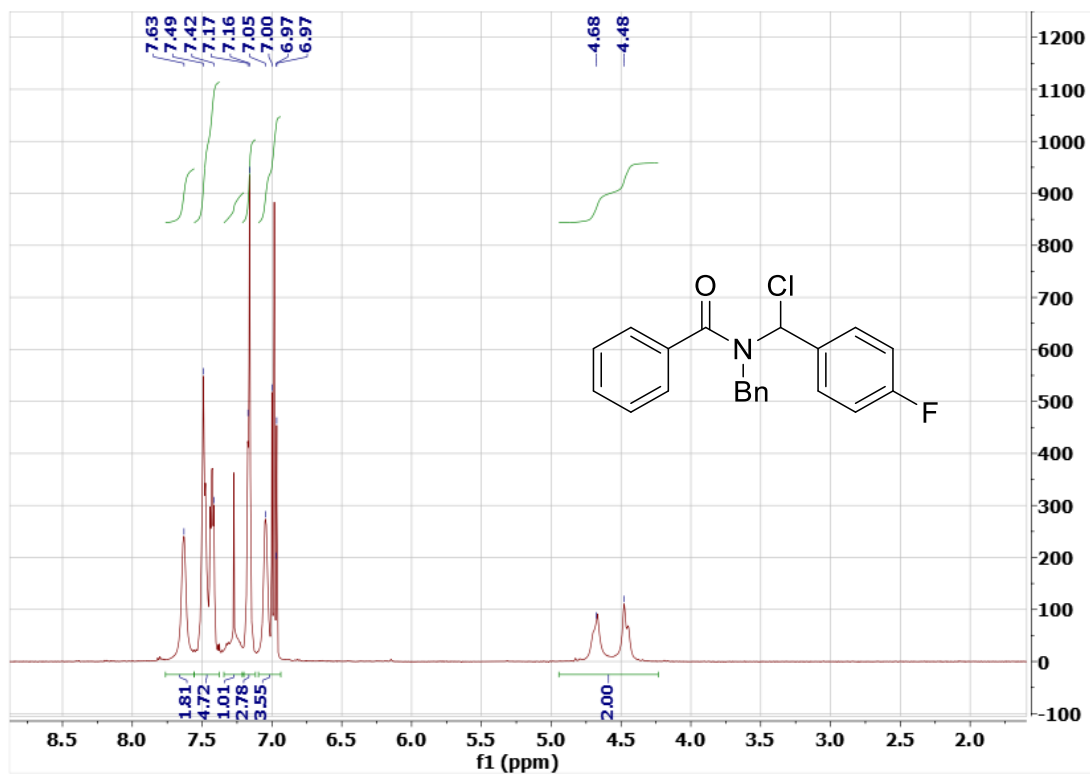
¹H and ¹³C NMR Spectra of 4.3ga (CDCl₃) at 5°C

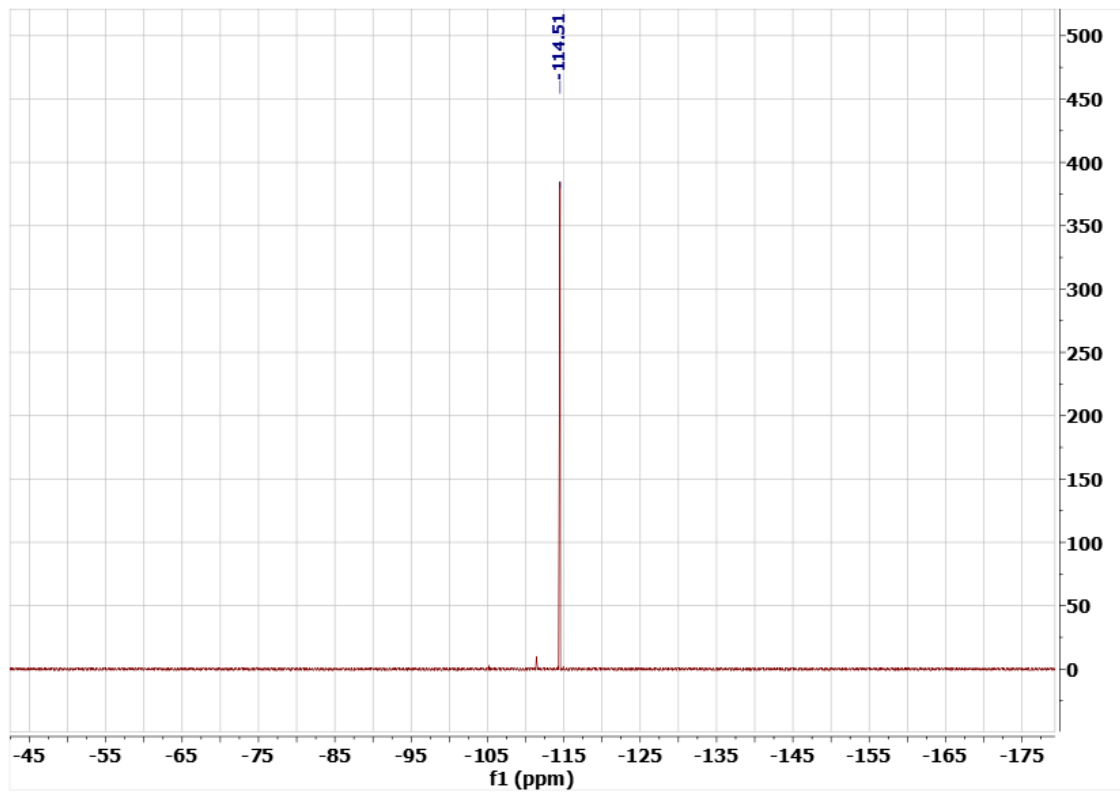


¹H and ¹³C NMR Spectra of 4.3ha (CDCl₃) at 5°C

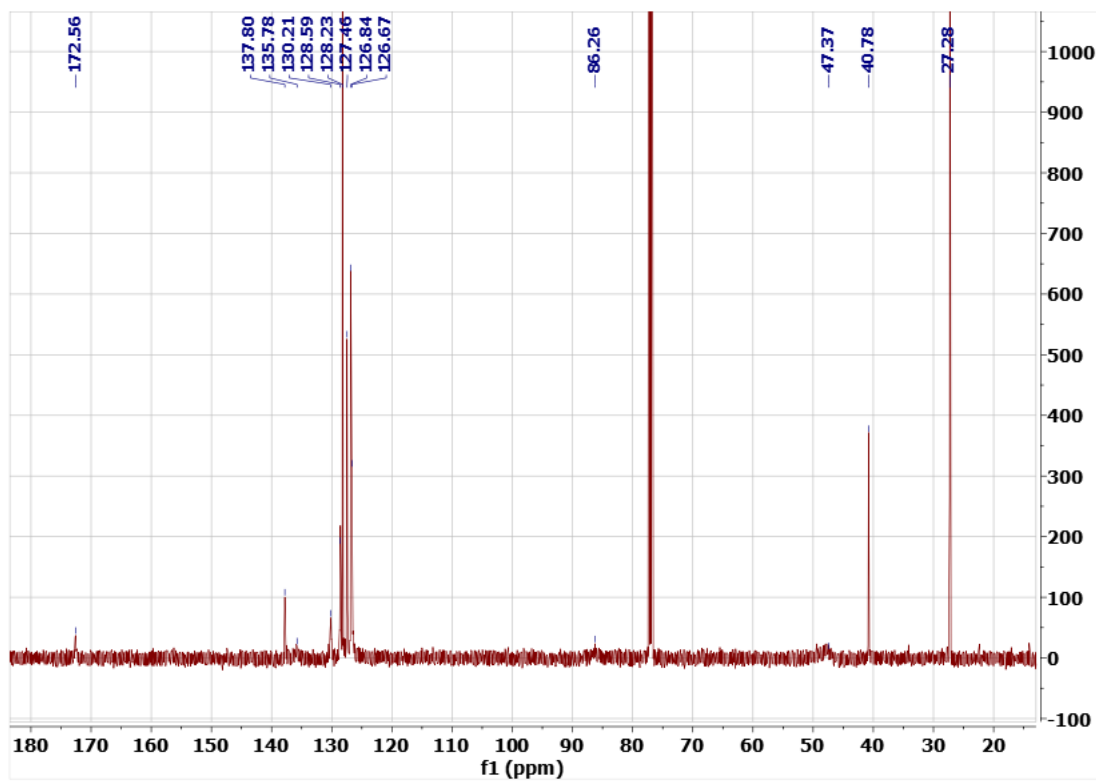
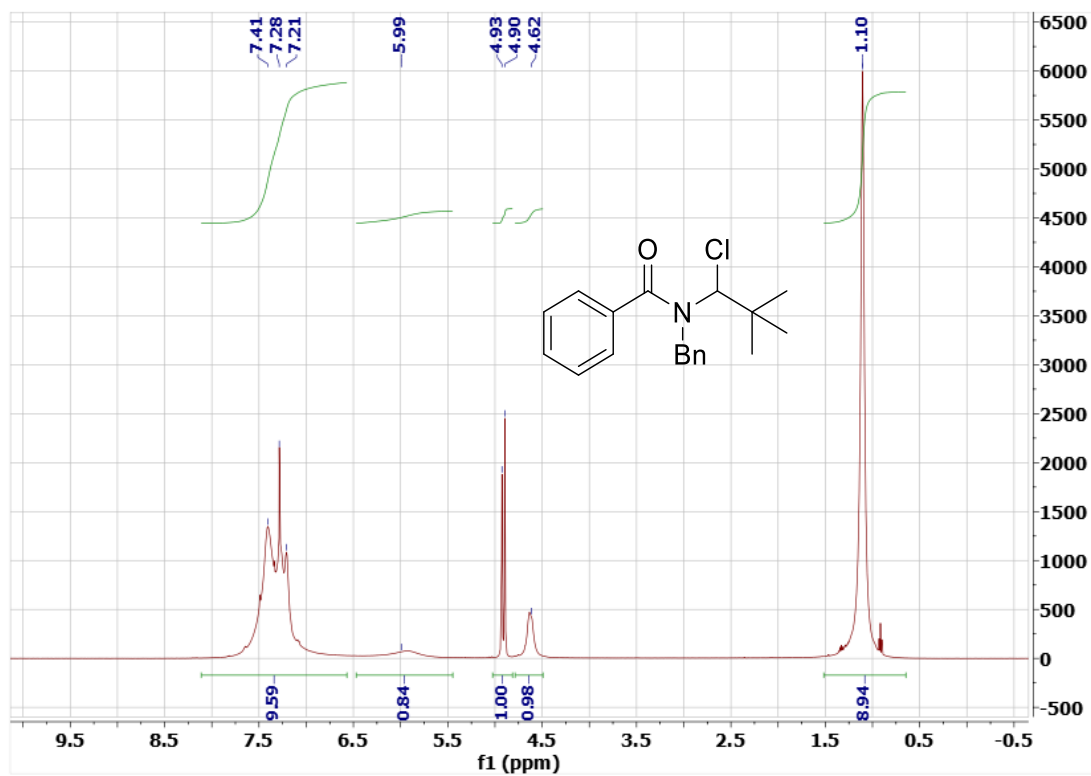


^1H , ^{13}C and ^{19}F NMR Spectra of 4.3ia (CDCl_3) at 5°C

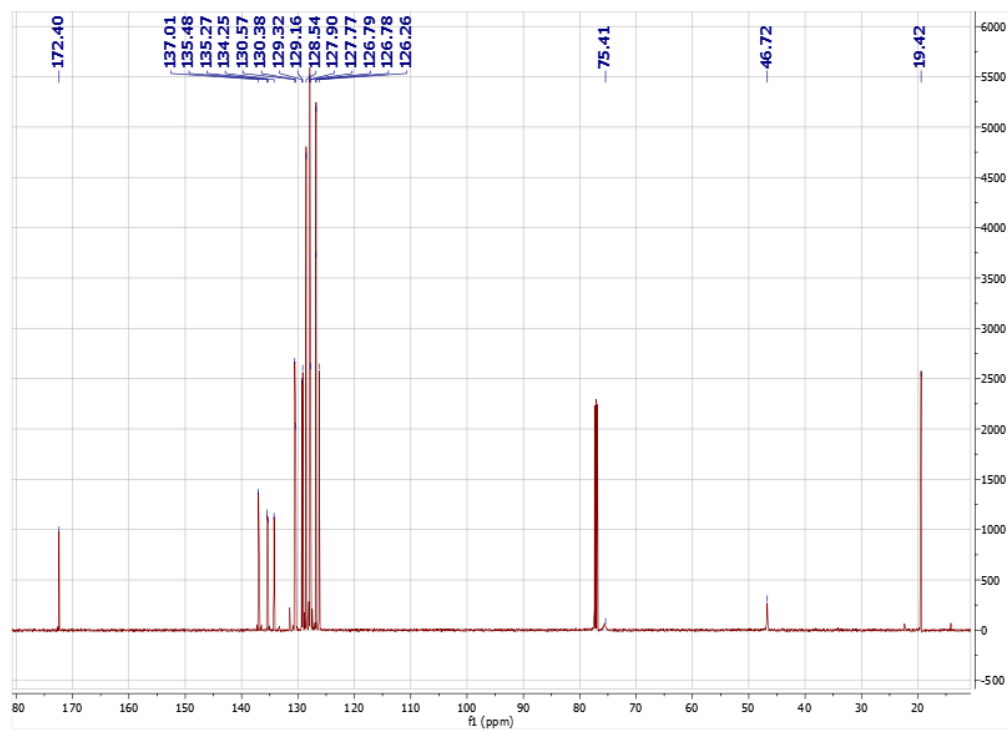
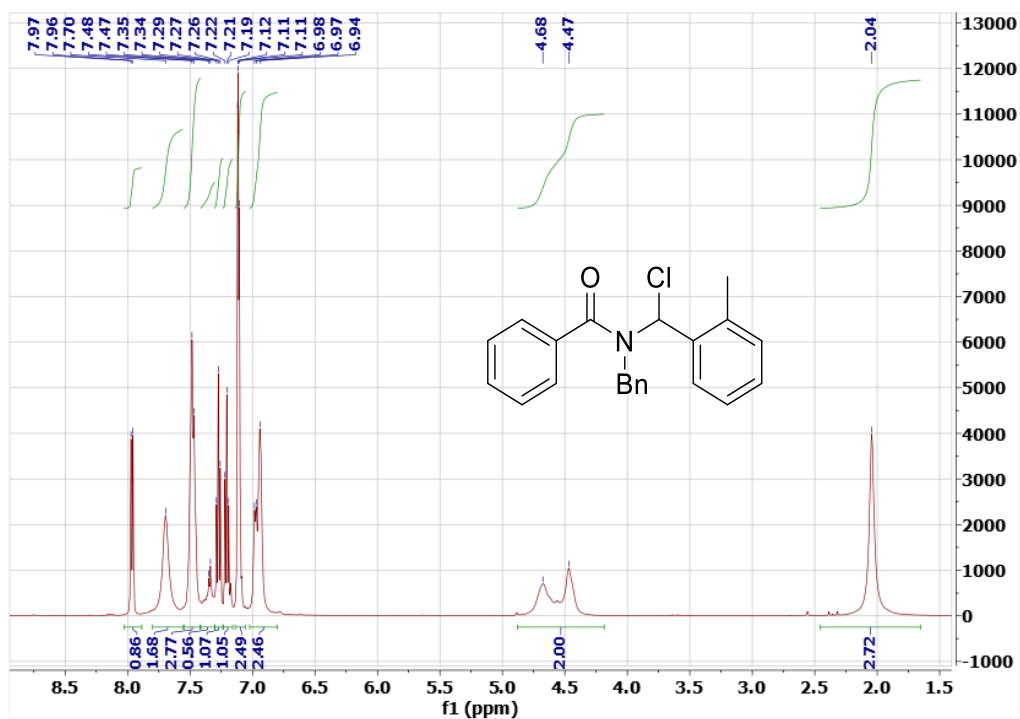




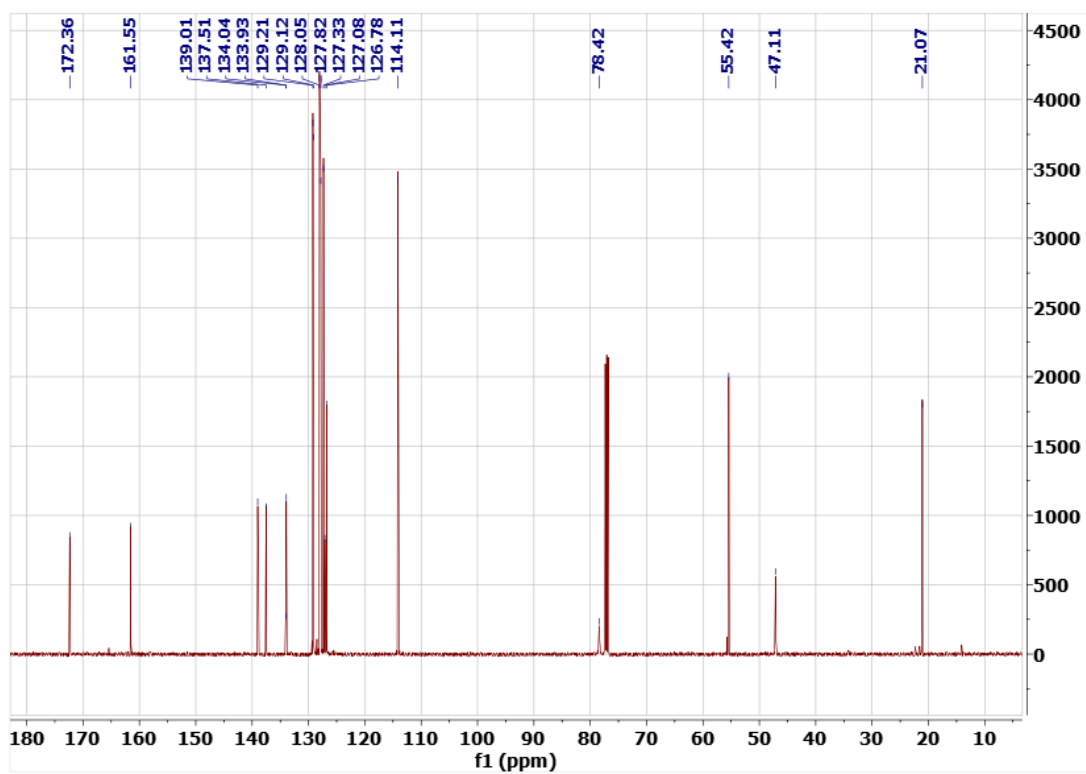
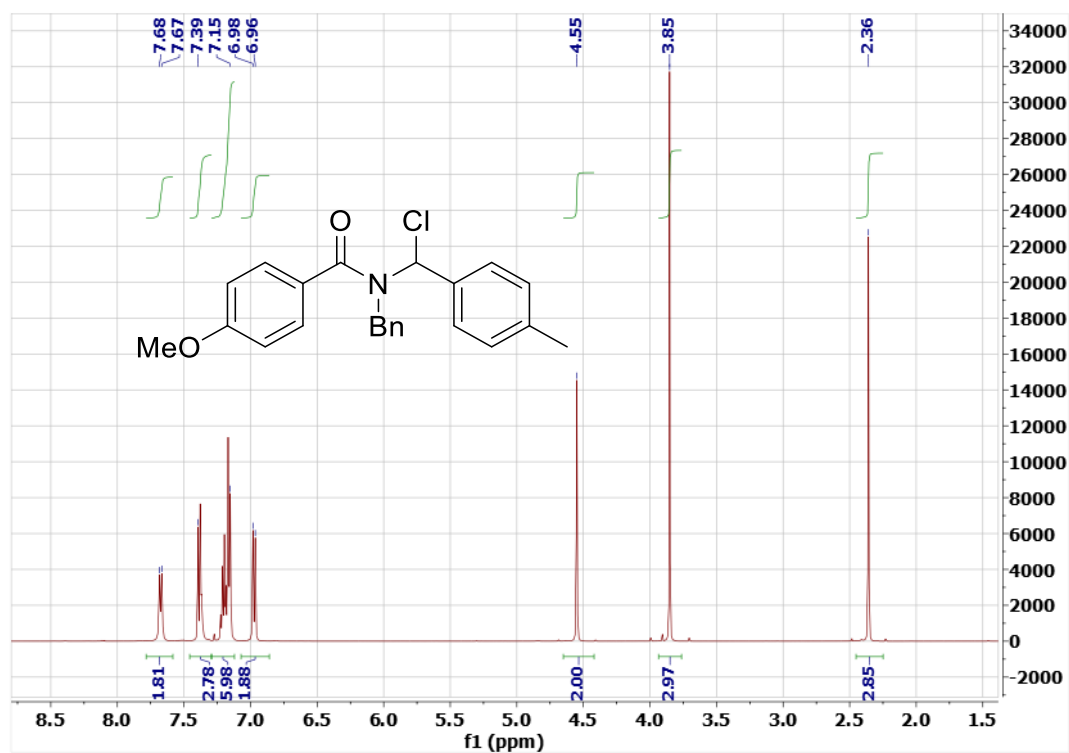
¹H and ¹³C NMR Spectra of 4.3ja (CDCl₃) at 5°C



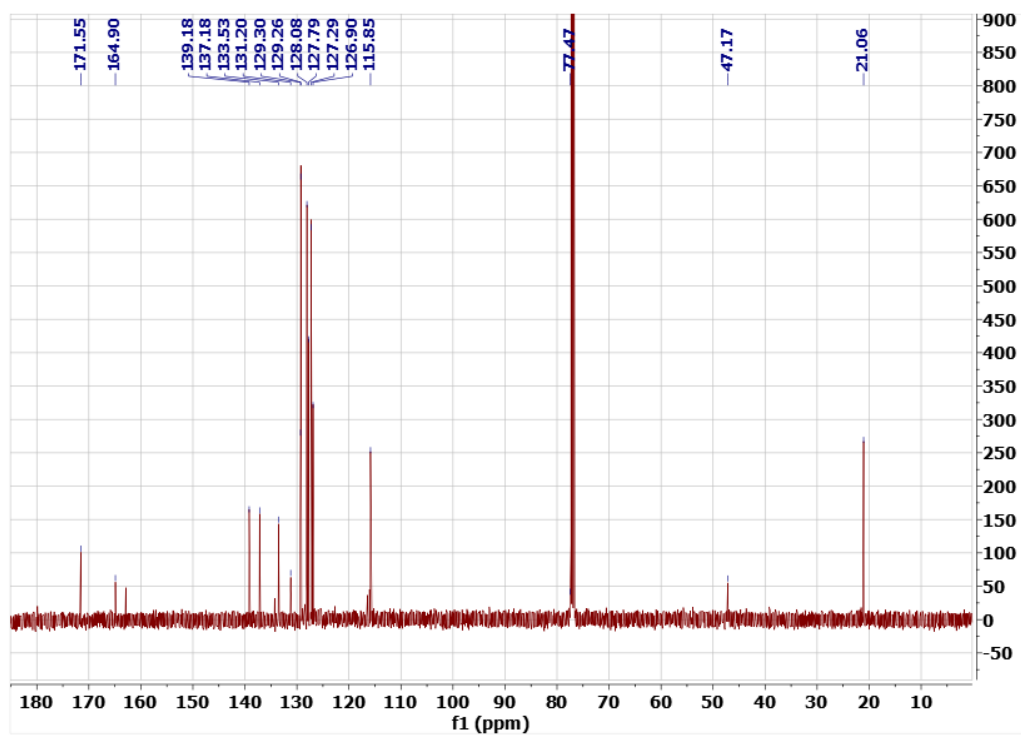
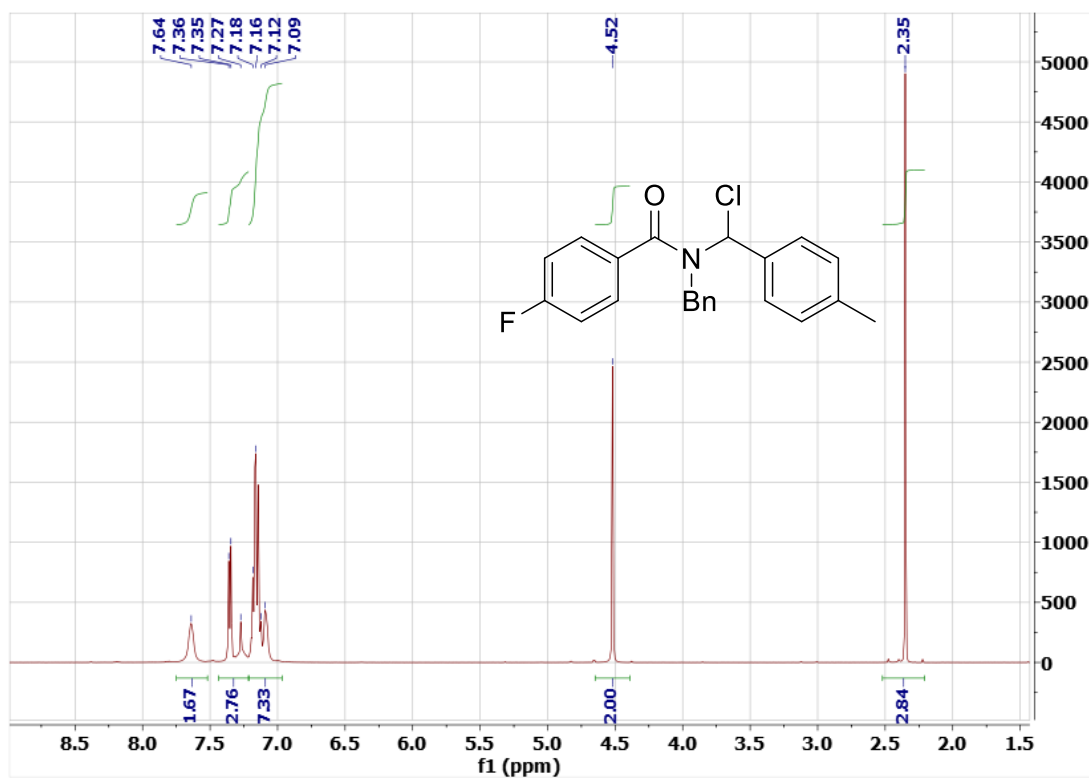
¹H and ¹³C NMR Spectra of 4.3ka (CDCl₃) at 5°C

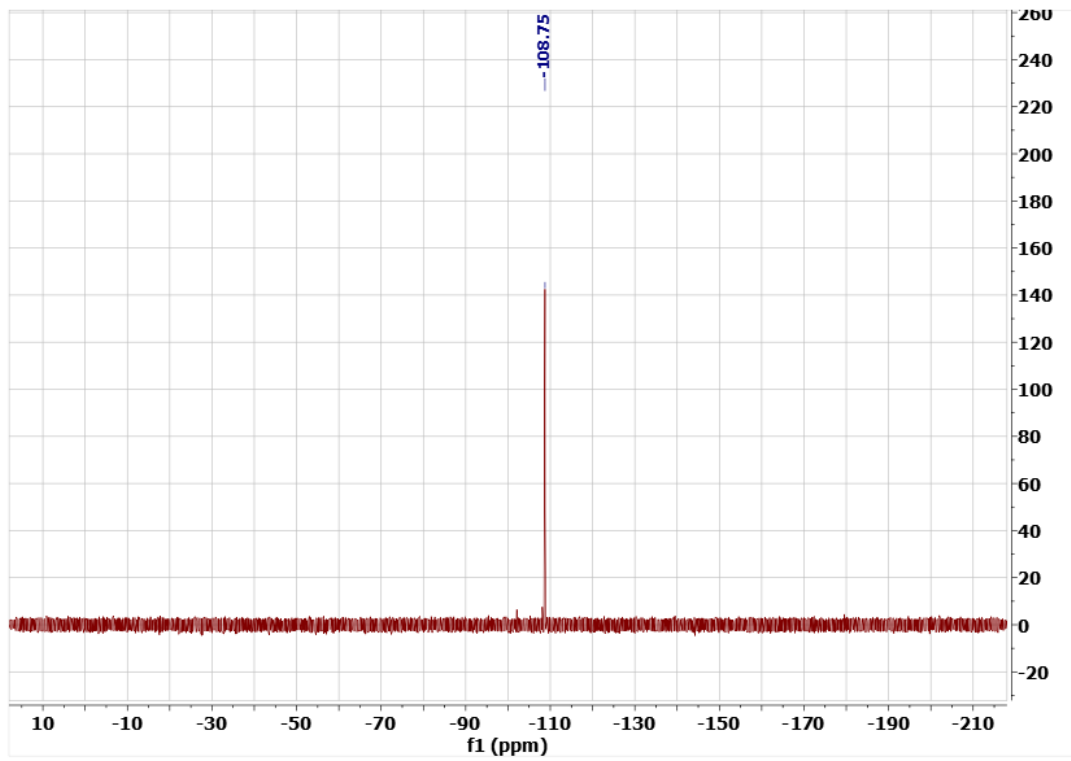


¹H and ¹³C NMR Spectra of 4.3ab (CDCl₃) at 5°C

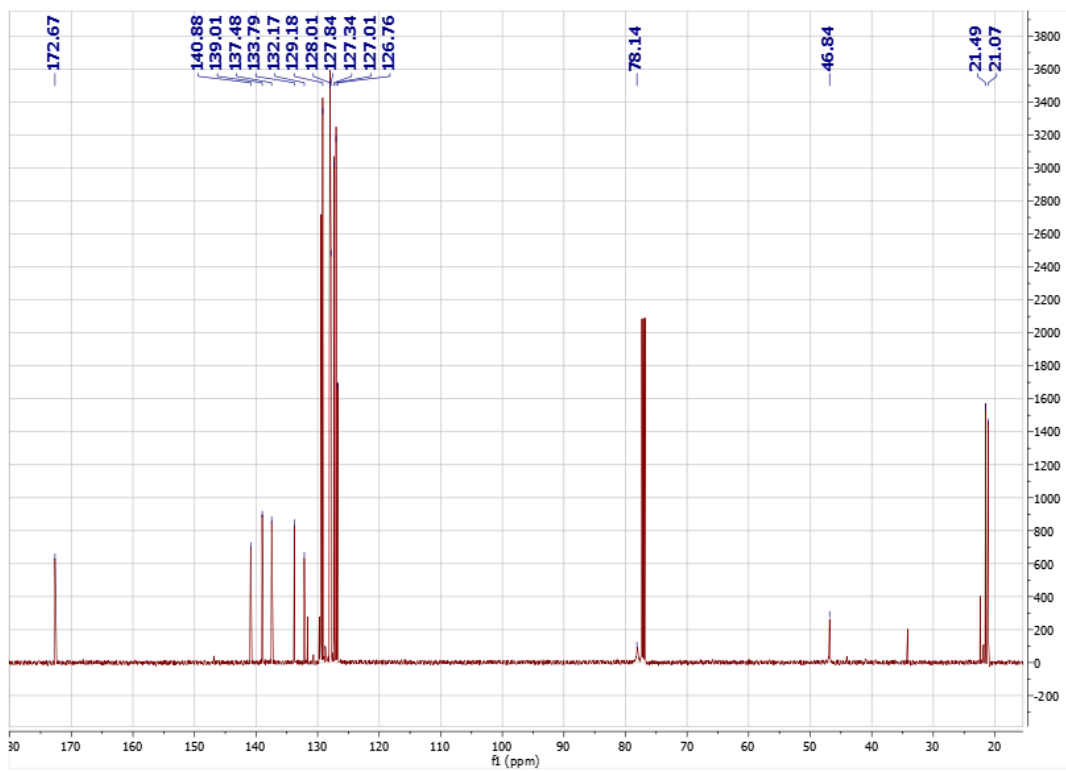
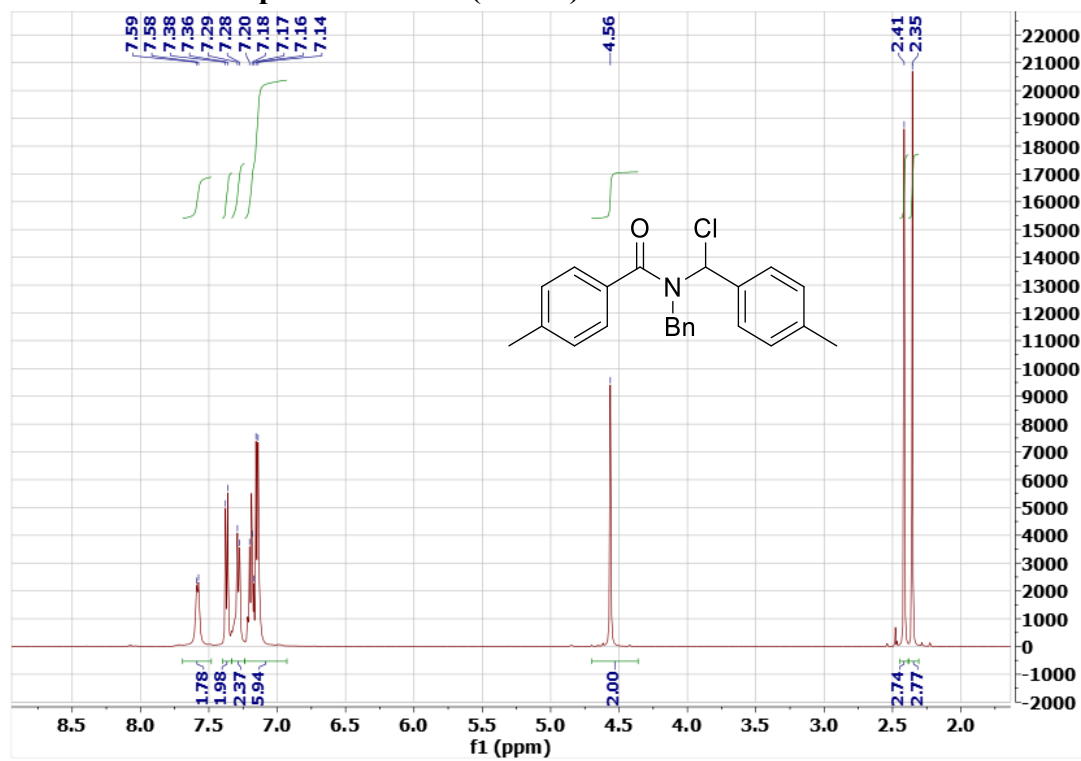


^1H , ^{13}C and ^{19}F NMR Spectra of 4.3ac (CDCl_3) at 5°C

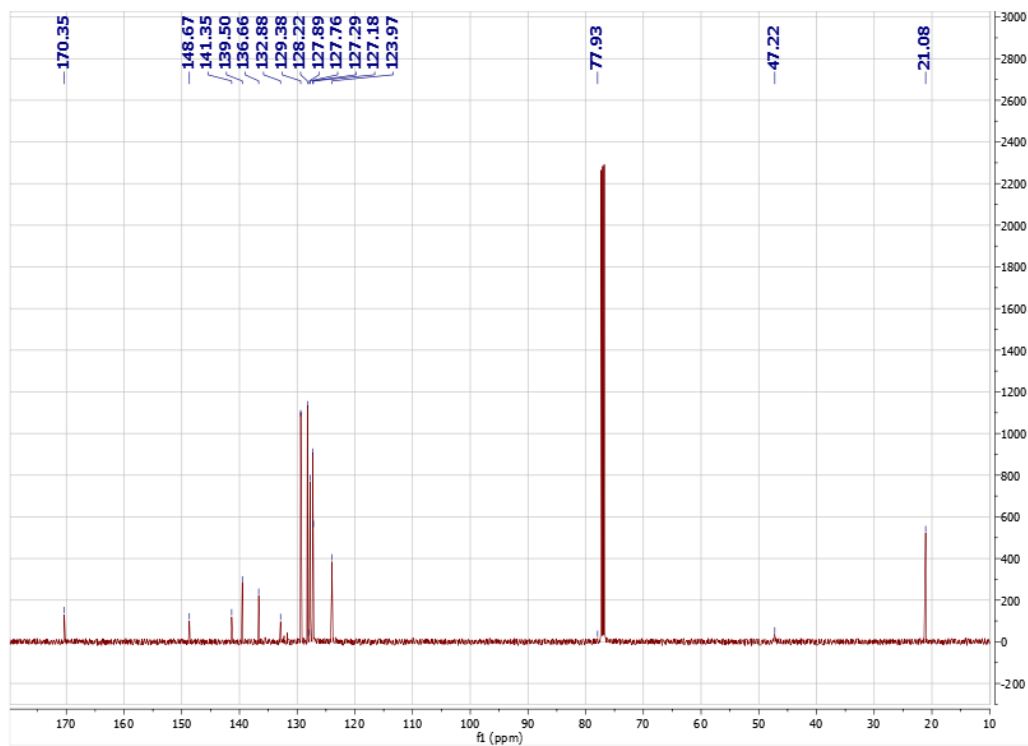
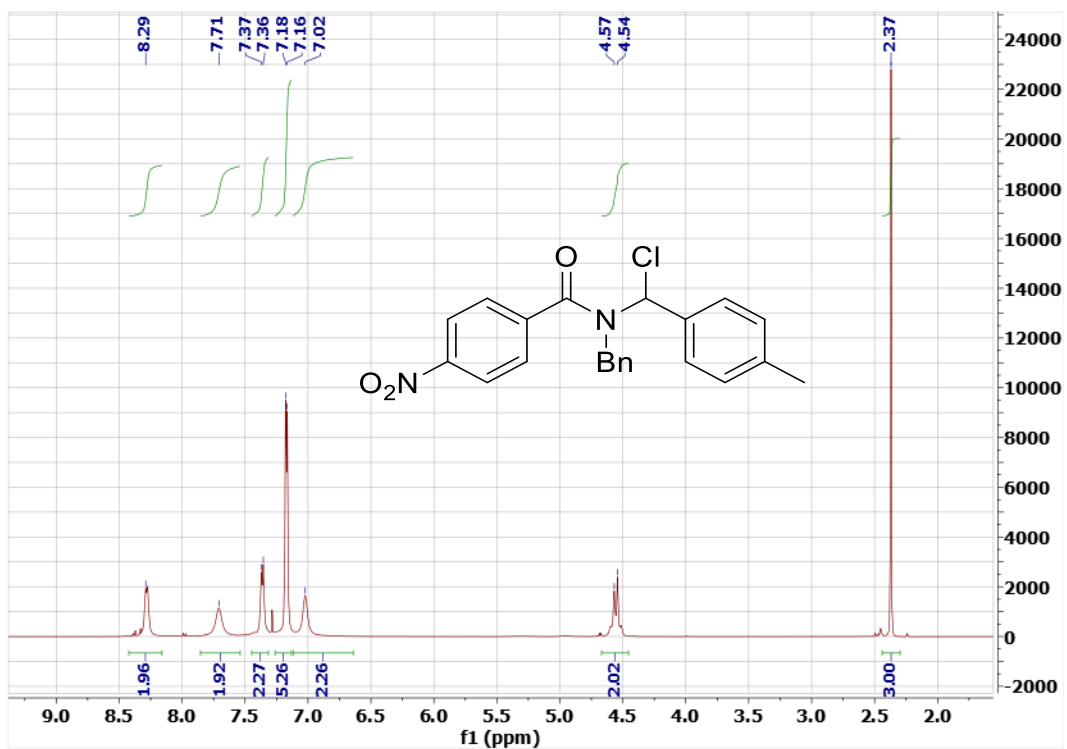




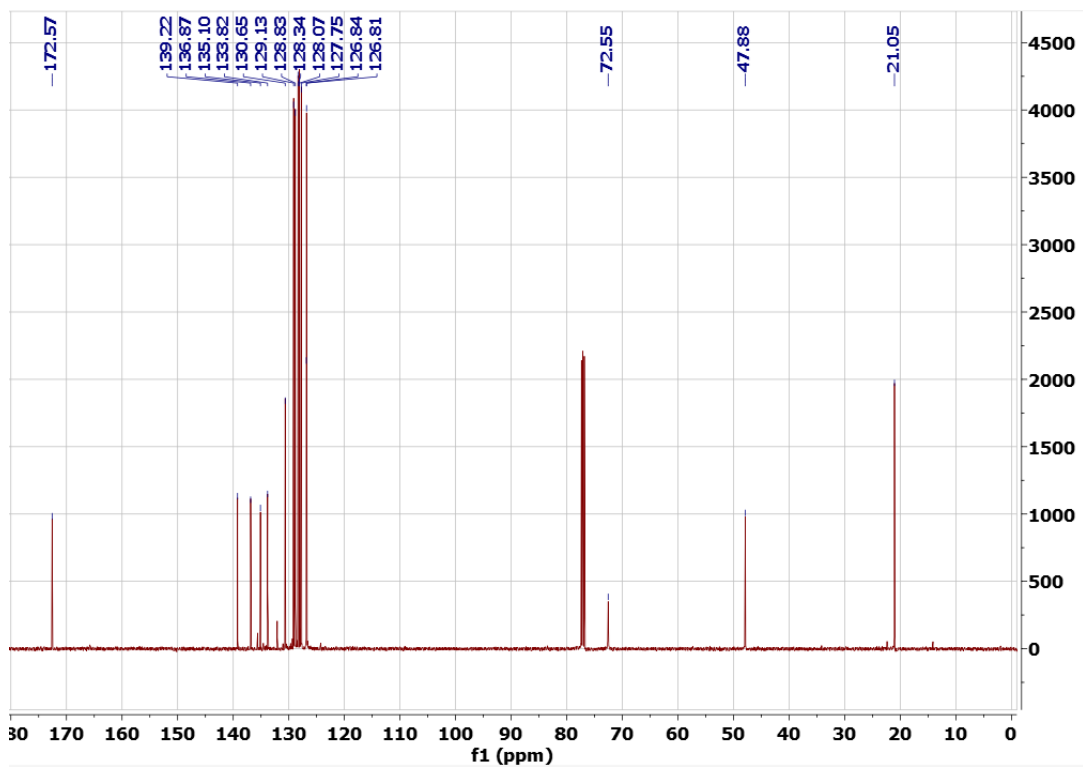
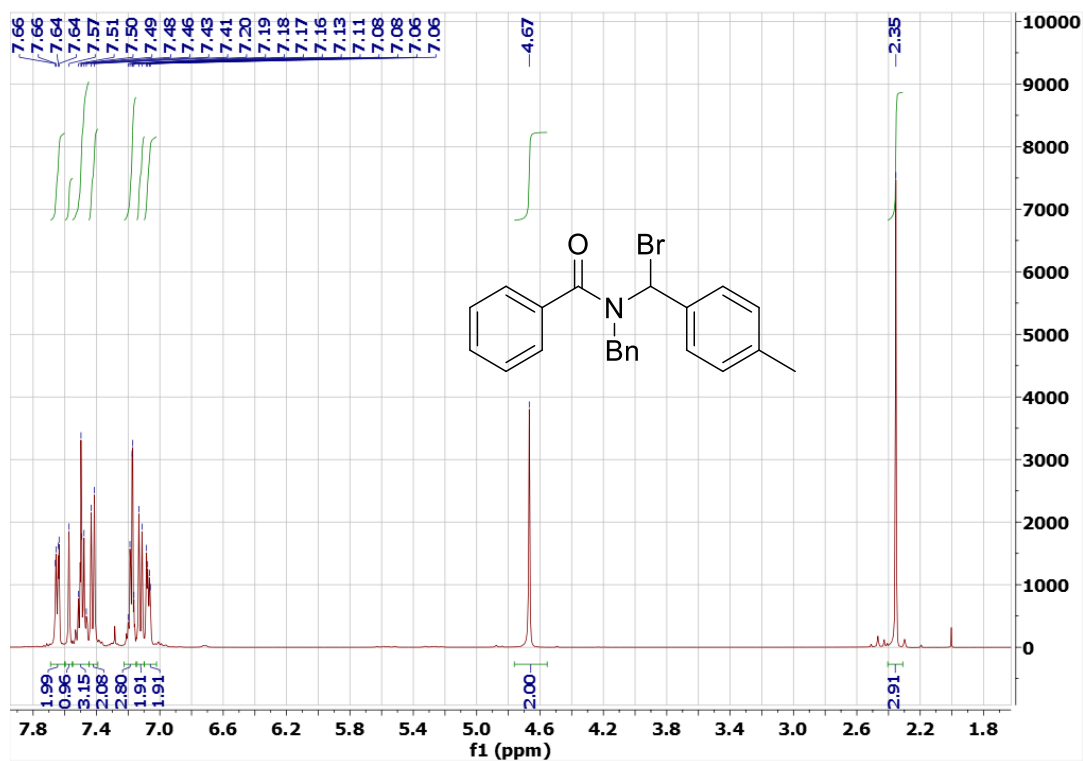
¹H and ¹³C NMR Spectra of 4.3ad (CDCl₃) at 5°C



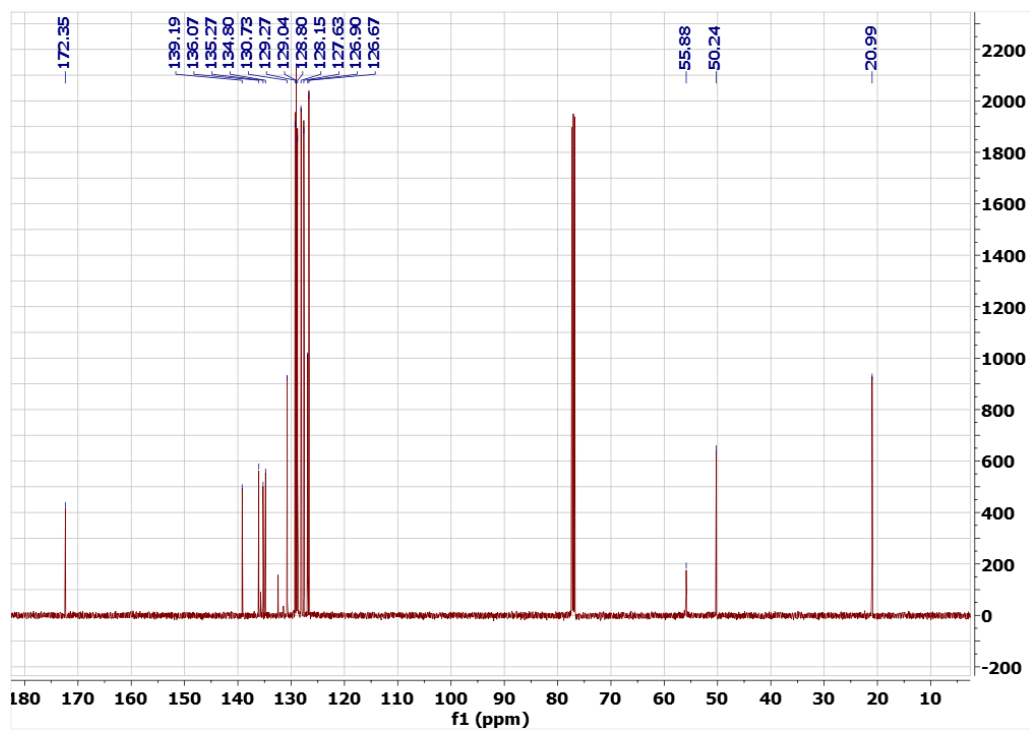
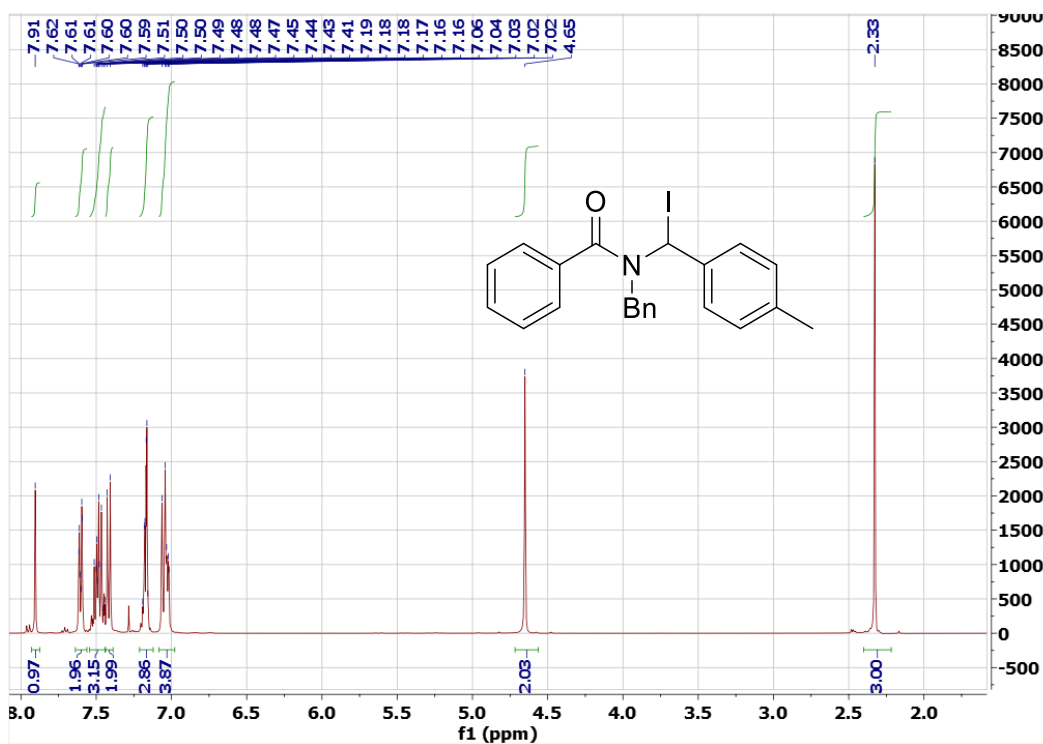
^1H and ^{13}C NMR Spectra of 4.3ae (CDCl_3) at 5°C



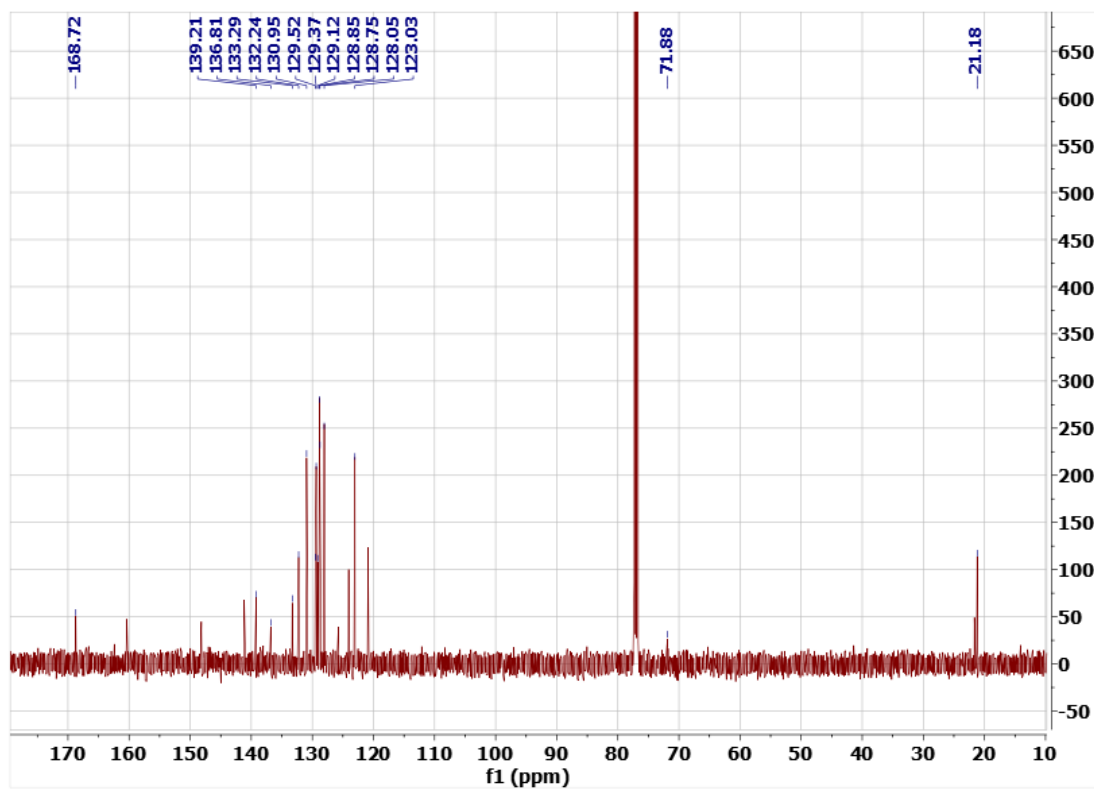
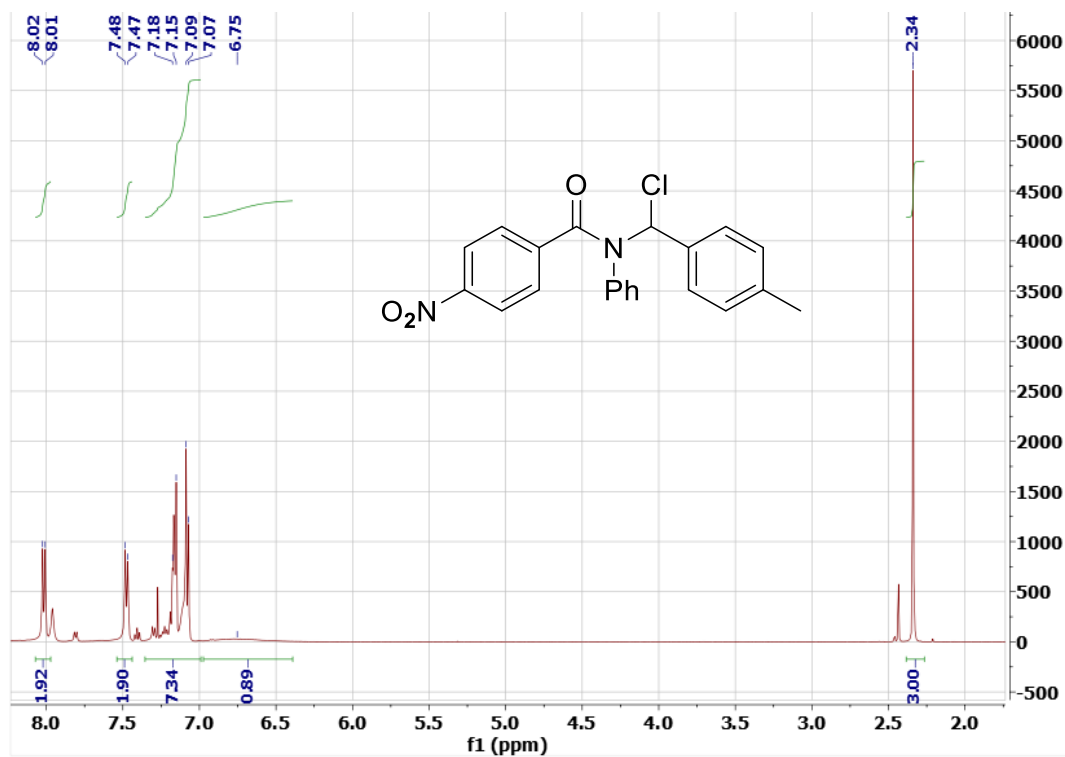
^1H and ^{13}C NMR Spectra of 4.3aa-Br (CDCl_3) at 5°C



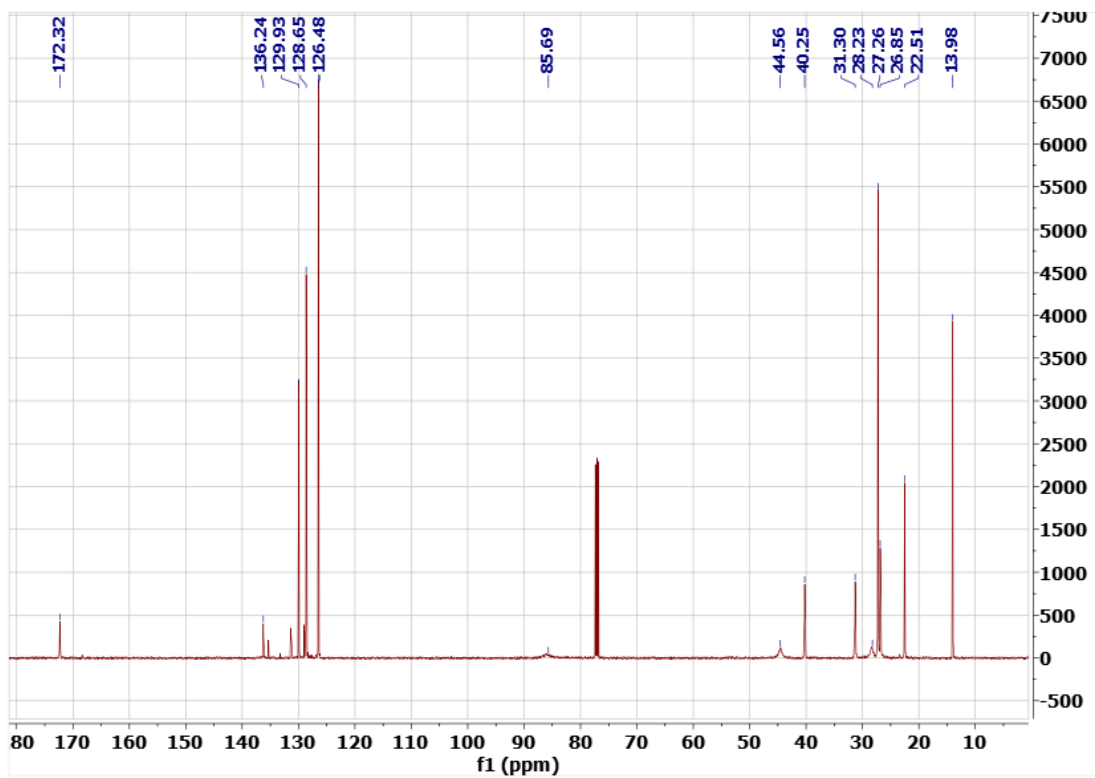
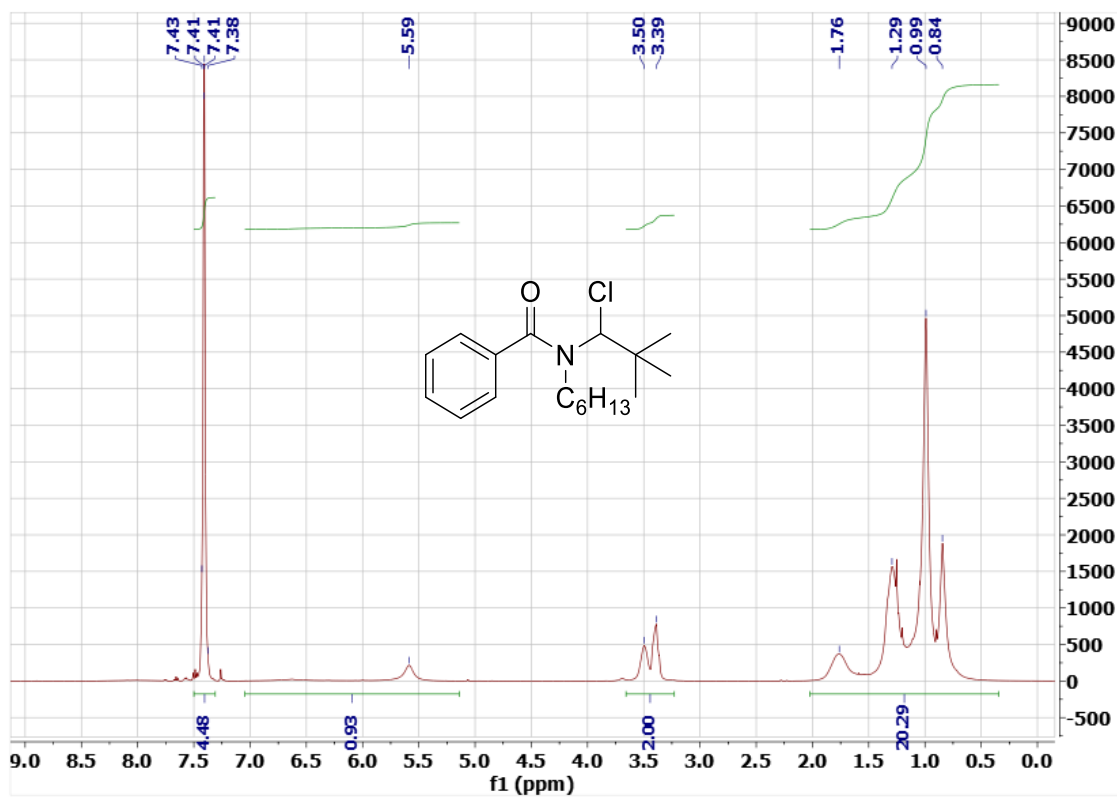
¹H and ¹³C NMR Spectra of 4.3aa-I (CDCl₃) at 5°C



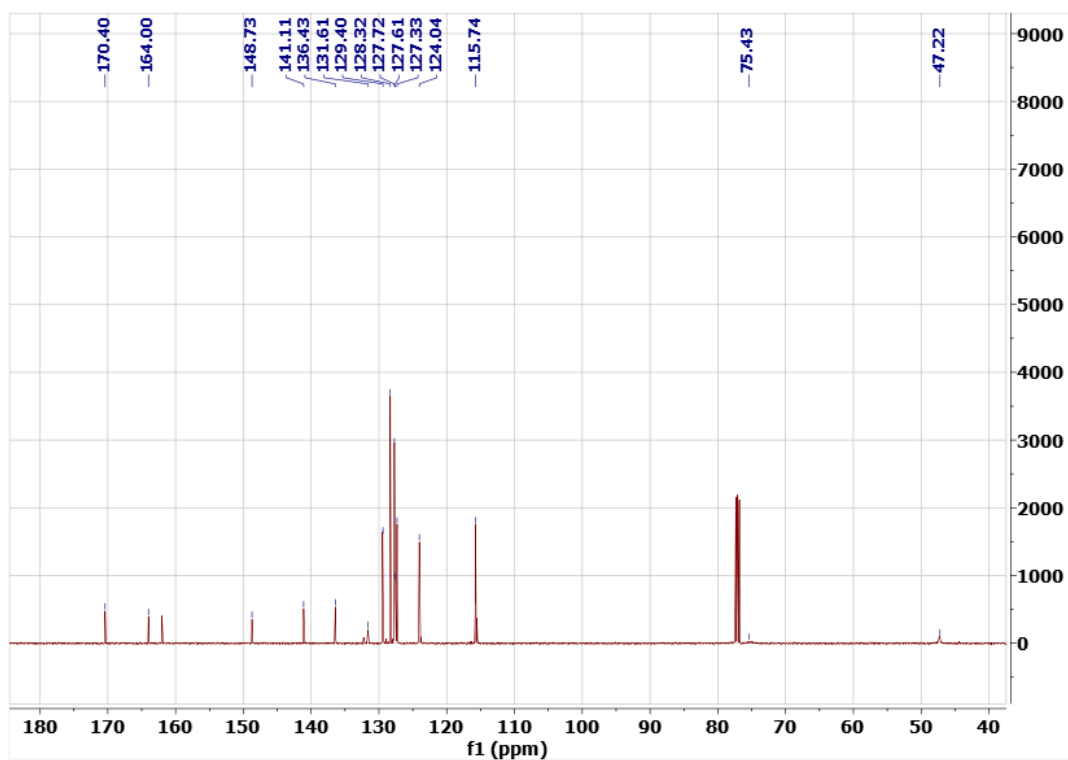
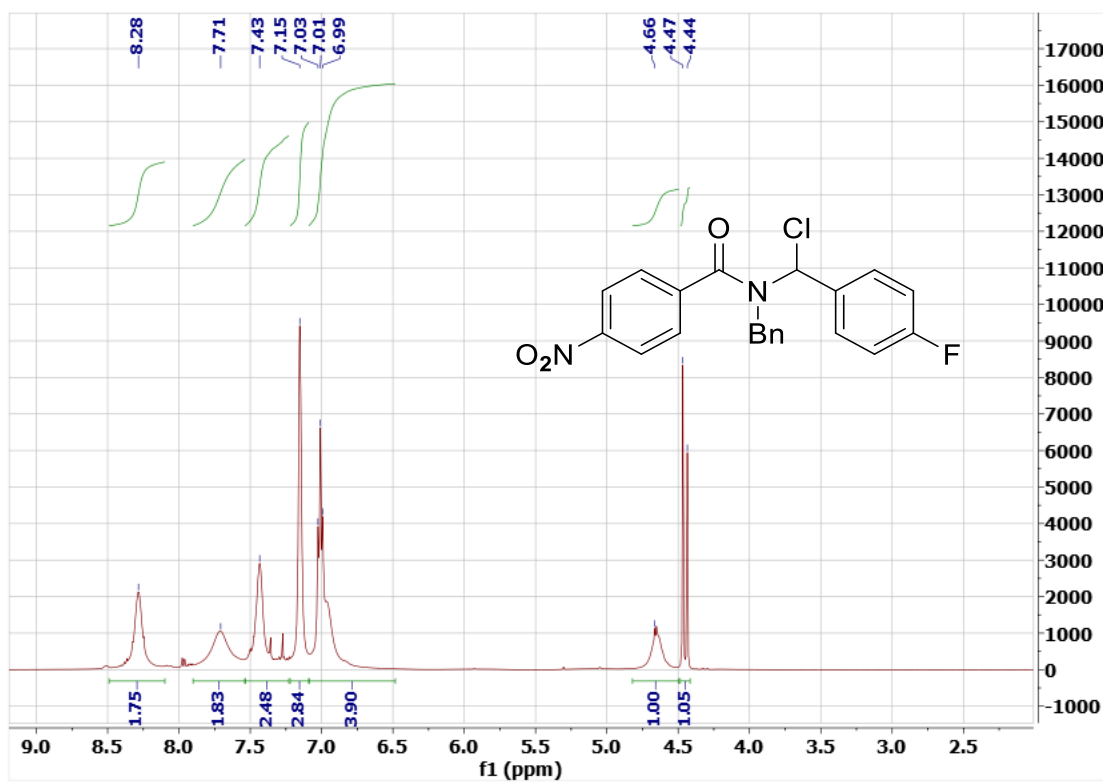
¹H and ¹³C NMR Spectra of 4.3ee (CDCl₃) at 5°C

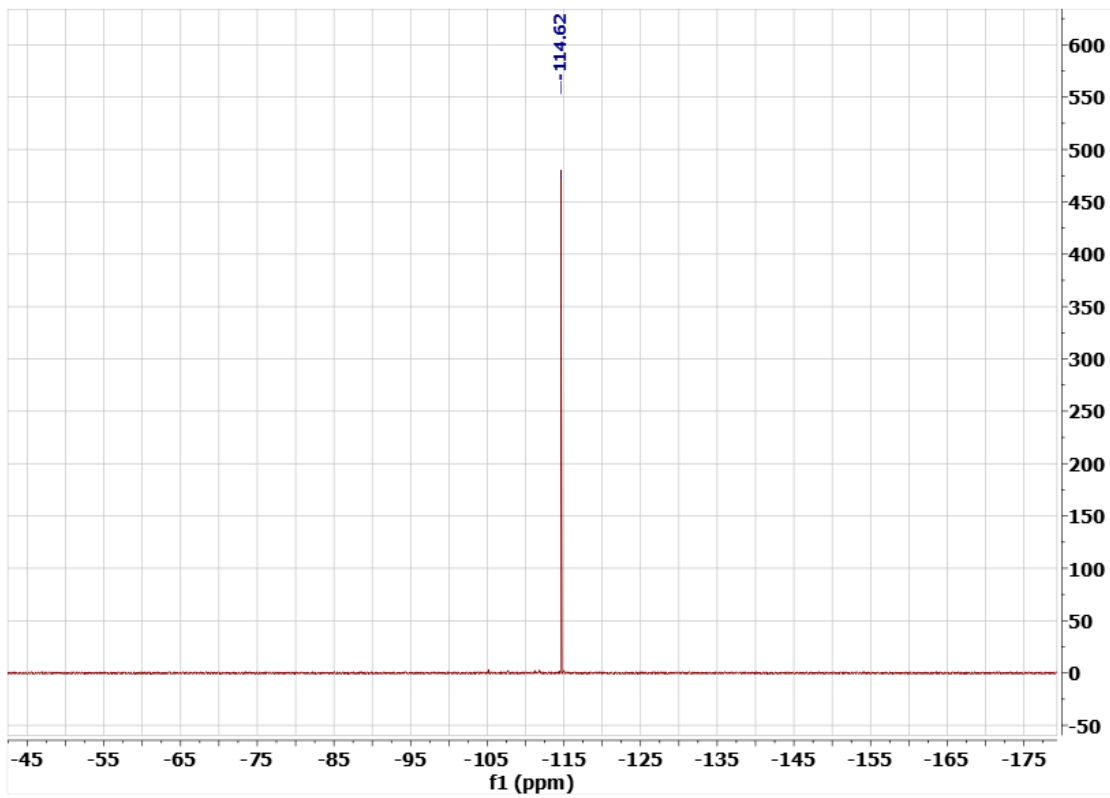


^1H and ^{13}C NMR Spectra of 4.31a (CDCl_3) at 5°C

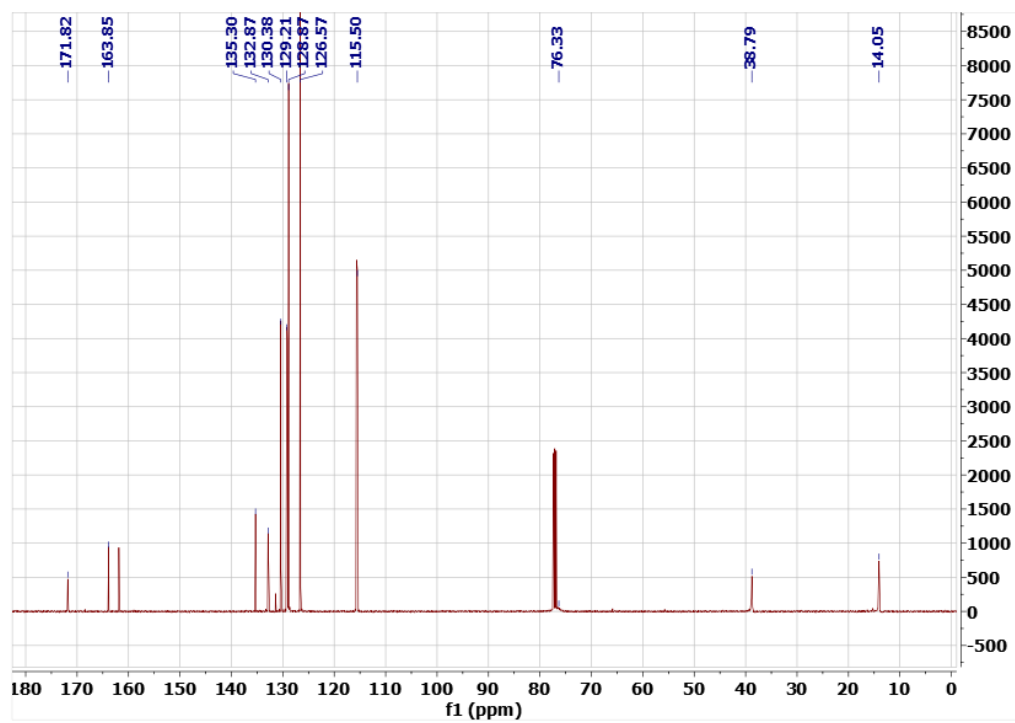
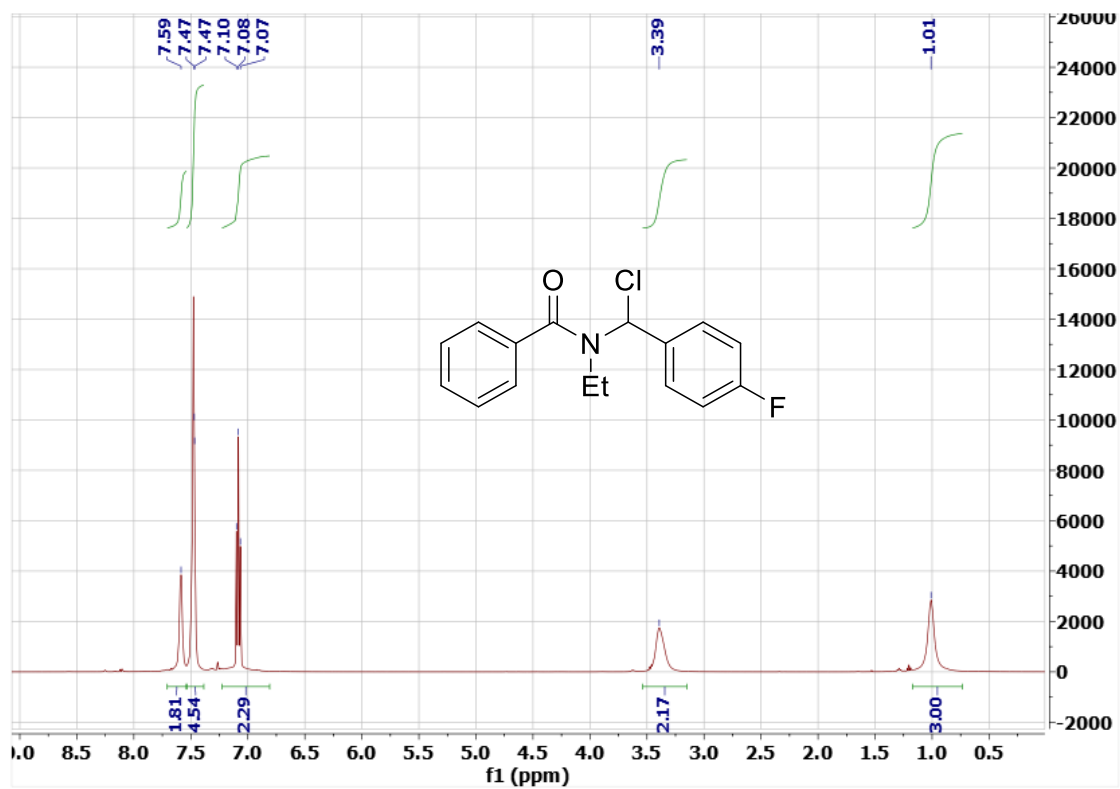


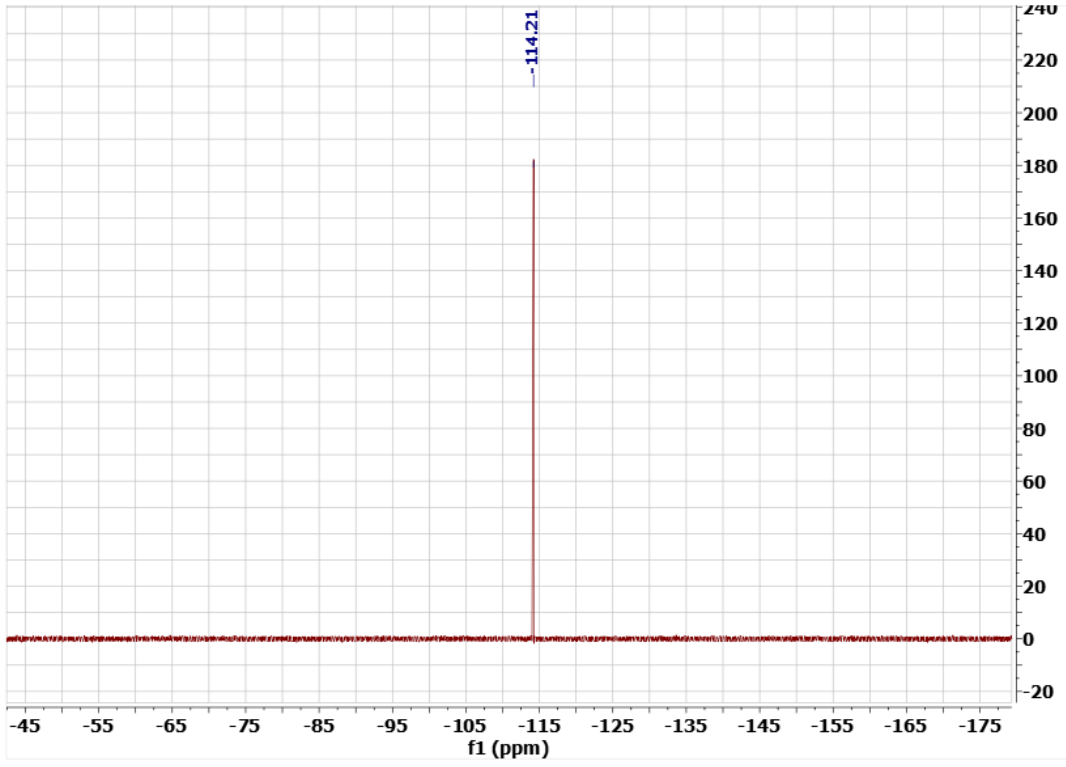
^1H , ^{13}C and ^{19}F NMR Spectra of 4.3ie (CDCl_3) at 5°C



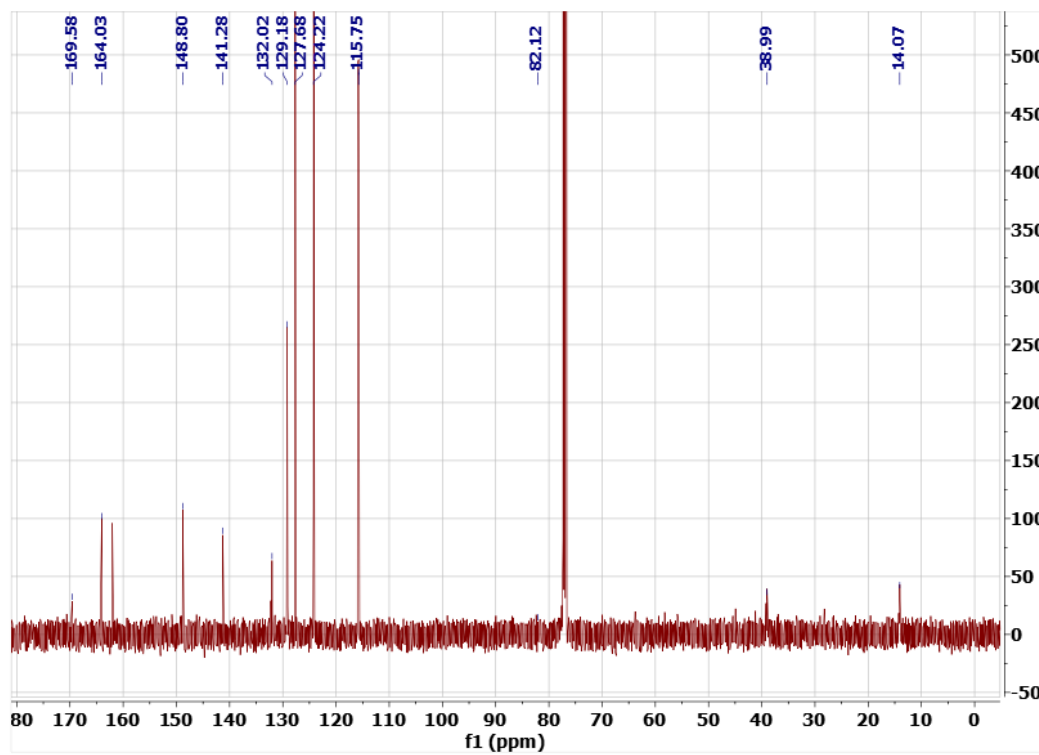
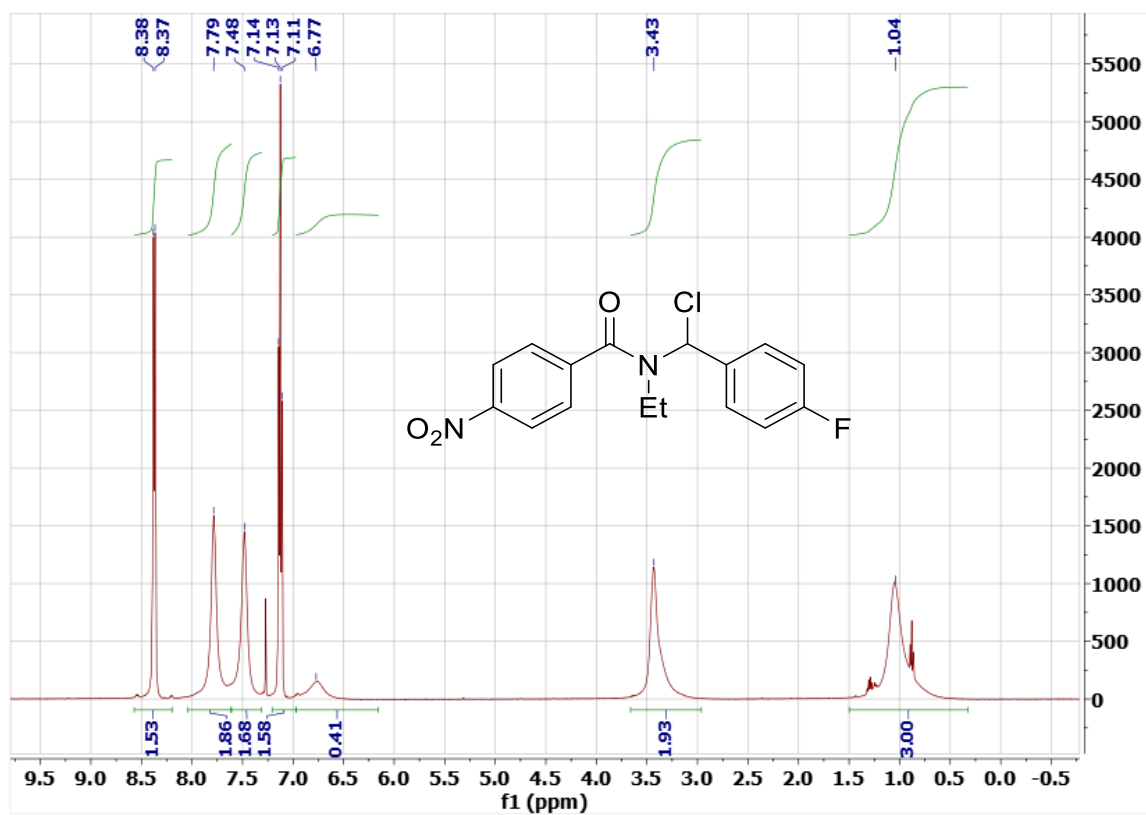


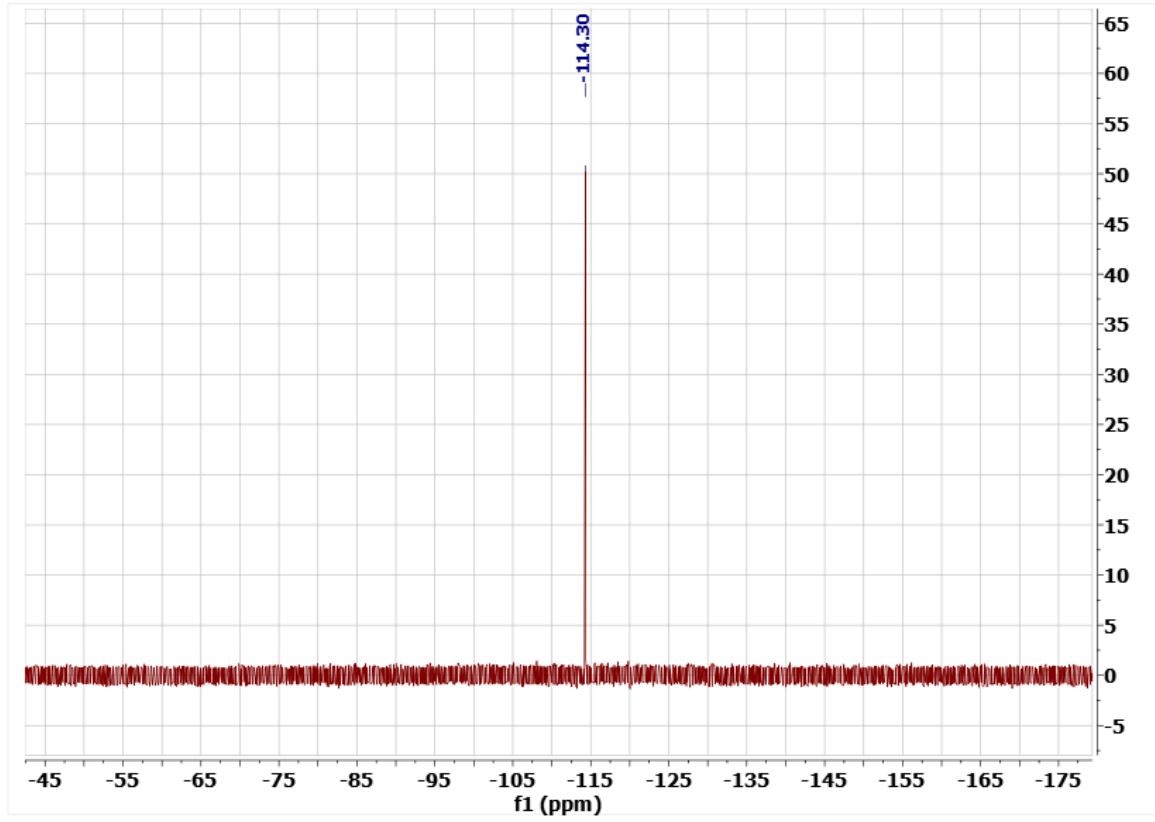
^1H , ^{13}C and ^{19}F NMR Spectra of 4.3ma (CDCl_3) at 5°C



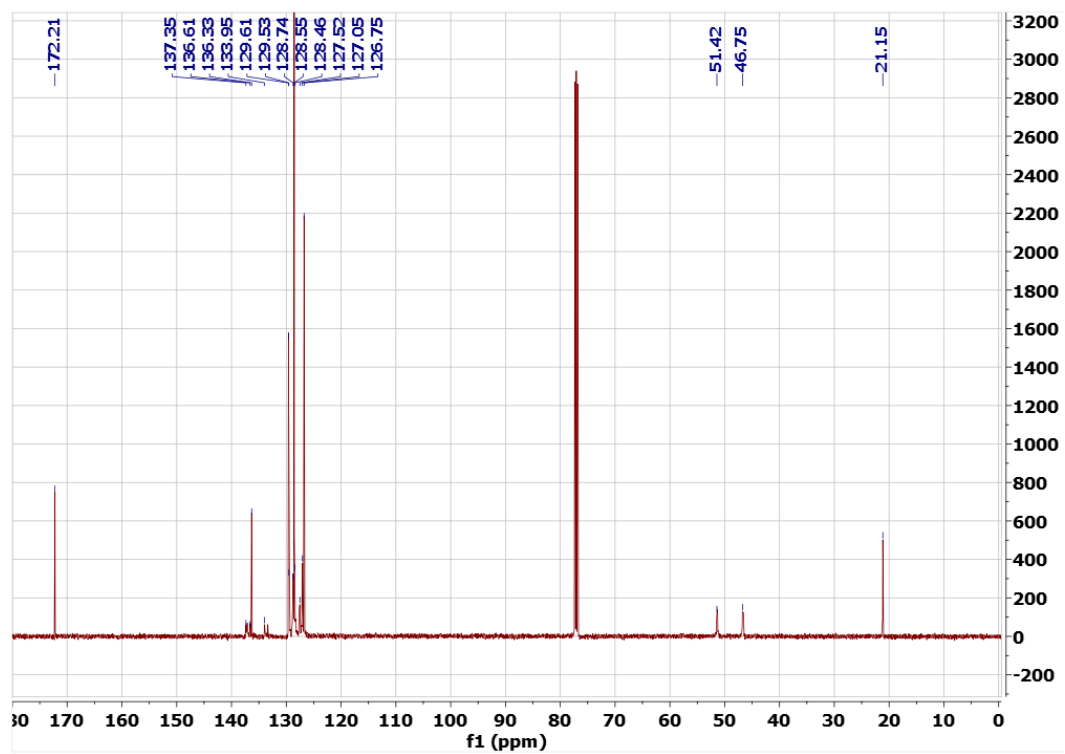
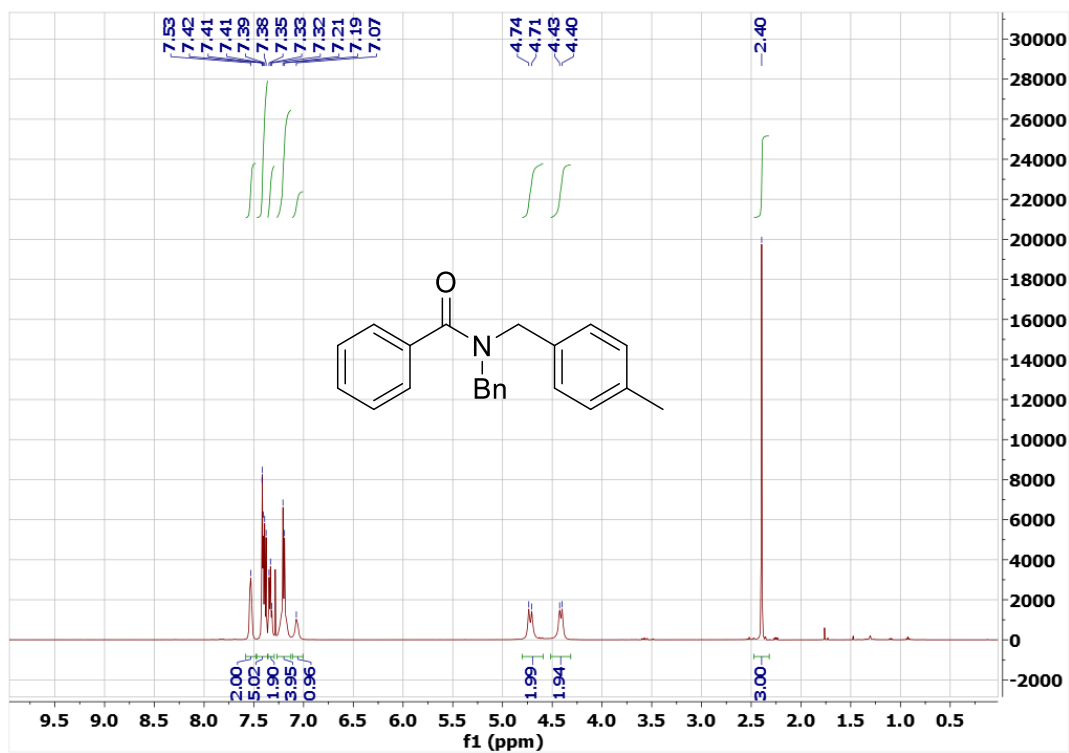


^1H , ^{13}C and ^{19}F NMR Spectra of 4.3me (CDCl₃) at 5°C

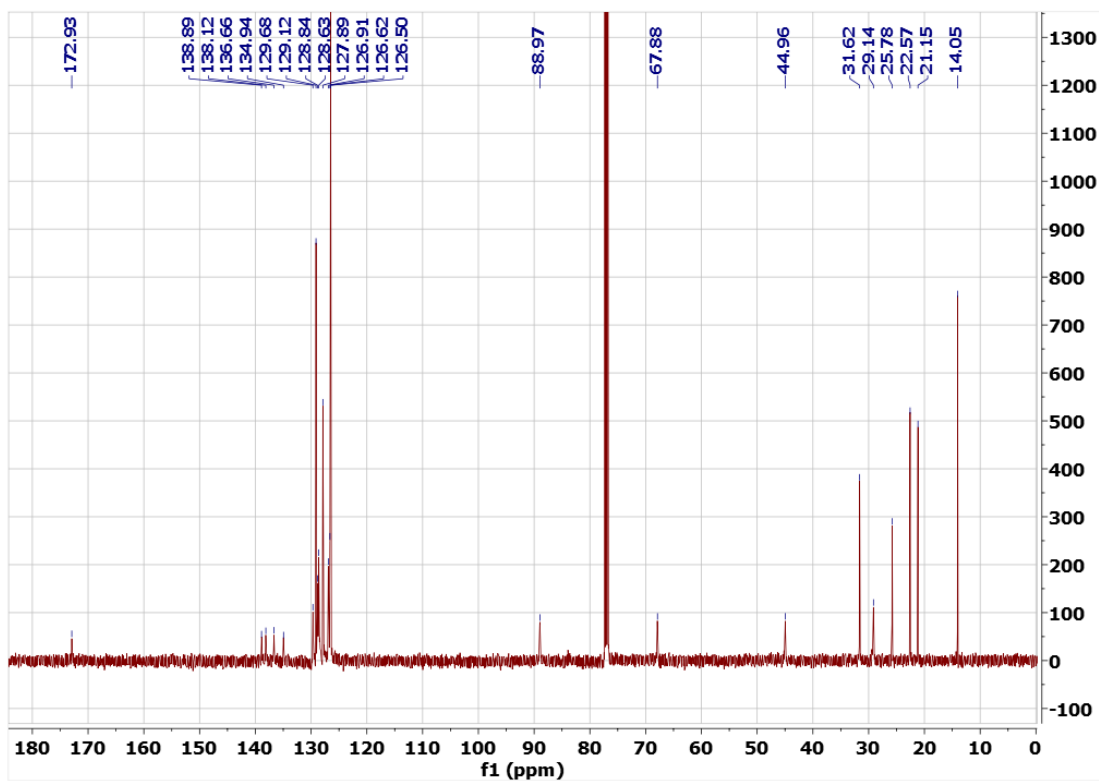
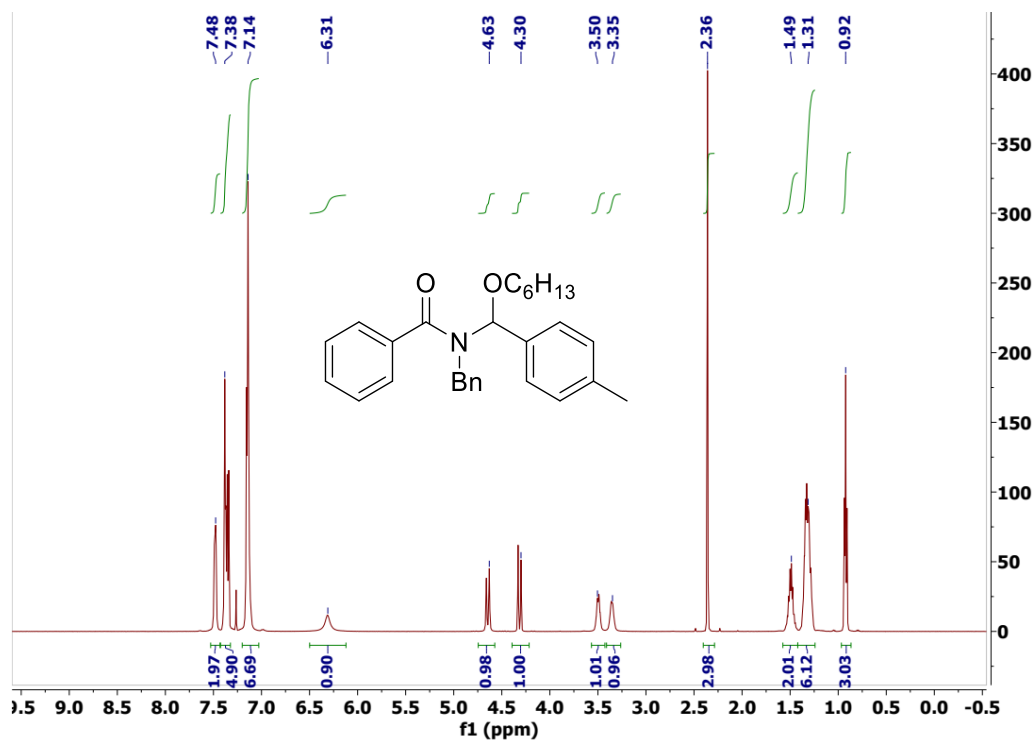




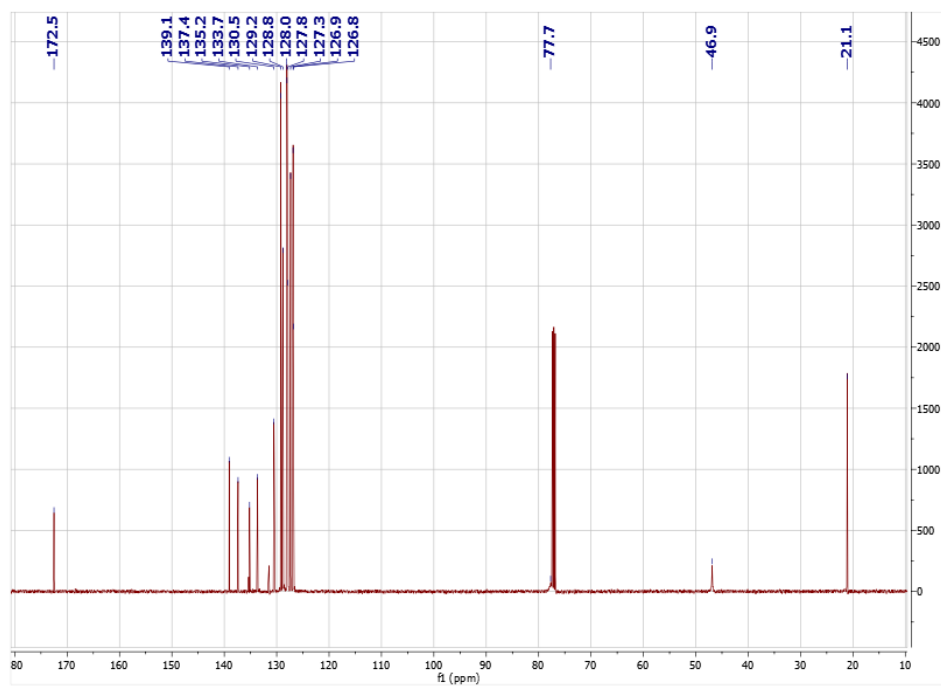
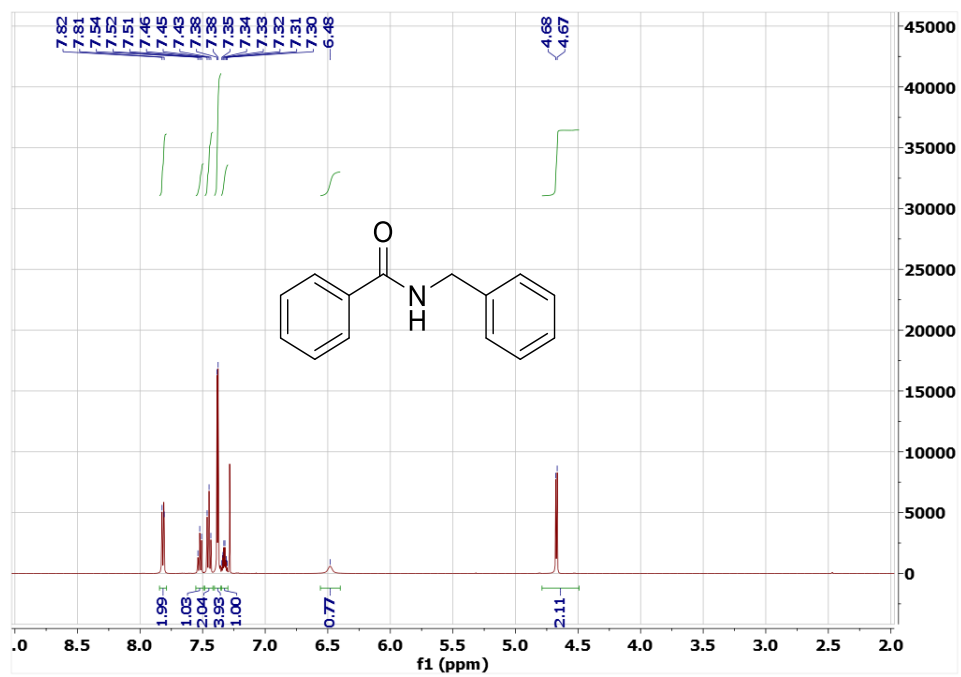
^1H and ^{13}C NMR Spectra of 4.4aa (CDCl_3)



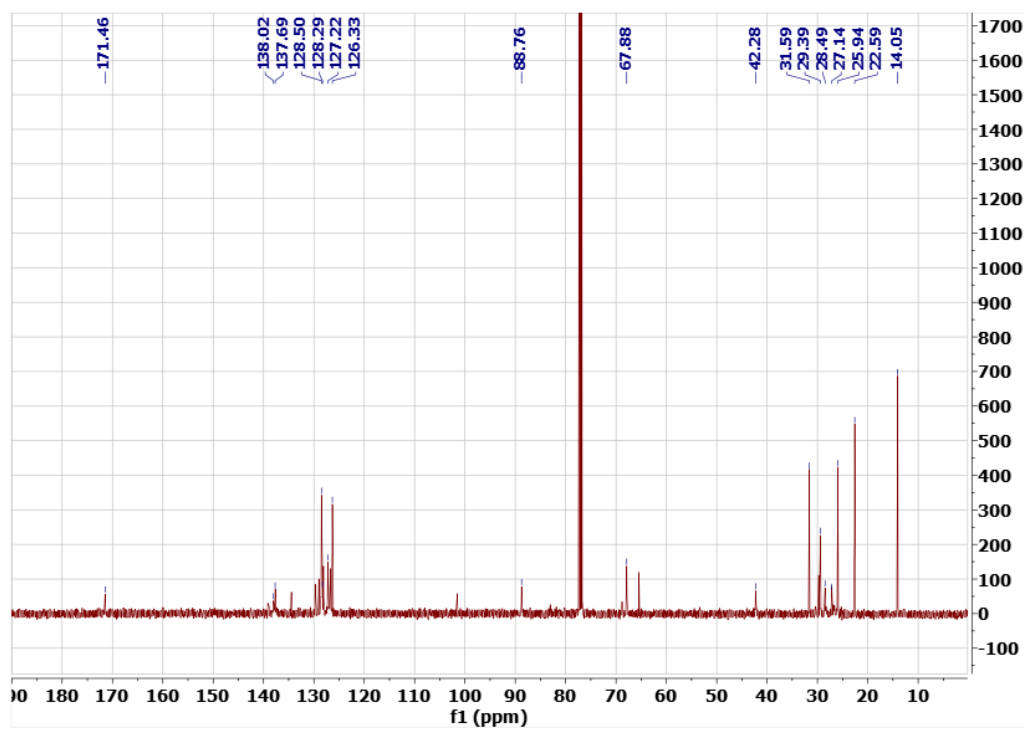
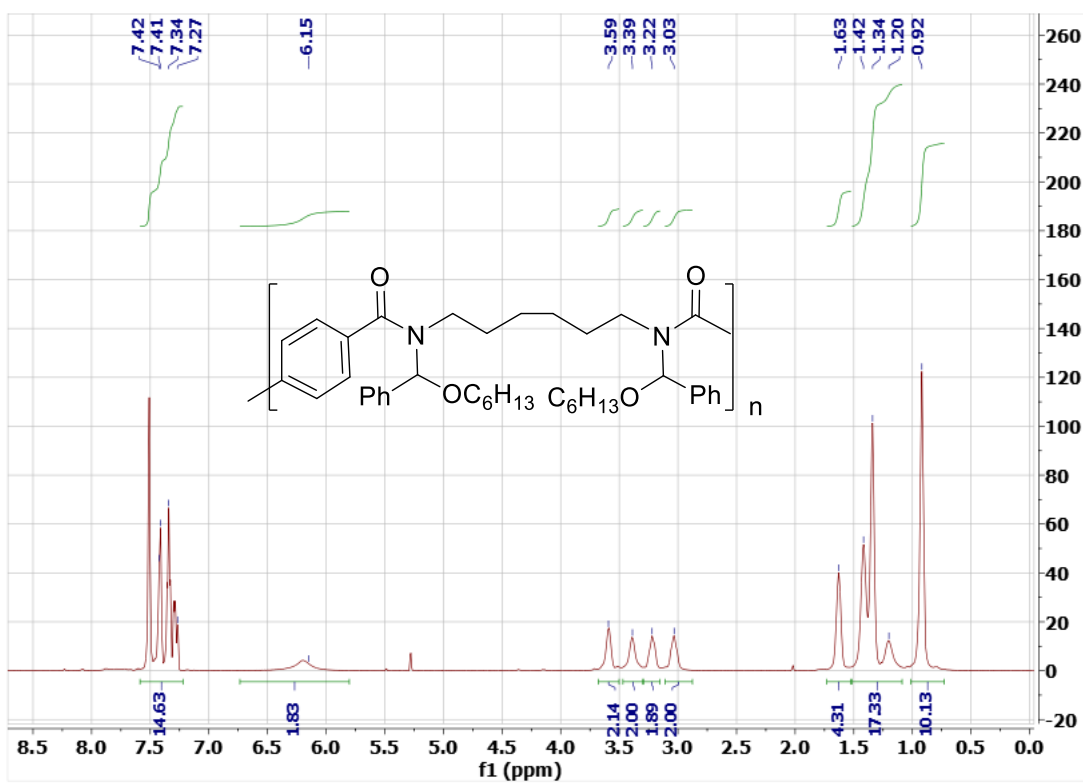
^1H and ^{13}C NMR Spectra of 4.5aa (CDCl_3) at 100°C



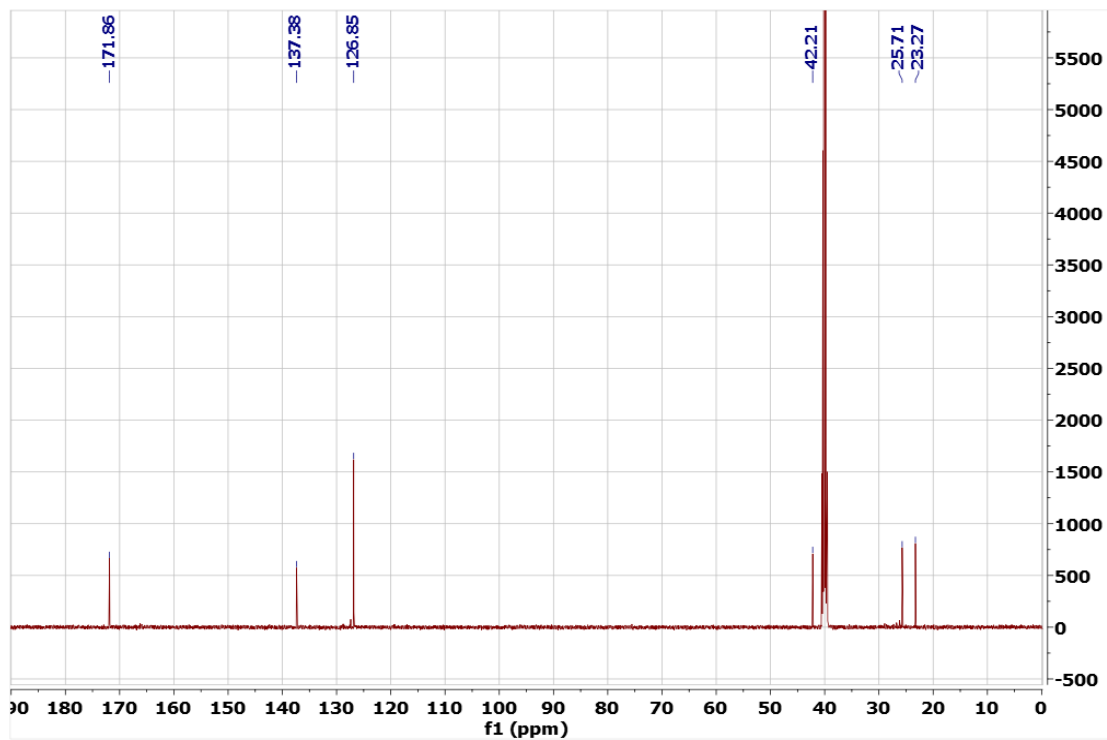
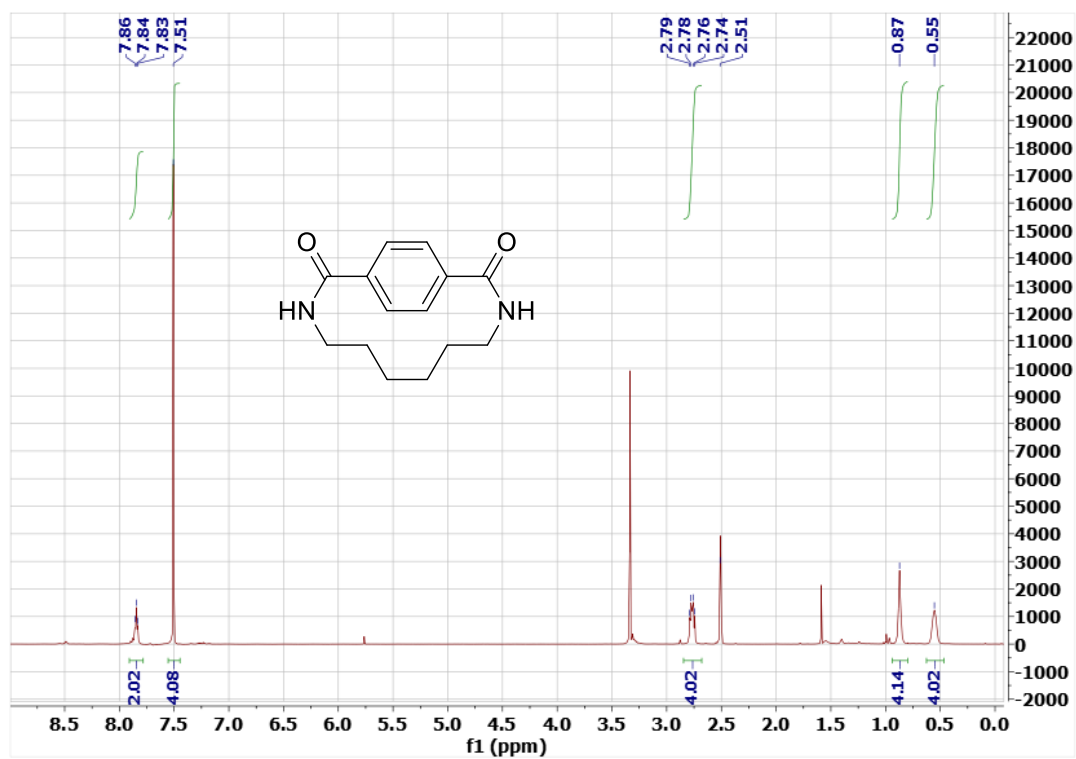
¹H and ¹³C NMR Spectra of 4.6a (CDCl₃)



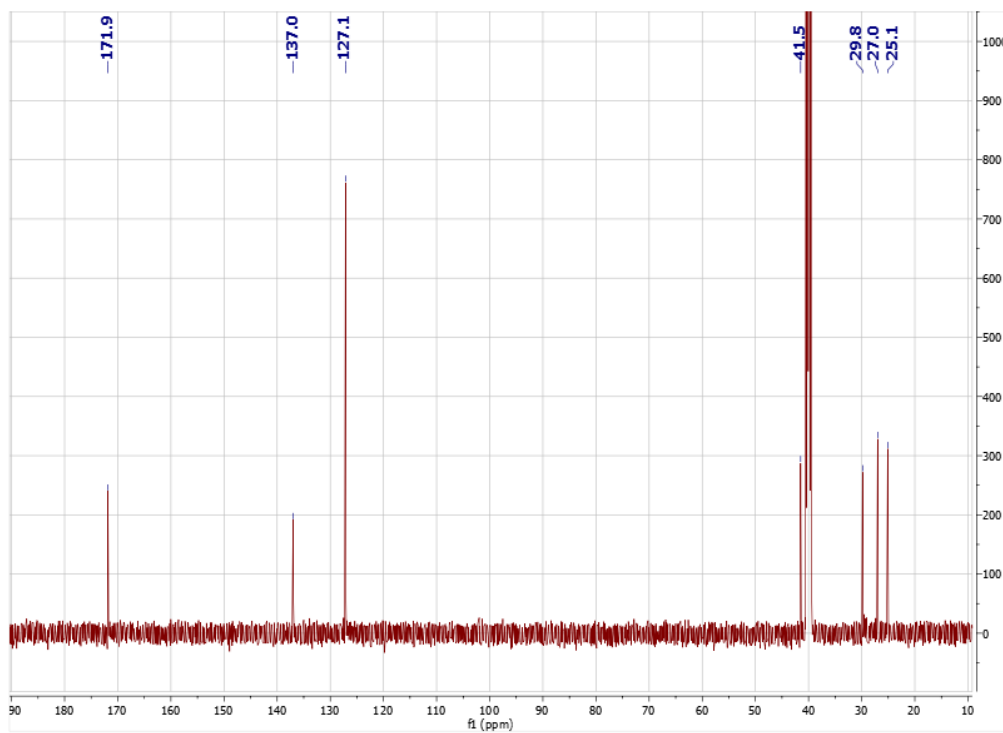
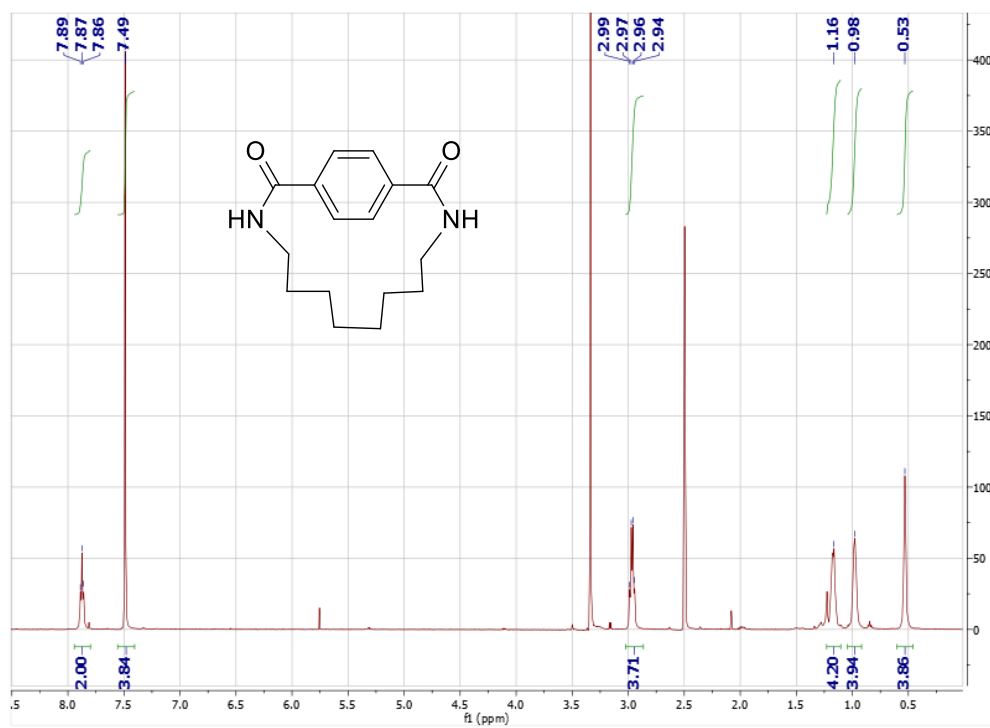
¹H and ¹³C NMR Spectra of 4.8 (CDCl₃) at 100°C



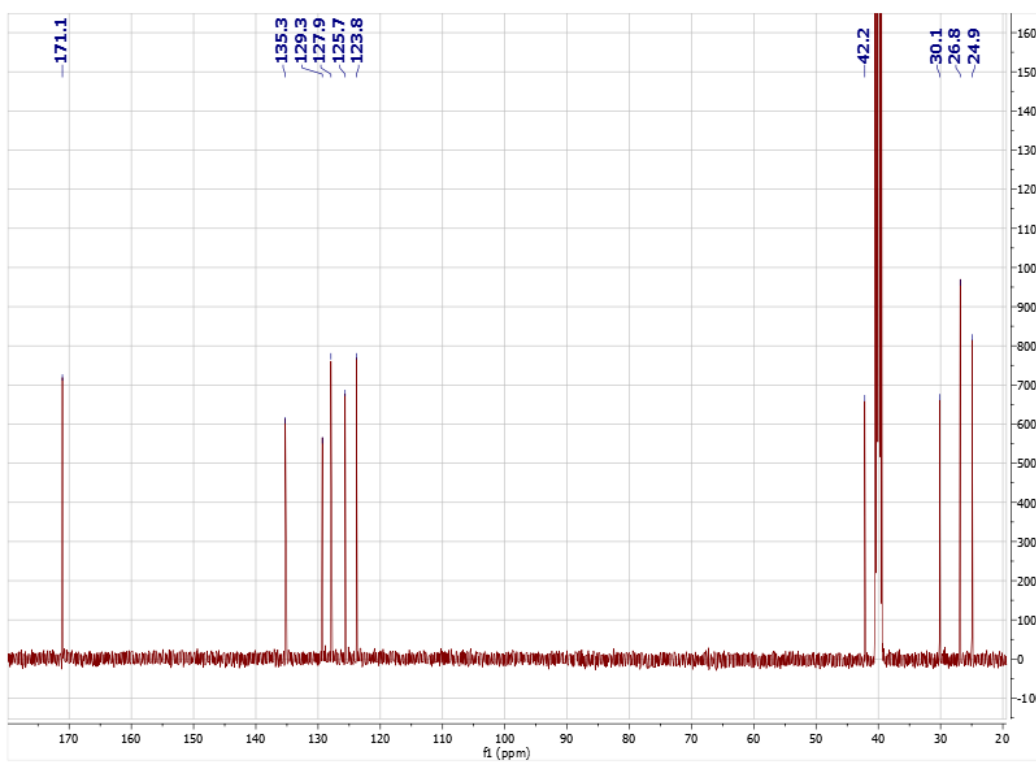
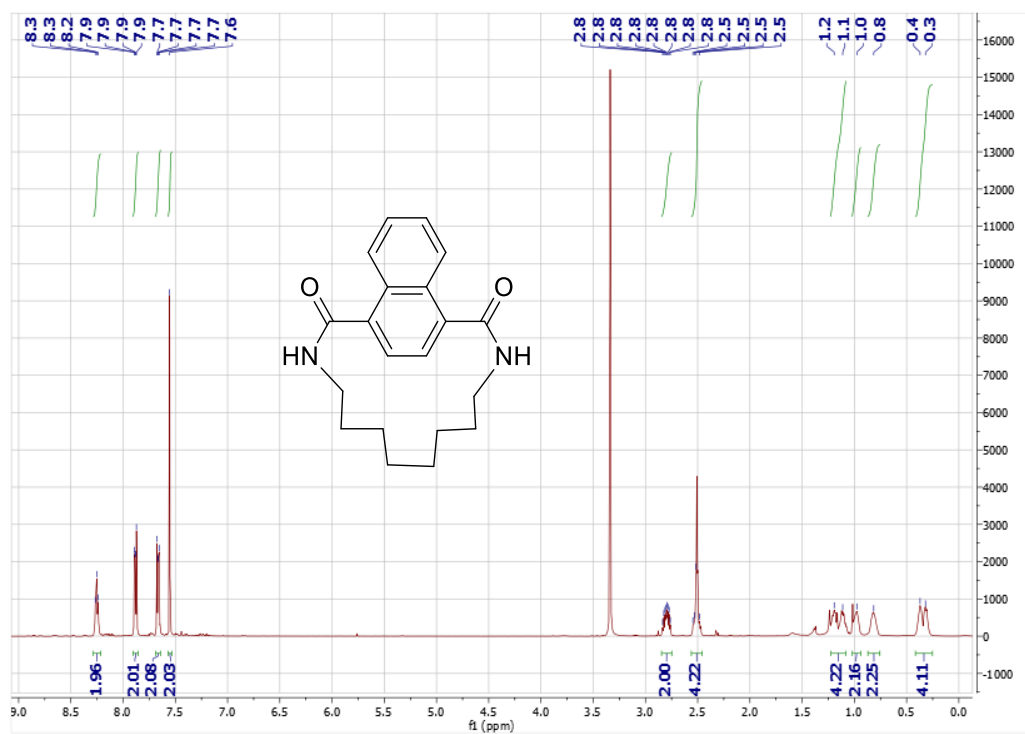
^1H and ^{13}C NMR Spectra of 4.9a (DMSO- d_6)



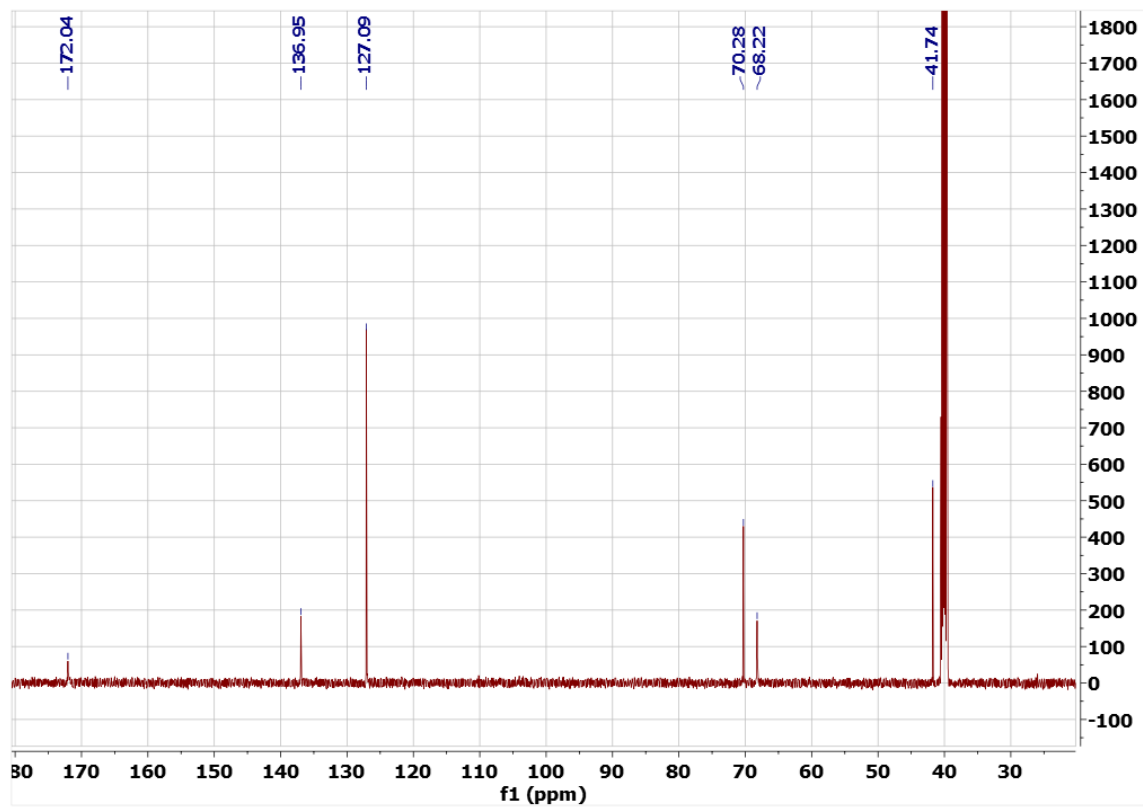
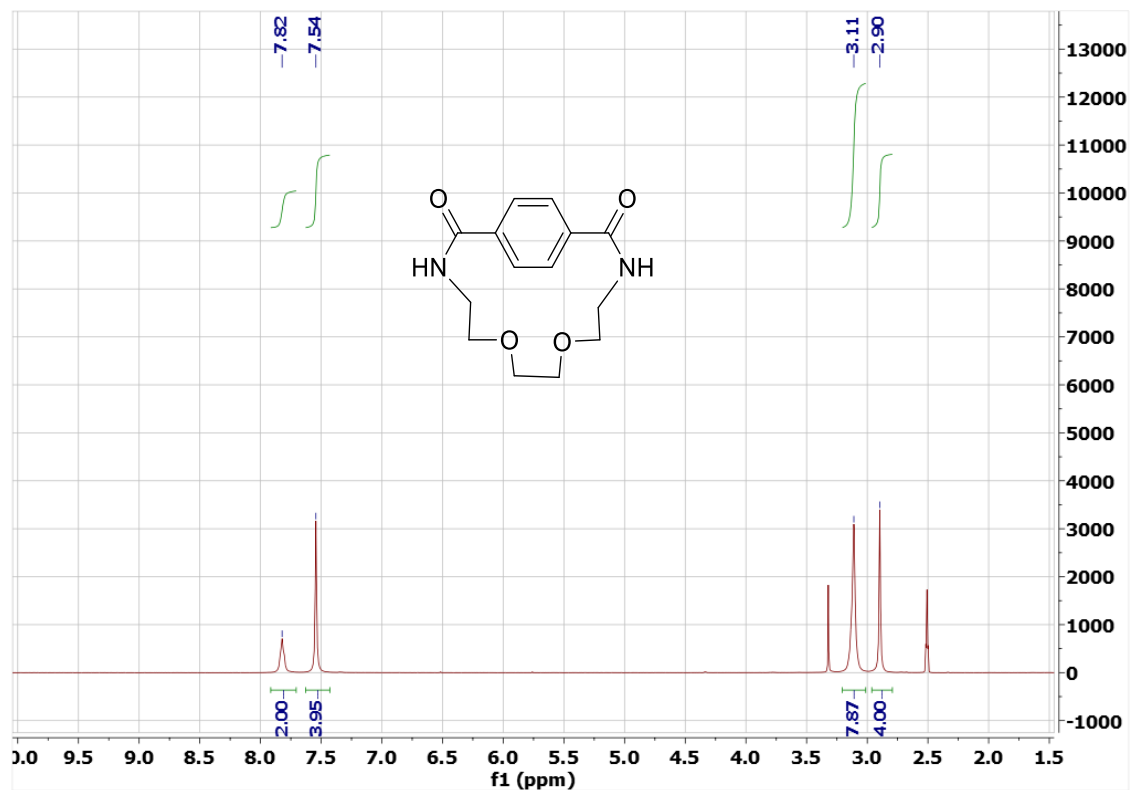
^1H and ^{13}C NMR Spectra of 4.9b (DMSO- d_6)



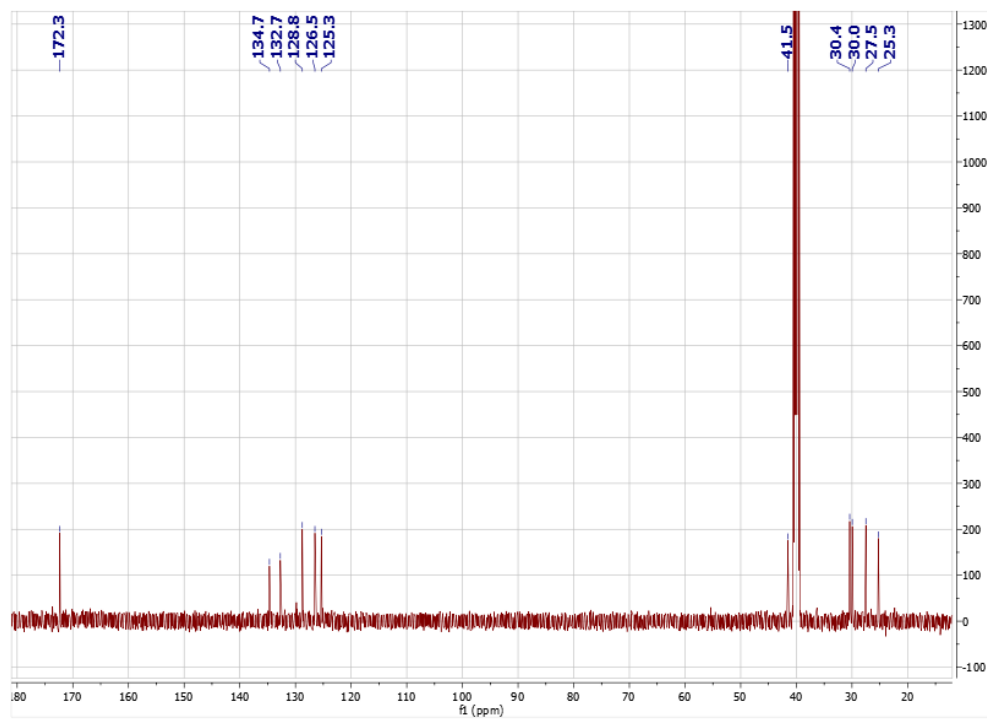
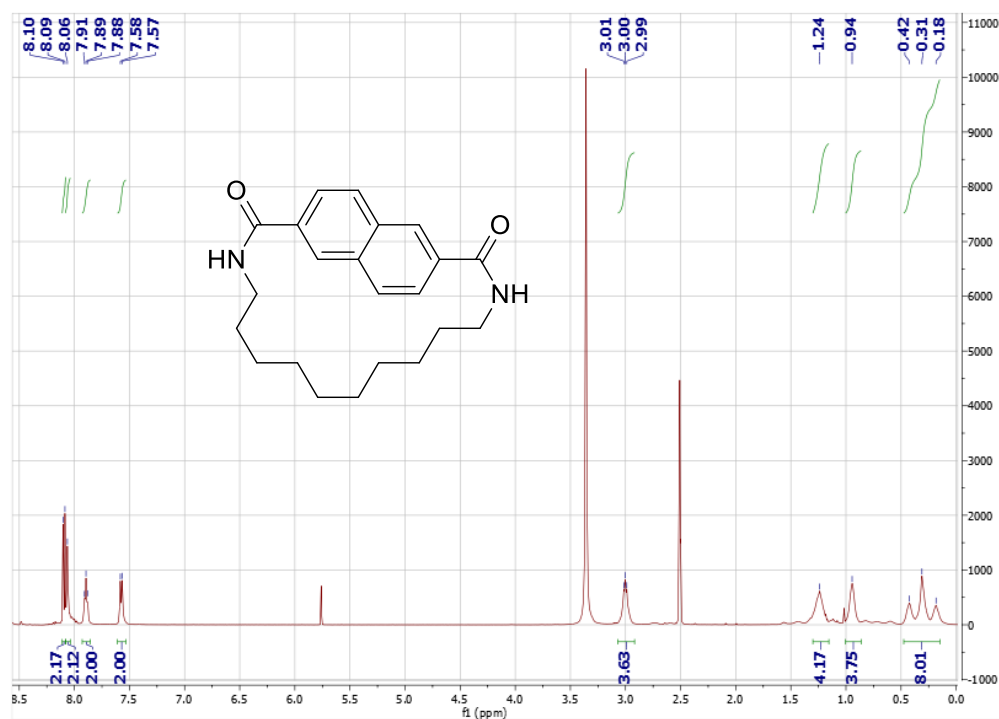
¹H and ¹³C NMR Spectra of 4.9c (DMSO-d₆)



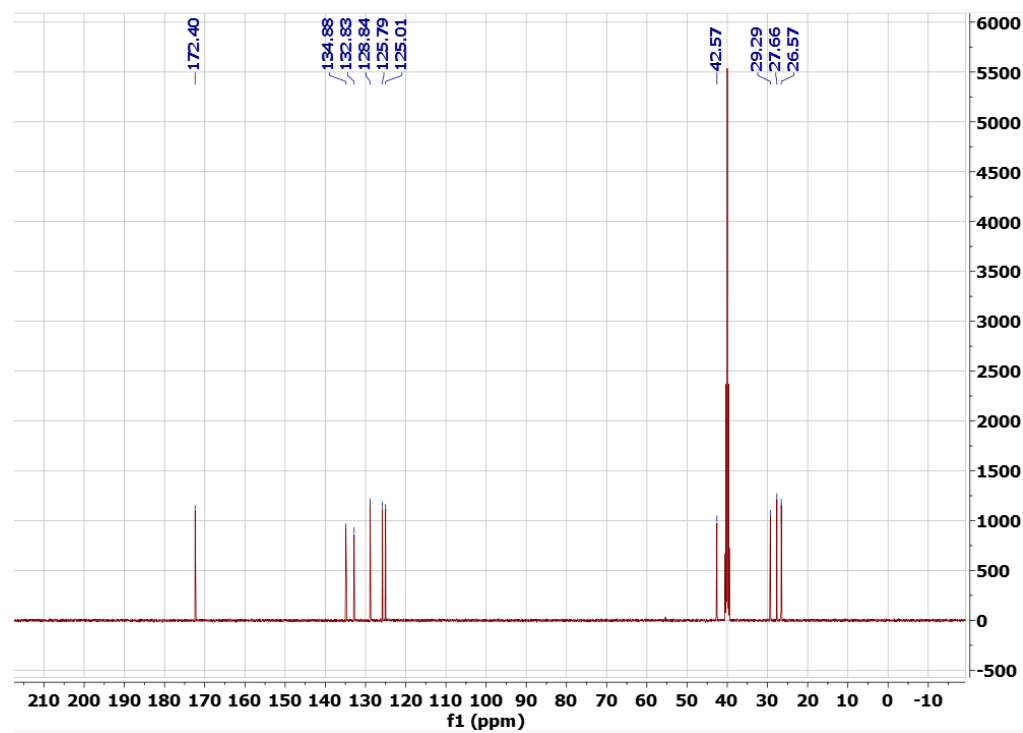
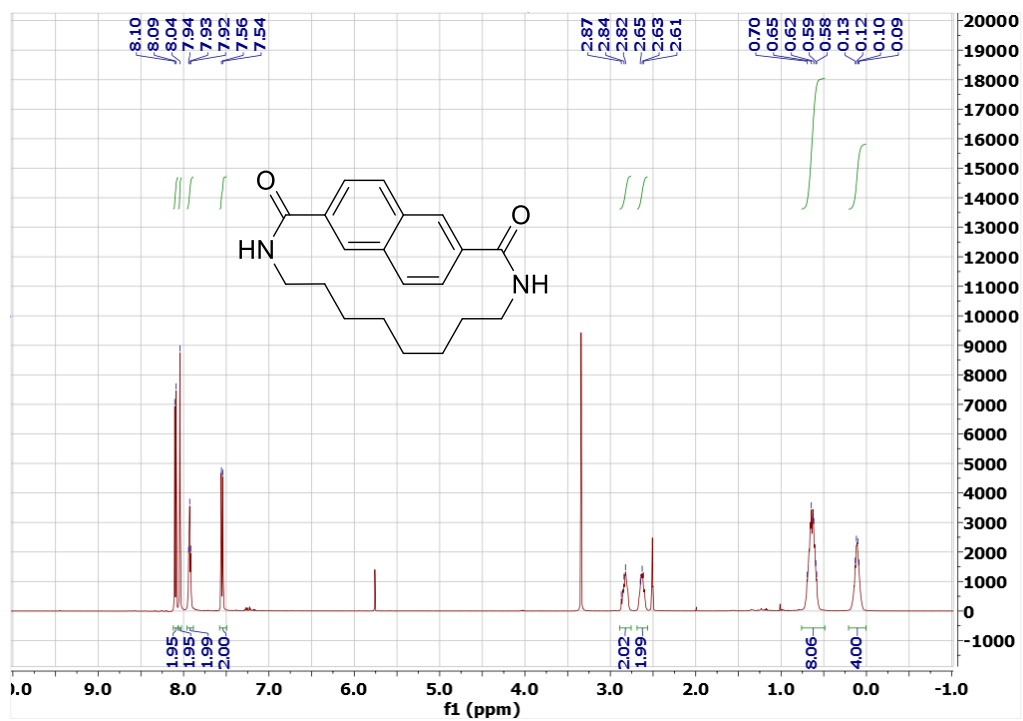
^1H and ^{13}C NMR Spectra of 4.9d (DMSO- d_6)



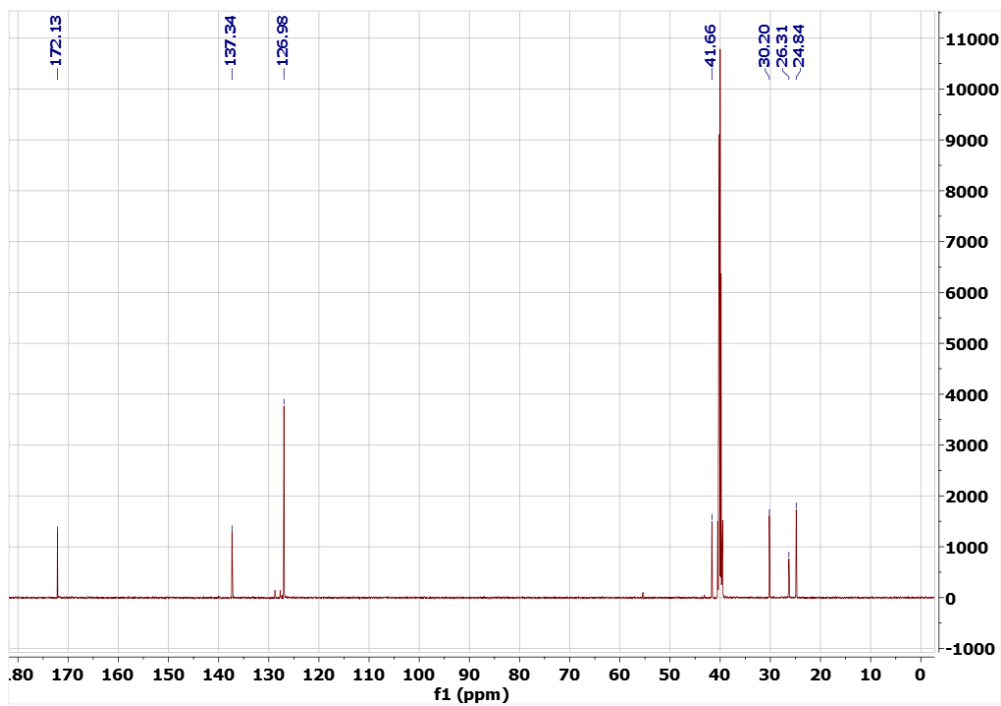
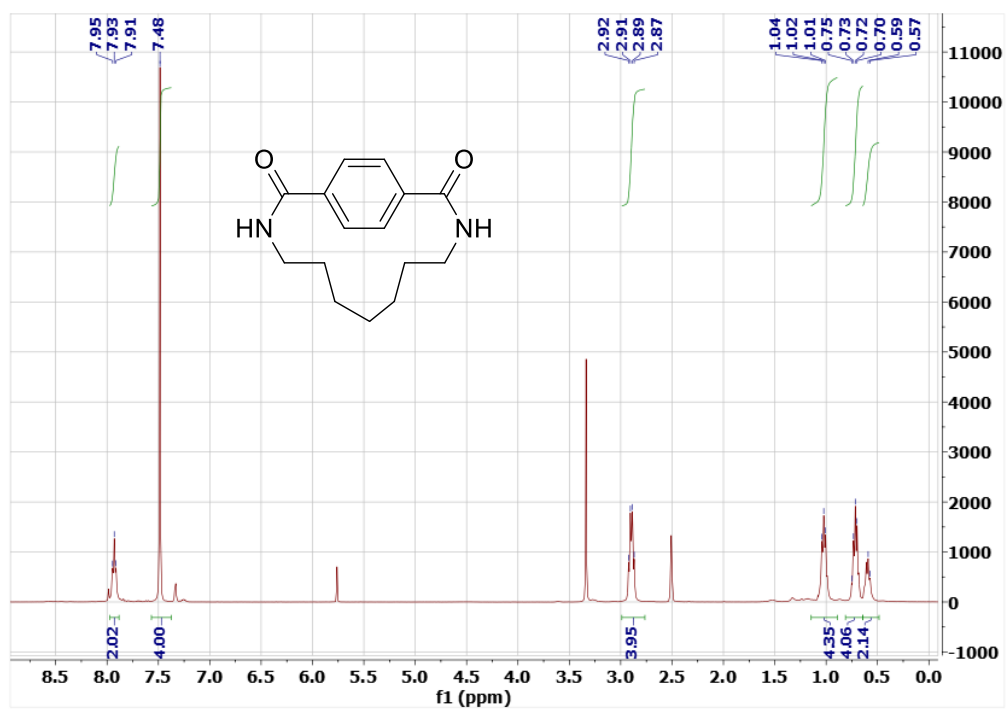
^1H and ^{13}C NMR Spectra of 4.9e (DMSO- d_6)



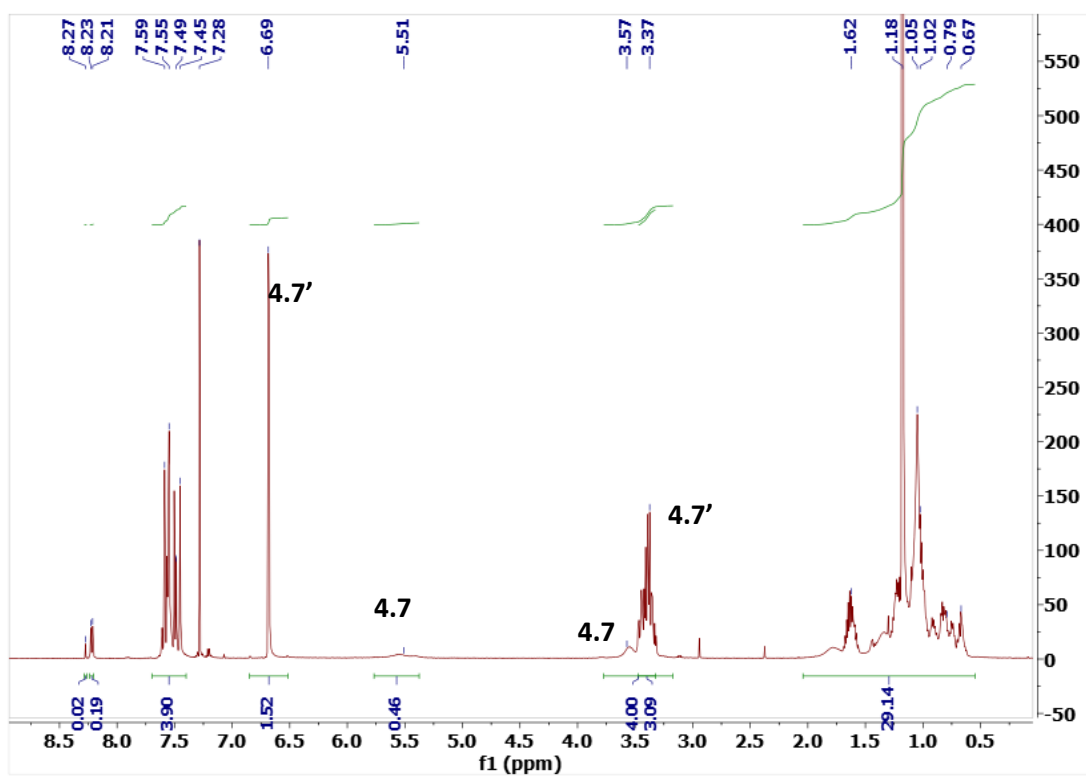
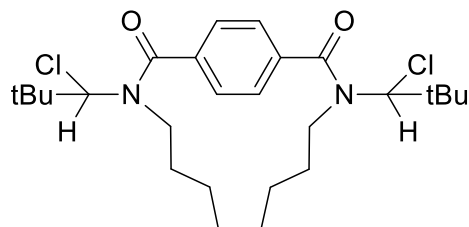
^1H and ^{13}C NMR Spectra of 4.9f (DMSO- d_6)



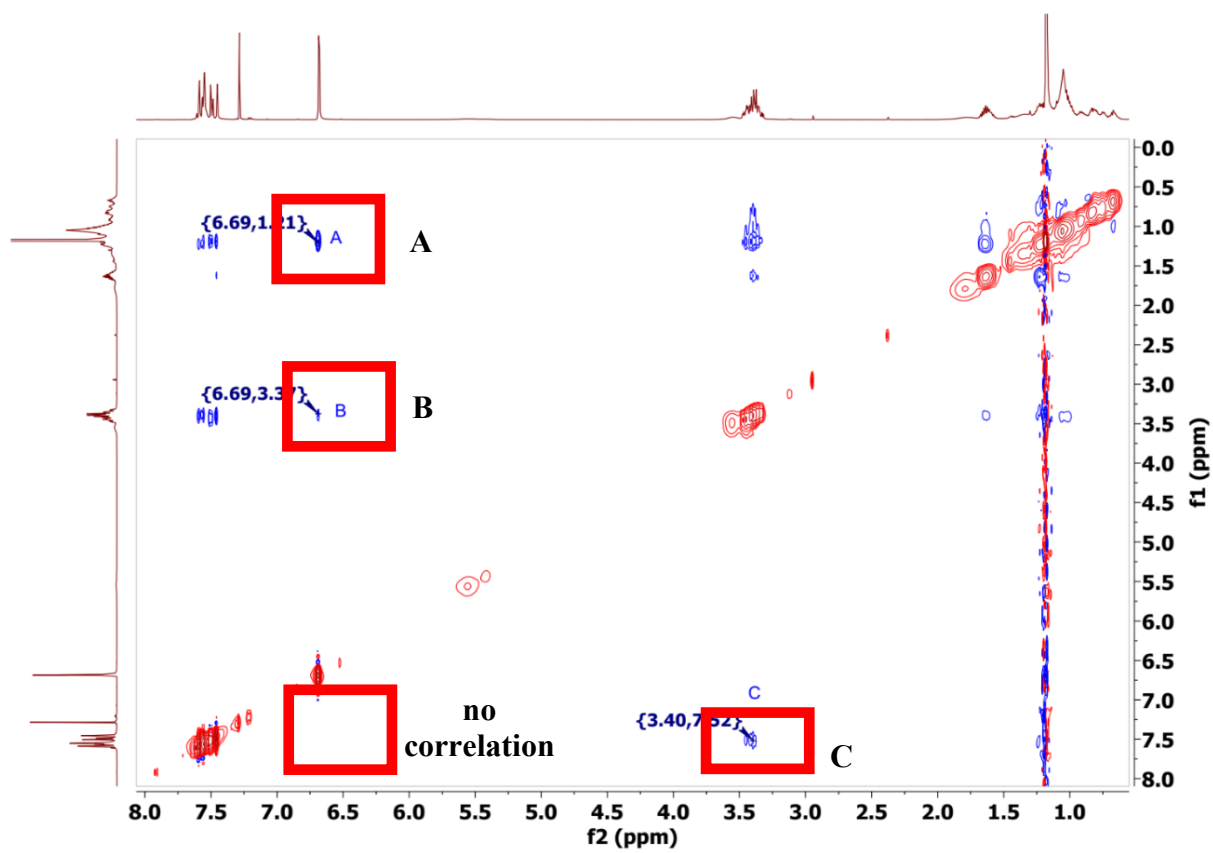
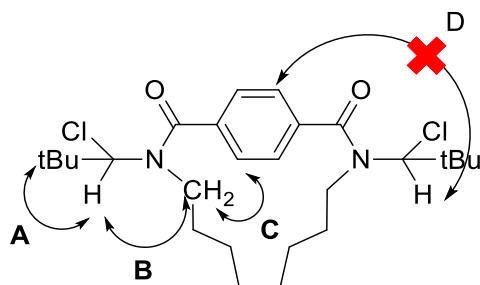
^1H and ^{13}C NMR Spectra of 4.9g (DMSO- d_6)



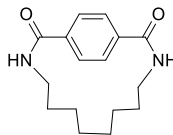
¹H NMR Spectra of 4.7-4.7' mixture (CDCl₃)



2D-NOE Spectra of 4.7' (CDCl₃)



Summary of Crystallographic Data of 4.9b (CCDC no: 1948563)



Empirical formula	C ₁₆ H ₂₂ N ₂ O ₂
Formula weight	274.35
Temperature/K	298(2)
Crystal system	monoclinic
Space group	P2 ₁ /n
a/Å	5.9945(2)
b/Å	18.5737(6)
c/Å	13.2381(4)
α/°	90
β/°	93.0910(10)
γ/°	90
Volume/Å ³	1471.79(8)
Z	4
ρ _{calc} /cm ³	1.238
μ/mm ⁻¹	0.654
F(000)	592.0
Crystal size/mm ³	0.400 × 0.150 × 0.150
Radiation	CuKα (λ = 1.54178)
2θ range for data collection/°	9.524 to 144.716
Index ranges	-7 ≤ h ≤ 6, -22 ≤ k ≤ 22, -16 ≤ l ≤ 16
Reflections collected	23429
Independent reflections	2884 [R _{int} = 0.0302, R _{sigma} = 0.0190]
Data/restraints/parameters	2884/0/181
Goodness-of-fit on F ²	1.045
Final R indexes [I ≥ 2σ (I)]	R ₁ = 0.0448, wR ₂ = 0.1192
Final R indexes [all data]	R ₁ = 0.0463, wR ₂ = 0.1207
Largest diff. peak/hole / e Å ⁻³	0.23/-0.17

Fractional Atomic Coordinates ($\times 10^4$) and Equivalent Isotropic Displacement Parameters ($\text{\AA}^2 \times 10^3$).
 U_{eq} is defined as 1/3 of the trace of the orthogonalised U_{ij} tensor.

Atom	<i>x</i>	<i>y</i>	<i>z</i>	U(eq)
C1	5956(2)	3918.8(6)	1158.2(9)	31.5(3)
C2	3795(2)	4026.3(7)	1470.0(10)	35.9(3)
C3	2795(2)	3496.9(7)	2029.3(10)	36.5(3)
C4	3910(2)	2866.5(6)	2296.0(9)	33.2(3)
C5	6011(2)	2744.2(6)	1938.6(10)	35.5(3)
C6	7001(2)	3262.8(7)	1363.1(9)	33.9(3)
C7	2782(2)	2317.5(7)	2932.1(10)	39.1(3)
O8	936.2(19)	2082.7(6)	2653.5(9)	60.0(3)
N9	3894(2)	2097.4(6)	3780.9(9)	45.8(3)
C10	5820(3)	2445.7(8)	4292.9(11)	49.0(4)
C11	5241(3)	3162.7(9)	4779.3(12)	54.4(4)
C12	7281(3)	3568.9(10)	5210.1(13)	64.7(5)
C13	8714(3)	3913.0(9)	4423.7(13)	57.2(4)
C14	7678(3)	4565.6(9)	3884.6(12)	52.3(4)
C15	9270(3)	4936.5(8)	3194.1(12)	49.6(4)
C16	8381(3)	5615.8(8)	2674.5(11)	51.7(4)
C17	6606(3)	5485.5(7)	1836.2(11)	45.6(3)
N18	7494(2)	5136.5(6)	947.8(8)	41.2(3)
C19	7307(2)	4461.5(7)	614.7(9)	34.8(3)
O20	8344.3(18)	4258.3(5)	-122.1(7)	47.7(3)

Anisotropic Displacement Parameters ($\text{\AA}^2 \times 10^3$). The Anisotropic displacement factor exponent takes the form: $-2\pi^2[h^2a^{*2}U_{11}+2hka^*b^*U_{12}+\dots]$.

Atom	U_{11}	U_{22}	U_{33}	U_{23}	U_{13}	U_{12}
C1	36.1(6)	28.9(6)	29.9(6)	-0.2(4)	4.5(5)	-3.2(5)
C2	35.7(6)	31.7(6)	40.6(7)	4.6(5)	3.7(5)	3.6(5)
C3	30.6(6)	37.2(6)	42.0(7)	1.8(5)	6.0(5)	0.3(5)
C4	36.1(6)	29.4(6)	34.4(6)	0.9(5)	4.0(5)	-4.6(5)
C5	38.2(6)	27.0(6)	41.7(7)	1.9(5)	5.3(5)	2.8(5)
C6	32.5(6)	32.9(6)	37.0(6)	-2.3(5)	8.1(5)	0.2(5)
C7	41.2(7)	30.9(6)	46.0(7)	2.1(5)	10.7(5)	-4.9(5)
O8	47.8(6)	58.5(7)	73.7(8)	14.0(6)	2.5(5)	-20.5(5)
N9	57.5(7)	34.9(6)	45.4(6)	10.7(5)	7.2(5)	-10.5(5)
C10	55.9(8)	48.8(8)	42.0(7)	10.3(6)	0.7(6)	-6.1(7)
C11	66.1(10)	51.4(9)	46.4(8)	2.7(7)	10.1(7)	-10.4(7)
C12	88.0(13)	59.1(10)	45.5(9)	8.5(7)	-8.9(8)	-18.2(9)
C13	62.1(10)	50.8(9)	57.8(9)	6.2(7)	-5.7(8)	-11.6(7)
C14	59.6(9)	49.0(8)	48.3(8)	3.2(6)	3.6(7)	-8.8(7)
C15	56.7(9)	43.7(8)	48.7(8)	-3.4(6)	4.3(7)	-10.0(6)
C16	75.9(10)	32.2(7)	48.2(8)	-7.1(6)	14.1(7)	-12.7(7)
C17	61.9(9)	30.0(6)	46.4(8)	-3.5(5)	15.0(6)	3.7(6)
N18	57.0(7)	29.0(5)	39.1(6)	0.9(4)	15.3(5)	-5.6(5)
C19	40.8(6)	31.1(6)	33.0(6)	0.6(5)	7.1(5)	-2.7(5)
O20	63.2(6)	38.4(5)	44.1(5)	-7.6(4)	25.3(5)	-12.2(4)

Bond Lengths

Atom	Atom	Length/Å	Atom	Atom	Length/Å
C1	C6	1.3902(17)	C10	C11	1.527(2)
C1	C2	1.3946(17)	C11	C12	1.522(2)
C1	C19	1.5009(16)	C12	C13	1.525(2)
C2	C3	1.3865(18)	C13	C14	1.522(2)
C3	C4	1.3847(18)	C14	C15	1.521(2)
C4	C5	1.3875(17)	C15	C16	1.520(2)
C4	C7	1.5058(16)	C16	C17	1.515(2)
C5	C6	1.3816(17)	C17	N18	1.4676(16)
C7	O8	1.2275(17)	N18	C19	1.3316(16)
C7	N9	1.3391(19)	C19	O20	1.2435(15)
N9	C10	1.458(2)			

Bond Angles

Atom	Atom	Atom	Angle/°	Atom	Atom	Atom	Angle/°
C6	C1	C2	118.92(11)	C7	N9	C10	126.89(11)
C6	C1	C19	115.67(11)	N9	C10	C11	112.98(14)
C2	C1	C19	125.41(11)	C12	C11	C10	113.19(15)
C3	C2	C1	119.45(11)	C11	C12	C13	115.01(13)
C4	C3	C2	121.27(11)	C14	C13	C12	115.04(16)
C3	C4	C5	119.08(11)	C15	C14	C13	112.89(14)
C3	C4	C7	119.35(11)	C16	C15	C14	115.58(14)
C5	C4	C7	121.53(11)	C17	C16	C15	114.47(12)
C6	C5	C4	119.90(11)	N18	C17	C16	112.77(13)
C5	C6	C1	121.08(11)	C19	N18	C17	130.81(11)
O8	C7	N9	122.92(12)	O20	C19	N18	120.58(11)
O8	C7	C4	119.82(12)	O20	C19	C1	118.55(11)
N9	C7	C4	117.25(11)	N18	C19	C1	120.77(11)

Hydrogen Atom Coordinates ($\text{\AA}\times 10^4$) and Isotropic Displacement Parameters ($\text{\AA}^2\times 10^3$)

Atom	x	y	z	U(eq)
H2	3031.98	4449.65	1304.19	43
H3	1347.01	3566.63	2229.12	44
H5	6751.08	2313.79	2086.1	43
H6	8388.77	3171.43	1108.72	41
H9	3422.22	1709.55	4052.92	55
H10A	6949.92	2527.41	3807.84	59
H10B	6450.69	2125.18	4811.64	59
H11A	4452.45	3462.26	4277.15	65
H11B	4242.07	3073.53	5318.28	65
H12A	8205.91	3238.3	5616.15	78
H12B	6785.79	3943.54	5656.66	78
H13A	10128.12	4056.36	4754.31	69
H13B	9030.14	3552.68	3920.59	69
H14A	6354.35	4414.72	3486.58	63
H14B	7216.07	4907.94	4385.79	63
H15A	10627.15	5057.55	3589.93	60
H15B	9669.59	4596.5	2677.82	60
H16A	7763.59	5926.14	3178.37	62
H16B	9619.97	5869.71	2394.58	62
H17A	5439.91	5185.3	2092.9	55
H17B	5939.09	5942.4	1633.01	55
H18	8263.63	5414.38	580.81	49